Postreplicative repair is an integral component of lagging strand DNA replication and a suppressor of replication stress

A DISSERTATION
SUBMITTED TO THE FACULTY OF THE GRADUATE SCHOOL
OF THE UNIVERSITY OF MINNESOTA
BY

Jordan Robert Becker

IN PARTIAL FULFILLMENT OF THE REQUIREMENTS
FOR THE DEGREE OF
DOCTOR OF PHILOSOPHY

Dr. Anja-Katrin Bielinsky

April 2016

Acknowledgements

I want to begin by thanking all of the current and former members of the Bielinsky lab that I've had the pleasure to meet and work with over the past 5.5 years. I would be lucky to work with any scientists of your caliber but am particularly fortunate in that you are also my close friends.

I must also give a deep thanks to my adviser, Anja. Not only have you taught me to hold myself to a high standard, but you have daily demonstrated the drive and work ethic necessary to be successful in this profession. I can never thank you enough for the time (and undoubtedly frustration) that you have expended in teaching me how to do science the right way. Thank you.

I am so incredibly lucky to have a family that is such an unyielding source of love and support. My brothers, Alex, Kyle and Aaron, and my sister Ellen. I love you all and even though many of us live far away from one another, when we all get together it's as if we never missed a beat. To my extended family, Janet and Dale, and my "in-laws" Andy, Sheila, and Paul who have all been so supportive through this process. In particular I would like to thank my parents, Brian and Jill. Mom and Dad, I love you so much and will never be able to thank you enough for everything that you've done for me. Thank you.

Finally and most importantly, my wife Abbey. We met in the first week of grad school and have shared this journey together from the beginning. I love you more than anything and cannot wait to share the rest of our lives adventures together.

Dedication

This thesis is dedicated to my family and friends for their unwavering love and support.

Abstract

Cell division is a basic requirement for the propagation of all organisms. This process begins with a parental cell which divides, leaving two daughter cells. Prior to division, it is necessary for the parental cell to generate a precise duplicate of its genetic material *via* the process of DNA replication, so that each resulting daughter segregates with a full genetic complement. Errors that occur during this process are thus inherited as mutations by the daughter cells and perpetuated in each subsequent generation along that lineage. Because an estimated 10,000 trillion cell divisions occur in the average lifetime of a human being, it is imperative that this process occurs with a minimum of errors [Quammen 2008]. In the event of difficulty or error, a network of repair and checkpoint pathways has arisen to facilitate the completion of replication with a minimum of inherited mutations [Myung *et al.* 2001]. The high level of conservation in these replication, repair and checkpoint pathways has allowed us to utilize relatively simple model organisms, such as *S. cerevisiae* (budding yeast), to better understand how these processes are carried out in more complex metazoan systems. My research has focused on one such group of pathways collectively referred to as postreplicative repair or "PRR" [Chen *et al.* 2011]. PRR is activated in response to a variety of stressors, which cause difficulty for the replication program and mitigates their impact on genome integrity. The findings included in this dissertation expand our knowledge of stressors, which impact the usage of PRR pathways and moreover describe PRR as an integral component of lagging strand DNA replication.

Table of Contents

List of Tables

List of Figures

Chapter 1: Introduction

Chapter 2: Mcm10 deficiency causes defective-replisome-induced mutagenesis and a dependence on error-free postreplicative repair

Chapter 3: Genetic interactions implicating postreplicative repair in Okazaki fragment processing

Abbreviations

A	alanine
APC	Anaphase promoting complex
ARS	autonomously replicating sequences
ATM	ataxia-telangiectasia mutated
ATR	ataxia-telangiectasia mutated- and Rad3-related
BER	base excision repair
Can1	canavanine resistance 1
Cas9	CRISPR associated protein 9
Cdc	cell division cycle
Cdk1	Cyclin dependent kinase 1
Cdt1	chromatin licensing and DNA replication factor 1
Chk	checkpoint kinase
Clb	B-type cyclin
Cln	G1 or A-type cyclin
CMG	Cdc45-Mcm2-7-GINS
CRISPR	Clustered regularly-interspaced short palindromic repeats
Ctf4	chromosome transmission fidelity 4
Ddc	DNA damage checkpoint
DDK	Dbf4-dependent Cdc7 kinase
DNA	Deoxyribonucleic acid
Dna2	DNA synthesis defective 2
Dnl4	DNA ligase 4
dNTPs	di-deoxynucleotide
DRIM	Defective-replisome-induced mutagenesis
ds	double-stranded
DSB	double-stranded break
E2	ubiquitin conjugating enzyme
E3	ubiquitin ligase
Elg1	enhanced level of genomic instability
Esp1	extra spindle pole bodies 1
Exo1	exonuclease 1
F	phenylalanine
FEN1	flap endonuclease 1
G	glycine
G1	Gap phase 1
G2	Gap phase 2
Gal-	Galactose inducible promoter
GINS	Go, Ichi, Nii, and San (5-1-2-3 in Japanese)

His	histidine
HR	homologous recombination
HU	hydroxyurea
K	lysine
kDa	Kilodalton
L	leucine
M	mitosis
Mcm	minichromosome maintenance
Mec1	mitotic entry checkpoint 1
MMS	methyl methansulfonate
Mms21	Methyl methanesulfonate sensitivity 21
Mrc1	mediator of replication checkpoint 1
NHEJ	non-homologous end joining
nt	nucleotide
ORC	origin recognition complex
PCNA	proliferating cell nuclear antigen
Pds1	precocious dissociation of sisters 1
PIP	PCNA-interacting peptide
Pol	polymerase
pre-IC	pre-initiation complex
pre-LC	pre-loading complex
pre-RC	pre-replicative complex
PRR	postreplicative repair
R	arginine
Rad	radiation sensitive
Rev	reversionless
RFC	replication factor C
RNA	ribonucleic acid
RPA	replication protein A
S	Synthesis phase
S. cerevisiae	*Saccharomyces cerevisiae*
S-CDK	S phase dependent-kinase
Sic1	substrate/subunit inhibitor of cyclin-dependent protein kinase 1
Sld	synthetic lethality with Dpb11
Srs2	suppressor of rad six 2
ss	single stranded
ssDNA	single-stranded DNA
SUMO	small ubiquitin-like modifier
Tdh1	triose-phosphate dehydrogenase 1
TLS	translesion synthesis

Ubc9	ubiquitin-conjugating 9
UV	Ultraviolet

CHAPTER 1

Introduction

Cell cycle regulation

The cell cycle has historically been divided into 4 phases: 1) G1 or “gap 1” phase in which the cell prepares by ensuring that it contains the necessary components to transit the cell cycle, 2) S or “synthesis” phase when the genome is replicated, 3) G2 or “gap 2” to ensure that replication is completed sufficiently for cell division, and finally 4) M or “mitosis” phase in which the chromosomes are separated and the cell divides.

The phases of this cycle are defined by the specific events outlined above, but are also defined and regulated by the interaction of cyclin dependent kinase 1 (Cdk1) with a cohort of nine different cyclins which regulate its activity [Hartwell *et al.* 1974, Reed *et al.* 1985]. These related proteins can be sub-classified and include three G1 cyclins (Cln) and six B-type cyclins (Clb) [Mendenhall and Hodge 1998]. Different cyclins are present at distinct stages of the cell cycle and their binding to Cdk1 specifies its activity to the correct substrates at the correct time [Reed *et al.* 1985, Mendenhall and Hodge 1998]. Being that the majority of my research has been carried out using the yeast model system, the nomenclature used herein is derived from *S. cerevisiae*.

In G1 phase, Cdk1 is bound by the G1 cyclins Cln1-3. There is no individual G1 cyclin that is essential, but at least one must be present to proceed from G1 phase past the restriction point or “Start” in yeast, into S phase [Richardson *et al.* 1989]. Despite this, Cln1-3 each have some unique molecular functions. The Cln3-Cdk1 complex plays a critical role by phosphorylating the transcriptional repressor

whiskey 5 (Whi5), enabling derepression of transcription of a massive cohort of genes involved in the upcoming cell cycle including Cln1/2 and Clb5/6 [Simon *et al.* 2001, Costanzo *et al.* 2004]. Following transcriptional derepression, Cln1 and Cln2 levels rise and when bound to Cdk1 they promote spindle pole body duplication, bud formation, and phosphorylation of substrate/subunit inhibitor of cyclin-dependent protein kinase 1 (Sic1) [Lew and Reed 1993, Dirick *et al.* 1995, Lew and Reed 1995, Schneider *et al.* 1996]. Phosphorylation of Sic1 results in its degradation, relieving the inhibition of Cdk1-Clb5 and Cdk1-Clb6 complexes and allowing entry into S phase [Hereford and Hartwell 1974, Tyers 1996, Feldman *et al.* 1997].

Progression through S, G2, and M phases sees a handoff from the G1 specific A-type (Cln1-3) to the early B-type (Clb5/6) cyclins. Clb5/6 are present in the beginning of S phase and are directly involved in assembling factors involved in the initiation of DNA replication [Tanaka *et al.* 2007]. Clb3/4 accumulate in mid-S phase and persist until the completion of mitosis, during which time they are partially redundant for Clb5/6 and support proper spindle assembly [Fitch *et al.* 1992, Schwob and Nasmyth 1993, Haase *et al.* 2001]. After the bulk of replication is completed, Clb1 and Clb2 accumulate during G2 phase where they promote the transition into and through M phase [Fitch *et al.* 1992, Seufert *et al.* 1995]. In M phase, Clb1/2-Cdk1 activates the anaphase promoting complex (APC), an E3 ubiquitin ligase which targets precocious dissociation of sisters 1 (Pds1) or “securin” for degradation [Cohen-Fix *et al.* 1996]. Pds1 degradation relieves its

inhibition of extra spindle pole bodies 1 (Esp1) or “separase”, which is then free to cleave cohesin and thereby allow separation of the chromosomes [Ciosk *et al.* 1998, Uhlmann *et al.* 1999]. APC then goes on to target the majority of the Clb cyclins for degradation by the 26S proteasome enabling exit from mitosis [Morgan 1999].

Mechanism of DNA replication

Origin licensing and activation

Origins of replication in budding yeast are located throughout the genome and are defined by related autonomous replicating sequences (ARSs) [Stinchcomb *et al.* 1979]. These ARS sequences are bound by a multiprotein origin recognition complex (ORC) in late M/G1 phase of the cell cycle which identifies them as potential origins of replication [Bell and Dutta 2002]. During G1 phase, ORC recruits cell division cycle 6 (Cdc6) and chromatin licensing and DNA replication factor 1 (Cdt1) before loading minichromosome maintenance 2-7 (Mcm2-7) helicase hexamers in a head-to-head fashion (Figure 1.1) [Liang *et al.* 1995, Coleman *et al.* 1996, Maiorano *et al.* 2000, Nishitani *et al.* 2000, Whittaker *et al.* 2000, Remus *et al.* 2009]. Loading of Mcm2-7 completes assembly of the pre-replication complex (pre-RC) and at this juncture the origins are inactive but considered to be “licensed” [Evrin *et al.* 2009, Remus *et al.* 2009].

With the transition from G1 to S phase and the initiation of DNA replication, the pre-RC is sequentially targeted by two S-phase specific kinases, Dbf4-

dependent kinase (DDK) and S-cyclin-dependent kinase (S-CDK), stimulating formation of the pre-initiation complex (pre-IC) (Figure 1.1) [Heller *et al.* 2011]. This is marked by the recruitment of a series of additional replication factors including GINS (Go, Ichi, Nii, and San) and Cdc45 which together with Mcm2-7 forms the Cdc45-Mcm2-7-GINS (CMG) holoenzyme [Zou and Stillman 2000, Moyer *et al.* 2006]. After activation, CMG will translocate along the chromosome unwinding DNA [Moyer *et al.* 2006]. In the first event of activation, DDK phosphorylates Mcm4 and Mcm6 stimulating the recruitment of synthetically lethal with *dpb11-1* (Sld3) and Cdc45 [Randell *et al.* 2006, Sheu and Stillman 2010]. Then, Clb5/6-Cdk1 or "S-CDK" phosphorylates Sld3 and Sld2, enabling their interaction with Dpb11 [Zegerman and Diffley 2007]. Dpb11 recruits Pol-ε and GINS, which along with Sld2 forms the pre-loading complex (pre-LC) and delivers Pol-ε and GINS to origins (Figure 1.1) [Muramatsu *et al.* 2010]. However, before the helicase can become fully activated the Mcm2-7 helicase ring, which loads encircling double-stranded (ds)DNA, must melt the two strands, extruding one from the inner pore of the ring [Costa *et al.* 2011]. Mcm2-7 is then positioned encircling the leading strand template and unwinds the two strands for replication as it travels along the chromosome [Fu *et al.* 2011]. The precise mechanism by which melting and strand extrusion occurs is not yet entirely understood but is an active area of study [Gai *et al.* 2010].

One of the final steps in origin activation is the recruitment of Mcm10 to the pre-IC. This serves two proposed roles: 1) binding and stabilization of single-

stranded (ss)DNA upon melting of the two DNA strands, allowing replication protein A (RPA) recruitment, and 2) recruitment of polymerase (Pol-) α primase in concert with chromosome transmission fidelity 4 (Ctf4) [Ricke and Bielinsky 2004, Ricke and Bielinsky 2006, Warren *et al.* 2008, Gambus *et al.* 2009, Warren *et al.* 2009, Baxley *et al.* 2016]. Pol-α primase is necessary to generate primers with a 3'-OH end that can be extended by the replicative polymerases Pol-ε and Pol-δ [Bell and Dutta 2002]. Mcm10 then travels with the replication fork in association with proliferating cell nuclear antigen (PCNA), moving away from the origin as a component of the DNA elongation machinery (Figure 1.1) [Ricke and Bielinsky 2004, Das-Bradoo *et al.* 2006]. In a recent and exciting development, the Diffley laboratory at the Francis Crick Institute in London has reconstituted origin assembly and activation completely *in vitro* using only purified yeast protein components [Yeeles *et al.* 2015]. This has for the first time undisputedly established the minimum number and identity of essential components necessary for origin assembly and replication start [Yeeles *et al.* 2015].

DNA synthesis and Okazaki fragment maturation

Replication proceeds bidirectionally from the sites of origin activation with complete CMG complexes moving away in both directions (Figure 1.2) [Bell and Dutta 2002, Fu *et al.* 2011]. Synthesis of the DNA is primed by Pol-α primase, generating short (20-30 nucleotide) RNA-DNA fragments *de novo* on a ssDNA template [Arezi and Kuchta 2000]. The 3'-OH end of the primer plays 2 crucial roles

in enabling bulk DNA synthesis: 1) unlike Pol-α primase, the replicative polymerases Pol-ε and Pol-δ are unable to polymerize DNA on unprimed ssDNA and require a starting 3'-OH for nucleotide addition which the primer provides, and 2) the 3' end is recognized by the replication factor C (RFC) clamp loader complex which loads the homotrimeric replication clamp and polymerase processivity factor PCNA [Majka and Burgers 2004]. Because replicative polymerases only synthesize DNA in one direction (5' to 3'), one strand is replicated continuously following in the same direction as the helicase. This is referred to as the leading strand and is thought to be synthesized primarily by Pol-ε [Pursell *et al.* 2007]. In contrast, the lagging strand is replicated by Pol-δ in the opposite direction and is carried out in short bursts called Okazaki fragments (Figure 1.2) [Sakabe and Okazaki 1966, McElhinny *et al.* 2007]. Each Okazaki fragment requires the synthesis of a short RNA-DNA primer by Pol-α primase, DNA synthesis by Pol-δ, and processing by the combined efforts of a number of enzymes, which act to join the newly synthesized Okazaki fragment with the 5' end of the preceding fragment (Figure 1.2) [Burgers 2009].

The joining of Okazaki fragments is a regulated multistep process collectively referred to as Okazaki fragment maturation [Hubscher and Seo 2001]. It begins when DNA synthesis by Pol-δ collides with the 5' end of the previous Okazaki fragment and displaces it into a 5' flap [Burgers 2009]. PCNA then coordinates the processing of this flap in a manner that is dependent on a conserved interaction between the PCNA interacting peptide (PIP) box of the flap

endonuclease radiation sensitive 27 (Rad27) and the interdomain connector loop of PCNA [Gary *et al.* 1999, Chapados *et al.* 2004, Tsutakawa *et al.* 2011]. Flaps that escape processing by Rad27 are degraded by the endonuclease/helicase Dna2 in a reaction that depends on RPA binding to the flap [Bae and Seo 2000, Bae *et al.* 2001]. Successful flap cleavage results in a ligatable nick, which is joined by DNA ligase I [Pascal *et al.* 2004, Tomkinson *et al.* 2006]. After ligation, PCNA is unloaded in an enhanced level of genomic instability (Elg1)-dependent reaction, completing Okazaki fragment maturation [Kubota *et al.* 2013, Kubota *et al.* 2015]. Because of their relatively small size (100-200 nucleotides), one round of replication of the yeast genome includes the priming, synthesis, and processing of ~100,000 Okazaki fragments [Jin *et al.* 2003]. This fact underlines the importance to genome stability of reliably completing maturation with a minimum of errors. In human cells with a much larger genome, the lagging strand is synthesized in an estimated 26,000,000 Okazaki fragments [Hubscher and Seo 2001]. If even a small percentage of these fail to efficiently join and result in mutations or breaks in the DNA, the effect on genome stability is profoundly disastrous. In the next section, I will focus on the cellular response to such DNA damage and more generally stress on the replication machinery. This will be described with particular emphasis on PRR as it pertains to my own research.

Cellular response to DNA damage/replication stress

"Replication stress" is a complex condition that can be generally characterized as a cellular environment in which replication is impaired by any exogenous or endogenous factors that impinge on its normal regulation or successful completion. The primary signal for replication stress is unreplicated ssDNA which becomes coated with the ssDNA binding protein complex RPA [Branzei and Foiani 2010]. As discussed in the previous section, ssDNA is an important and natural intermediate in many of the DNA/protein transactions that occur during unperturbed replication. However, in the presence of replication stressors, either in the form of chemical damage to the DNA that impedes polymerase progress, or inherent defects within the replication machinery, ssDNA gaps can persist for an inordinate amount of time [Lopes *et al.* 2006]. These ssDNA gaps act as a marker for replication stress or DNA damage that – if unaddressed – can lead to unintended breakage or recombination events, translocation, mutation, or loss of genetic material [Zou and Elledge 2003, Branzei and Foiani 2010, Flynn and Zou 2011]. RPA binds ssDNA with high affinity and acts as a platform to initiate checkpoint and rescue pathways to mitigate the effects of replication stress [Zou and Elledge 2003].

The S-phase checkpoint is activated by replication stress

The S phase checkpoint acts as a sort of pause button when DNA replication encounters any of a variety of obstacles and promotes its completion

with a minimum of heritable mutations. Activation of the checkpoint begins with the binding of mitotic entry checkpoint 1 (Mec1) kinase and its partner DNA damage checkpoint 2 (Ddc2) to RPA-coated ssDNA [Rouse and Jackson 2000, Zou and Elledge 2003]. Mec1 and Ddc2 are homologs of the mammalian ATR kinase and ATR interacting protein (ATRIP), respectively [Zou and Elledge 2003]. Mec1 then acts through two independently operating mediator proteins, mediator of the replication checkpoint 1 (Mrc1) and Rad9 which when phosphorylated are capable of activating the checkpoint kinase Rad53 (homolog of the human kinase CHK2) (Figure 1.3) [Sanchez *et al.* 1996, Sun *et al.* 1996, Vialard *et al.* 1998, Alcasabas *et al.* 2001]. Activation of Rad53 serves several important roles in response to replication stress. First, it inhibits origins that have not yet fired [Santocanale and Diffley 1998]. Rad53 targets the initiation factors Sld3 and DDK, inactivating them and preventing the creation of additional replication forks until the source of replication stress has been addressed [Lopez-Mosqueda *et al.* 2010, Zegerman and Diffley 2010]. Second, it upregulates cellular dNTP pools, promoting efficient replication under conditions of replication stress [Chabes *et al.* 2003]. Finally, and perhaps most importantly, Rad53 activation stabilizes stressed replication forks, preventing their collapse and preserving them for resumption of replication when the checkpoint signal subsides [Tercero and Diffley 2001].

Postreplicative repair

In parallel to the S phase checkpoint and activated through the same RPA-ssDNA stimulus are the so-called postreplicative repair or “PRR” pathways. The role of PRR in facilitating replication under various adverse conditions has been the primary focus of my thesis research and as such I will devote extended space to the details underlying PRR and related pathways along with a historical perspective.

PRR, which is also referred to as DNA damage tolerance, can be divided into two general pathways: 1) Error-prone, which relies on low fidelity translesion polymerases to bypass lesions on the template strand DNA, completing replication and avoiding ssDNA persistence at the cost of an increased mutation load, and 2) Error-free, whereby the template strand for replication is switched from the damaged strand to the nascent strand of its newly replicated sister chromatid in a recombination-like process (Figure 1.4) [Prakash *et al.* 2005, Branzei 2011]. The importance of completing replication in a timely manner is underlined by the observation that cells will knowingly take on additional mutations by utilizing the error-prone branch of PRR to fill ssDNA gaps. The “DNA damage tolerance” terminology which is often used to describe PRR is literally accurate in the sense that both pathways enable the tolerance of DNA damage and promote bypass by the replication machinery [Branzei and Foiani 2010]. Neither pathway is directly involved in the repair of DNA damage, which is carried out afterward by independent repair pathways [Ganesan 1974]. The “postreplicative” moniker is

derived from early studies in which it was erroneously assumed that these pathways are active exclusively after the bulk of replication had taken place [Rupp and Howard-Flanders 1968]. However, more recent work has demonstrated that while PRR can be functional after S phase, it is also at work in the context of active replication forks [Branzei and Foiani 2010, Daigaku *et al.* 2010, Karras and Jentsch 2010]. Despite the literal accuracy of “DNA damage tolerance”, PRR is the preferred terminology in the field and will thus be the primary term in this dissertation.

PRR was first described in *E. coli* by Rupp and Howard-Flanders in a 1968 study in which they provided evidence for the exchange of genetic information between sister chromatids after UV irradiation [Rupp and Howard-Flanders 1968]. Such a model is consistent with what we now know about error-free PRR and the use of undamaged sister chromatid DNA as a replication template (Figure 1.4) [Branzei 2011]. The authors observed that the chromosomes of UV irradiated cells incorporated less [^{3}H]thymidine than non-irradiated cells and inferred that UV-induced lesions impaired the completion of replication, leaving unreplicated gaps. However, if the cells were incubated for a longer time after radiation they were able to fully incorporate [^{3}H]thymidine and complete replication. Rupp and Howard-Flanders named the process by which this occurs “postreplication repair”. It is remarkable that these early researchers were able to devise such an accurate model based solely on the pattern of [^{3}H]thymidine incorporation into the DNA of excision repair deficient cells following UV irradiation.

As indicated earlier, the error-prone branch of PRR gains its name from a reliance on low fidelity translesion polymerases [Prakash *et al.* 2005]. These were first identified in a 1971 study in which the translesion polymerase genes reversionless 1 and 3 (*REV1* and *REV3*) (although they were not known to be polymerases at the time) were found to be responsible for the majority of mutations in *S. cerevisiae* after UV treatment [Lemontt 1971, Quah *et al.* 1980]. We now know that Rev1 is a highly conserved translesion polymerase present throughout evolution and Rev3 is the catalytic subunit of another highly conserved translesion polymerase, Pol-ζ [Prakash *et al.* 2005]. The study by J.F. Lemontt that identified these genes turned out to be seminal, as many of the additional translesion polymerases in yeast, mammalian, and *E. coli* systems were later identified by their homology to *REV1* [Kenyon and Walker 1980, McDonald *et al.* 1997, McDonald *et al.* 1999]. A subsequent genetic screen for alleles, which confer sensitivity to UV radiation in yeast confirmed for the first time that genes involved in error-prone PRR belong to an epistasis group downstream of *RAD6* [Lawrence and Christensen 1976]. This so-called *RAD6* epistasis group, which originally included *REV1*, *REV3*, and *RAD18*, was later connected to error-free PRR by the inclusion of *RAD5* [Johnson *et al.* 1992]. Rad5 acts downstream of Rad6 and regulates the initiation of error-free PRR [Branzei 2011]. Thus, error-prone and error-free PRR are co-regulated by Rad6, but at the time the basis for this regulation was not clear.

Mechanistically, the regulation of PRR by Rad6 remained something of a mystery until 1986 when it was demonstrated to be a ubiquitin conjugating enzyme [Jentsch *et al.* 1986]. Several studies at the time described Rad6 ubiquitination of histones H2A and H2B, although these did not turn out to be the key targets for PRR regulation [Jentsch *et al.* 1986, Sung *et al.* 1988]. It was not until 2002 that the critical target of Rad6 was identified as PCNA by Hoege and colleagues in the laboratory of Stefan Jentsch (Figure 1.3) [Hoege *et al.* 2002]. Interestingly, it was Dr. Jentsch who had first described the enzymatic activity of Rad6 as a postodoctoral researcher 15 years earlier [Jentsch *et al.* 1986]. In a proteomic screen for small ubiquitin-like modifier (SUMO) conjugates in response to DNA damage induced by the base alkylating agent methylmethane sulfonate (MMS), PCNA was identified as a target for both ubiquitination and sumoylation at the same residue of lysine (K)164. Further analysis confirmed that this conserved residue was indeed the crucial elusive target of Rad6 which regulates PRR. It emerged that the ubiquitin conjugating enzyme Rad6 in conjunction with the E3 ubiquitin ligase Rad18 targets PCNA-K164 for mono-ubiquitination in response to DNA damage that cannot be replicated by Pol-δ or -ε and leads to their stalling [Hoege *et al.* 2002]. This results in a loss of coordination between the unwinding activity of the CMG helicase and the DNA synthesis activity of the polymerases [Byun *et al.* 2005]. Loss of coordination promotes the formation of ssDNA regions, which rapidly become coated with RPA, and recruits Rad6-Rad18 to mono-ubiquitinate PCNA [Byun *et al.* 2005, Lopes *et al.* 2006, Davies *et al.* 2008]. This

mono-ubiquitin moiety can then be extended to a K63-linked poly-ubiquitin chain by the Rad5-Mms2-Ubc13 complex [Hoege *et al.* 2002]. The length of this ubiquitin chain plays a crucial role in determining which of the two PRR pathways is activated. Mono-ubiquitin facilitates the error-prone pathway for lesion bypass dependent on translesion polymerase activity [Hoege *et al.* 2002, Stelter and Ulrich 2003, Garg and Burgers 2005, Freudenthal *et al.* 2010]. Alternatively, poly-ubiquitin chains enable the error-free template switching pathway [Branzei 2011]. This extremely satisfying result finally put into place the activities of the various genes, which had for a quarter of a century been implicated in the *RAD6* epistasis group and PRR without a clear mechanistic understanding of how they functioned.

As mentioned earlier, K164 was identified as the attachment site for both ubiquitin and SUMO. This added a layer of complexity to our understanding of PRR regulation [Hoege *et al.* 2002]. Unlike ubiquitination, sumoylation occurs in the absence of DNA damage and inhibits illegitimate recombination between nascent sister chromatids. This is executed by recruiting the helicase/anti-recombinase suppressor of rad six 2 (Srs2) [Papouli *et al.* 2005, Pfander *et al.* 2005]. Srs2 inhibits recombination at replication forks by disrupting the formation of Rad51 nucleoprotein filaments that are necessary for strand invasion, a key step in homologous recombination (HR). The default suppression of HR during normal replication ultimately prevents formation of undesirable recombination intermediates between the two nascent strands [Krejci *et al.* 2003, Veaute *et al.* 2003].

The identification of PCNA ubiquitination as a mediator of PRR also offered a second physical marker (besides RPA-ssDNA) for replication stress. Until this point, I have described PRR exclusively as a mechanism for the tolerance of physical damage to the DNA in the form of UV-induced lesions or chemically-induced alkyl adducts. However, it became apparent that certain mutations in replication factors, which impair their function, cause constitutive PRR activation in the absence of exogenous DNA damage [Northam *et al.* 2006, Becker *et al.* 2014, Becker *et al.* 2015]. This was first described by the Shcherbakova laboratory, which reported hypomorphic mutants for Pol-α, Pol-ε, and Pol-δ triggering constitutive ubiquitination of PCNA and activation of PRR [Northam *et al.* 2006]. Later work in other laboratories and work contained in this dissertation reported similar results in additional polymerase and non-polymerase replication mutants [Karras and Jentsch 2010, Becker *et al.* 2014, Becker *et al.* 2015].

Ubiquitination at residues different from K164 has also been reported in response to specific forms of replication stress, initially by our laboratory and later by other groups [Das-Bradoo *et al.* 2010, Das-Bradoo *et al.* 2010, Povlsen *et al.* 2012, Nguyen *et al.* 2013, Elia *et al.* 2015]. There is some indication that alternate sites of ubiquitination coordinate non-PRR pathways, but the details are poorly understood [Das-Bradoo *et al.* 2010]. In particular, yeast cells deficient for DNA ligase I exhibit ubiquitination of PCNA at K107 [Das-Bradoo *et al.* 2010]. This modification is essential for the viability of ligase mutants and appears to

coordinate a Rad59-dependent rescue pathway independently of PRR [Nguyen *et al.* 2013, Lee *et al.* 2014].

Genome stability and cancer

In the second edition of their comprehensive “Hallmarks of Cancer” review, Hanahan and Weinberg included genome instability and mutation as the most prominent enabling characteristics of cancer [Hanahan and Weinberg 2011]. In general, this refers to the acquisition of mutations and genomic rearrangements, which impair the function of checkpoint and repair pathways, inactivate tumor suppressors, or activate oncogenes. We now know that the vast majority of mutations and genomic rearrangements occurs during S phase and results from defects in replication, repair, or checkpoint activation [Myung *et al.* 2001, Kolodner *et al.* 2002]. As such, the integrity of these pathways is imperative for the maintenance of genome stability and acts a critical anti-cancer barrier.

This point is best illustrated by the clinical predisposition to cancer in patients with germline mutations that impair the function of replication or repair genes [Jackson and Bartek 2009, Zeman and Cimprich 2014]. These include components of PRR, such as the translesion polymerase Pol-η. Pol-η specializes in the bypass of thymidine dimers resulting from UV damage to DNA. Bulky lesions cannot be replicated by Pol-ε and Pol-δ [Prakash *et al.* 2005], leading to the formation of RPA-ssDNA structures and subsequent ubiquitination of PCNA [Lopes *et al.* 2006, Davies *et al.* 2008]. This facilitates the recruitment of Pol-η to

bypass the UV lesion [Watanabe *et al.* 2004]. Patients with inherited mutations that inactivate Pol-η suffer from a disorder known as *Xeroderma Pigmentosum* (XP) that renders them highly sensitive to UV light [Masutani *et al.* 1999]. When the skin of XP patients is exposed to sunlight it results in painful sores and a dramatic increase in the incidence of skin cancers [Cleaver 2005].

In addition to inherited mutations, early tumorigenic events are also thought to put stress on DNA replication and repair pathways, thereby promoting cancer progression [Bartkova *et al.* 2005]. In these cases, it is more difficult to assess whether a specific mutation played a role as a "driver" in cancer development. Due to the prominence of genome instability and mutation in carcinogenesis, such clinical specimens typically have a high mutation load and determining the stage at which each occurred is often not possible after the fact [Kolodner *et al.* 2002]. However, recapitulating mutations of interest in model organisms can be informative in learning whether they have the potential to drive tumorigenesis. One such example is FEN1, the human homolog of the yeast gene *RAD27* which, as described earlier, cleaves 5' flaps that are generated during lagging strand replication [Hubscher and Seo 2001]. Mutations that impair the catalytic function of FEN1 were observed in a wide variety of cancers, and subsequently recapitulated in mouse models to establish their potential to promote cancer formation [Zheng *et al.* 2007, Larsen *et al.* 2008].

We now appreciate genome instability to be a unifying characteristic of most human cancers [Hanahan and Weinberg 2011]. The high level of evolutionary

conservation in replication and checkpoint pathway components has made *S. cerevisiae* particularly useful in characterizing this relationship [Kolodner *et al.* 2002]. While recent advances in genome engineering with the CRISPR-Cas9 system have drastically reduced the time requirement and complexity of addressing targeted genetic questions in human cells, the genetic malleability and speed of yeast research remains unparalleled [Ran *et al.* 2013].

Rationale

Replication stress is a prominent contributor to genome instability and mutation, both enabling characteristics of cancer. Over the past half-century we have come to understand PRR as a crucial mechanism by which cells minimize the negative impact of replication stress and promote the timely completion of S phase. The subject of this dissertation has been to better understand the cellular conditions that lead to a requirement for PRR in the absence of exogenous DNA damage. A clearer picture for the genetic conditions under which PRR is required holds the potential to identify unique cancer vulnerabilities that could be explored as novel targets for cancer therapy. The studies presented herein have served to build a better understanding of PRR as a potential therapeutic target as well as an anti-cancer barrier.

Figure 1.1

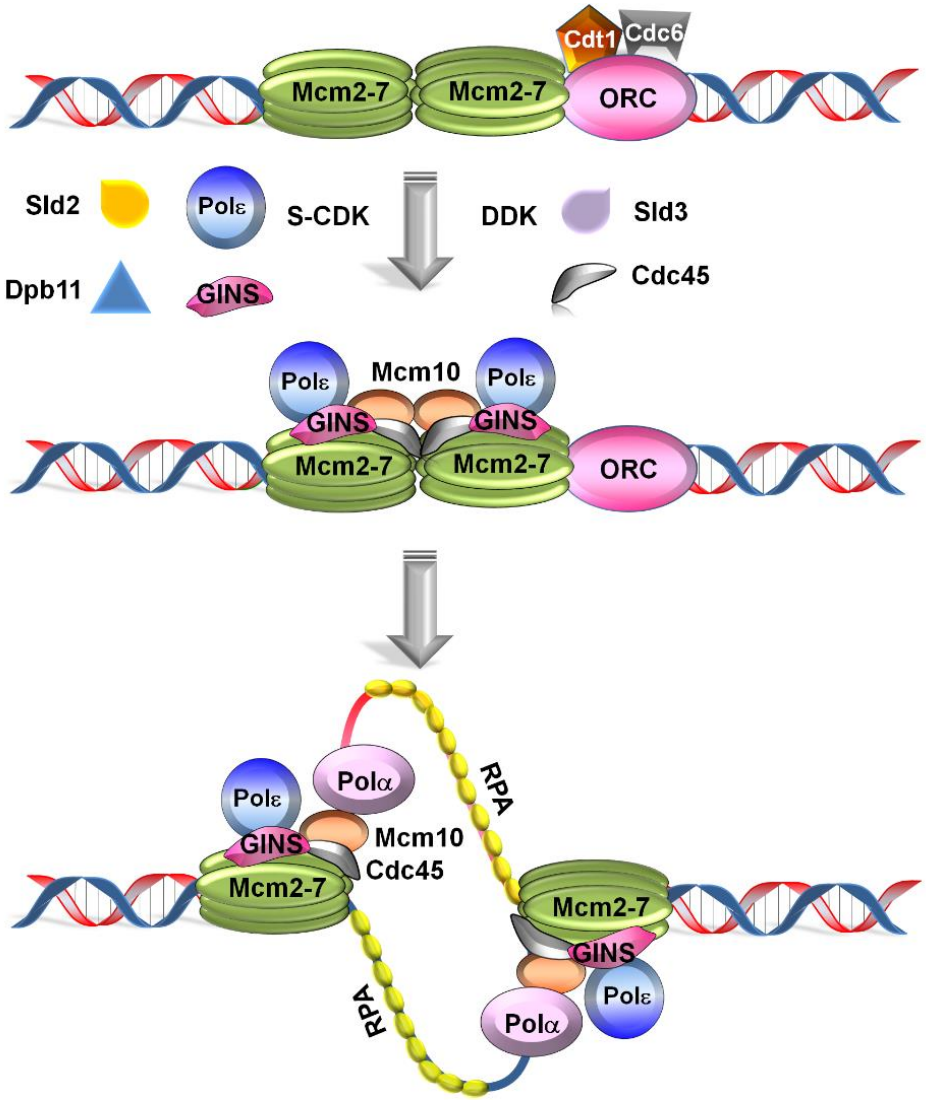
Cdt1
Cdc6
Mcm2-7
Mcm2-7
ORC
Sld2
Polε
S-CDK
DDK
Sld3
Dpb11
GINS
Cdc45
Polε
Mcm10
Polε
GINS
GINS
Mcm2-7
Mcm2-7
ORC
Polα
Polε
RPA
GINS
Mcm10
Cdc45
Mcm2-7
Mcm2-7
GINS
Polε
Polα
RPA

Figure 1.1. Origin licensing and activation. ORC binds origins and recruits Cdt1, Cdc6 and Mcm2-7, forming the pre-RC and "licensing" the origin (top panel). DDK phosphorylation of Mcm4 and Mcm6 recruits Cdc45 and Sld3. This is followed by the formation and recruitment of the pre-LC, composed of Dpb11, Pol-ε, Sld2, and GINS in an S-CDK dependent manner. This completes pre-IC formation (middle panel). Recruitment of Mcm10, Pol-α, and RPA then enables DNA unwinding and origin firing, beginning DNA synthesis (bottom panel). This figure was adapted from Thu and Bielinksy, 2014 [Thu and Bielinsky 2014].

Figure 1.2

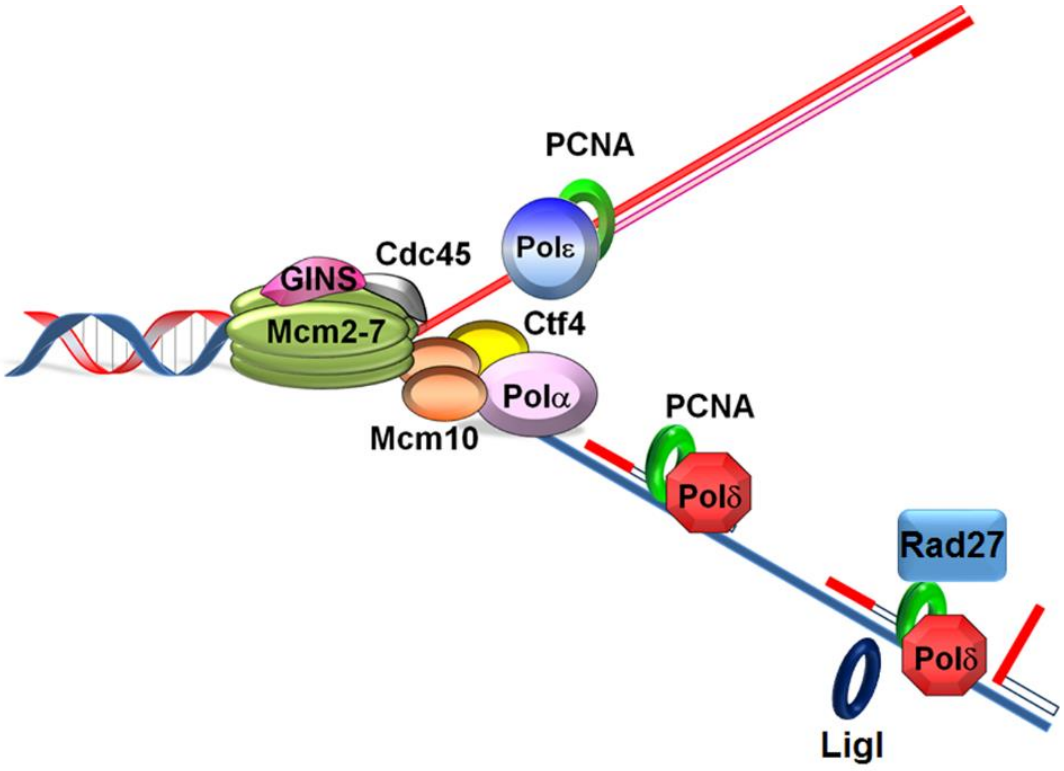
PCNA
Cdc45
GINS
Polε
Mcm2-7
Ctf4
Polα
Mcm10
PCNA
Polδ
Rad27
Polδ
LigI

Figure 1.2. The eukaryotic replication fork. The mechanism of DNA replication is semiconservative and antiparallel in nature. The leading strand (top) is replicated in the same direction as helicase unwinding and occurs in a more or less continuous manner. Lagging strand replication (bottom) moves in the opposite direction of helicase unwinding and therefore must be constantly re-primed (Mcm10, Ctf4, and Pol-α) as the helicase unspools new regions of template strand. These discontinuous segments are referred to as Okazaki fragments and are synthesized by Pol-δ. Following synthesis, each fragment is processed and ligated to the adjacent fragment by the combined activities of Pol-δ, Rad27 and DNA ligase I (LigI). Adapted from Thu and Bielinsky, 2014 [Thu and Bielinsky 2014].

Figure 1.3

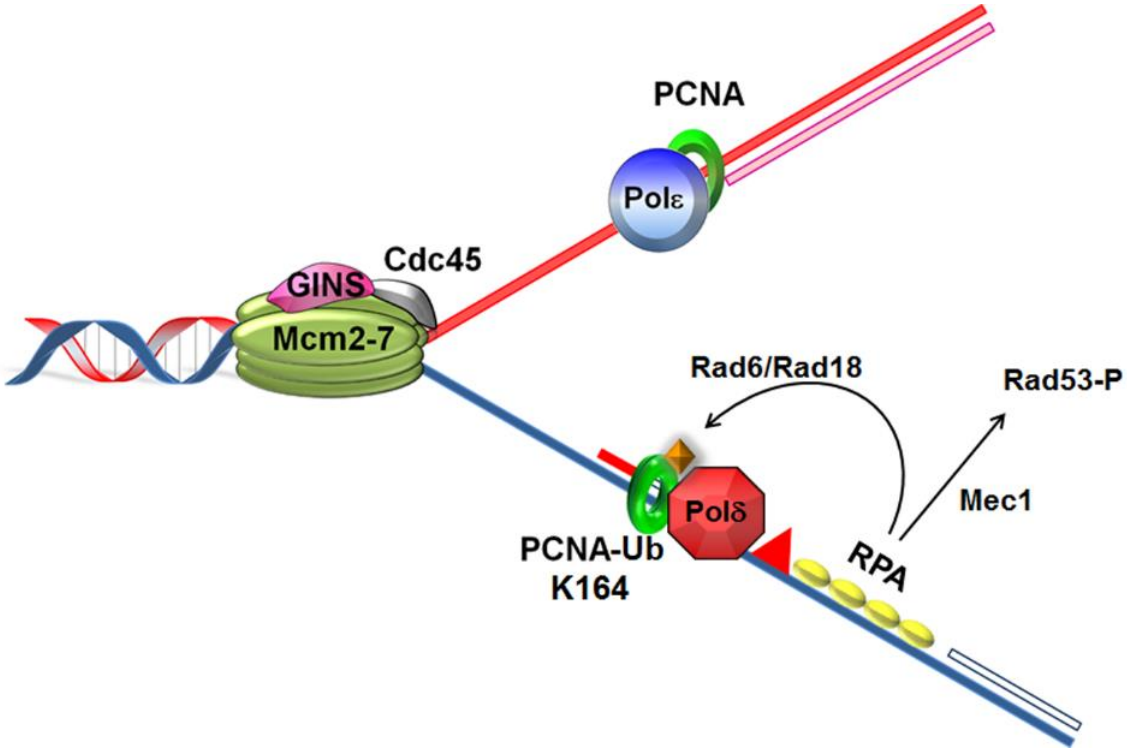
PCNA
Polε
Cdc45
GINS
Mcm2-7
Rad6/Rad18
Rad53-P
Mec1
Polδ
PCNA-Ub
K164
RPA

Figure 1.3. The eukaryotic replication stress response. In response to DNA damage or replication stress (symbolized by the red triangle) that leads to the formation of RPA-coated ssDNA there are two critical responses that act in parallel. One is activation of the checkpoint kinase Rad53 by the ATR homolog Mec1, which serves to initiate the S phase checkpoint. The other is recruitment of the Rad6-Rad18 ubiquitination complex to ubiquitinate (orange diamond) PCNA at K164 and trigger activation of PRR (see Figure 1.1). Adapted from Thu and Bielinsky, 2014 [Thu and Bielinsky 2014].

Figure 1.4

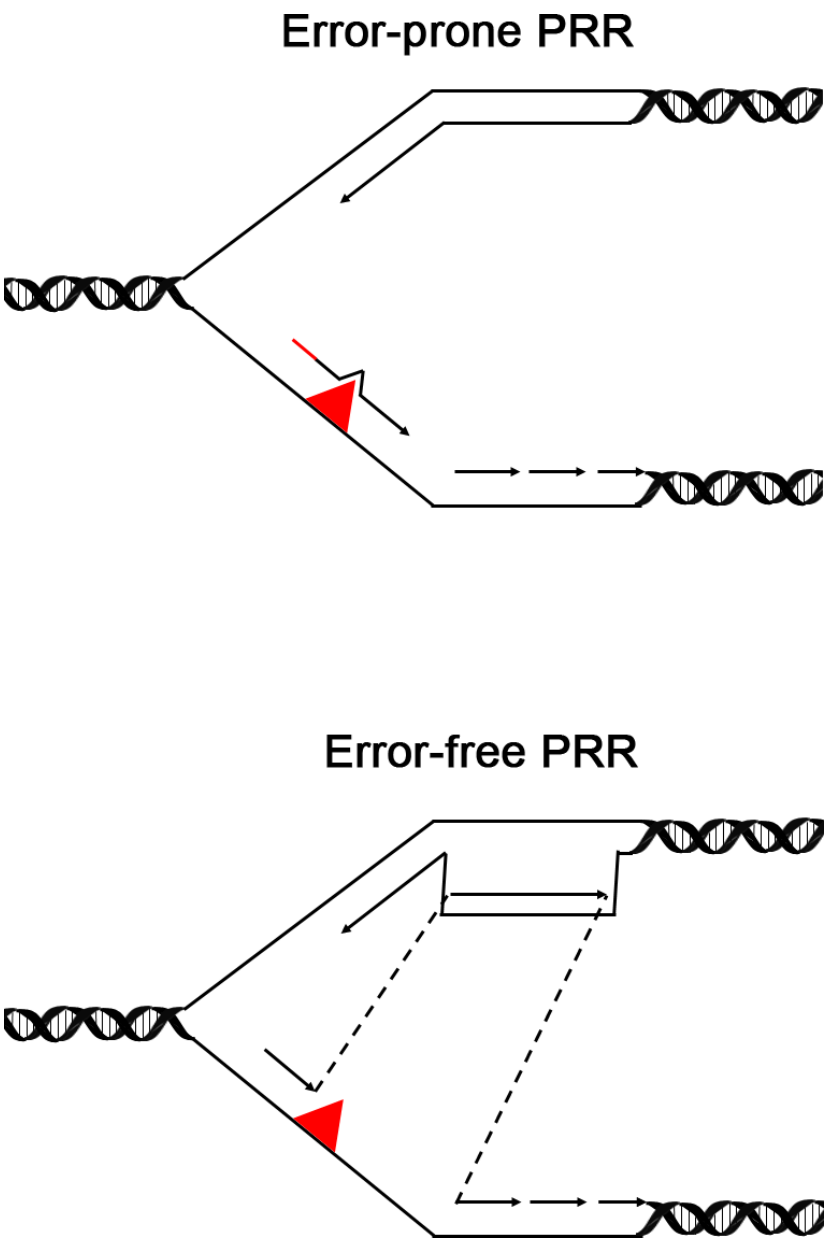

Figure 1.4. Postreplicative repair pathways. Lesions in template strand DNA (red triangle) lead to PCNA-K164 ubiquitination and activation of PRR pathways to facilitate damage bypass. Error-prone PRR (top) utilizes mutagenic translesion polymerases to replicate past lesions, incurring mutations to avoid the greater risk that is replication stalling and fork breakage. In error-free PRR (bottom) the nascent strand of the undamaged sister chromatid is used as a template to replicate past the lesion before re-annealing to the original damaged template.

CHAPTER 2

Mcm10 deficiency causes defective-replisome-induced mutagenesis and a dependency on error-free postreplicative repair

(The work in this chapter was published in Becker, J.R., Nguyen, H.D., Wang X., and Bielinsky, A.K. (2014) *Cell Cycle* 1;13(11):1737-48. PMID: 24674891)

Author contributions:

Experiments were designed by J.R.B., H.D.N., and A.K.B and performed by J.R.B. with assistance from X.W. The data was analyzed and prepared for publication by J.R.B. and A.K.B.

Mcm10 is a multifunctional replication factor with reported roles in origin activation, polymerase loading, and replication fork progression. The literature supporting these variable roles is controversial and it has been debated whether Mcm10 has an active role in elongation. Here, we provide evidence that the *mcm10-1* allele confers alterations in DNA synthesis that lead to defective-replisome-induced mutagenesis (DRIM). Specifically, we observed that *mcm10-1* cells exhibited elevated levels of PCNA ubiquitination and activation of the translesion polymerase, pol-ζ. Whereas translesion synthesis had no measurable impact on viability, *mcm10-1* mutants also engaged in error-free PRR, and this pathway promoted survival at semi-permissive conditions. Replication gaps in *mcm10-1* were likely caused by elongation defects, as *dbf4-1* mutants, which are compromised for origin activation did not display any hallmarks of replication stress. Furthermore, we demonstrate that deficiencies in priming, induced by a *pol1-1* mutation, also resulted in DRIM, but not in error-free PRR. Similar to *mcm10-1* mutants, DRIM did not rescue the replication defect in *pol1-1* cells. Thus, it appears that DRIM is not proficient to fill replication gaps in *pol1-1* and *mcm10-1* mutants. Moreover, the ability to correctly prime nascent DNA may be a crucial prerequisite to initiate error-free PRR.

INTRODUCTION

Timely and accurate replication of the genome is critical for the long-term health and viability of eukaryotic organisms and their offspring. Accomplishing this task requires the precise orchestration of a multitude of enzymatic and non-enzymatic factors. Errors in this process can cause mutations and genomic rearrangements, which are both hallmarks of cancer [Hanahan and Weinberg 2011]. In particular, defects in replication genes are a contributing source of errors that can engender genome instability [Myung *et al.* 2001]. A detailed mechanistic knowledge of how DNA replication is regulated and how cells counteract replication stress is thus intimately linked to our understanding of carcinogenesis.

At the center of both normal DNA replication and the response to replication stress is the homotrimeric clamp, proliferating cell nuclear antigen (PCNA). PCNA is loaded onto primed template DNA and – spatially and temporally – coordinates the action of a multitude of proteins involved in DNA polymerization and nascent DNA processing [Moldovan *et al.* 2007]. During normal replication, PCNA binds the replicative polymerases, pol-ε and pol-δ, to facilitate leading and lagging strand synthesis, respectively, acting as a processivity factor to promote efficient replication [Burgers 2009]. When these processive DNA polymerases encounter bulky lesions in the template strand that they are unable to bypass, they will stall, leaving regions of unreplicated single-stranded (ss)DNA [Lopes *et al.* 2006]. This ssDNA rapidly becomes coated with replication protein A (RPA), which facilitates the recruitment of the E2-E3 ubiquitination complex Rad6-Rad18 to catalyze the

transfer of mono-ubiquitin onto lysine (K)164 of PCNA [Hoege *et al.* 2002, Davies *et al.* 2008]. Mono-ubiquitination at K164 can subsequently be extended to a K63-linked poly-ubiquitin chain by Mms2-Ubc13-Rad5. Mono- *versus* poly-ubiquitination of PCNA-K164 plays a crucial role in determining the downstream pathway that will be activated to bypass the lesion. Poly-ubiquitination promotes error-free postreplication repair (PRR) by template switching, whereas mono-ubiquitination is necessary for the activation of specialized translesion synthesis (TLS) polymerases that temporarily replace the processive replicative polymerases, albeit at the cost of an elevated intrinsic error rate [Branzei and Foiani 2010, Branzei 2011]. Higher eukaryotes possess a wide variety of TLS polymerases, however, yeast expresses only Rev1, pol-ζ (composed of Rev3 and Rev7) and pol-η (Rad30) [Prakash *et al.* 2005]. Pol-ζ is responsible for nearly all subsequent replication-generated mutations induced by treatment with DNA-damaging agents *in vivo* [Prakash *et al.* 2005]. Pol-ζ works in conjunction with pol-η to bypass UV light-induced pyrimidine dimers and has a structural requirement for Rev1 in TLS [Waters *et al.* 2009]. Thus, loss of pol-ζ leads to an almost complete reduction in the mutational load accrued in response to DNA damage [Prakash *et al.* 2005]. Although originally described as a response to obstructive template strand lesions, PCNA ubiquitination and TLS by pol-ζ have more recently been implicated in the response to non-template-altering sources of replication stress [Northam *et al.* 2006, Northam *et al.* 2010]. In an elegant set of genetic experiments, Northam and co-workers showed that replication impediments,

including hydroxyurea (HU), as well as defective copies of pol-α, -δ and -ε induce pol-ζ synthesis independently of DNA damage [Northam *et al.* 2006, Northam *et al.* 2010]. This phenomenon, termed defective-replisome-induced mutagenesis (DRIM), occurs on undamaged template DNA, but nonetheless results in PCNA-K164 ubiquitination and a pol-ζ–dependent elevation of the mutation rate.

PCNA ubiquitination and DRIM occur in a *pol1* mutant that exhibits abnormal priming [Suzuki *et al.* 2009]. It is notable that priming must take place every 100-200 base pairs along the lagging strand template to initiate the synthesis of a new Okazaki fragment, making its accuracy and regulation critical to successful replication [Burgers 2009]. Unlike Pol1, Mcm10 is a non-catalytic scaffold protein that has been implicated in multiple steps during DNA replication [Thu and Bielinsky 2013]. Early work analyzing Mcm10 in *Xenopus* egg extract indicated that it was recruited to replication origins after licensing and required for DNA unwinding [Wohlschlegel *et al.* 2002]. Additional reports in yeast have shed light on the mechanistic role of Mcm10 in replication complex assembly and helicase activation [Heller *et al.* 2011, Kanke *et al.* 2012, van Deursen *et al.* 2012, Watase *et al.* 2012]. These studies came to the conclusion that Mcm10 is essential to activate the unwinding of DNA duplexes at origins by the Cdc45-Mcm2-7-GINS (CMG) helicase complex. It remains unclear whether Mcm10 acts as a *bona fide* helicase activator or is simply needed by its virtue of stabilizing ssDNA.

In addition to origin unwinding, multiple laboratories in various model systems have demonstrated that Mcm10 binds the catalytic subunit of pol-α, Pol1,

and facilitates its chromatin association [Fien *et al.* 2004, Ricke and Bielinsky 2004, Yang *et al.* 2005, Ricke and Bielinsky 2006, Chattopadhyay and Bielinsky 2007, Zhu *et al.* 2007, Warren *et al.* 2009, Haworth *et al.* 2010, Lee *et al.* 2010, Robertson *et al.* 2010]. Moreover, Mcm10 is post-transcriptionally modified during G1 and S phase, resulting in non-proteolytic ubiquitination at two distinct lysines. This modification is a prerequisite for Mcm10's interaction with PCNA, which is essential for cell proliferation [Das-Bradoo *et al.* 2006]. In addition, Mcm10 travels with the replication fork, pointing to a function in DNA elongation [Ricke and Bielinsky 2004, Pacek *et al.* 2006, Raveendranathan *et al.* 2006, Taylor *et al.* 2011]. Although roles for Mcm10 in origin unwinding, elongation and pol-α regulation are not mutually exclusive, the notion that Mcm10 is part of the eukaryotic replisome is a matter of ongoing debate in the field [Kanke *et al.* 2012, van Deursen *et al.* 2012, Watase *et al.* 2012, Thu and Bielinsky 2013].

Here, we exploited the fact that PCNA ubiquitination and DRIM can be utilized as a sensitive biological readout for the accumulation of ssDNA gaps. Consistent with a previous report, we detected both ubiquitination of PCNA and DRIM in *pol1-1* cells [Northam *et al.* 2006]. In support of a role for Mcm10 in DNA synthesis, we also detected these two diagnostic markers in *mcm10-1*, but not *dbf4-1* mutants known to be compromised in origin firing similarly to *mcm10-1* cells [Zou and Stillman 2000, Varrin *et al.* 2005]. Interestingly, *mcm10-1* – but not *pol1-1* – engaged in error-free PRR to promote completion of DNA replication and cell survival. Together, these results argue that reduced origin activation is unlikely to

trigger gap formation in the genome of budding yeast. We propose that defective priming in *pol1-1* and *mcm10-1* leads to ubiquitination of PCNA and DRIM. Moreover, wild-type priming activity appears to be required to initiate template switch events.

RESULTS

Mutants defective in Mcm10 exhibit PCNA ubiquitination

Translesion polymerases are not only required to bypass DNA lesions, but also act in response to intrinsic defects of the replicative polymerases, pol-α, -δ and -ε.[Northam *et al.* 2006, Northam *et al.* 2010] Specifically, the *pol1-L868F* mutant, which has a higher rate of nucleotide misincorporation than the wild-type enzyme and therefore produces mismatched primers that are unsuitable for extension by pol-δ, displays constitutive PCNA ubiquitination [Suzuki *et al.* 2009]. We addressed whether other types of defects in pol-α or pol-α-associated proteins, such as Mcm10, have a similar effect. We examined two different temperature-sensitive mutations, *pol1-1* and *mcm10-1*. The former is a G493R substitution in the N-terminus that does not alter the active site nor the expression level of Pol1 [Lucchini *et al.* 1988, Pizzagalli *et al.* 1988, Lucchini *et al.* 1990]. However, the mutated protein no longer assembles into a stable pol-α/primase complex, which almost certainly affects the catalytic rate of RNA/DNA primer synthesis [Lucchini *et al.* 1988]. In addition, it has been proposed that the positive charge interferes with chromatin association, and independent evidence supports

that the enzyme is prone to replication slippage [Schweitzer and Livingston 1998, Gutiérrez and Wang 2003]. All of these effects are more pronounced at non-permissive conditions, under which cells arrest in mid-to-late S phase (Figure 2.1). The P269L mutation in *mcm10-1*, on the other hand, confers lower steady-state protein levels than wild-type under permissive conditions and these further diminish at elevated temperatures [Merchant *et al.* 1997, Sawyer *et al.* 2004]. We monitored the status of PCNA ubiquitination in *pol1-1*, *mcm10-1*, and their respective parental wild-type strains at permissive and various elevated temperatures (Figure 2.2). Whereas *pol1-1* mutants exhibited constitutive PCNA ubiquitination (Figure 2.2A), the modification was first induced at semi-permissive conditions in *mcm10-1* cells (Figure 2.2B). To ascertain that PCNA ubiquitination was triggered by the loss of Mcm10, we complemented the *mcm10-1* strain with a wild-type *MCM10* transgene under the control of its endogenous promoter. Expression of the transgene alleviated PCNA ubiquitination at 35°C (Figure 2.2C) and complemented the temperature-sensitive growth of the mutant (Figure 2.2D). Since ubiquitination of PCNA is diagnostic for replication stress that interferes with normal elongation, these results suggest that both the *pol1-1* and *mcm10-1* mutations result in aberrant DNA synthesis and ssDNA gaps.

To further corroborate this notion, we determined whether ubiquitin was attached to K164. To this end, we generated double mutants that expressed His_6-tagged PCNA that was either wild-type or carried a K164R substitution. Asynchronous cell cultures were shifted to 35°C for 3h and PCNA was purified

under denaturing conditions on Ni-NTA agarose [Ulrich 2009]. The eluates were then analyzed for ubiquitin and small ubiquitin-like modifier (SUMO). Sumoylation of PCNA occurs constitutively during S phase at K127 and K164 [Hoege *et al.* 2002]. Both *pol1-1* and *mcm10-1* mutants displayed mono- and poly-ubiquitination as well as mono- and poly-sumoylation (Figure 2.3A and B). The K164R substitution in PCNA eliminated most of these modifications, except for mono-sumoylation at K127, a known alternate sumoylation site to K164 [Hoege *et al.* 2002]. To ensure that the mutants used in these experiments behaved in a manner consistent with previous reports, we treated *mcm10-1* and *mcm10-1 pol30-K164* mutants with methyl methanesulfonate (MMS) at room temperature, demonstrating that K164-specific ubiquitin attachment can be observed in these strains (Figure 2.3B) [Hoege *et al.* 2002]. When we shifted *mcm10-1 pol30-K164R* double mutants to 35°C, ubiquitination was slightly reduced, but we consistently observed measurable mono- and poly-ubiquitination, raising the possibility that alternate lysine residues are targeted for ubiquitin conjugation in this mutant (Figure 2.3B) [Das-Bradoo *et al.* 2010, Das-Bradoo *et al.* 2010, Nguyen *et al.* 2013]. To verify that the *pol30* mutations conferred the expected DNA damage sensitivity in the *mcm10-1* background, we exposed *mcm10-1 pol30* double and triple mutants to UV light. Consistent with previous reports, the *pol30-K164R* mutation rendered cells UV-sensitive. This sensitivity was partially alleviated in the *pol30-KK127/164RR* mutant (Figure 2.4) [Hoege *et al.* 2002, Stelter and Ulrich 2003]. In summary, these pull down experiments unequivocally identify PCNA-

K164 as the target site for ubiquitination in *pol1-1* mutants. Furthermore, they independently confirm the presence of ubiquitinated PCNA in *mcm10-1* cells, albeit ubiquitin conjugation does not occur exclusively at K164.

Spontaneous mutations in *mcm10-1* cells are dependent on K164 of PCNA and the translesion polymerase genes *REV1* and *REV3*

Since the biochemical data for *mcm10-1* remained ambiguous with respect to the site of ubiquitin attachment on PCNA, we explored this issue genetically. To validate that PCNA-K164 played a functional role in both *pol1-1* and *mcm10-1* strains, we determined whether it had any effect on their respective spontaneous mutation rates. To this end, we quantified the frequency of canavanine resistance by a standard fluctuation analysis at semi-permissive growth conditions. For *pol1-1*, the mutation rate was elevated ~15-fold over wild-type controls (Figure 2.5A). Interestingly, a K164R substitution in PCNA reduced this mutation rate approximately 4-fold, but did not decrease it to wild-type levels. This is consistent with a previous report that suggested that the replication fidelity of Pol1-1-containing pol-α/primase complexes is lower than that of its wild-type counterpart [Gutiérrez and Wang 2003, Northam *et al.* 2006]. This would result in mutations that are independent of K164, due to an intrinsic catalytic dysfunction as observed in Figure 2.5A. In contrast, spontaneous mutations in *mcm10-1* cells were exclusively dependent on K164 of PCNA (Figure 2.5B). Furthermore, the K164-dependent mutation rate was very similar between the *pol1-1* and *mcm10-1*

strains. These results strongly suggested that *mcm10-1* mutants ubiquitinated PCNA at K164, and that DRIM was the primary source of the measured mutagenic events. To address this issue experimentally, we deleted *REV1*, *REV3* and *RAD30*, respectively, in both *pol1-1* and *mcm10-1* cells. Loss of either Rev1 or Rev3 had a comparable effect to that caused by the K164R substitution in PCNA (compare Figure 2.5A to Figure 2.6A, and 2.5B to 2.6B), whereas ablation of *RAD30* triggered no significant alterations. These results are in agreement with the fact that Rev3 and its accessory subunit Rev7 are exchanged with the catalytic subunit of pol-δ to form a chimeric translesion polymerase complex known as pol-ζ, which works in conjunction with Rev1 [Prakash *et al.* 2005, Baranovskiy *et al.* 2012, Makarova *et al.* 2012]. Unlike pol-ζ, Rad30 specifically promotes UV-induced DNA damage tolerance (DDT), but has not been implicated in DRIM [Northam *et al.* 2010]. To exclude the possibility that Rad30 was not active in the *pol1-1* and *mcm10-1* strains, we exposed cells to UV light and measured the resulting mutation frequencies. Both strains showed a significant increase in UV-induced mutations (Figure 2.7). Consistent with the results shown in Figures 3 and 4, *pol1-1* cells displayed a higher frequency of mutagenesis than *mcm10-1* mutants relative to their corresponding wild-type strains (Figure 2.7A). *mcm10-1* cells exhibited the same relative increase in UV-induced mutagenesis as wild-type controls (Figure 2.7B), whereas this was not the case for *pol1-1* mutants (Figure 2.7A). The underlying reason is unknown. Nevertheless, these findings argue that neither the *pol1-1* nor the *mcm10-1* mutation compromises TLS in response to UV

irradiation. This suggests that despite not being involved in spontaneous mutagenesis (Figures 2.6A and 2.6B), Rad30 is not otherwise disabled, confirming that only Rev1 and pol-ζ are participating in DRIM.

RAD5 and *POL30-K164* but not *REV3* suppress *mcm10-1* temperature sensitivity

Our finding that PCNA is ubiquitinated at K164 in *pol1-1* and *mcm10-1* and facilitates pol-ζ dependent DRIM led us to examine the importance of PCNA-K164 for cell viability. Interestingly, we found that *mcm10-1 pol30-K164R* double mutants showed an approximately 10-fold growth defect at 33°C in comparison to the *mcm10-1* single mutant (Figure 2.8A). In contrast, *pol1-1 pol30-K164R* double mutants exhibited no enhanced growth defect at any of the temperatures analyzed (Figure 2.8A). As previously indicated, mono- and poly-ubiquitination of PCNA at K164 are known to facilitate distinct PRR pathways, and thus we dissected the relative contribution of each of these pathways in promoting survival of *mcm10-1* cells [Branzei and Foiani 2010]. Because we had previously observed that deletion of *REV3* was sufficient to abrogate DRIM (Figure 2.6B), we generated a *mcm10-1 rev3Δ* double mutant. To disable the error-free branch of PRR we combined *mcm10-1* with *rad5Δ*. Finally, to inhibit both pathways, we created *mcm10-1 rad5Δ rev3Δ* triple mutants. Whereas deletion of *REV3* did not have any effect at the temperatures examined, deletion of *RAD5* alone or in combination with *REV3* caused a 10-fold reduction in viability at 33°C (Figure 2.8B). This is consistent with

the 10-fold growth defect observed in *mcm10-1 pol30-K164* mutants (Figure 2.8A) and suggests that the *RAD5*-dependent error-free branch of PRR suppresses the temperature sensitivity of the *mcm10-1* strain. Importantly, the growth defects in *mcm10-1 pol30-K164R* and *mcm10-1 rad5Δ* mutants were rescued by expression of a wild-type *MCM10-2HA* transgene (Figure 2.8C). Similar to *pol1-1 pol30-K164R* cells (Figure 2.8A), neither *pol1-1 rev3Δ* double-, *pol1-1 rad5Δ* double-, nor *pol1-1 rad5Δ rev3Δ* triple mutants exhibited any growth alterations compared to the *pol1-1* parental strain (Figure 2.8B). These findings suggest that DRIM is not proficient to promote survival of *pol1-1* or *mcm10-1* strains. Additionally, there must be an intrinsic difference between these mutants in their ability to engage into *RAD5*-dependent PRR. Despite the fact that both *pol1-1* and *mcm10-1* exhibit poly-ubiquitin chains (Figure 2.3), the former do not efficiently utilize error-free PRR to complete replication.

PCNA ubiquitination in *mcm10-1* mutants is not the result of a defect in origin activation

Mcm10 has been implicated in the activation of the replicative helicase and its role in elongation has been disputed [Kanke *et al.* 2012, van Deursen *et al.* 2012, Watase *et al.* 2012, Thu and Bielinsky 2013]. Theoretically, it was therefore possible that defects in origin unwinding triggered PCNA ubiquitination in *mcm10-1* mutants in an indirect manner by increasing inter-origin distances and thus raising the overall probability of spontaneous fork arrest. To address this issue, we

analyzed the well-defined *dbf4-1* mutant [Zou and Stillman 2000]. Dbf4 is required for Cdc7-dependent phosphorylation of the Mcm 2, 4 and 6 subunits which enables the subsequent formation of the pre-initiation complex [Lei *et al.* 1997, Sheu and Stillman 2006, Sheu and Stillman 2010, Heller *et al.* 2011]. In addition it has been reported that Dbf4 may play a direct or indirect role in PRR [Pessoa-Brandão and Sclafani 2004, Harkins *et al.* 2009]. To ensure that disruption of Dbf4 did not inhibit ubiquitination of PCNA, we grew asynchronous cultures of *dbf4-1* cells for 3 h in the presence and absence of MMS, a known inducer of replication stress. When treated with MMS at 25°C or the semi-permissive temperature of 35°C, *dbf4-1* cells were able to efficiently ubiquitinate PCNA (Figure 2.9B). Importantly, this modification was not observed at 35°C in the absence of MMS despite a significant accumulation of cells in mid-to-late S phase (Figure 2.9A). Consistent with these findings, introduction of a *pol30-K164R* mutation had no effect on the temperature sensitivity of *dbf4*-1 cells (Figure 2.9C). The level of MMS-induced PCNA ubiquitination in *dbf4-1* cells at 35°C was slightly lower than that observed in wild-type (Figure 2.9B), likely because *dbf4-1* mutants arrested significantly earlier in S phase and therefore had fewer active replication forks (Figure 2.9A). In contrast, MMS-treated *mcm10-1* and wild-type cells exhibited similar levels of PCNA ubiquitination (Figure 2.9B). When shifted to 35°C in the absence of MMS, PCNA ubiquitination in *mcm10-1* was elevated to similar levels as those induced by MMS treatment (Figure 2.9B). Together, these data suggest that despite significant disruptions to cell cycle progression, and a severe S phase delay, defects in origin

activation do not lead to the formation of ssDNA gaps. This is further corroborated by the finding that *dbf4-1* cells grown at 35°C did not exhibit activation of the Rad53 checkpoint kinase, nor did they exhibit elevated levels of histone H2A phosphorylation at S129, both known Mec1 targets and markers of replication stress and DNA damage, respectively (Figure 2.9D) [Downs *et al.* 2000, Osborn and Elledge 2003]. In contrast, the *mcm10-1* mutation caused Rad53 hyperphosphorylation at 35°C. We did not detect any significant phosphorylation of histone H2A-S129 3h after temperature shift, arguing that Rad53 activation was not primarily due to double-strand breaks, but rather ssDNA regions. However, we detected histone H2A phosphorylation after prolonged exposure to semi-permissive conditions (Figure 2.10). These results support the conclusion that *mcm10-1* mutants form extended regions of ssDNA, whereas *dbf4-1* cells do not. Because it has been reported that Cdc7/Dbf4 acts upstream of Rad53, we included MMS treatment as a positive control to ascertain that *dbf4-1* mutants are capable of activating the intra-S-phase checkpoint (Figure 2.9D) [Zhong *et al.* 2013]. Lastly, the lack of PCNA ubiquitination in *dbf4-1* cells was also confirmed in experiments in which we arrested cells in G1 and released them synchronously into S phase at 35°C (Figure 2.11). In summary, we conclude that a defect in origin activation is unlikely to be the crucial trigger of PCNA ubiquitination in *mcm10-1* mutants.

DISCUSSION

Hypomorphic mutations in the DNA replication genes *POL1* and *MCM10* cause replication stress, which activates ubiquitination of PCNA at K164 and pol-ζ-dependent DRIM. Although DRIM has been described for strains defective in all three replicative polymerases, it has not been reported in the context of dysregulating scaffold proteins, such as Mcm10 [Northam *et al.* 2006, Northam *et al.* 2010]. Moreover, the biological impact of DRIM on cell viability had not been explored. Despite the fact that TLS is error-prone, it has a clear role in DNA damage resistance and contributes to cell growth under conditions of nucleotide shortage [Hoege *et al.* 2002, Lazzaro *et al.* 2012]. However, DRIM had no beneficial effect on cell survival in the *pol1-1* or *mcm10-1* strains, suggesting that it is not proficient to fill gaps, at least in these two mutants. This result is also consistent with the observation that half of the *pol1-1* population arrested in mid S phase and did not reach G2 (Figure 2.1). In contrast, *mcm10-1* mutants were able to engage in error-free PRR and arrested uniformly in G2 (Figure 2.9A). Our findings are in line with reports that argued that TLS is most active in late S/G2 phase, due to the cell cycle-specific upregulation of Rev1 and that error-free PRR has a predominant role earlier in S phase to facilitate completion of genome duplication [Branzei *et al.* 2004, Waters and Walker 2006, Hishida *et al.* 2009, Huang *et al.* 2013, Karras *et al.* 2013].

Our results further suggest that replication defects in *pol1-1* and *mcm10-1* mutants are leading to persistent regions of unreplicated ssDNA, which recruit the

E2-E3 ligase complexes, Rad6-Rad18 and Mms2-Ubc13-Rad5, to modify PCNA at K164 [Hoege *et al.* 2002, Davies *et al.* 2008]. How are these gaps generated? We envision that the two mutants are deficient in proper initiation of nascent DNA, leading to similar but not identical types of replication stress. The G493R missense mutation in *pol1-1* impairs pol-α/primase complex assembly [Pizzagalli *et al.* 1988]. This increases the probability for larger gaps, especially along the lagging strand template (Figure 2.12), and these activate the *RAD6* pathway, even in the absence of any DNA damaging agents [Karras and Jentsch 2010]. Moreover, the structural alterations caused by the *pol1-1* mutation negatively affect the fidelity of pol-α, resulting in increased levels of nucleotide misincorporation during primer synthesis. This was revealed by the finding that neither the K164R substitution in PCNA nor the deletion of *REV1* or *REV3* reduced the *pol1-1*-dependent mutation rate completely to wild-type levels (Figs. 2.5A and 2.6A). As a result, *pol1-1* mutants likely initiate Okazaki fragments much more infrequently than wild-type cells and with a higher propensity for mismatches. In fact, these mismatches might contribute to the formation of ssDNA gaps, as they are poor substrates for pol-δ [Haracska *et al.* 2001, Acharya *et al.* 2006]. It is tempting to speculate that pol-ζ is required in conjunction with Rev1 to extend synthesis from mismatched primers in *pol1-1*, especially since there is precedence for such a scenario from the study of a different *pol1* mutant (L868F) that has elevated levels of nucleotide misincorporation [Suzuki *et al.* 2009]. Therefore, DRIM might in fact be necessary for primer extension, but it may not work at a sufficiently high level during S phase

to rescue viability, which would explain why we did not detect any genetic interaction between *pol1-1* and *REV3* (Figure 2.8B).

Unlike Pol1, Mcm10 is a non-catalytic, multifunctional replication factor active at various steps of DNA replication [Thu and Bielinsky 2013]. The ubiquitination of PCNA (Figures 2.2 and 2.3) and activation of Rad53 (Figure 2.9D and Figure 2.10B) indicate the presence of persistent regions of ssDNA in *mcm10-1* cells that can be rescued by complementation with the wild-type gene. Mcm10 interacts with Pol1 and acts as a chromatin recruitment factor [Fien *et al.* 2004, Ricke and Bielinsky 2004, Yang *et al.* 2005, Das-Bradoo *et al.* 2006, Ricke and Bielinsky 2006, Chattopadhyay and Bielinsky 2007, Zhu *et al.* 2007, Warren *et al.* 2009, Haworth *et al.* 2010, Robertson *et al.* 2010]. Therefore, our data is consistent with the notion that inefficient chromatin assembly of pol-α/primase complexes in both *pol1-1* and *mcm10-1* mutants may be responsible for the impairment of DNA synthesis, which triggers DRIM. However, we cannot exclude that Mcm10 depletion interferes with DNA synthesis in a manner unrelated to priming. Nevertheless, in *mcm10-1* mutants, all pol-α/primase complexes that are brought to chromatin have wild-type function. In our view, this is a critical difference between the two mutants and provides a rationale for the finding that *mcm10-1* cells were able to engage in error-free PRR, whereas *pol1-1* cells did not appear to utilize this pathway efficiently (Figure 2.8A and B). Primer elongation in *mcm10-1* should not require pol-ζ, but could simply be carried out by pol-δ (Figure 2.12). We propose that longer nascent DNA strands in *mcm10-1* mutants are proficient

for Rad5-dependent template switching, which facilitates gap filling. It is not immediately obvious why gap filling requires Rad5 in the absence of DNA damage, and not just pol-δ. It is possible that error-free PRR is necessary in specific regions of the genome or at particularly large gaps. Moreover, we cannot exclude the possibility that Mcm10 may have a role during replication fork restart and that this function leads to an increase in the half-life of ssDNA at stalled forks. Although we consider this scenario unlikely, we cannot formally exclude it.

Lastly, Mcm10's proposed role in stimulating origin unwinding led us to consider the possibility that PCNA ubiquitination in *pol1-1* and *mcm10-1* cells may not be the result of a common defect in priming [Kanke *et al.* 2012, van Deursen *et al.* 2012, Watase *et al.* 2012, Thu and Bielinsky 2013]. Less efficient origin firing in *mcm10-1* mutants may increase the likelihood of incomplete replication. To address this issue, we compared the level of PCNA ubiquitination in *mcm10-1* and *dbf4-1* mutants. Our finding that *dbf4-1* mutants did not exhibit any sign of replication stress (Figures 2.9, 2.10 and 2.11), argues that defects in origin firing are probably not the trigger of PCNA ubiquitination in *mcm10-1*. However, the study of additional origin activation mutants is required to further substantiate this conclusion.

Taken together, our observations support a role for Mcm10 in the synthesis of nascent DNA fragments, possibly by regulating the turnover and/or chromatin association of Pol1 [Ricke and Bielinsky 2004, Zhu *et al.* 2007, Haworth *et al.* 2010, Lee *et al.* 2010]. Importantly, we also demonstrate that disruption of Mcm10

function leads to pol-ζ-dependent DRIM. This is particularly relevant to cancer biology because dysregulation of translesion polymerases is strongly associated with tumor formation [Jiyang *et al.* 2001, Lee *et al.* 2003, Yang *et al.* 2004, Albertella *et al.* 2005, Lee and Matsushita 2005, Sakiyama *et al.* 2005] and negative clinical outcomes [Lemée *et al.* 2010].

MATERIALS AND METHODS

Strains and plasmids

All strains are derived from W303-1a or SSL204 parental strains (Table 2.1). All *mcm10*-1 strains are isogenic derivatives of W303-1a, whereas all *pol1-1* strains are isogenic derivatives of SSL204. Strains carrying gene deletions (including *REV1, REV3*, *RAD30*, *RAD5, BAR1*, and *POL30*) were constructed by PCR-based gene disruption [Lorenz *et al.* 1995]. The deletions were subsequently confirmed by PCR and sequencing.

The expression vector pRS316-*MCM10*-2HA used for *mcm10-1* complementation was generated by insertion of *MCM10* and its endogenous promoter into the pRS316 backbone.

PCNA lysine mutants for the canavanine assays were generated using pCH1572 (a gift from L. Prakash, UTMB, USA). Fragments composed of PCNA, its endogenous promoter and a *LEU2* marker were amplified by PCR and integrated at the endogenous PCNA locus. Integration and clonal homogeneity were confirmed by PCR. PCNA mutations were confirmed by sequencing.

His_6-tagged PCNA strains were constructed using YIp128-P30-POL30wt (a gift from H.D. Ulrich, IMB Mainz, Germany). Lysine mutations were introduced using the QuikChange Lightning Site-Directed Mutagenesis Kit (Agilent Technologies). The plasmid was linearized by AflII (NEB) and integrated at the *LEU2* locus. Expression of His_6-tagged PCNA was confirmed by western blot analysis. Endogenous PCNA was knocked out by PCR-mediated gene disruption.

The *can1-100::CAN1(HIS1)* allele was generated by two-step gene replacement.[76] Briefly, DNA fragments containing wild-type *CAN1* and *HIS1* with complementary linker sequences were generated by PCR. Equal molar amounts of the two fragments were mixed, denatured at 95°C for 5 min and allowed to re-anneal at room temperature. The resulting mixture was transformed into yeast and integration was confirmed by PCR and sequencing.

Yeast culture conditions

All temperature shift experiments were carried out in yeast peptone dextrose (YPD). Asynchronous cultures were grown to OD_{600}=0.6 at 25°C before shifting to various temperatures. MMS was added immediately before the temperature shift where indicated. Strains carrying pRS316 or pRS316-*MCM10*-2HA were grown to OD_{600} = 0.6 in medium lacking uracil at 25°C and shifted to 35°C in pre-warmed YPD.

Ni-Purification of His_6-tagged PCNA

Cultures were grown to OD_{600} = 0.6 at 25°C and shifted to 35°C for 3 h before harvesting. His_6-tagged PCNA was purified from whole cell extracts prepared under denaturing conditions as described [Ulrich 2009]. Briefly, extracts were incubated overnight with Ni-NTA agarose beads (Qiagen) also under denaturing conditions. After binding, the His_6-tagged PCNA conjugated beads were washed with buffers of increasing stringency before elution into EDTA-containing loading buffer. Eluted proteins were fractionated by SDS-PAGE and analyzed by western blot.

Protein preparation and western blotting

Total protein extracts were obtained by trichloroacetic acid (TCA) precipitation and analyzed by western blot analysis [Ricke and Bielinsky 2006]. In all experiments, PCNA was detected using an anti-PCNA antibody (clone S871, a gift from B. Stillman, CSHL, NY). In pull-down experiments, His_6-tagged PCNA-ubiquitin conjugates were detected with an anti-ubiquitin antibody (P4D1, Covance) and His_6-tagged PCNA-SUMO conjugates were detected with an anti-SUMO antibody (a gift from X. Zhao, MSKCC, NY). Rad53 was detected using an anti-Rad53 antibody (a gift from JFX Diffley, LRI, UK). Phospho-histone H2A was detected using a phospho-S129 specific anti-histone H2A antibody (ab15083, Abcam). Tubulin served as loading control (MMS-407R, Covance).

Measurement of mutation rate and frequency

Measurement of the rate of forward mutations in *CAN1* was determined from at least 12 independent yeast cultures for each strain. Cultures were inoculated from single colonies and grown to stationary phase in YPD for 4 days at semi-permissive temperatures (30°C for *pol1-1* and 33°C for *mcm10-1*). Cells were then treated with 10 J/m^2 of UV before plating where indicated. After appropriate dilution, cells were plated on solid medium lacking arginine, but containing 60 mg/L canavanine to select for mutants and on YPD to obtain a viable cell count. Colonies were counted after 3-4 days of growth. Mutation rates and frequencies were calculated as described [Drake 1991, Foster 2006]. Significance was determined using the Mann-Whitney U test [Mann and Whitney 1947].

Cell cycle arrest and flow cytometry

For G1 arrest, cultures were grown to OD_{600} = 0.2 to 0.3 and α-factor was added to a final concentration of 150 ng/ml. Cultures were incubated with shaking for 2 h at 25°C and then shifted to 35°C for 1 h. To release cells from the G1 arrest, cultures were washed once in water and re-suspended in medium pre-warmed to 35°C with 0.1 mg/ml pronase (Sigma-Aldrich). DNA was stained for flow cytometry analysis with sytox green (Invitrogen). Cell cycle progression was monitored as described [Das-Bradoo *et al.* 2010]. All samples were analyzed using a Becton Dickinson FACSCalibur.

Figure 2.1

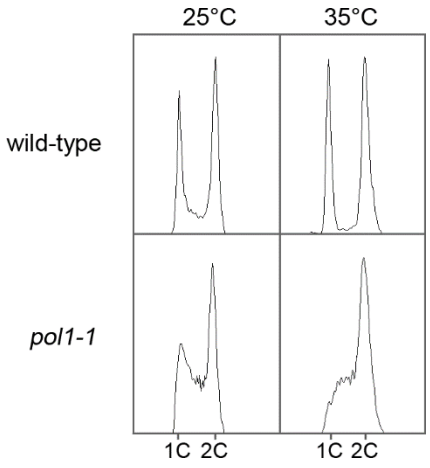

Figure 2.1. *pol1-1* mutants arrest in mid-to-late S phase at 35°C. Asynchronous cultures of *pol1-1* and wild-type parental cells were grown to OD_{600}=0.6 at 25°C. They were then split and incubated for 3 h at 25°C or 35°C as indicated.

Figure 2.2

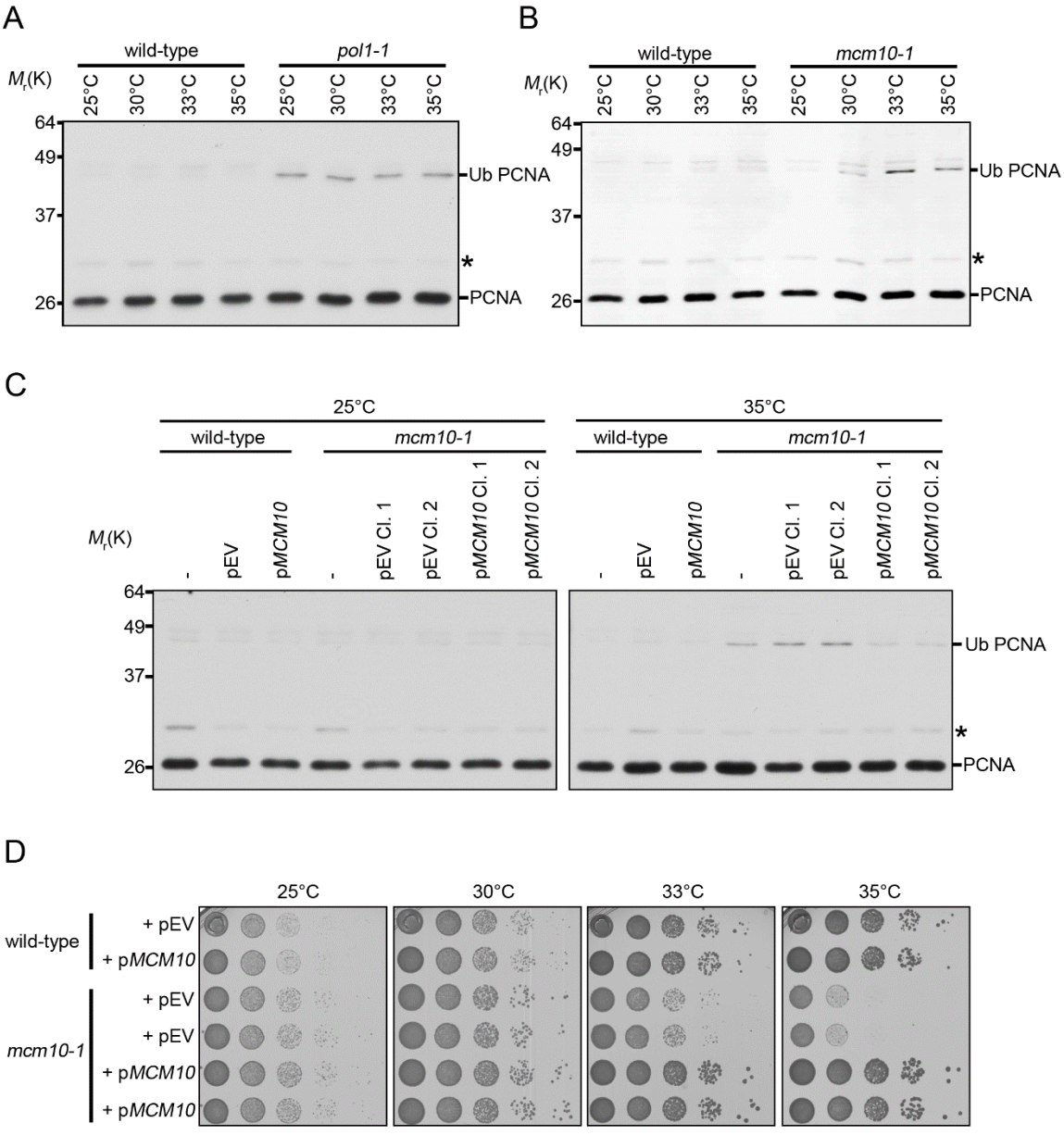
A
wild-type
pol1-1
M_r(K)
25°C
30°C
33°C
35°C
64
49
37
26
Ub PCNA
*
PCNA
B
wild-type
mcm10-1
C
25°C
35°C
wild-type
mcm10-1
-
pEV
pMCM10
pEV Cl. 1
pEV Cl. 2
pMCM10 Cl. 1
pMCM10 Cl. 2
D
25°C
30°C
33°C
35°C
wild-type
+ pEV
+ pMCM10
mcm10-1
+ pEV
+ pEV
+ pMCM10
+ pMCM10

Figure 2.2. *pol1-1* and *mcm10-1* mutations stimulate mono-ubiquitination of PCNA. (**A, B**) Cultures of *mcm10-1*, *pol1-1* and the corresponding parental strains were grown to mid-log phase at 25°C and shifted to varying temperatures as indicated for 3 h. Total protein was precipitated with TCA and fractionated by SDS-PAGE for western blot analysis with an anti-PCNA antibody. The asterisk indicates a PCNA form with a low molecular weight post-translational modification (or a non-specific band) visible in darker exposures. (**C**) *mcm10-1* and wild-type parental strains containing no vector DNA (-), empty vector (pEV), or a wild-type *MCM10* transgene expressed from the endogenous *MCM10* promoter (p*MCM10*) were cultured to mid-log phase at 25°C. Cultures were then split and shifted to 25°C or 35°C as indicated for 3 h before harvesting. Unmodified and ubiquitinated PCNA were monitored as mentioned above. (**D**) 10-fold serial dilutions of strains from **C** were grown on synthetic complete medium lacking uracil for 3 days at the indicated temperatures.

Figure 2.3

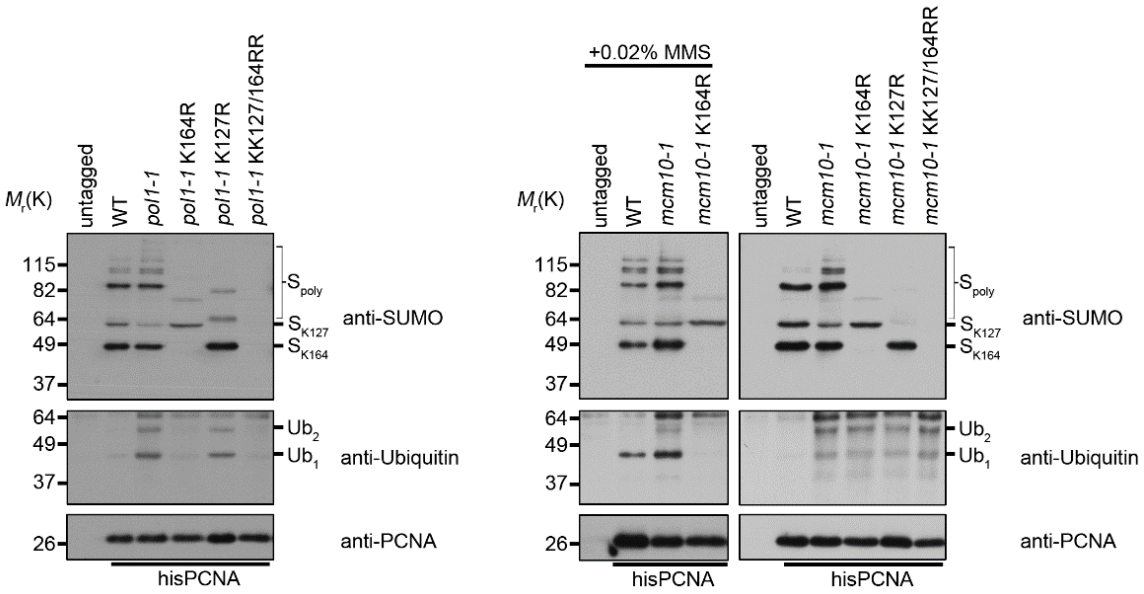

Figure 2.3. Ubiquitination and sumoylation patterns of PCNA in *pol1-1* and *mcm10-1* mutants. (**A, B**) *mcm10-1*, *pol1-1*, and the corresponding parental strains expressing His_6-tagged PCNA were grown to mid-log phase at 25°C and shifted to 35°C for 3 h. Cultures were treated with MMS immediately prior to temperature shift where indicated. PCNA was purified under denaturing conditions and the eluates fractionated by SDS-PAGE for western blot analysis with anti-PCNA, anti-ubiquitin, and anti-SUMO antibodies as indicated. Ubiquitinated forms of PCNA are denoted as Ub_1 and Ub_2 for mono- and di-ubiquitin, respectively. SUMO attachment is indicated as S_{K164} for K164 and S_{K127} for K127. Poly-sumoylated species are represented by S_{poly}.

Figure 2.4

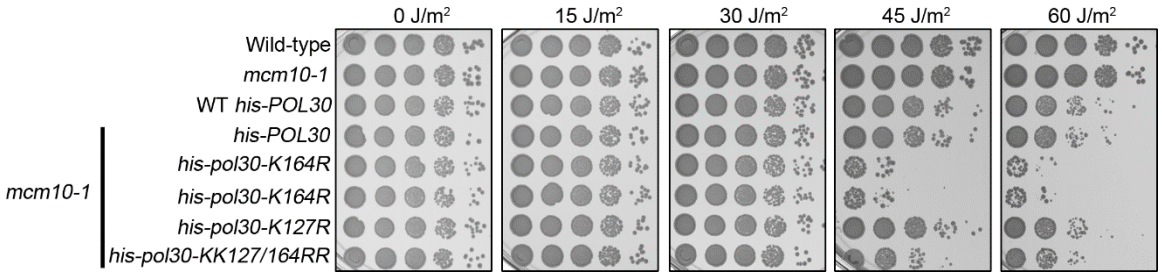

Figure 2.4. *mcm10-1 his-pol30-K164R* mutants are UV sensitive. The indicated strains were grown for two days in liquid culture at 25°C until they had reached saturation. Serial 10-fold dilutions were plated on YPD and immediately exposed to UV light. Images were taken after 2 days.

Figure 2.5

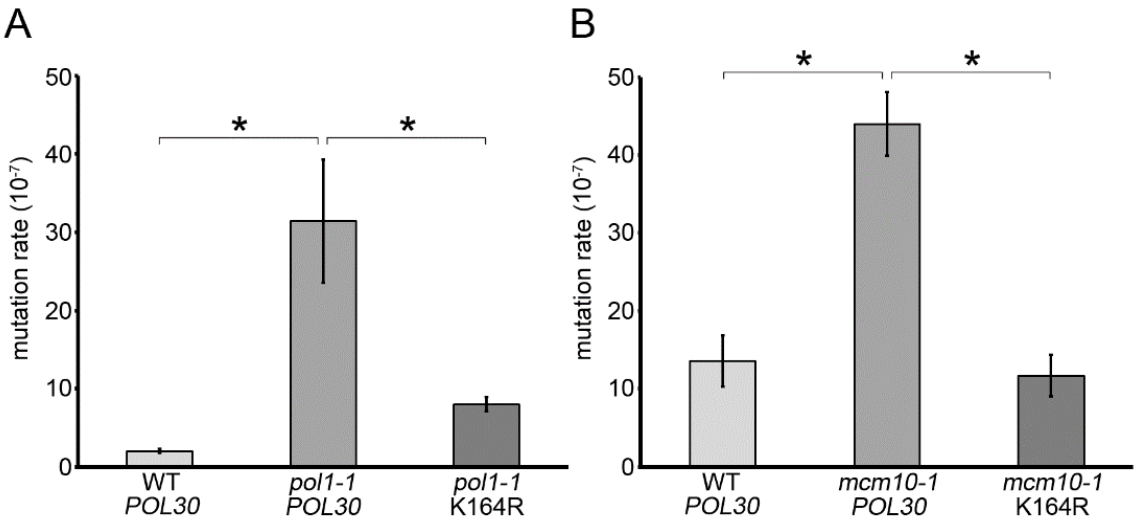

Figure 2.5. Elevated mutation rates in *pol1-1* and *mcm10-1* mutants are PCNA-K164 dependent. Bars indicate the mutation rates in *pol1-1* (**A**), *mcm10-1* (**B**), and the corresponding parental strains expressing either wild-type PCNA (*POL30*) or PCNA carrying a substitution in K164R (K164R). Each mutation rate represents the median of at least 12 independent measurements. Significance was determined by the Mann-Whitney U test and is indicated by an asterisk.

Figure 2.6

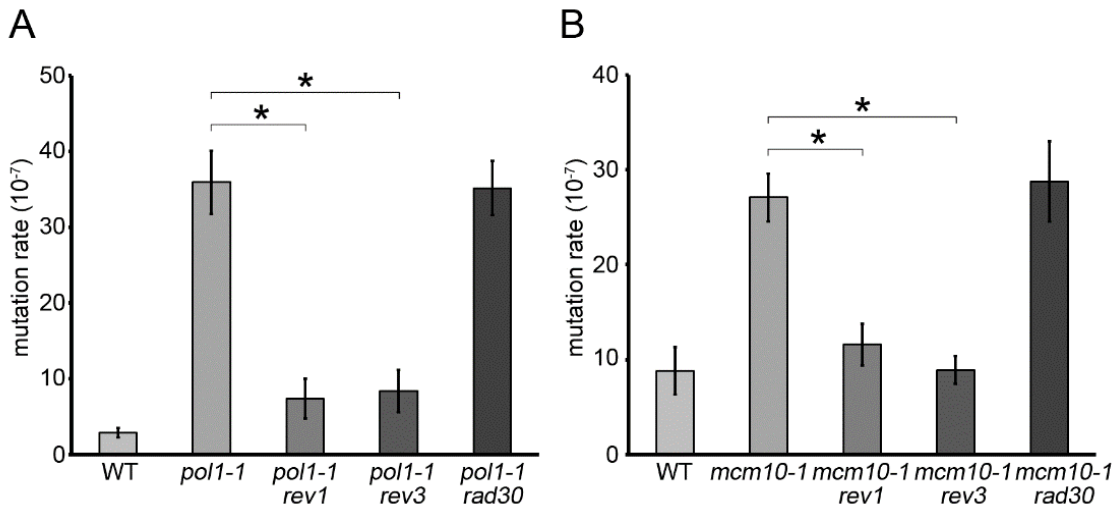

Figure 2.6. Elevated mutation rates in *pol1-1* and *mcm10-1* are dependent on Rev1 and Rev3. Bars indicate the mutation rates in *pol1-1* (**A**), *mcm10-1* (**B**), and the corresponding parental strains, carrying deletions of *REV1*, *REV3*, or *RAD30* as indicated. Each mutation rate represents the median of at least 12 independent measurements. Significance was determined by the Mann-Whitney U test and is indicated by an asterisk.

Figure 2.7

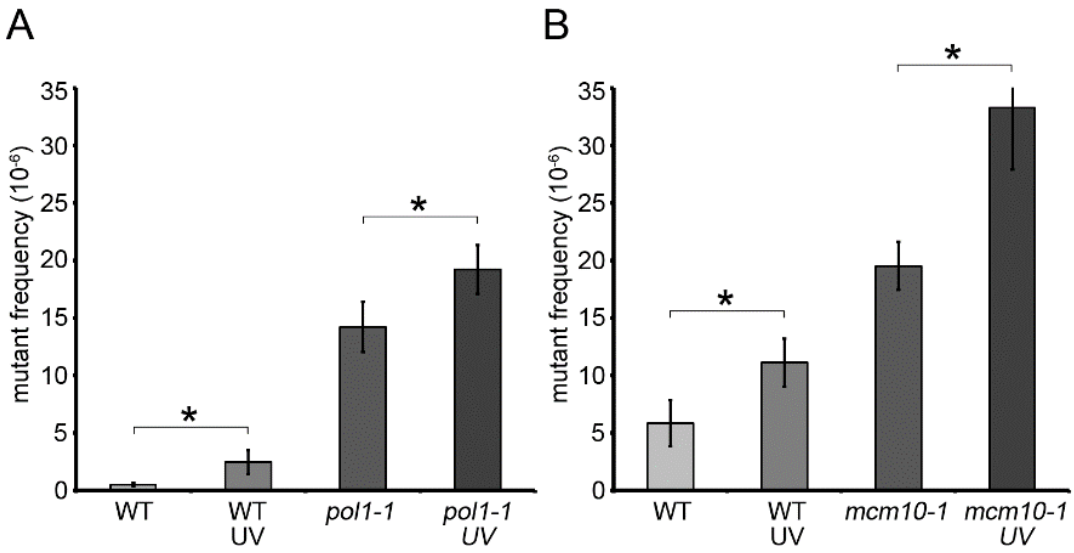

Figure 2.7. *pol1-1* and *mcm10-1* mutations do not impact the normal TLS response to UV damage. Bars indicate the mutation frequencies in *pol1*-1 (**A**), *mcm10-1* (**B**), and the corresponding parental strains in the presence or absence of UV light (10 J/m^2) treatment. Each bar represents the median of at least 12 independent measurements. Significance was determined by the Mann-Whitney U test and is indicated by an asterisk.

Figure 2.8

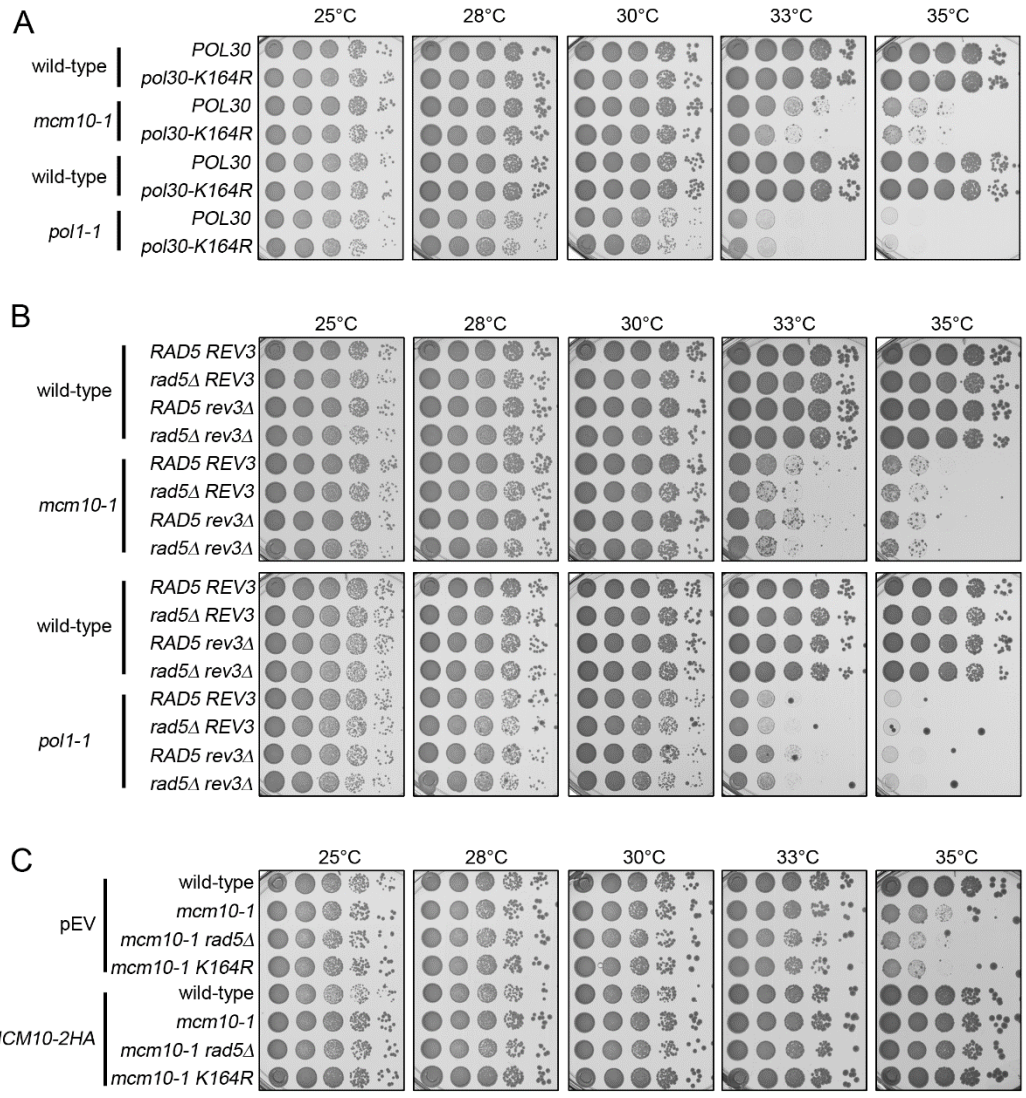

Figure 2.8. Error-free PRR but not TLS suppresses the temperature sensitivity of *mcm10-1.* (**A**) (**B**) Serial 10-fold dilutions of the indicated strains were grown on YPD plates for 2 days at the indicated temperatures. (**C**) Serial 10-fold dilutions of the indicated strains were grown on SC plates lacking uracil for 3 days at the indicated temperatures.

Figure 2.9

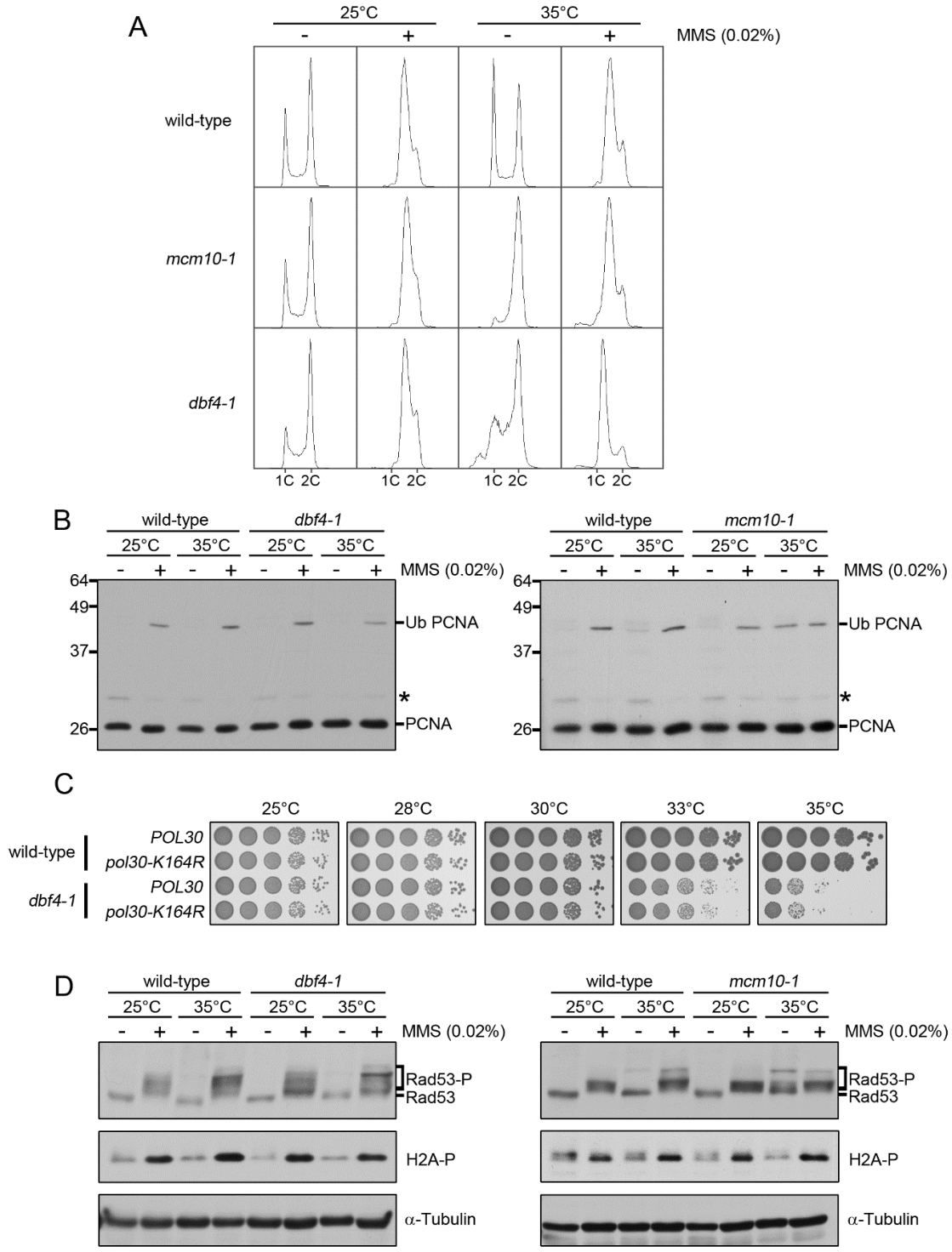
A
25°C
35°C
- + - +
MMS (0.02%)
wild-type
mcm10-1
dbf4-1
1C 2C 1C 2C 1C 2C 1C 2C
B
wild-type
dbf4-1
mcm10-1
25°C 35°C 25°C 35°C
MMS (0.02%)
64
49
37
26
Ub PCNA
*
PCNA
C
25°C
28°C
30°C
33°C
35°C
wild-type
dbf4-1
POL30
pol30-K164R
D
Rad53-P
Rad53
H2A-P
α-Tubulin

Figure 2.9. Origin activation defects do not trigger PCNA ubiquitination in asynchronous cultures. (**A**) Asynchronous cultures of wild-type, *mcm10-1* and *dbf4-1* cells were grown to mid-log phase and then shifted to either 25°C or 35°C for 3 h in the absence or presence of 0.02% MMS. Cells were then harvested and analyzed for DNA content. (**B**) Protein extracts were prepared from cells treated as described in panel **A**. Modified and unmodified forms of PCNA were detected using an anti-PCNA antibody. (**C**) Serial 10-fold dilutions of the indicated strains were grown on YPD plates for 2 days at various temperatures as marked. (**D**) Wild-type, *mcm10-1*, and *dbf4-1* cells were harvested from the cultures analyzed in panel **A** and protein extracts were prepared. Modified and unmodified forms of Rad53 were detected with an anti-Rad53 antibody. Phosphorylated histone H2A was detected using a phospho-S129 specific anti-histone H2A antibody. Tubulin served as a loading control.

Figure 2.10

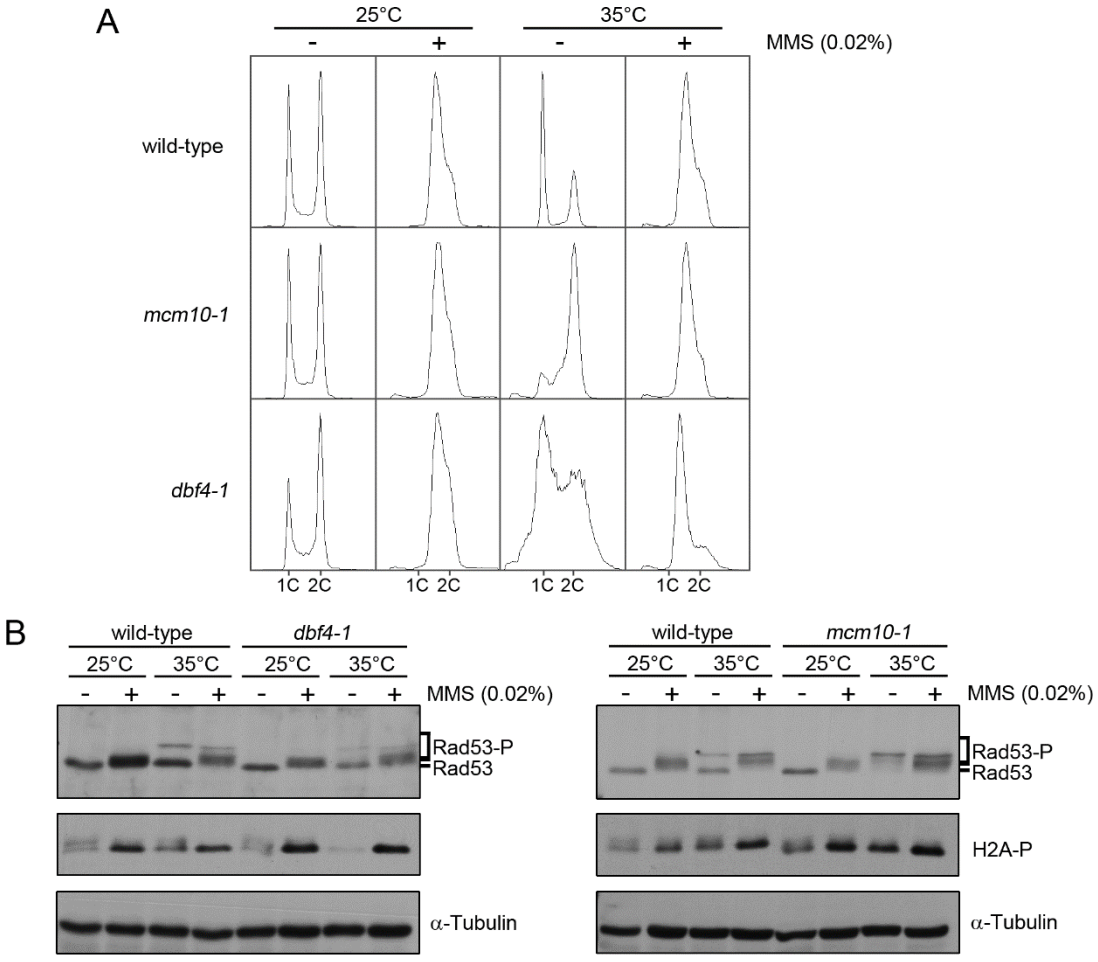
A
25°C
35°C
- + - +
MMS (0.02%)
wild-type
mcm10-1
dbf4-1
1C 2C
B
wild-type
dbf4-1
mcm10-1
25°C 35°C
MMS (0.02%)
Rad53-P
Rad53
H2A-P
α-Tubulin

Figure 2.10. *dbf4-1* mutants do not trigger checkpoint activation in asynchronous cultures. (**A**) Asynchronous cultures of wild-type, *mcm10-1* and *dbf4-1* cells were grown to OD_{600}=0.6 and then shifted to either 25°C or 35°C for 5 h in the presence or absence of 0.02% MMS. Cells were harvested and analyzed for DNA content. (**B**) Wild-type, *mcm10-1*, and *dbf4-1* cells were harvested from the cultures analyzed in panel **A** and protein extracts were prepared. Modified and unmodified forms of Rad53 were detected with an anti-Rad53 antibody. Phosphorylated histone H2A was detected using a phospho-S129 specific anti-histone H2A antibody. □-tubulin served as a loading control.

Figure 2.11

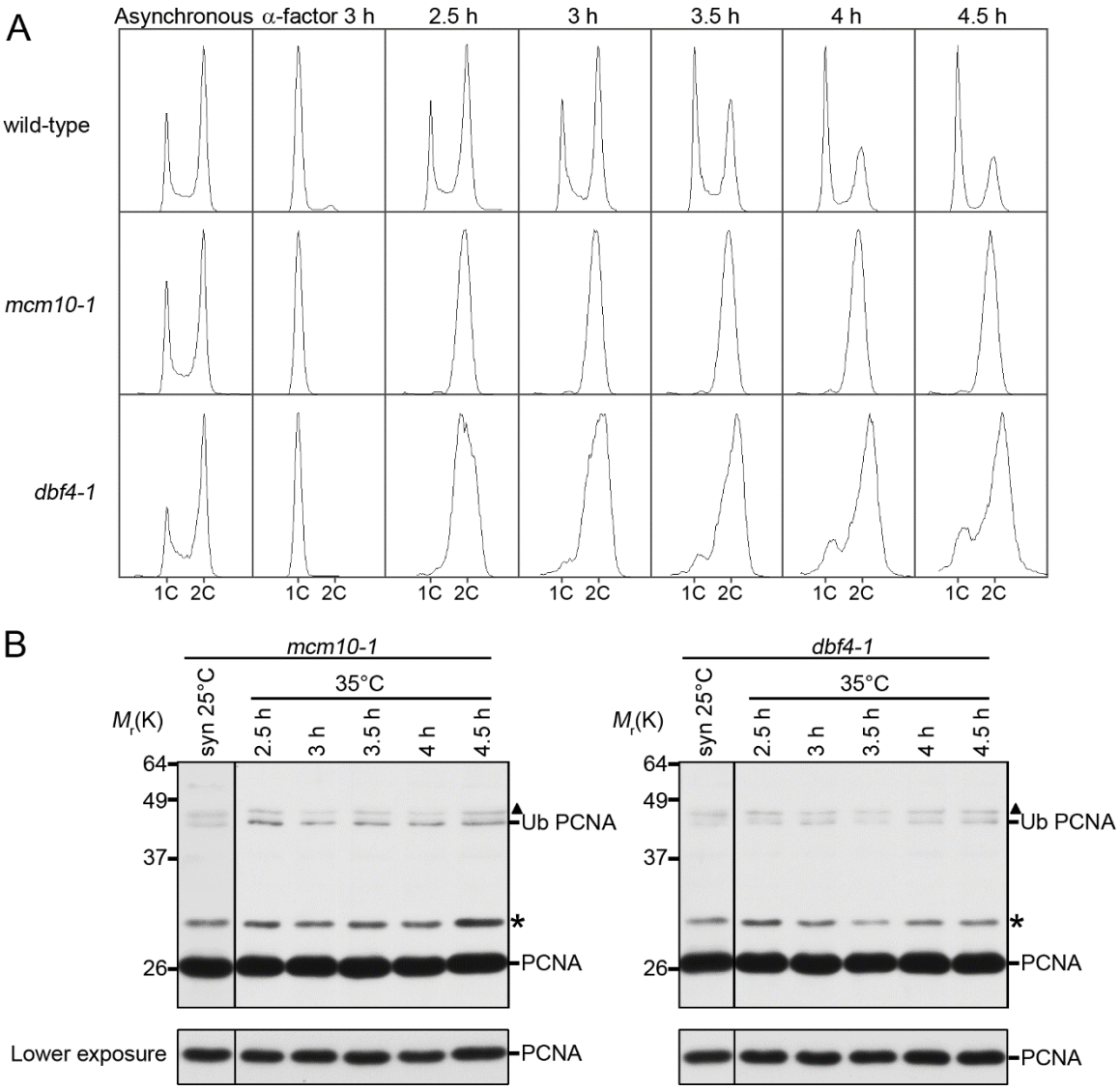

Figure 2.11. *dbf-1* mutants do not trigger PCNA ubiquitination in S-phase. (**A**) Asynchronous cultures of *mcm10-1* and *dbf4-1* strains were arrested in G1 phase with 150 ng/ml □-factor for 3 h. Cultures were released at 35°C and analyzed for cell cycle progression (**A**) and PCNA ubiquitination (**B**) at the indicated time points. The asterisks and triangles indicate bands of unknown origin.

Figure 2.12

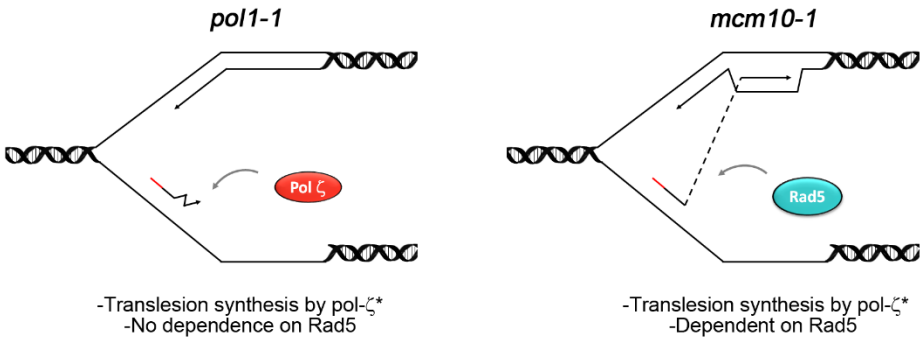

Figure 2.12. Primer quality affects PRR pathway choice. The cartoon depicts the inherent differences between *pol1-1* and *mcm10-1* mutants in PRR pathway dynamics. (Left) In *pol1-1*, intrinsically inaccurate primer synthesis by the Pol1-1 enzyme leads to mismatches unsuitable for pol-□ extension. These primers are likely extended, at least initially, by pol-ζ, which is efficient in adding to terminal mismatche [Prakash et al. 2005]. It is possible that mismatched primers are also unsuitable to initiate template switching, explaining why the Rad5-dependent error-free pathway is not efficiently utilized in these mutants. (Right) Primers in *mcm10-1* are synthesized by a wild-type Pol1 enzyme, allowing for engagement in template switching, which promotes cell survival. The dashed line denotes the actual switch from the lagging strand template to the nascent leading strand. *Although the translesion polymerase pol- ζ is activated in both *pol1-1* and *mcm10-1* mutants, it does not impact survival of either strain.

.

Table 2.1

Table 2.1. Yeast Strains used in Chapter 2.

Strain Name	Relevant Genotype	Source
	W303-1a-derived strains	
W303-1a	*MATa ade2-1 can1-100 his3-11,15 leu2-3,112 trp1-1 ura3-52*	[Thomas and Rothstein 1989]
BTY100	*mcm10-1*	[Homesley *et al.* 2000]
ABy1702	*can1-100::CAN1 (HIS1), bar1::TRP1*	This Study
ABy1703	*mcm10-1*, *can1-100::CAN1 (HIS1), bar1::TRP1*	This Study
ABy1704	*mcm10-1, rev1::URA3, can1-100::CAN1 (HIS1)*	This Study
ABy1705	*mcm10-1, rev3::URA3, can1-100::CAN1 (HIS1)*	This Study
ABy1706	*mcm10-1, rad30::URA3, can1-100::CAN1 (HIS1)*	This Study
ABy1737	*pol30::POL30 (LEU2), can1-100::CAN1 (HIS1)*	This Study
ABy1740	*mcm10-1, pol30::POL30 (LEU2), can1-100::CAN1 (HIS1)*	This Study
ABy1742	*mcm10-1, pol30::pol30-K164R (LEU2), can1-100::CAN1 (HIS1)*	This Study

Strain Name	Relevant Genotype	Source
ABy1900	*leu2::his-POL30 (LEU2)*, *pol30::URA3*	This Study
ABy1901	*mcm10-1, leu2::his-POL30 (LEU2)*, *pol30::URA3*	This Study
ABy1903	*mcm10-1, leu2::his-pol30-K164R (LEU2)*, *pol30::URA3*	This Study
ABy1937	pRS316	This Study
ABy1938	pRS316-*MCM10-2HA*	This Study
ABy1898	*mcm10-1,* pRS316 Cl. 1	This Study
ABy1939	*mcm10-1,* pRS316 Cl. 2	This Study
ABy1899	*mcm10-1,* pRS316-*MCM10-2HA* Cl. 1	This Study
ABy1940	*mcm10-1,* pRS316-*MCM10-2HA* Cl. 2	This Study
ABy1885	*dbf4-1*, *bar1::TRP1*	[Zou and Stillman 2000]
ABy2009	*rev3::URA3*	This Study
ABy2012	*rad5::LEU2*	This Study
ABy2013	*mcm10-1, rad5::LEU2*	This Study
ABy2021	*mcm10-1, rev3::URA3, rad5::LEU2*	This Study

Strain Name	Relevant Genotype	Source
ABy2025	*rev3::URA3, rad5::LEU2*	This Study
ABy2026	*mcm10-1, pol30::pol30-K164R (LEU2),* pRS316	This Study
ABy2028	*mcm10-1, pol30::pol30-K164R (LEU2),* pRS316-*MCM10-2HA*	This Study
ABy2030	*mcm10-1, rad5::LEU2,* pRS316	This Study
ABy2032	*mcm10-1, rad5::LEU2,* pRS316-*MCM10-2HA*	This Study
ABy2035	*mcm10-1, leu2::his-pol30-K127R (LEU2)*, *pol30::URA3*	This Study
ABy2036	*mcm10-1, leu2::his-pol30-K127/164R (LEU2)*, *pol30::URA3*	This Study
ABy2044	*dbf4-1, pol30::POL30 (LEU2)*	This Study
ABy2045	*dbf4-1, pol30::pol30-K164R (LEU2)*	This Study
	SSL204-derived strains	
SSL240	*MATa, ade2, his3D200, trp1, leu2, ura3-52*	[Dornfeld and Livingston 1991]
SSL530	*SSL240*, *pol1-1*	[Schweitzer and Livingston 1999]
ABy1589	*SSL240*, *bar1::TRP1*	This Study
ABy1590	*pol1-1*, *bar1::TRP1*	This Study

Strain Name	Relevant Genotype	Source
ABy1533	*pol1-1*, *pol30::POL30 (LEU2)*	This Study
ABy400	*pol30::POL30 (LEU2)*	This Study
ABy1426	*pol30::pol30-K164R (LEU2)*	This Study
ABy1412	*rev1::URA3*	This Study
ABy1414	*rev3::URA3*	This Study
ABy1443	*rad30::URA3*	This Study
ABy1409	*pol1-1*, *rev1::URA3*	This Study
ABy1410	*pol1-1*, *rev3::URA3*	This Study
ABy1445	*pol1-1*, *rad30::URA3*	This Study
ABy1591	*pol1-1*, *leu2::his-POL30 (LEU2)*, *pol30::URA3*	This Study
ABy1592	*pol1-1, leu2::hispol30-K164R (LEU2)*, *pol30::URA3*	This Study
ABy1600	*leu2::his-POL30 (LEU2)*, *pol30::URA3*	This Study
ABy2010	*rad5::LEU2*	This Study
ABy2015	*pol1-1, rev3::URA3, rad5::LEU2*	This Study

Strain Name	Relevant Genotype	Source
ABy2020	*pol1-1, rad5::LEU2*	This Study
ABy2023	*rev3::URA3, rad5::LEU2*	This Study
ABy2037	*pol1-1, leu2::his-pol30-K127R (LEU2)*, *pol30::URA3*	This Study
ABy2038	*pol1-1, leu2::his-pol30-K127/164R (LEU2)*, *pol30::URA3*	This Study

CHAPTER 3

Genetic interactions implicating postreplicative repair in Okazaki fragment processing

(The work in this chapter was published in Becker, J.R., Pons, C., Nguyen, H.D., Costanzo, M., Boone, C., Myers, C.L., and Bielinsky, A.K. (2015) *PLOS Genetics* 6;11(11) PMID: 26545110)

Author contributions:

Experiments were designed and conceived by J.R.B., H.D.N., and A.K.B. and performed by J.R.B. The synthetic lethality screen was designed and performed by M.C. and C.B. Screen results were analyzed by C.P. and C.L.M. All results were interpreted and prepared for publication by J.R.B., C.P. and A.K.B.

Ubiquitination of the replication clamp PCNA at the conserved residue lysine K164 triggers PRR to fill single-stranded gaps that result from stalled DNA polymerases. However, it has remained elusive as to whether cells engage PRR in response to replication defects that do not directly impair DNA synthesis. To experimentally address this question, we performed synthetic genetic array (SGA) analysis with a ubiquitination-deficient K164 to arginine (K164R) mutant of PCNA against a library of *S. cerevisiae* temperature-sensitive alleles. The SGA signature of the K164R allele showed a striking correlation with profiles of mutants deficient in various aspects of lagging strand replication, including *rad27Δ* and *elg1Δ*. Rad27 is the primary flap endonuclease that processes 5' flaps generated during lagging strand replication, whereas Elg1 has been implicated in unloading PCNA from chromatin. We observed chronic ubiquitination of PCNA at K164 in both *rad27Δ* and *elg1Δ* mutants. Notably, only *rad27Δ* cells exhibited a decline in cell viability upon elimination of PRR pathways, whereas *elg1Δ* mutants were not affected. We further provide evidence that K164 ubiquitination suppresses replication stress resulting from defective flap processing during Okazaki fragment maturation. Accordingly, ablation of PCNA ubiquitination increased S phase checkpoint activation, indicated by hyperphosphorylation of the Rad53 kinase. Furthermore, we demonstrate that alternative flap processing by overexpression of catalytically active exonuclease 1 eliminates PCNA ubiquitination. This suggests a model in which unprocessed flaps may directly participate in PRR signaling. Our findings demonstrate that PCNA ubiquitination at K164 in response to replication

stress is not limited to DNA synthesis defects but extends to DNA processing during lagging strand replication.

INTRODUCTION

The accurate copying of a cellular genome and subsequent transmission of genetic material to two daughter cells occurs on a microscopic scale, but is nonetheless a prodigious task. Considering the difficulty of accomplishing this fundamental process for living cells, it is hardly surprising that evolution has selected for a complex and multi-layered system of checkpoints and redundancies that promote its completion under sub-optimal conditions [Myung *et al.* 2001, Cremona *et al.* 2012]. Many of these processes are regulated by post-translational modification of proteins that act as molecular switches to regulate downstream responses.

The replication clamp, proliferating cell nuclear antigen (PCNA), is one such target for a variety of post-translational modifications that trigger an array of downstream effects. Known modifications include the covalent attachment of ubiquitin and the small ubiquitin-like modifier (SUMO) to specific lysine (K) residues [Hoege *et al.* 2002]. SUMO modification of chromatin-bound PCNA, or sumoylation, occurs during an unperturbed S phase at K164 and – to a lesser extent – at K127 [Hoege *et al.* 2002]. Sumoylation acts primarily to recruit the helicase/anti-recombinase suppressor of rad six 2 (Srs2), which prevents

illegitimate recombination at replication forks [Haracska *et al.* 2004, Papouli *et al.* 2005, Pfander *et al.* 2005].

Ubiquitination of PCNA occurs predominately at K164, however, alternative attachment sites have been mapped in yeast and human cells [Das-Bradoo *et al.* 2010, Xu *et al.* 2010, Povlsen *et al.* 2012, Nguyen *et al.* 2013, Elia *et al.* 2015]. In contrast to sumoylation, ubiquitination is induced by replication stress [Hoege *et al.* 2002]. PCNA-K164 ubiquitination was initially identified as a response to template strand lesions, which stall the highly selective processive polymerases (Pol-) δ and Pol-ε [Hoege *et al.* 2002]. Polymerase stalling leads to the accumulation of single-stranded (ss) DNA, which quickly becomes coated with replication protein A (RPA) [Lopes *et al.* 2006]. This allows for the recruitment of the E2-E3 ubiquitin ligase complex radiation sensitive-6 and -18 (Rad6-Rad18) to mono-ubiquitinate PCNA-K164 [Davies *et al.* 2008]. Mono-ubiquitin can be subsequently extended to K63-linked poly-ubiquitin chains by methyl methanesulfonate sensitive 2-ubiquitin conjugating 13-radiation sensitive 5 (Mms2-Ubc13-Rad5) [Hoege *et al.* 2002]. The length of the ubiquitin chain plays a crucial role in determining which of two PRR pathways is activated. Mono-ubiquitin facilitates an error-prone pathway for lesion bypass dependent on translesion polymerase activity [Hoege *et al.* 2002, Stelter and Ulrich 2003, Garg and Burgers 2005, Freudenthal *et al.* 2010]. Recent data indicates that replication past lesions by the mutagenic translesion polymerase Pol-ζ may continue for up to 1 kilobase beyond the lesion [Kochenova *et al.* 2015]. Alternatively, poly-ubiquitin chains

enable a template switching pathway in which the nascent DNA of the sister chromatid acts as a template, allowing for lesion bypass and filling of ssDNA gaps [Branzei 2011]. This process is considered to be “error-free”, because it does not rely on the intrinsically mutagenic translesion polymerases of the error-prone pathway [Vanoli *et al.* 2010]. The precise mechanism of this branch is not yet well understood.

In addition to the originally described function of PRR in DNA damage tolerance and lesion bypass, recent work has suggested that mutants with impaired replisome function also activate these pathways for replication of undamaged template strands [Northam *et al.* 2006, Karras and Jentsch 2010, Northam *et al.* 2010, Becker *et al.* 2014]. We have previously demonstrated that PRR promotes the viability of *mcm10* mutants in the absence of DNA damage [Becker *et al.* 2014]. To systematically explore the role of PCNA-K164 in response to intrinsic cellular dysfunction, we performed SGA analysis of a PCNA-K164 to arginine (PCNA-K164R) mutant. Interestingly, we found that the genetic interaction profile of the PCNA-K164R mutant closely resembled that of many alleles of lagging strand replication factors, including those involved in Okazaki fragment processing. This observation was particularly intriguing, as PRR has not been implicated in tolerating Okazaki fragment processing defects. As a result, we further investigated the activity of PCNA-K164-dependent pathways in mutants disrupting normal lagging strand replication. Specifically, we focused on the role of PCNA-K164 in cells deficient for the flap endonuclease radiation sensitive 27

(Rad27) or enhanced level of genomic instability 1 (Elg1), a homolog of replication factor C (RFC) subunit Rfc1 [Bellaoui *et al.* 2003].

Rad27 processes 5' flaps generated during lagging strand replication when DNA synthesis by Pol-δ collides with the 5' end of the RNA-DNA primer of the previous Okazaki fragment, displacing it into a small <10-nucleotide (nt) flap [Ayyagari *et al.* 2003, Jin *et al.* 2003]. If the 5' flap escapes processing by Rad27 and grows long enough to bind replication protein A (RPA), it is then cleaved by Dna2 [Bae *et al.* 2001, Jin *et al.* 2003, Levikova and Cejka 2015]. RPA binding of the flap serves both to inhibit Rad27, and to recruit Dna2 [Bae *et al.* 2001]. Dna2 cleaves the long ~30-nt flap to a short flap (5-10 nt), which can then be further processed by Dna2 or Rad27 into a ligatable nick [Bae and Seo 2000, Bae *et al.* 2001, Ayyagari *et al.* 2003, Levikova and Cejka 2015]. Although processing of long flaps must be relatively efficient under normal conditions, *rad27Δ* mutants exhibit a temperature dependent slow-growth phenotype [Reagan *et al.* 1995]. This is best explained by an increased rate in DNA replication and concomitant increase in the formation of long flaps [Reagan *et al.* 1995, Tishkoff *et al.* 1997]. At the restrictive temperature of 37°C, *rad27Δ* mutants are unable to meet flap processing demands, resulting in lethality, whereas at the semi-permissive temperature of 35°C growth is merely impaired [Reagan *et al.* 1995, Symington 1998]. In the absence of complete flap removal – even at lower temperatures – Pol δ-exonuclease (exo) activity can resect the nascent 3' end allowing the small 5' flap to re-anneal and form a ligatable nick [Jin *et al.* 2001, Jin *et al.* 2003]. After ligation

of the nick by DNA ligase I (Cdc9), PCNA is unloaded from chromatin by the Elg1:Rfc2-5 complex [Parnas *et al.* 2010, Kubota *et al.* 2013, Kubota *et al.* 2015]. In the present study, we report that PCNA is ubiquitinated in *rad27Δ* and *elg1Δ* mutants. Whereas ablation of PRR is inconsequential in the *elg1Δ* strain, both translesion synthesis (TLS) and template switching promote *rad27Δ* viability, possibly by enabling alternative flap processing. Furthermore, the long RPA-coated flaps generated in the absence of Rad27 play an active role in promoting the ubiquitination of PCNA at K164 and initiating PRR.

RESULTS

PCNA-K164R mutants resemble lagging strand replication mutants

To examine the global role of PCNA-K164 in the absence of exogenous DNA replication stressors, we performed SGA analysis of two independently isolated PCNA-K164R mutant clones (identified as PCNA-K164R clone 1 and PCNA-K164R clone 2, respectively) against a library of temperature-sensitive (TS) alleles and a full genome (FG) array as previously described (Tables 3.1 and 3.2) [Baryshnikova *et al.* 2010, Li *et al.* 2011]. Parallel analyses were performed against the TS array using a decreased abundance by mRNA perturbation (DAmP) allele of PCNA or a wild type (WT) allele as the query strain [Schuldiner *et al.* 2005, Beltrao *et al.* 2010]. Since ubiquitination or sumoylation of K164 facilitates only a subset of PCNA functions, we anticipated that interactions identified in the PCNA-K164R SGA screens should represent a small part of those identified in the PCNA-

DAmP analysis. Indeed the vast majority of hits identified in the K164R mutant screen with the TS array were also identified with the PCNA-DAmP allele (for PCNA-K164R clone 1: 18/26 hits overlapped with PCNA-DAmP with p-value < 10^{-11}, and for PCNA-K164R clone 2: 11/14 hits overlapped with p-value < 10^{-8} as determined by Fisher's test) (Table 3.1 and Figure 3.1A). Furthermore, the negative genetic interactions were largely consistent with previous reports, including a requirement for PRR when thiol-specific antioxidant 1 (*TSA1*) is deficient [Huang and Kolodner 2005]. Mutants of *TSA1* have reduced ability to neutralize reactive oxygen species, leading to increased DNA damage and synthetic sickness with PRR mutation [Huang and Kolodner 2005]. We also observed a modest requirement for homologous recombination (HR) components in K164R mutants (Figure 3.1A) [Motegi *et al.* 2006]. This gave us confidence that genes identified in the PCNA-K164R screens represented *bona fide* genetic interactions.

The most informative results were revealed when examining the similarity of the PCNA-K164R SGA profiles with the interaction signatures of other mutants. Strong Pearson correlation coefficient (PCC) values between PCNA-K164R clones and *rad5Δ* and *rad6Δ* mutants were consistent with the known functions of K164 in facilitating PRR (Figure 3.1B and Table 3.3). Strikingly, PCNA-K164R also exhibited strong correlation with many mutant alleles of genes involved in lagging strand replication, suggesting that those mutants have replication defects similar to those in the PCNA-K164R mutants (Figure 3.1B and Table 3.3). To validate this

observation in an unbiased manner, we performed a Gene Ontology (GO) enrichment analysis (http://www.ebi.ac.uk/QuickGO/). Alleles with SGA profiles similar to that of PCNA-K164R against the FG array (PCC > 0.15) were significantly associated with leading and lagging strand replication GO terms (Figure 3.1C). Interestingly, the list of enriched GO terms included “Okazaki fragment processing”, which has not been associated with PCNA-K164-dependent pathways (Fig 1C). GO enrichment of SGA profiles similar to PCNA-K164R against the TS array (PCC > 0.2) also showed nearly 25-fold enrichment with the “Okazaki fragment processing” term (Table 3.5). Because this initial analysis relied on existing GO annotations, we manually compiled an informed list of genes associated with leading and lagging strand replication for further analysis (Table 3.6). We found that PCNA-DAmP and PCNA-K164R profiles against the TS array were highly similar (PCC > 0.2) to profiles of genes implicated in leading and lagging strand replication (Figure 3.2A-D). We confirmed these results when we compared the profile of a second PCNA-K164R query strain (Table 3.3 and Figure 3.3). The PCNA-WT profile did not show any significant similarities (Table 3.3 and Figure 3.3).

Altogether, these findings suggested that PCNA-K164 may have an active role in lagging strand replication, even in the absence of exogenous DNA damage. Strong correlations with PCNA-K164R included *pol1* mutants, which we previously described to activate PRR pathways, and *pol3* mutants (deficient in Pol-δ) which have also been described to elicit PCNA ubiquitination and TLS (Table 3.3)

[Northam *et al.* 2006, Becker *et al.* 2014]. Additional strong correlations were observed for *rfc5*, *pol31*, *rad27*, and *elg1* mutants (Figure 3.1B and Table 3.3). These genes have been implicated in different steps of Okazaki fragment synthesis and processing, suggesting that PCNA-K164 is required at multiple junctions when lagging strand replication is impaired. This was surprising, as K164 ubiquitination of PCNA is dependent on the formation of ssDNA and is typically associated with DNA synthesis defects only [Davies *et al.* 2008]. The source of ssDNA – particularly in Okazaki fragment processing mutants, such as *rad27Δ* – was thus not immediately obvious. Nonetheless, these results led us to hypothesize that PCNA-K164-dependent pathways may be required to tolerate defects in lagging strand maturation. Because the function of K164 in PRR is dependent on its modification by ubiquitin, we hypothesized that lagging strand defects would result in chronic PCNA ubiquitination and activation of PRR pathways. To experimentally address this question, we assayed PCNA ubiquitination in *rad27Δ* and *elg1Δ* mutants, both of which had interaction profiles that correlated strongly with the PCNA-K164R alleles (Figure 3.1B and Table 3.3).

rad27Δ and *elg1Δ* mutants constitutively ubiquitinate PCNA at K164

rad27Δ is a temperature-sensitive allele, and for all subsequent experiments we shifted these mutants to 37°C for 3 h prior to analysis. To determine whether PCNA is ubiquitinated at K164 in *rad27Δ* and *elg1Δ* mutants,

we purified histidine tagged PCNA (His_6-PCNA) on Ni-NTA agarose and analyzed the eluates with PCNA-, ubiquitin- and SUMO-specific antibodies by western blot (Figure 3.4A and 3B). PCNA was indeed ubiquitinated in both mutants and ubiquitin attachment was completely ablated when PCNA carried a K164R substitution (Figure 3.4A and 3B), indicating that alternative attachment sites were not targeted. PCNA-K164R mutants also exhibited loss of K164-dependent sumoylation, consistent with previous reports [Hoege *et al.* 2002, Windecker and Ulrich 2008]. Interestingly, when we introduced the PCNA-K164R mutation in *elg1Δ* cells, we reproducibly observed a minor PCNA-SUMO species of a slightly lower molecular weight than K164-SUMO (marked by an asterisk), consistent with an earlier study that revealed an alternative sumoylation site (Figure 3.4B) [Windecker and Ulrich 2008]. As shown previously, K127-SUMO migrated markedly slower than K164-SUMO. Moreover, levels of K127-SUMO were elevated in PCNA-K164R mutants [Hoege *et al.* 2002]. Both *rad27Δ* and *elg1Δ* exhibited increased PCNA sumoylation at K127 and K164 compared to wild type (Figure 3.4A and 3B).

Next we asked whether PCNA-K164 modifications were important for viability of these two strains. Spotting analysis revealed that *rad27Δ* mutants had a significant reduction in growth at the semi-permissive temperature of 35°C when combined with the PCNA-K164R (*pol30-K164R*) mutation, whereas *elg1Δ* cells exhibited no such sensitivity at any temperature tested (Figure 3.4C), nor when they were exposed to UV light (Figure 3.4D). In contrast, *rad27Δ pol30-K164R*

double mutants were acutely sensitive even to low doses of UV, showing a severe reduction in growth after exposure to 1J/m^2 (Figure 3.4D). Together, these results suggested that K164-dependent pathways are important for the growth of *rad27Δ*, but not *elg1Δ* cells.

TLS and template switching play redundant roles in *rad27Δ* mutants

Because ubiquitination of PCNA at K164 is necessary for both TLS and template switching, we sought to determine which of these pathways are active in *rad27Δ* cells. Spotting analysis revealed that *pol30-K164R* and *rad18Δ* mutations each significantly reduced the viability of *rad27Δ* cells at 35°C (Figure 3.5A). The *rad27Δ rad18Δ* double mutant reproducibly appeared to have a slightly more severe growth defect than the *rad27Δ pol30-K164R* strain (Figure 3.5A). We attribute this finding to the known fact that PCNA-K164 sumoylation suppresses HR, and therefore substitution of K164 upregulates HR [Papouli *et al.* 2005, Pfander *et al.* 2005]. To address whether sumoylation of PCNA-K164 affected the viability of *rad27Δ* mutants, we deleted *SIZ1*, which encodes the SUMO E3 ligase that catalyzes this reaction. Consistent with published reports, *rad27Δ siz1Δ* double mutants did not exhibit any increased temperature sensitivity [Motegi *et al.* 2006, Chen *et al.* 2007]. These results strongly suggest that the PCNA-K164 dependent phenotype is solely due to the loss of ubiquitination.

To estimate the relative contribution of TLS and template switching to *rad27Δ* viability, we generated *rad27Δ* strains with *rev3Δ* or *rad5Δ* mutations

rendering them deficient in TLS and template switching, respectively. In addition, we analyzed a *rad27Δ rev3Δ rad5Δ* triple mutant, defective in both branches. We found that *rad27Δ rev3Δ* double mutants did not display any significant growth defects, whereas the *rad27Δ rad5Δ* cells exhibited a mild but noticeable growth delay, suggesting that the template switching pathway is the more prominent of the two (Figure 3.5B). However, loss of both pathways in the *rad27Δ rev3Δ rad5Δ* triple mutant resulted in a synergistic effect, resembling that of the *rad27Δ rad18Δ*double mutant (Figure 3.5A and 3.5B). These results argue that the two branches of PRR are both active in *rad27Δ* cells and have partially redundant roles in promoting viability.

The finding that *REV3* affected the survival of *rad27Δ* mutants in the absence of *RAD5* encouraged us to further examine the activity of the TLS branch of PRR. To accomplish this, we took advantage of the fact that TLS employs intrinsically mutagenic polymerases, which have a higher rate of nucleotide misincorporation combined with a lack of proofreading activity [Waters *et al.* 2009]. We predicted that TLS induced mutations would be dependent on K164. Mutation of K164 to arginine disables DNA synthesis by pol-ζ and its binding partner Rev1, which are responsible for the vast majority of TLS induced mutations [Nelson *et al.* 1996]. Consistent with previous reports, fluctuation analysis revealed that *rad27Δ* mutants have a drastically increased rate of mutation (Figure 3.5C) [Tishkoff *et al.* 1997, Serero *et al.* 2014]. Addition of the *pol30-K164R* allele led to a significant decrease in the mutation rate that accounted for 20-25% of total alterations,

confirming that TLS was active in these cells (Figure 3.5C). Because the *pol30-K164R* mutation also removes the suppressive effect of PCNA-SUMO on HR, an increase in gross chromosomal rearrangements may mask the decrease in mutation rate due to the loss of TLS. Therefore, the K164-dependent reduction is likely an underestimation of the contribution by TLS [Haracska *et al.* 2004, Papouli *et al.* 2005, Pfander *et al.* 2005]. In agreement with this notion, deletion of the pol-ζ catalytic subunit *REV3* results in a more severe reduction in the mutation rate than the *pol30-K164R* mutation (Figure 3.5C). Nonetheless, our observations are consistent with a recent report that had estimated point mutations in *rad27Δ* mutants to account for ~40% of all genomic aberrations [Serero *et al.* 2014]. Our results support the idea that the majority of these single nucleotide variations are a result of translesion polymerase activity.

PCNA-K164 suppresses *rad27Δ* replication defects

To further explore how PCNA-K164 aids in cell survival, we analyzed activation of the Rad53 kinase, a downstream target of the mitotic entry checkpoint kinase 1 (Mec1), the homolog of human *ATR (ataxia telangiectasia mutated- and Rad3-related) [Osborn and Elledge 2003]. rad27Δ pol30-K164R* double mutants showed increased phosphorylation of Rad53 relative to *rad27Δ* cells after they were shifted to the restrictive temperature of 37°C for 3 and 4 h. This was indicative of enhanced replication stress (Figure 3.6A). Consistently, the double mutants also displayed a robust late S/G2 phase arrest at those time points (Figure 3.6B). Since

rad27Δ cells passed more proficiently through mitosis (indicated by the higher G1 peak marked with a red arrow at 3 and 4 h in Figure 3.6B), we concluded that PRR pathways likely facilitated the completion of S phase and ultimately allowed for entry into mitosis. Therefore, without PRR cells have a reduced ability to tolerate Rad27 deficiency. Altogether, our findings support a role for PRR pathways in suppressing replication defects when Rad27 is absent. In contrast, *elg1Δ pol30-K164R* double mutants did not display any Rad53 activation or observable alterations in cell cycle distribution relative to *elg1Δ* (Figure 3.7).

Overexpression of *EXO1* eliminated PCNA ubiquitination in *rad27Δ*

Previous work demonstrated that ubiquitination of PCNA at K164 by Rad6-Rad18 requires persistent regions of RPA-coated ssDNA [Davies *et al.* 2008]. These normally accumulate if the replicative polymerases are impeded [Lopes *et al.* 2006]. However, in the context of Rad27 deficiency, the source of ssDNA was not readily apparent. Earlier studies established that in the absence of Rad27, Okazaki fragment flaps are processed through a “long flap” pathway by the combined activities of Dna2 and Pol3-exo [Jin *et al.* 2001, Ayyagari *et al.* 2003, Jin *et al.* 2003, Garg *et al.* 2004, Burgers 2009]. In this pathway short flaps become longer through enhanced strand displacement until they are sufficiently large to be bound by RPA [Budd *et al.* 2006, Rossi *et al.* 2008]. Binding by RPA serves to recruit Dna2 and stimulate its nuclease activity, reducing the flap to approximately 5 nt [Bae *et al.* 2001, Levikova and Cejka 2015]. Although Dna2 has been shown

to be competent to subsequently cleave the remaining short flap *in* vitro [Levikova and Cejka 2015], Pol3-exo activity is clearly essential in *rad27Δ* mutants at all temperatures [Jin *et al.* 2001]. Pol3-exo is thought to resect the 3' end of the preceding Okazaki fragment, allowing the remaining 5' flap to re-anneal and form a ligatable nick [Jin *et al.* 2001, Jin *et al.* 2003]. It is conceivable that both Dna2 and Pol3-exo contribute to the resolution of short flaps in *rad27Δ* cells. The binding of RPA to long flap intermediates *prior* to processing by Dna2 led us to consider that long ssDNA flaps themselves could provide the stimulus for PCNA ubiquitination. We inferred that the close proximity of these RPA-bound structures to PCNA should allow for recruitment of the Rad6-Rad18 complex and subsequent PCNA ubiquitination. To test this hypothesis, we sought to modulate flap processing by overexpression of *DNA2* [Bae and Seo 2000]. Because the current model for Dna2 processing of 5' flaps proposes that RPA binding occurs prior to cleavage, we expected that recruitment of Rad6 and Rad18 may not be significantly reduced upon *DNA2* overexpression (Figure 3.8A) [Bae *et al.* 2001, Stewart *et al.* 2008], unless it would directly compete with the E2-E3 complex. Notably, overexpression of *DNA2* did not reduce PCNA ubiquitination in *rad27Δ* (Figure 3.8B). We also considered the possibility that Pol3-exo activity during long flap processing could generate ssDNA regions sufficiently large to bind RPA (Figure 3.9A). However, overexpression of an exonuclease-dead allele of *POL3* (*pol3-01*) failed to reduce PCNA ubiquitination in *rad27Δ* (Figure 3.9B). Consistent

with previous reports, *pol3-01* expression was lethal in combination with *rad27Δ* (Figure 3.9C) [Gary *et al.* 1999].

We next sought to modulate flap processing in a manner that reduced the formation of long RPA-bound flaps. Multiple studies have demonstrated that overexpression of exonuclease 1 (*EXO1*) rescues the DNA damage sensitivity of *rad27Δ* mutants [Tishkoff *et al.* 1997, Moreau *et al.* 2001, Lewis *et al.* 2002, Sun *et al.* 2003]. Exo1 and Rad27 are both Rad2 family nucleases and crystal structures of their human homologs, FEN1 and EXO1, reveal highly conserved mechanisms of substrate binding and cleavage [Orans *et al.* 2011, Tsutakawa *et al.* 2011, Miętus *et al.* 2014]. Thus, we hypothesized that Exo1, like Rad27, may cleave flaps *before* RPA can bind to them. If this were true, Exo1 overexpression should reduce PCNA ubiquitination in *rad27Δ* cells (Figure 3.8C). Indeed, overexpression of *EXO1* from a galactose inducible promoter eliminated PCNA ubiquitination in *rad27Δ* mutants (Figure 3.8D). Furthermore, this phenotype was dependent on the catalytic activity of *EXO1,* as overexpression of a nuclease-dead *exo1-D173A* allele had no impact on PCNA ubiquitination (Figure 3.8D) [Moreau *et al.* 2001, Tran *et al.* 2002]. Furthermore, *EXO1* overexpression did not rescue the temperature sensitivity of *rad27Δ* (Figure 3.10). In summary, our results suggest that the majority of PCNA ubiquitination in *rad27Δ* is dependent on RPA-coated ssDNA intermediates, which recruit the Rad6-Rad18 complex and are degraded by Exo1.

PCNA ubiquitination caused by ssDNA gaps is not impacted by EXO1 overexpression

To examine whether the effect of *EXO1* overexpression on PCNA ubiquitination in *rad27Δ* mutants could be due to indirect suppression of ssDNA gap formation, we exposed *EXO1* overexpressing cells to 50 J/m^2 of UV light, which has been proven to cause ssDNA gaps (Figure 3.11A) [Lopes *et al.* 2006]. Overexpression of *EXO1* had no impact on the level of PCNA ubiquitination under these conditions (Figure 3.11B). Moreover, we did not observe any differences in ubiquitination when cells were treated with 100 J/m^2 of UV light, arguing that Exo1 did not act directly or indirectly to eliminate ssDNA regions (Figure 3.11B). In support of this conclusion, overexpression of *EXO1* had no impact on PCNA ubiquitination in cells harboring the temperature sensitive *pol1-1* allele (Figure 3.11C and 7D). This allele is thought to generate ssDNA regions as a result of reduced efficiency in the priming of Okazaki fragments (Figure 3.11C) [Gutiérrez and Wang 2003, Fumasoni *et al.* 2015], and causes ubiquitination of PCNA at K164 at the non-permissive temperature of 35°C [Becker *et al.* 2014]. Taken together, these findings indicate that Exo1 does not suppress the formation of ssDNA gaps.

DISCUSSION

The power of SGA analysis to identify networks of genetic interactors has greatly increased our knowledge of cellular pathway control and carries the

considerable advantage of being an unbiased systems-level approach to complex biological questions [Tong *et al.* 2001]. However, such screens are useful not only for identifying direct genetic interactors, but also in revealing functional relationships between genes through comparison of their SGA signatures [Nagai *et al.* 2008, Baryshnikova *et al.* 2010, Li *et al.* 2011]. Using this type of comparative analysis we identified a pattern of correlation between the profiles of PCNA-K164R mutants and the profiles of several lagging strand replication and Okazaki fragment processing mutants, including *rad27Δ* (Figure 3.1B and Table 3.3). The high degree of similarity between the *rad27Δ* and PCNA-K164R profiles suggested to us that PCNA-K164-mediated pathways may counteract replication defects in *rad27Δ*. Proof of PCNA ubiquitination in *rad27Δ* cells and synthetic sickness in *rad27Δ pol30-K164R* and *rad27Δ rad18Δ*, but not *rad27Δ siz1Δ* double mutants further substantiated this notion and led us to focus on the role of K164 ubiquitination-dependent pathways in the absence of flap endonuclease (Figures. 3.4A and 3.5A).

Long ssDNA flaps are a platform for PRR activation

The primary replication defect in *rad27Δ* cells is caused by impaired processing of 5' flaps generated during Okazaki fragment processing [Tishkoff *et al.* 1997]. At elevated temperatures, DNA replication proceeds more rapidly, likely leading to an increase in the formation of long flap intermediates, which must bind RPA before they can be efficiently processed [Bae *et al.* 2001]. We speculated that

these long RPA-coated flaps may serve as a platform to promote PCNA ubiquitination. To examine this hypothesis, we modulated flap length by overexpression of *EXO1*, a close relative of *RAD27* with a highly conserved mechanism of substrate binding and cleavage [Orans *et al.* 2011, Tsutakawa *et al.* 2011]. A number of prior studies have demonstrated that overexpression of *EXO1* suppresses the intrinsic mutagenicity of the *rad27Δ* allele [Tishkoff *et al.* 1997, Sun *et al.* 2003]. In particular, *EXO1* overexpression suppresses the duplication of short direct repeats that have been hypothesized to result from longer flap structures generated in *rad27Δ*, which is consistent with Exo1 activity preventing long RPA-coated flap formation [Tishkoff *et al.* 1997, Sun *et al.* 2003]. Thus, our finding that catalytically active Exo1 counteracts PCNA ubiquitination in *rad27Δ*, but has no effect on ubiquitination in *pol1-1* cells or after UV treatment, argues that the DNA structures mediating ubiquitination in flap endonuclease deficient cells are different from ssDNA gaps (Figs. 6 and 7).

It has been speculated that long unprocessed flaps could participate in the replication stress response [Budd *et al.* 2006, Budd *et al.* 2011, Nguyen *et al.* 2013]. Campbell and colleagues found that constitutive Mec1 activation is responsible for *dna2Δ* lethality [Budd *et al.* 2011]. They hypothesized that Mec1 activation originated from long RPA-coated flaps that accumulate in these mutants [Budd *et al.* 2011]. Interestingly, *EXO1* overexpression partially rescues the temperature sensitivity of a viable *dna2-1* mutant, consistent with the notion that Exo1 acts upstream of long flap formation [Budd *et al.* 2005].

Another well-documented hallmark of Okazaki fragment processing mutants is profound instability of trinucleotide repeat (TNR) regions [Freudenreich *et al.* 1998, Callahan *et al.* 2003]. This raises the question as to whether a requirement for PCNA-K164 in *rad27Δ* mutants is specific to the replication of TNR regions. A previous study had linked error-free PRR to the suppression of TNR expansion in *rad27Δ* cells [Daee *et al.* 2007]. However, error-prone TLS did not appear to regulate TNR expansion at all [Collins *et al.* 2007, Daee *et al.* 2007]. Our finding that both TLS and error-free PRR are active in *rad27Δ* cells therefore leads us to conclude that the role of PCNA-K164 in these mutants is not restricted to genomic regions that encompass TNRs (Figure 3.5B).

PCNA ubiquitination is a sensor of Okazaki fragment processing defects

Historically, PCNA ubiquitination and PRR were considered rescue pathways for template strand lesions that impair polymerase progression and require TLS or template switching for bypass [Hoege *et al.* 2002]. Later work from the Shcherbakova group demonstrated that intrinsic replisome deficiencies in hypomorphic alleles of the replicative polymerases *POL2* and *POL3* also lead to PCNA ubiquitination and activation of TLS on undamaged DNA templates [Northam *et al.* 2006]. This important finding described ubiquitination of PCNA and activation of PRR in the absence of replication stressors that damage DNA. Nevertheless, the essential effect of DNA damaging agents and hypomorphic polymerases on replication is a disruption of DNA synthesis. Both therefore

intuitively lead to ssDNA gaps, triggering PCNA ubiquitination and subsequent gap-filling by PRR.

In contrast, our study describes PCNA ubiquitination under conditions in which DNA synthesis is not impaired. Rad27 catalyzes Okazaki fragment flap cleavage, which does not occur until *after* Okazaki fragment synthesis, yet we see a requirement for PRR to support the viability of Rad27 deficient cells. This distinction suggests that PCNA-K164 is active in mediating DNA processing defects that are unlinked to problems in DNA synthesis. It is tempting to speculate that PRR pathways are promoting processing of Okazaki fragments by Dna2 or potentially an alternative mechanism. Error-free template switching could allow for synthesis past multiple Okazaki fragments using the sister chromatid as a template and reducing the overall requirement for flap endonuclease. A role for PRR in promoting flap processing and thereby reducing the half-life of long flaps is consistent with our observation of elevated Rad53 phosphorylation in *rad27Δ pol30-K164R* double mutants (Figure 3.6A). The mechanism by which PRR promotes flap processing or bypass is currently unclear.

PRR does not sustain survival of *elg1Δ* mutants

Similar to *RAD27, ELG1* has been described as an important protector of genome stability [Bellaoui *et al.* 2003, Ben-Aroya *et al.* 2003, Kanellis *et al.* 2003, Smith *et al.* 2004, Davidson *et al.* 2012]. Recent reports have identified Elg1 as a crucial component of an alternative RFC complex that unloads PCNA from double-

stranded DNA [Parnas *et al.* 2010, Kubota *et al.* 2013]. Our SGA screen revealed that the genetic interaction profile of ***elg1Δ*** correlates strongly with the PCNA-K164R and PCNA-DAmP profiles, leading us to investigate ubiquitination of PCNA at K164 in this mutant (Figures. 3.1B, 3.4B and Table 3.3). Unlike *rad27Δ*, ***elg1Δ*** cells did not exhibit synthetic sickness with the K164R mutation and displayed no acute requirement for PRR pathways to tolerate intrinsic replication stress or mild UV treatment (Figure 3.4C and 3D). We speculate that replication defects in ***elg1Δ*** are mimicking those present in PCNA-DAmP mutants in that both are limiting the amount of free PCNA in the nucleus that is available to load onto chromatin and engage in replication. In the case of the PCNA-DAmP allele this is simply the result of lower steady-state levels of PCNA protein, whereas in *elg1Δ*, PCNA is likely sequestered on DNA due to diminished unloading [Parnas *et al.* 2010, Kubota *et al.* 2013, Yu *et al.* 2014].

In summary, our results suggest that during the processing of Okazaki fragments *via* the long flap pathway, the flap itself is likely not an inert DNA processing intermediate, but may play an active role in signaling replication stress through PCNA. It is conceivable that under normal conditions a division of labor between long and short flap processing is required for efficient Okazaki fragment maturation [Bae *et al.* 2001, Kao *et al.* 2004, Rossi and Bambara 2006, Balakrishnan *et al.* 2010]. In ***rad27Δ*** cells, the balance is pushed severely to the long flap pathway, leading to the accumulation of RPA bound ssDNA structures that can be eliminated by Exo1. This becomes particularly problematic at elevated

temperatures when the kinetics of DNA replication are increased and flaps are produced at a higher rate. The mechanism by which PRR is suppressing replication stress under these conditions is not clear at this time, but we speculate that it is helping to circumvent flap processing.

These findings are salient in light of the relationship between the regulation of flap processing and cancer. Homozygous deletion of the *RAD27* homolog FEN1 in mice is lethal, but heterozygous deletion in combination with mutation of the adenomatous polyposis coli (Apc) gene results in increased numbers of adenocarcinomas, enhanced tumor progression and decreased survival [Kucherlapati *et al.* 2002]. Mutations which reduce FEN1 activity have also been demonstrated to vastly increase cancer incidence in mouse models [Zheng *et al.* 2007]. This study provides molecular evidence for the pathways contributing to mutagenesis when flap endonuclease function is compromised and gives insight into how cells sustain viability under these conditions.

MATERIALS AND METHODS

Strains and plasmids

All yeast strains used in this study are isogenic derivatives of wild type E133 cells, which were derived from CG379 [Tran *et al.* 1997], with the exception of *pol1-1* strains which are derived from SSL204 [Becker *et al.* 2014]. Strains with gene deletions were generated by PCR mediated gene disruption [Lorenz *et al.* 1995]. All clones were verified by PCR and sequencing of the modified locus. Strains

carrying *pol30-K164R* mutations were generated by PCR mediated gene disruption as follows: continuous PCR fragments consisting of PCNA, its endogenous promoter and a *LEU2* marker were amplified from pCH1654 (a gift from L Prakash, UTMB) and integrated at the endogenous PCNA locus. Integration and clonal homogeneity were verified by PCR and sequencing. All strains generated in this study are listed in Table 3.7.

His_6-tagged PCNA strains were constructed using Yip128-P30-POL30wt (gift from HD Ulrich, IMB Mainz). Plasmid variants with lysine mutations were constructed using the QuikChange Lightning (Agilent Technologies) site-directed mutagenesis kit. Briefly, the plasmid was linearized at an AflII restriction site in the *LEU2* coding sequence and transformed. Clones were screened by PCNA western blot to ensure that His_6-PCNA expression was equivalent to endogenous (untagged) expression levels. The endogenous copy of PCNA was then knocked out via PCR mediated gene disruption.

In experiments using galactose inducible gene expression, liquid cultures were grown to OD_{600}=0.600 at 25°C in raffinose containing medium. Galactose was then added to a final concentration of 2% and the cultures were shifted to 37°C for 3 h before collecting. Overexpression of *POL3* and *pol3-01* was induced by adding galactose to cells carrying the plasmids pBL336 and pBL336-01, respectively (gifts from D. Gordenin, NIEHS, originally constructed in P.M.J. Burgers laboratory, Washington University in St. Louis) [Jin *et al.* 2003]. Expression of *DNA2* was induced with galactose in cells carrying pgal-*DNA2* (a

gift from R. Wellinger, Université de Sherbrooke, Québec) [Parenteau and Wellinger 1999]. *EXO1* overexpression was induced by adding galactose to cells carrying pcDNA50.1, a derivative of pRS316 that was referred to as gal-*EXO1* (a gift from K. Lewis, Texas State University) [Lewis *et al.* 2002]. The *exo1-D173A* variant was generated using the QuikChange Lightning (Agilent Technologies) site-directed mutagenesis kit.

UV treatment (254nm) of liquid cultures was applied using a UV crosslinker (CL-1000, UVP). Cultures were transferred to a sterile tray and treated in the crosslinker before being returned to flasks and cultured an additional 40 min before harvesting.

Synthetic Genetic Array (SGA) screen

A genome-wide screen for genetic interactions with four *POL30* alleles as query strains (PCNA-DAmP, PCNA-WT, PCNA-K164R Cl.1, and PCNA-K164R Cl.2) was conducted at 30°C as previously described [Baryshnikova *et al.* 2010]. Because the screens are performed at 30°C they did not uncover a synthetic interaction between PCNA-K164R and *rad27Δ*. Briefly, the query strains, marked with a nourseothricin (NatMX4) resistance cassette and harboring the SGA haploid specific markers and reporter [Baryshnikova *et al.* 2010], were mated to an array of 786 temperature-sensitive and 175 viable deletion mutants (TS array: manuscript in preparation) (Table 3.1). Additionally, PCNA-K164R Cl.1 and Cl.2 were mated to an array of 3827 viable deletion mutants (FG array). Nourseothricin-

and geneticin-resistant heterozygous diploid mutants were selected and sporulated with MATa pol30 double mutants as described [Baryshnikova *et al.* 2010] (Table 3.2). Different PCC cutoffs were applied to the FG and TS array data (0.15 and 0.2, respectively) in order to enrich for the top 2% of all profile correlations.

His_6-PCNA purification

Cultures were grown to OD_{600}=0.600 at 25°C and then shifted to 37°C for 3 h before harvesting (with the exception of ***elg1Δ*** strains which remained at 25°C for 3 h after reaching OD_{600}=0.600). Cell pellets were frozen at -80°C. Briefly, cells were lysed under denaturing conditions and protein extracts were prepared as previously described [Ulrich 2009]. Extracts were incubated rotating overnight at room temperature with Ni-NTA conjugated agarose (Qiagen) to bind His_6PCNA. After incubation, His_6PCNA-bound beads were washed with buffers of decreasing pH to increase stringency with successive washes. His_6-PCNA was eluted from the beads with an EDTA-containing buffer and eluates were fractionated by SDS-PAGE. Purified PCNA and modified forms were then analyzed by western blot using specific antibodies against PCNA, ubiquitin, and SUMO.

Protein extraction and western blotting

Whole cell protein extraction was accomplished by TCA precipitation as previously described and fractionated by SDS-PAGE [Ricke and Bielinsky 2006].

Western blots were probed using the following antibodies; anti-PCNA at 1:4000 dilution (S871, a gift from B. Stillman, CSHL), anti-SUMO at 1:3000 dilution (A gift from X. Zhao, MSKCC), anti-ubiquitin at 1:1000 dilution(P4D1, Covance), anti-Rad53 at 1:1000 dilution (A gift from JFX Diffley, LRI, UK), anti-phospho-S129 H2A at 1:1000 dilution (ab15083, Abcam), and anti-tubulin at 1:5000 dilution (MMS-407R, Covance).

Mutation rate analysis

Mutation rates were estimated by measuring the forward rate of mutations at the *CAN1* locus that confer resistance to canavanine [Whelan *et al.* 1979]. Determinations were made from the median of at least 14 independent cultures for each strain. Cultures were inoculated from single colonies in 5 ml of YPD medium and grown to saturation for 5 days at 30°C. Cells were then washed and diluted to appropriate concentrations before plating on medium lacking arginine and containing canavanine (60 mg/L). Dilutions were also plated on non-selective YPD to obtain a viable cell count. Mutation rates were calculated using Drake's formula as previously described [Drake 1991, Foster 2006]. Significance was determined by the Mann Whitney U test as previously described [Mann and Whitney 1947].

Cell viability analysis

Relative cell viability was measured using an assay referred to as the "spotting assay". In this assay, 10 ml cultures were grown to saturation for 4 days

at 25°C. Cells were then harvested, washed with water, quantified, and diluted to equal volumes containing $2x10^7$ cells. 10-fold serial dilutions were made from these $2x10^7$ cells in a 96-well plate and then “spotted” on rich medium using a multi-pronged spotting manifold. Replicates were generated for incubation at various temperatures. UV treatment (254nm) was applied where indicated after plating using a UV crosslinker (CL-1000, UVP). Plates were imaged after 1.5 days of growth except where indicated.

Cell Cycle Analysis

Cell cycle progression was measured by flow cytometry as previously described [Das-Bradoo *et al.* 2010]. Briefly, 1 ml of liquid culture was pelleted and fixed in ice-cold 70% ethanol overnight. DNA was stained with Sytox Green (Invitrogen) and cells were analyzed using a BD Accuri C6 flow cytometer (BD Biosciences). Peaks were quantified using the quantification feature of the BD Accuri C6 software.

Figure 3.1

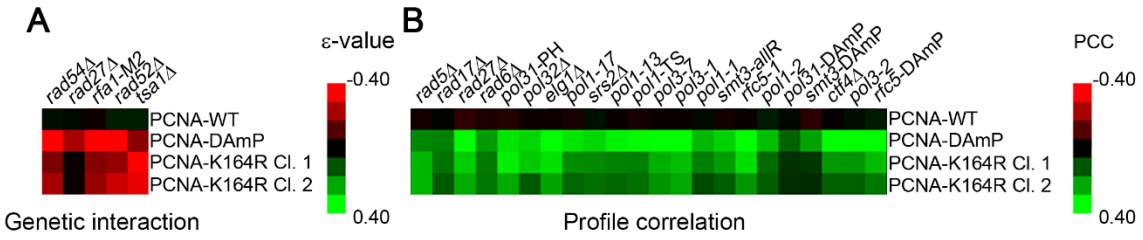

C

GO Term	Set	Expected	Fold Enrichment	1 Sided Fisher (p-value)
leading strand elongation	5 of 36 (13.9%)	0.08	61.54	5.52e-09
DNA strand elongation involved in DNA replication	6 of 36 (16.7%)	0.22	27.69	4.19e-08
DNA strand elongation	6 of 36 (16.7%)	0.23	26.59	5.48e-08
DNA replication, removal of RNA primer	4 of 36 (11.1%)	0.06	63.30	1.92e-07
mismatch repair	5 of 36 (13.9%)	0.15	32.58	2.57e-07
DNA replication	9 of 36 (25.0%)	1.04	8.67	4.94e-07
DNA replication, Okazaki fragment processing	4 of 36 (11.1%)	0.08	49.23	6.83e-07
postreplication repair	5 of 36 (13.9%)	0.21	24.08	1.35e-06
lagging strand elongation	4 of 36 (11.1%)	0.12	34.09	3.78e-06
base-excision repair	4 of 36 (11.1%)	0.12	34.09	3.78e-06
DNA repair	10 of 36 (27.8%)	1.78	5.62	5.68e-06
DNA-dependent DNA replication	7 of 36 (19.4%)	0.75	9.34	6.72e-06
RNA-dependent DNA replication	4 of 36 (11.1%)	0.15	26.07	1.23e-05
response to DNA damage stimulus	10 of 36 (27.8%)	2.07	4.84	2.17e-05
cellular response to stress	13 of 36 (36.1%)	3.84	3.39	4.41e-05

Figure 3.1. The PCNA-K164R SGA profile exhibits a limited set of direct genetic interactions but correlates strongly with other replication mutants. **(A)** Heat map of selected significant negative genetic interactions identified by SGA against the TS array for 2 independently isolated PCNA-K164R mutants. PCNA-WT and PCNA-DAmP are shown for comparison. The scale indicates epsilon- (ε-) values for the reported genetic interactions with negative interactions in red and positive interactions in green. **(B)** Heat map denoting the strength of correlation (measured by PCC) between PCNA-WT, PCNA-DAmP, PCNA-K164R clone 1 (Cl. 1) and PCNA-K164R clone 2 (Cl. 2) signatures against the TS array with the SGA signatures of the indicated strains. The scale denotes the strength of correlation between the indicated profiles with green being positive correlation and red being negative **(C)** Top 15 GO terms (http://www.ebi.ac.uk/QuickGO/) for alleles with PCC > 0.15 with the PCNA-K164R Cl. 1 profile against the FG array. This list is derived from a representative allele randomization (complete results in Table 3.4). Nine other randomizations were performed with similar results.

Figure 3.2

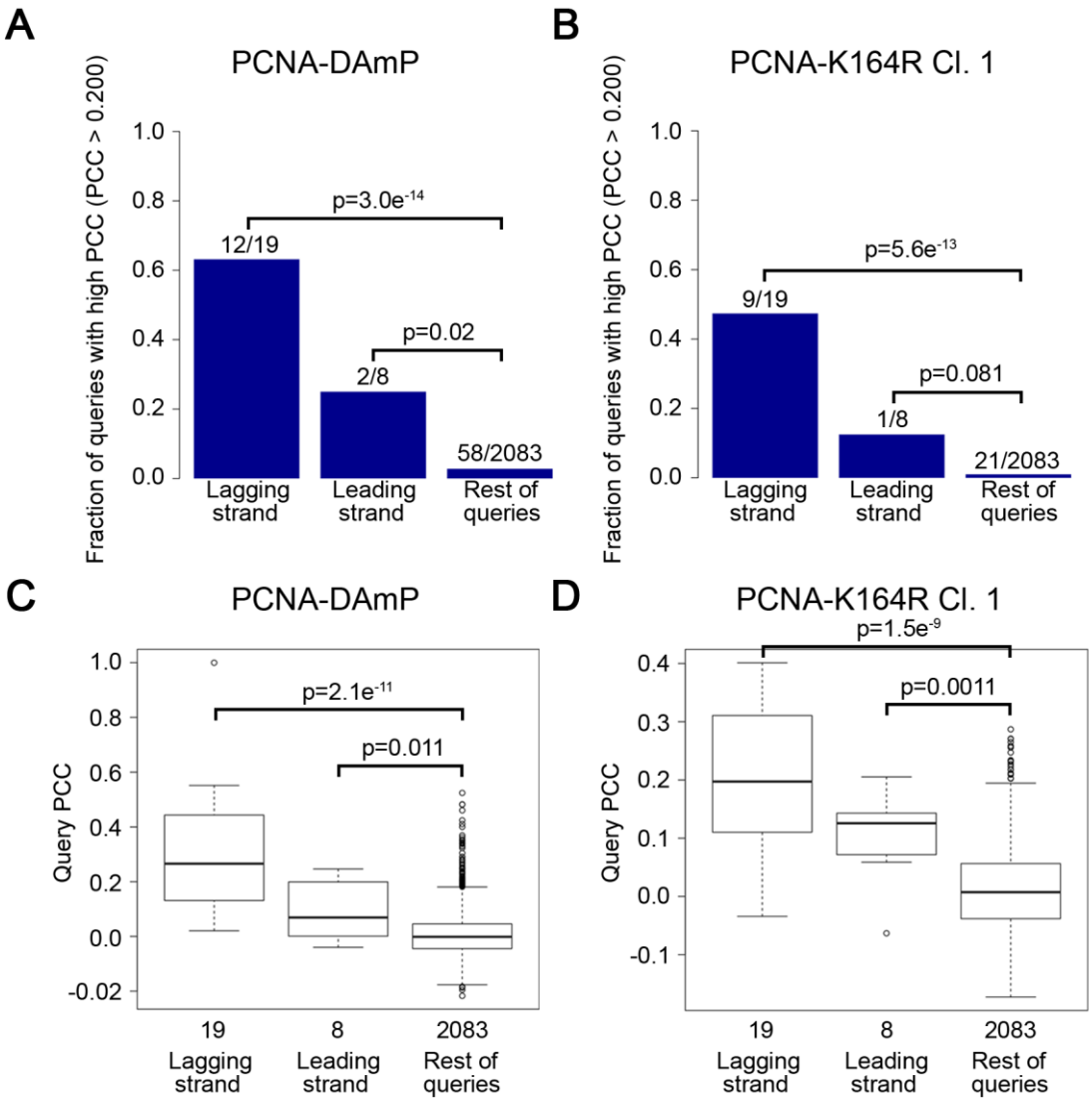
A
PCNA-DAmP
Fraction of queries with high PCC (PCC > 0.200)
1.0
0.8
0.6
0.4
0.2
0.0
p=3.0e-14
12/19
p=0.02
2/8
58/2083
Lagging strand
Leading strand
Rest of queries
B
PCNA-K164R Cl. 1
Fraction of queries with high PCC (PCC > 0.200)
p=5.6e-13
9/19
p=0.081
1/8
21/2083
Lagging strand
Leading strand
Rest of queries
C
PCNA-DAmP
Query PCC
1.0
0.8
0.6
0.4
0.2
0.0
-0.02
p=2.1e-11
p=0.011
19
Lagging strand
8
Leading strand
2083
Rest of queries
D
PCNA-K164R Cl. 1
Query PCC
0.4
0.3
0.2
0.1
0.0
-0.1
p=1.5e-9
p=0.0011
19
Lagging strand
8
Leading strand
2083
Rest of queries

Figure 3.2. The PCNA-K164R SGA profile strongly resembles lagging strand replication mutant profiles. (A and B) The fraction of leading and lagging strand mutants with a similar profile (PCC > 0.2) to that of the PCNA-DAmP and PCNA-K164R alleles, respectively. PCNA-K164R Cl.1 was used for this analysis. All mutants were queried against the TS array. Significance was determined using Fisher's exact test. **(C and D)** The distribution of profile similarities (calculated using PCC) between PCNA-DAmP or PCNA-K164R, respectively, and leading or lagging strand replication terms. All mutants were queried against the TS array for this analysis. Horizontal lines within the boxes indicate the median PCC. Error bars encompass the middle quartiles of the PCC value distribution. Outliers are represented with circular dots. Significance was determined by the Wilcoxon rank sum test [Mann and Whitney 1947].

Figure 3.3

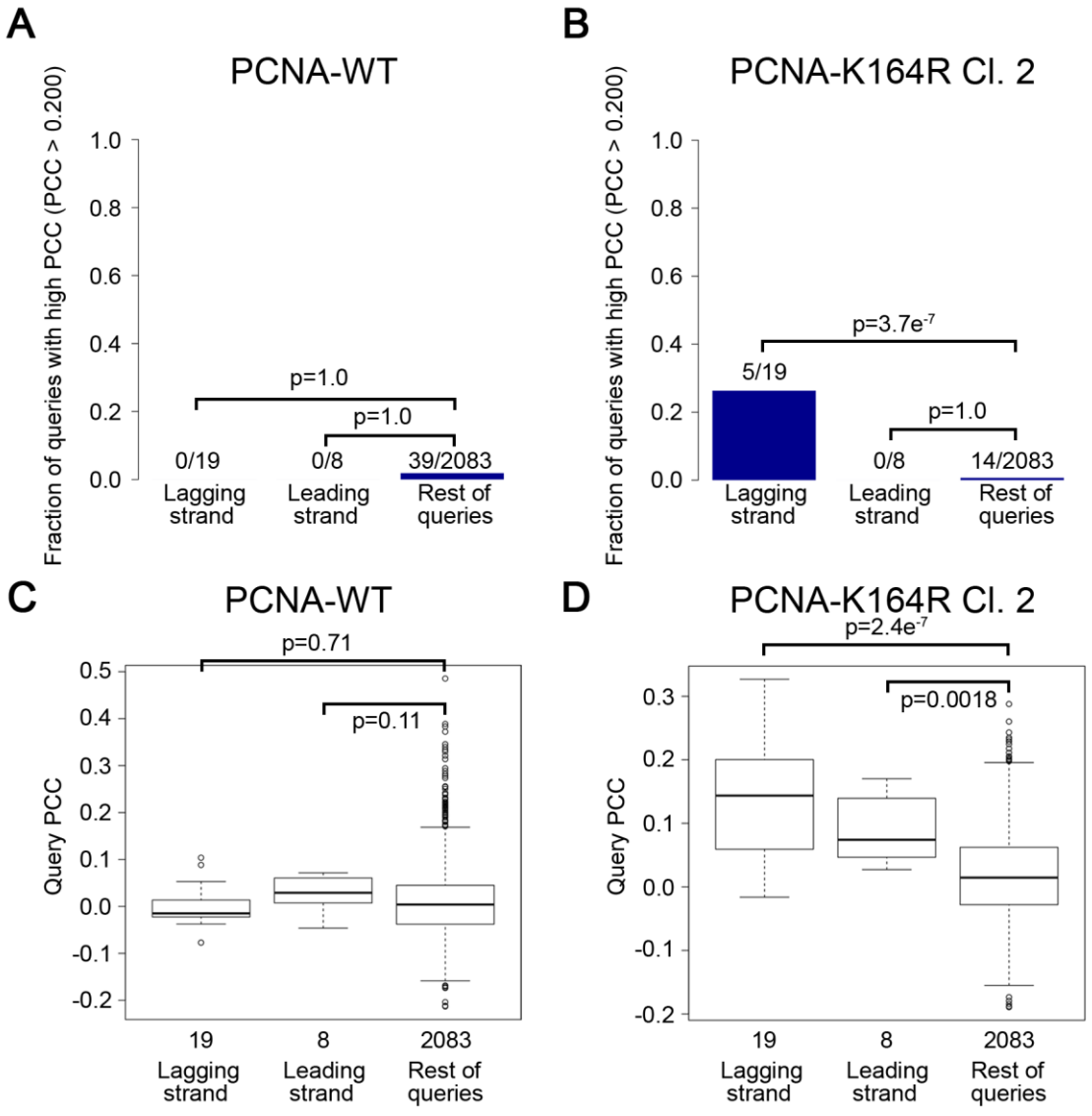
A
PCNA-WT
Fraction of queries with high PCC (PCC > 0.200)
1.0
0.8
0.6
0.4
0.2
0.0
p=1.0
p=1.0
0/19
0/8
39/2083
Lagging strand
Leading strand
Rest of queries
B
PCNA-K164R Cl. 2
Fraction of queries with high PCC (PCC > 0.200)
p=3.7e-7
5/19
p=1.0
0/8
14/2083
Lagging strand
Leading strand
Rest of queries
C
PCNA-WT
Query PCC
p=0.71
p=0.11
0.5
0.4
0.3
0.2
0.1
0.0
-0.1
-0.2
19
8
2083
Lagging strand
Leading strand
Rest of queries
D
PCNA-K164R Cl. 2
Query PCC
p=2.4e-7
p=0.0018
0.3
0.2
0.1
0.0
-0.1
-0.2
19
8
2083
Lagging strand
Leading strand
Rest of queries

Figure 3.3. The PCNA-K164R Cl. 2 SGA profile, but not that of PCNA-WT, strongly resembles the genetic interactions of lagging strand replication mutants. (A and B) The fraction of leading and lagging strand mutants with a similar profile (PCC > 0.2) to that of the PCNA-WT and PCNA-K164R alleles, respectively. PCNA-K164R Cl.2 was used for this analysis. All mutants were queried against the TS array. Significance was determined using Fisher's exact test. **(C and D)** The distribution of profile similarities (calculated using PCC) between PCNA-WT or PCNA-K164R, respectively, and leading or lagging strand replication terms. PCNA-K164R Cl.2 was used for this analysis. All mutants were queried against the TS array. Horizontal lines within the boxes indicate the median PCC. Error bars encompass the middle quartiles of the PCC value distribution. Outliers are represented with circular dots. Significance was determined by the Wilcoxon rank sum test [Mann and Whitney 1947].

Figure 3.4

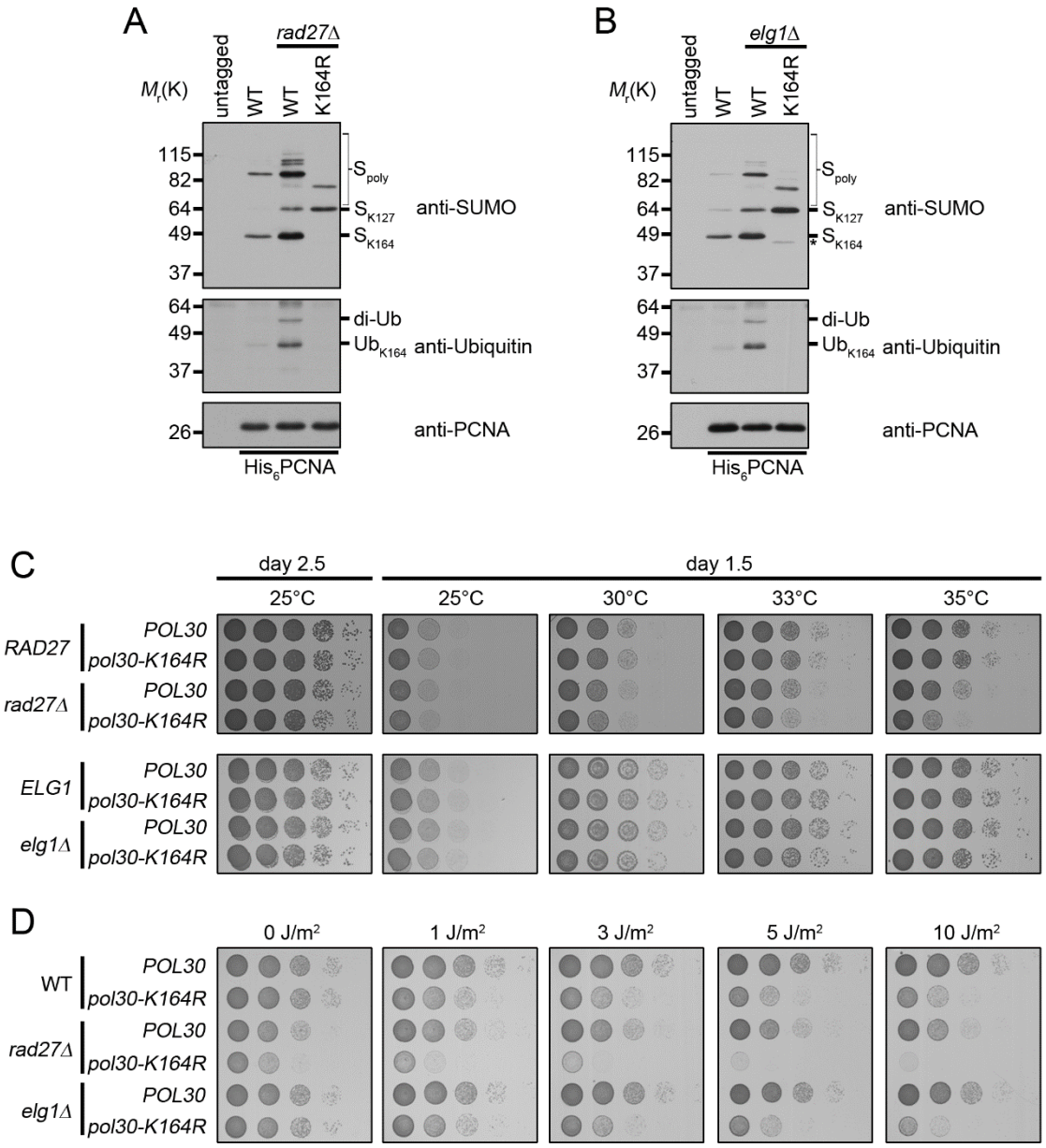
A
rad27Δ
untagged
WT
WT
K164R
Mr(K)
115
82
64
49
37
Spoly
SK127
SK164
anti-SUMO
64
49
37
di-Ub
UbK164
anti-Ubiquitin
26
anti-PCNA
His6PCNA
B
elg1Δ
untagged
WT
WT
K164R
Mr(K)
115
82
64
49
37
Spoly
SK127
*SK164
anti-SUMO
64
49
37
di-Ub
UbK164
anti-Ubiquitin
26
anti-PCNA
His6PCNA
C
day 2.5
day 1.5
25°C
25°C
30°C
33°C
35°C
RAD27
POL30
pol30-K164R
rad27Δ
POL30
pol30-K164R
ELG1
POL30
pol30-K164R
elg1Δ
POL30
pol30-K164R
D
0 J/m2
1 J/m2
3 J/m2
5 J/m2
10 J/m2
WT
POL30
pol30-K164R
rad27Δ
POL30
pol30-K164R
elg1Δ
POL30
pol30-K164R

Figure 3.4. *rad27Δ* and *elg1Δ* mutants ubiquitinate PCNA at K164. (A) Asynchronous cultures were grown to OD_{600}=0.600 at 25°C and then shifted to 37°C for 3 h before harvesting. His_6-PCNA was purified under denaturing conditions and analyzed by western blot using specific antibodies against PCNA, ubiquitin, and SUMO as indicated. **(B)** Asynchronous cultures were grown to OD_{600}=1.0 at 25°C before harvesting. PCNA was purified as in **(A)**. The asterisk (*) indicates a minor PCNA-SUMO species observed in *elg1Δ pol30-K164R* mutants. **(C)** 10-fold serial dilutions of the indicated strains were incubated 1.5 or 2.5 days on YPD plates at varying temperatures. **(D)** 10-fold serial dilutions of the indicated strains were spotted on YPD plates and subsequently treated with UV. Plates were imaged 1.5 days after spotting.

Figure 3.5

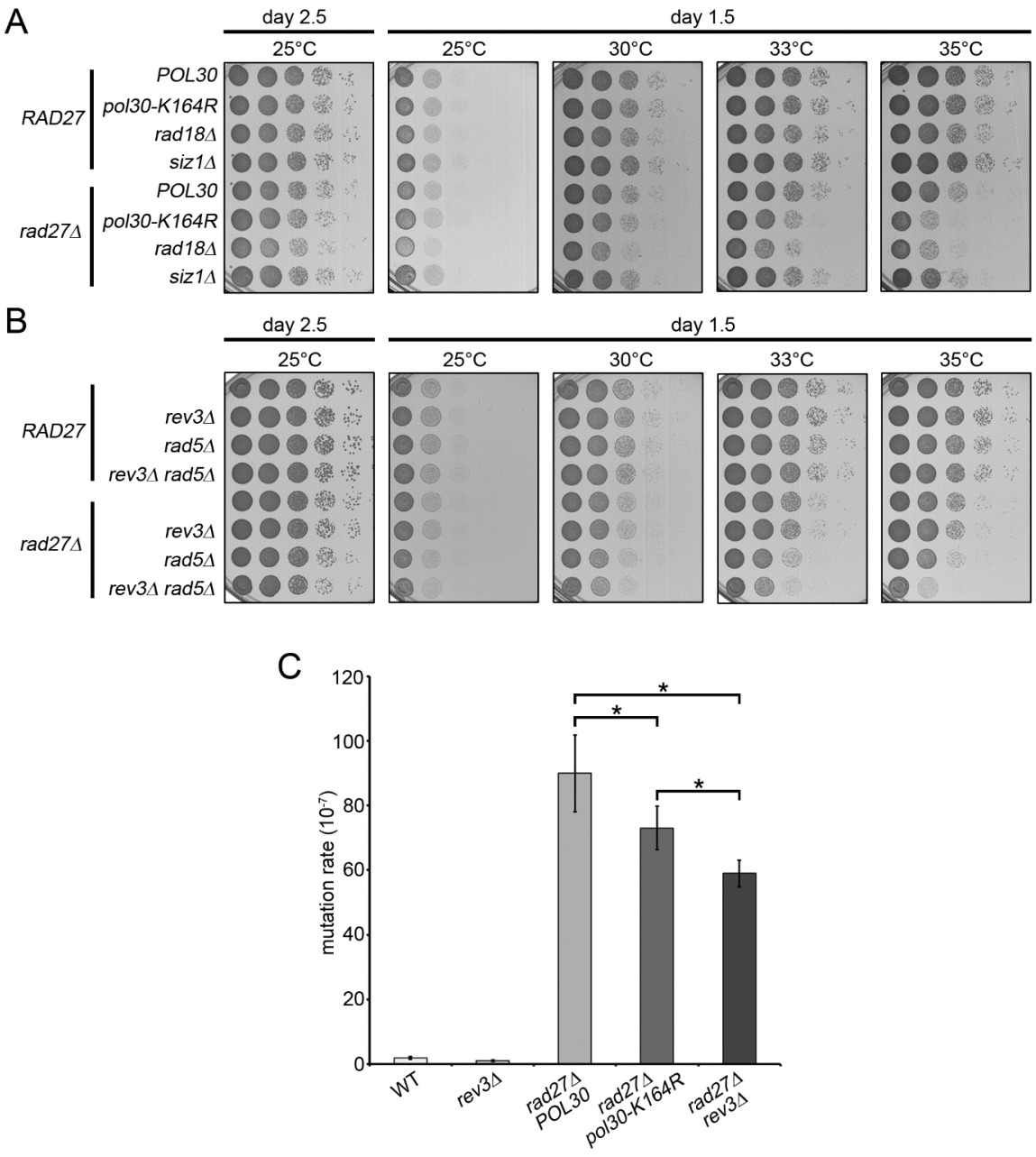
A
day 2.5
day 1.5
25°C
25°C
30°C
33°C
35°C
RAD27
POL30
pol30-K164R
rad18Δ
siz1Δ
rad27Δ
POL30
pol30-K164R
rad18Δ
siz1Δ
B
day 2.5
day 1.5
25°C
25°C
30°C
33°C
35°C
RAD27
rev3Δ
rad5Δ
rev3Δ rad5Δ
rad27Δ
rev3Δ
rad5Δ
rev3Δ rad5Δ
C
mutation rate (10-7)
120
100
80
60
40
20
0
*
*
*
WT
rev3Δ
rad27Δ POL30
rad27Δ pol30-K164R
rad27Δ rev3Δ

Figure 3.5. TLS and template switching are redundant in promoting *rad27Δ* viability. (A and B) 10-fold serial dilutions of the indicated strains were incubated 1.5 or 2.5 days on YPD plates at varying temperatures. **(C)** Bars indicate the rate of mutation at the *CAN1* locus for the indicated strains. Each measurement represents the median of at least 14 independent determinations. Significance was determined using the Mann-Whitney U test.

Figure 3.6

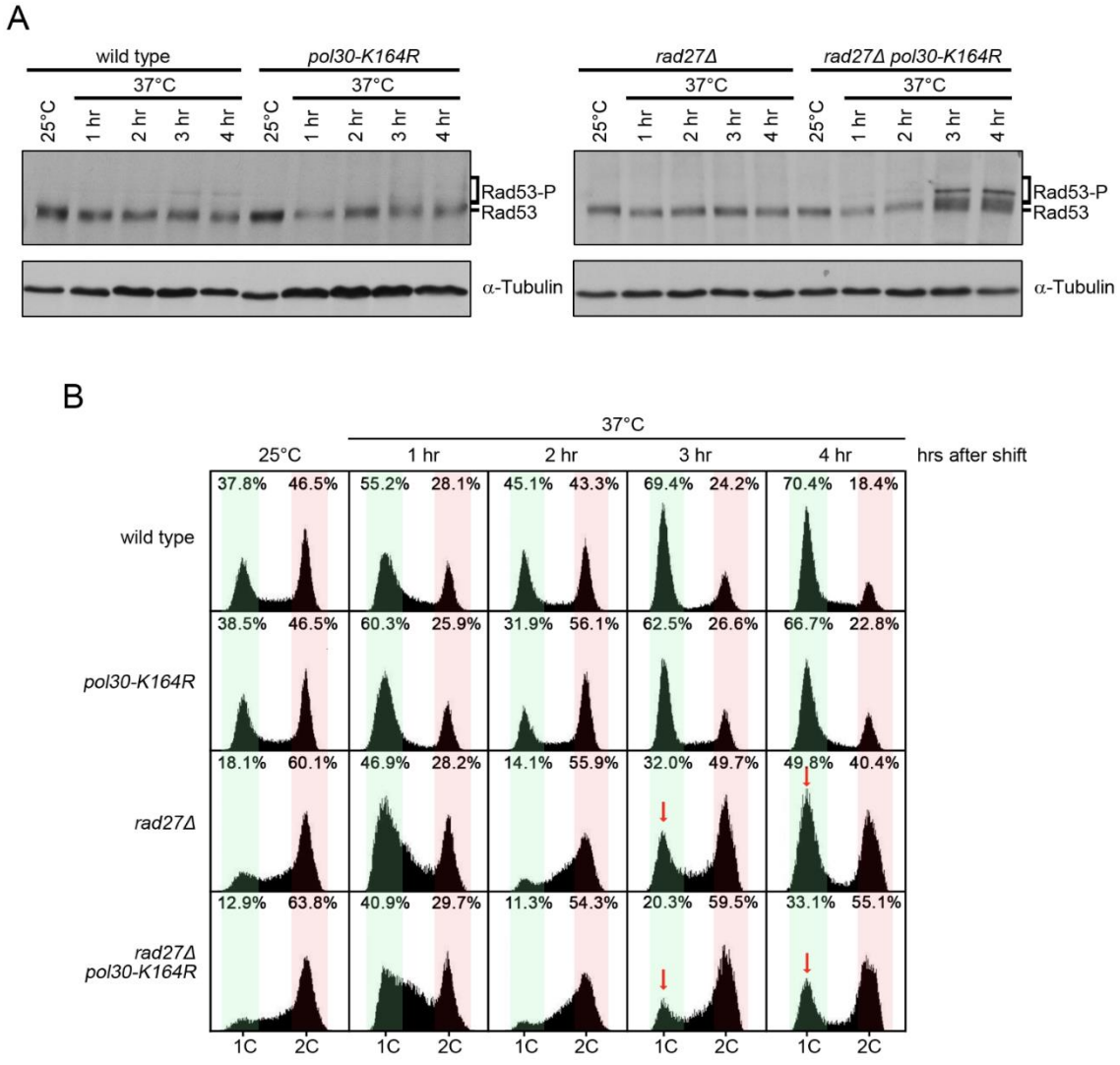
A
wild type
pol30-K164R
rad27Δ
rad27Δ pol30-K164R
37°C
25°C
1 hr
2 hr
3 hr
4 hr
Rad53-P
Rad53
α-Tubulin
B
37°C
25°C
1 hr
2 hr
3 hr
4 hr
hrs after shift
wild type
pol30-K164R
rad27Δ
rad27Δ pol30-K164R
37.8% 46.5%
55.2% 28.1%
45.1% 43.3%
69.4% 24.2%
70.4% 18.4%
38.5% 46.5%
60.3% 25.9%
31.9% 56.1%
62.5% 26.6%
66.7% 22.8%
18.1% 60.1%
46.9% 28.2%
14.1% 55.9%
32.0% 49.7%
49.8% 40.4%
12.9% 63.8%
40.9% 29.7%
11.3% 54.3%
20.3% 59.5%
33.1% 55.1%
1C
2C

Figure 3.6. *rad27Δ pol30-K164R* double mutants exhibit increased checkpoint activation and cell cycle arrest. **(A)** The indicated strains were grown to OD_{600}=0.600 at 25°C and then shifted to 37°C for 4 h. Samples were harvested immediately before the temperature shift and every hour for 4 h afterward. Protein was subsequently extracted by TCA precipitation. Extracts were fractionated by SDS-PAGE and analyzed by western blot with anti-Rad53 and anti-tubulin antibodies. Tubulin served as a loading control. **(B)** Aliquots of the same cultures from **(A)** were analyzed for DNA content by flow cytometry. Red arrows indicate the G1 peaks of *rad27Δ* and *rad27Δ pol30-K164R* after 3 and 4 h at 37°C for comparison. Percentages indicate the percent of all cells analyzed that fall within the highlighted area. Green regions indicate G1 phase peaks while red regions mark late S and G2/M phases.

Figure 3.7

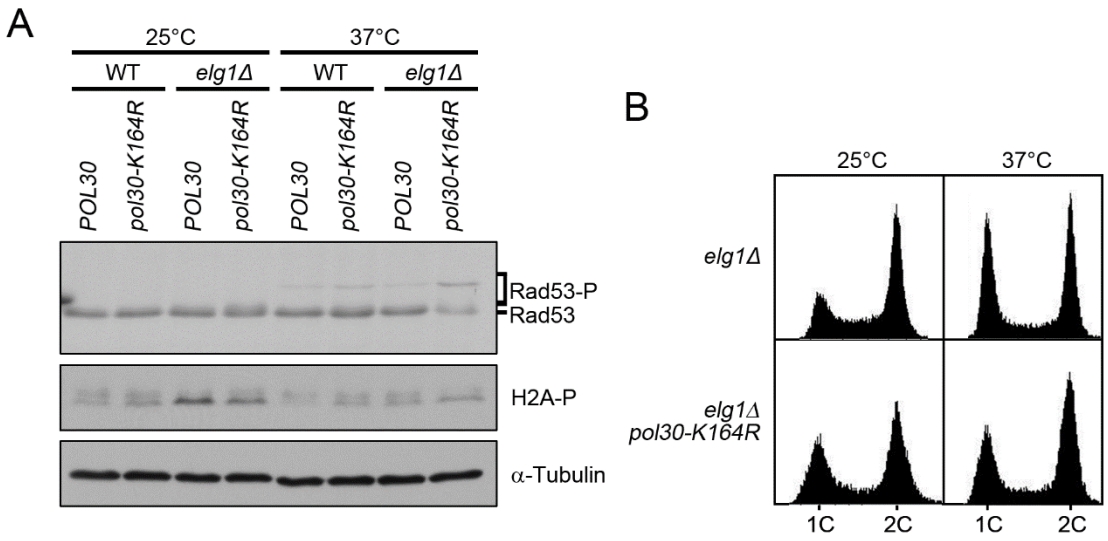

Figure 3.7. *elg1Δ pol30-K164R* double mutants do not exhibit increased replication defects. (A) The indicated strains were grown to OD_{600}=0.600 at 25°C and then split in half, either remaining at 25°C or being shifted to 37°C. Both cultures were harvested after 3 h growth and protein was extracted by TCA precipitation. Extracts were fractionated by SDS-PAGE and analyzed by western blot with antibodies specific to Rad53 and phospho-H2A-S129. Tubulin served as a loading control. **(B)** Aliquots of the same cultures from **(A)** were analyzed for DNA content by flow cytometry.

Figure 3.8

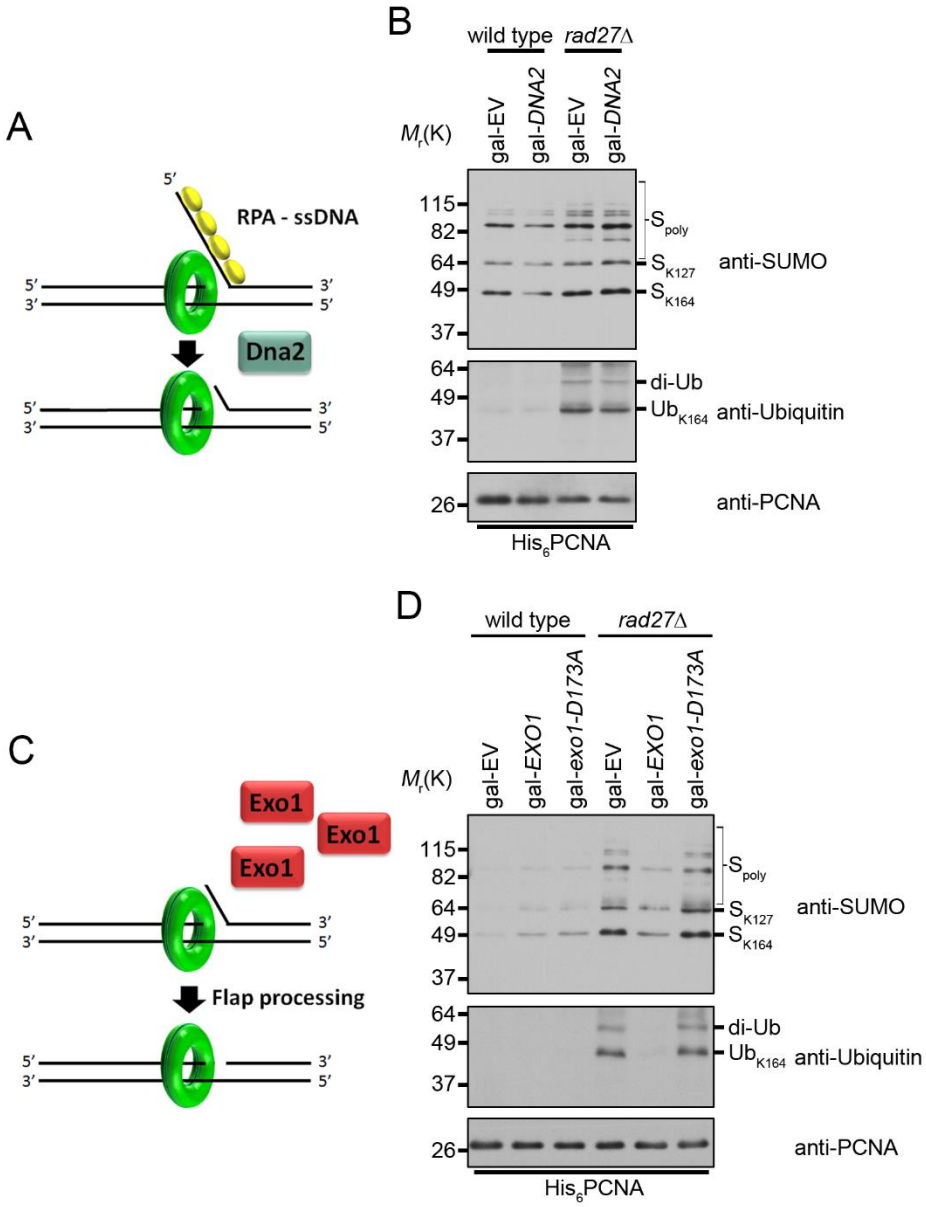
A
5′
RPA - ssDNA
5′
3′
3′
5′
Dna2
5′
3′
3′
5′
B
wild type
rad27Δ
gal-EV
gal-DNA2
gal-EV
gal-DNA2
Mr(K)
115
82
64
49
37
Spoly
SK127
SK164
anti-SUMO
64
49
37
di-Ub
UbK164
anti-Ubiquitin
26
anti-PCNA
His6PCNA
C
Exo1
Exo1
Exo1
5′
3′
3′
5′
Flap processing
5′
3′
3′
5′
D
wild type
rad27Δ
gal-EV
gal-EXO1
gal-exo1-D173A
gal-EV
gal-EXO1
gal-exo1-D173A
Mr(K)
115
82
64
49
37
Spoly
SK127
SK164
anti-SUMO
64
49
37
di-Ub
UbK164
anti-Ubiquitin
26
anti-PCNA
His6PCNA

Figure 3.8. Overexpression of *EXO1* suppresses PCNA ubiquitination in *rad27Δ*. (A) RPA binding to long ssDNA flaps occurs *prior* to processing by Dna2. Therefore overexpression of *DNA2* is unlikely to interfere with RPA binding. **(B)** Wild type and *rad27Δ* cells carrying gal-EV or gal-*DNA2* plasmids were grown to OD_{600}=0.600 at 25°C in raffinose containing medium lacking uracil. Galactose was then added to a final concentration of 2% and the cultures we shifted to 37°C for 3 h before harvesting. His_6-PCNA was purified under denaturing conditions and analyzed by western blot with antibodies specific to PCNA, ubiquitin, and SUMO as indicated. **(C)** Cartoon depicting the effect of *EXO1* overexpression in the absence of flap endonuclease. If long RPA-coated flaps are the stimulus for PCNA ubiquitination in *rad27Δ*, we hypothesize that *EXO1* overexpression and processing of flaps before they are long enough to bind RPA will reduce ubiquitination. **(D)** Wild-type and *rad27Δ* cells carrying gal-EV, gal-*EXO1*, or gal-*exo1-D173A* plasmids were treated as in **(B)** in medium lacking uracil and purified PCNA was analyzed by western blot with antibodies specific to PCNA, ubiquitin and SUMO as indicated.

Figure 3.9

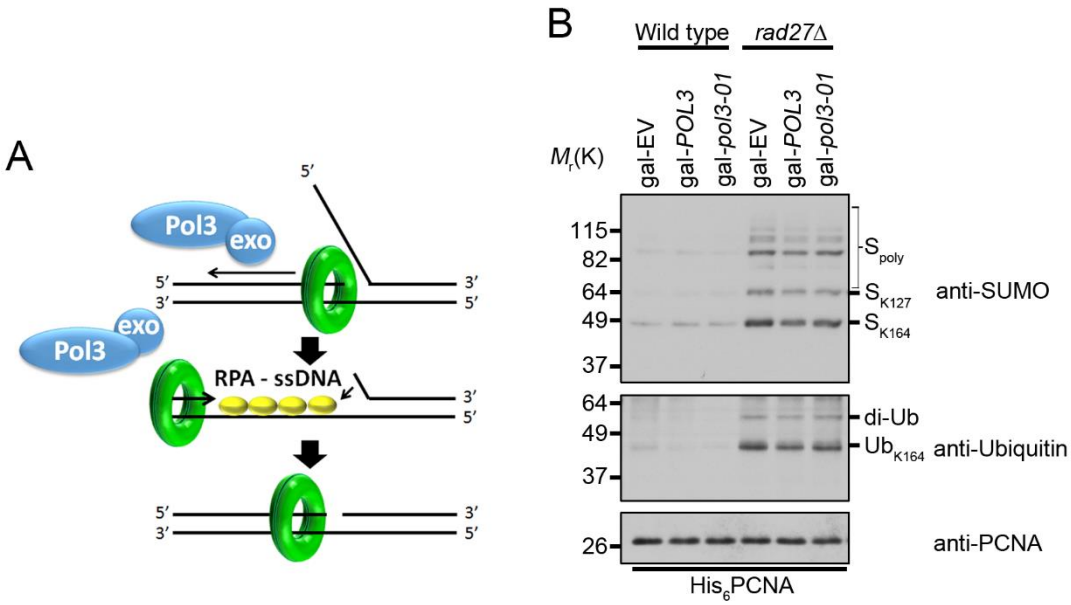
A
5′
Pol3
exo
5′
3′
3′
5′
Pol3
exo
RPA - ssDNA
3′
5′
5′
3′
3′
5′
B
Wild type
rad27Δ
gal-EV
gal-POL3
gal-pol3-01
gal-EV
gal-POL3
gal-pol3-01
Mr(K)
115
82
64
49
37
Spoly
SK127
SK164
anti-SUMO
64
49
37
di-Ub
UbK164
anti-Ubiquitin
26
anti-PCNA
His6PCNA

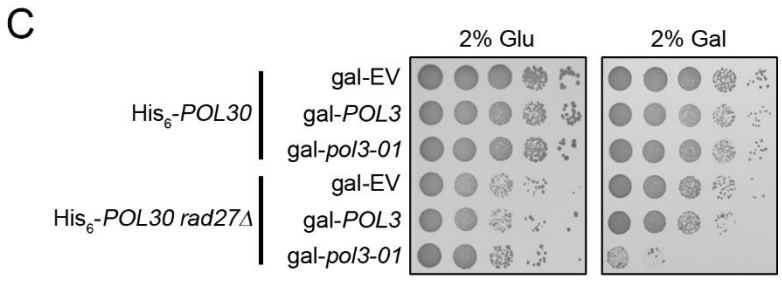
C
2% Glu
2% Gal
His6-POL30
gal-EV
gal-POL3
gal-pol3-01
His6-POL30 rad27Δ
gal-EV
gal-POL3
gal-pol3-01

Figure 3.9. Overexpression of *pol3-01* does not suppress PCNA ubiquitination in *rad27Δ*. (A) Long flaps generated in the absence of Rad27 are processed into short flaps before Pol3-exo activity resects the 3' end of the nascent DNA strand allowing for the short flap to re-anneal and form a ligatable nick. If 3' resection is extensive enough to form a ssDNA region sufficient to bind RPA we considered that this could serve as the stimulus for PCNA ubiquitination in *rad27Δ*. **(B)** Wild type and *rad27Δ* cells carrying gal-EV, gal-*POL3*, or gal-*pol3-01* plasmids were grown to OD_{600}=0.600 at 25°C in raffinose containing medium lacking tryptophan. Galactose was then added to a final concentration of 2% and the cultures were shifted to 37°C for 3 h before harvesting. His_6-PCNA was purified under denaturing conditions and analyzed by western blot with antibodies specific to PCNA, ubiquitin, and SUMO as indicated. **(C)** 10-fold serial dilutions of the indicated strains were incubated 3 days at 35°C on medium lacking tryptophan and containing either 2% glucose or 2% galactose.

Figure 3.10

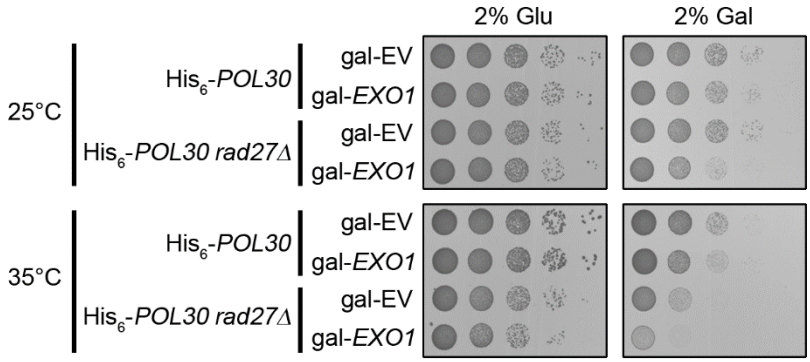

Figure 3.10. *EXO1* overexpression does not rescue the temperature sensitivity of *rad27Δ* mutants. 10-fold serial dilutions of the indicated strains were incubated 3 days at 25°C or 35°C on medium lacking uracil and containing either 2% glucose or 2% galactose.

Figure 3.11

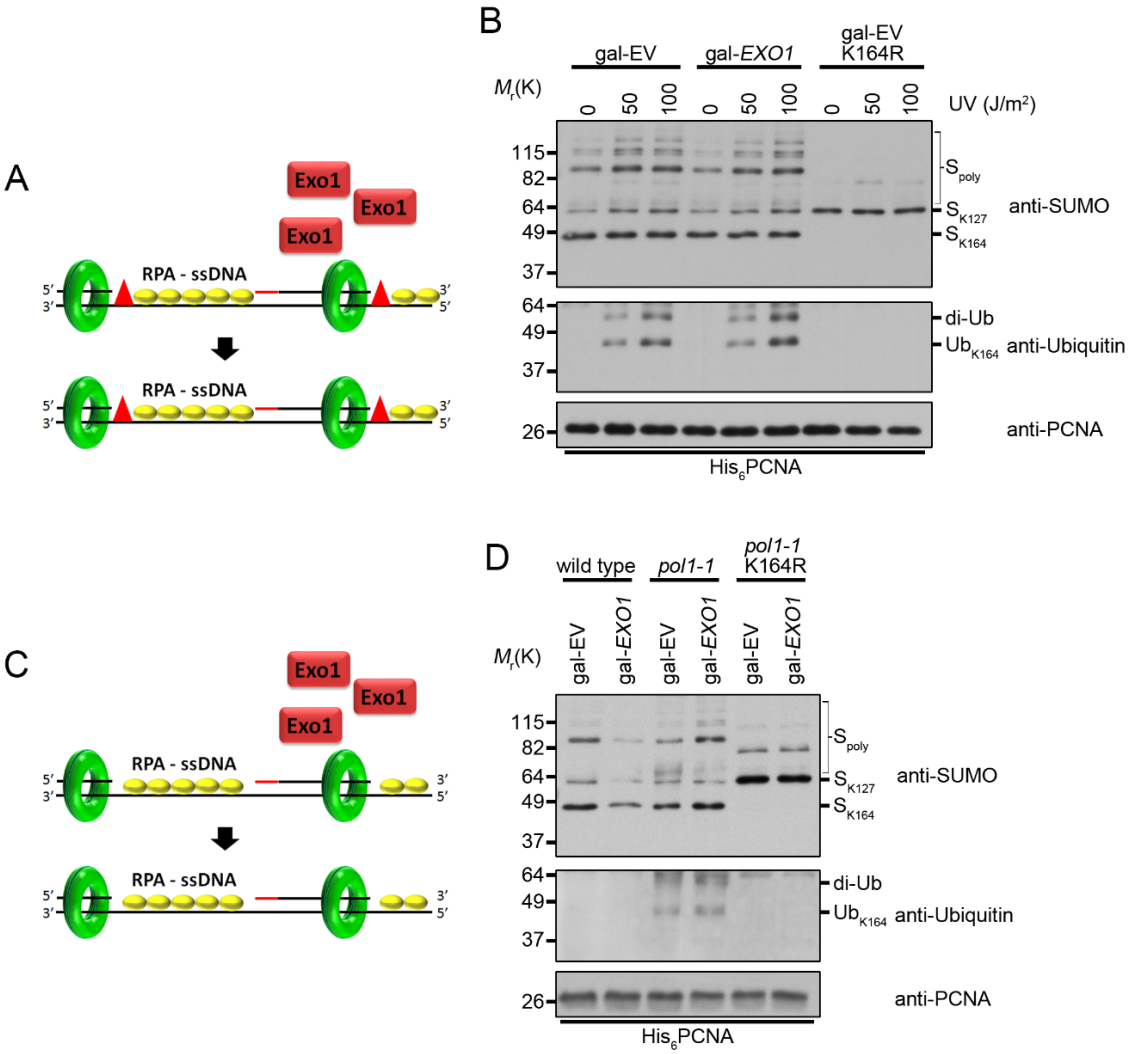
A
Exo1
Exo1
Exo1
RPA - ssDNA
5′
3′
3′
5′
RPA - ssDNA
B
gal-EV
gal-EXO1
gal-EV K164R
M_r(K)
0
50
100
0
50
100
0
50
100
UV (J/m²)
115
82
64
49
37
S_{poly}
S_{K127}
S_{K164}
anti-SUMO
64
49
37
di-Ub
Ub_{K164}
anti-Ubiquitin
26
anti-PCNA
His_6PCNA
C
Exo1
Exo1
Exo1
RPA - ssDNA
RPA - ssDNA
D
wild type
pol1-1
pol1-1 K164R
M_r(K)
gal-EV
gal-EXO1
gal-EV
gal-EXO1
gal-EV
gal-EXO1
115
82
64
49
37
S_{poly}
S_{K127}
S_{K164}
anti-SUMO
64
49
37
di-Ub
Ub_{K164}
anti-Ubiquitin
26
anti-PCNA
His_6PCNA

Figure 3.11. Overexpression of EXO1 does not alter PCNA ubiquitination under conditions that cause ssDNA gap formation. (A) UV treatment leads to the formation of ssDNA gaps in replicating cells [Lopes et al. 2006]. Overexpression of EXO1 has no impact on ssDNA gap formation. The red triangles indicate UV-induced lesions. RPA-coated ssDNA is marked as RPA-ssDNA. **(B)** Cells carrying gal-EV or gal-EXO1 plasmids were grown to OD_{600}=0.600 at 25°C in raffinose containing medium lacking uracil. Galactose was then added to a final concentration of 2% and the cells were grown an additional 2 h at 25°C. Each culture was then split into 3 parts and treated with either 0, 50, or 100 J/m^2 UV and left to recover for 40 min at 25°C before harvesting. His_6-PCNA was purified under denaturing conditions and analyzed by western blot with antibodies specific to PCNA, ubiquitin, and SUMO as indicated. **(C)** Inefficient priming along the lagging strand template leads to the formation of RPA-coated ssDNA gaps (RPA-ssDNA) in pol1 mutants [Gutiérrez and Wang 2003, Suzuki et al. 2009, Becker et al. 2014]. Overexpression of EXO1 has no impact on ssDNA gap formation. **(D)** Wild-type and pol1-1 cells carrying gal-EV or gal-EXO1 plasmids were grown to OD_{600}=0.600 at 25°C in raffinose containing medium lacking uracil. Galactose was then added to a final concentration of 2% and the cultures we shifted to 35°C for 3 h before harvesting. His_6-PCNA was purified under denaturing conditions and analyzed by western blot with antibodies specific to PCNA, ubiquitin, and SUMO as indicated.

Table 3.1

Table 3.1. SGA screen of PCNA DAmP, PCNA-WT, PCNA-K164R Cl. 1, and PCNA-K164R Cl. 2 against temperature sensitive array. Genetic interactions were scored as described in [Baryshnikova *et al.* 2010]. Only genetic interactions with epsilon scores ε<-0.09 or ε> 0.09 are included.

Query systematic name	Query standard name	Array systematic name	Array standard name	Epsilon score	p-value
PCNA-DAmP					
YBR088C	PCNA-DAmP	YJL074C	SMC3	-0.6853	0.00e+00
YBR088C	PCNA-DAmP	YGL163C	RAD54	-0.6681	8.40e-83
YBR088C	PCNA-DAmP	YFR027W	ECO1	-0.6374	3.41e-33
YBR088C	PCNA-DAmP	YAR007C	RFA1	-0.5941	5.39e-99
YBR088C	PCNA-DAmP	YFL008W	SMC1	-0.5894	0.00e+00
YBR088C	PCNA-DAmP	YOL094C	RFC4	-0.5412	0.00e+00
YBR088C	PCNA-DAmP	YML032C	RAD52	-0.5407	0.00e+00
YBR088C	PCNA-DAmP	YJR043C	POL32	-0.5395	1.41e-24
YBR088C	PCNA-DAmP	YPR085C	ASA1	-0.5196	0.00e+00
YBR088C	PCNA-DAmP	YFR004W	RPN11	-0.5158	0.00e+00
YBR088C	PCNA-DAmP	YJL074C	SMC3	-0.5127	3.26e-25
YBR088C	PCNA-DAmP	YPR135W	CTF4	-0.4709	9.70e-42
YBR088C	PCNA-DAmP	YMR076C	PDS5	-0.4588	4.07e-31
YBR088C	PCNA-DAmP	YOR259C	RPT4	-0.4526	1.56e-68
YBR088C	PCNA-DAmP	YMR224C	MRE11	-0.4476	9.07e-37
YBR088C	PCNA-DAmP	YFR004W	RPN11	-0.4173	6.43e-15

Query systematic name	Query standard name	Array systematic name	Array standard name	Epsilon score	p-value
YBR088C	PCNA-DAmP	YDL102W	POL3	-0.4111	5.26e-19
YBR088C	PCNA-DAmP	YDR180W	SCC2	-0.3927	1.85e-28
YBR088C	PCNA-DAmP	YCL061C	MRC1	-0.3659	8.19e-11
YBR088C	PCNA-DAmP	YMR190C	SGS1	-0.3483	1.56e-20
YBR088C	PCNA-DAmP	YFL008W	SMC1	-0.3351	2.04e-09
YBR088C	PCNA-DAmP	YMR198W	CIK1	-0.3332	4.62e-08
YBR088C	PCNA-DAmP	YFR052W	RPN12	-0.3317	0.00e+00
YBR088C	PCNA-DAmP	YLL002W	RTT109	-0.3298	0.00e+00
YBR088C	PCNA-DAmP	YGR092W	DBF2	-0.3246	2.72e-08
YBR088C	PCNA-DAmP	YIR011C	STS1	-0.3242	1.31e-15
YBR088C	PCNA-DAmP	YDL126C	CDC48	-0.316	3.06e-10
YBR088C	PCNA-DAmP	YHR191C	CTF8	-0.2988	3.70e-05
YBR088C	PCNA-DAmP	YPL055C	LGE1	-0.295	2.44e-04
YBR088C	PCNA-DAmP	YOR362C	PRE10	-0.2919	1.19e-07
YBR088C	PCNA-DAmP	YDL003W	MCD1	-0.2888	6.61e-09
YBR088C	PCNA-DAmP	YHR164C	DNA2	-0.2888	4.13e-21
YBR088C	PCNA-DAmP	YDL008W	APC11	-0.2883	3.46e-84
YBR088C	PCNA-DAmP	YHR191C	CTF8	-0.2755	4.29e-90
YBR088C	PCNA-DAmP	YNR003C	RPC34	-0.2726	9.44e-09
YBR088C	PCNA-DAmP	YKL113C	RAD27	-0.2688	1.25e-06
YBR088C	PCNA-DAmP	YNL064C	YDJ1	-0.2596	8.69e-04
YBR088C	PCNA-DAmP	YJL047C	RTT101	-0.2512	1.29e-05
YBR088C	PCNA-DAmP	YDL003W	MCD1	-0.2477	1.44e-06
YBR088C	PCNA-DAmP	YDL097C	RPN6	-0.2431	4.41e-05
YBR088C	PCNA-DAmP	YJR093C	FIP1	-0.2291	5.03e-08
YBR088C	PCNA-DAmP	YDR311W	TFB1	-0.2281	1.89e-05

Query systematic name	Query standard name	Array systematic name	Array standard name	Epsilon score	p-value
YBR088C	PCNA-DAmP	YDR083W	RRP8	-0.2277	6.55e-06
YBR088C	PCNA-DAmP	YPR108W	RPN7	-0.2277	8.00e-10
YBR088C	PCNA-DAmP	YOR259C	RPT4	-0.2269	7.91e-03
YBR088C	PCNA-DAmP	YMR078C	CTF18	-0.2195	8.41e-70
YBR088C	PCNA-DAmP	YHR118C	ORC6	-0.219	2.38e-03
YBR088C	PCNA-DAmP	YML028W	TSA1	-0.2186	1.63e-07
YBR088C	PCNA-DAmP	YER157W	COG3	-0.2172	6.79e-15
YBR088C	PCNA-DAmP	YHR191C	CTF8	-0.217	8.20e-06
YBR088C	PCNA-DAmP	YDR113C	PDS1	-0.2116	9.88e-06
YBR088C	PCNA-DAmP	YJL115W	ASF1	-0.2115	1.36e-04
YBR088C	PCNA-DAmP	YMR043W	MCM1	-0.2089	1.65e-20
YBR088C	PCNA-DAmP	YOR181W	LAS17	-0.2063	2.81e-139
YBR088C	PCNA-DAmP	YIL040W	APQ12	-0.1977	9.03e-03
YBR088C	PCNA-DAmP	YML065W	ORC1	-0.1926	1.97e-05
YBR088C	PCNA-DAmP	YLL004W	ORC3	-0.1915	3.06e-06
YBR088C	PCNA-DAmP	YLR452C	SST2	-0.1892	3.57e-02
YBR088C	PCNA-DAmP	YMR093W	UTP15	-0.1892	8.59e-04
YBR088C	PCNA-DAmP	YFR050C	PRE4	-0.1858	1.20e-03
YBR088C	PCNA-DAmP	YER147C	SCC4	-0.1812	4.77e-03
YBR088C	PCNA-DAmP	YLR078C	BOS1	-0.1804	0.00e+00
YBR088C	PCNA-DAmP	YER094C	PUP3	-0.1754	6.69e-17
YBR088C	PCNA-DAmP	YER147C	SCC4	-0.1737	1.33e-06
YBR088C	PCNA-DAmP	YCL016C	DCC1	-0.1729	1.15e-02
YBR088C	PCNA-DAmP	YML103C	NUP188	-0.1718	3.58e-03
YBR088C	PCNA-DAmP	YDR510W	SMT3	-0.1711	1.38e-03

Query systematic name	Query standard name	Array systematic name	Array standard name	Epsilon score	p-value
YBR088C	PCNA-DAmP	YLR007W	NSE1	-0.1699	5.87e-23
YBR088C	PCNA-DAmP	YDL102W	POL3	-0.167	1.04e-04
YBR088C	PCNA-DAmP	YDL105W	NSE4	-0.1666	1.84e-04
YBR088C	PCNA-DAmP	YHR196W	UTP9	-0.1646	1.03e-04
YBR088C	PCNA-DAmP	YNL153C	GIM3	-0.163	4.76e-02
YBR088C	PCNA-DAmP	YJR068W	RFC2	-0.1599	1.34e-02
YBR088C	PCNA-DAmP	YOR341W	RPA190	-0.1558	1.74e-04
YBR088C	PCNA-DAmP	YDR288W	NSE3	-0.1488	5.22e-03
YBR088C	PCNA-DAmP	YHR027C	RPN1	-0.1451	2.44e-08
YBR088C	PCNA-DAmP	YLR298C	YHC1	-0.1421	4.84e-03
YBR088C	PCNA-DAmP	YLR071C	RGR1	-0.1393	7.65e-11
YBR088C	PCNA-DAmP	YPR162C	ORC4	-0.1374	2.01e-02
YBR088C	PCNA-DAmP	YER125W	RSP5	-0.1369	1.16e-03
YBR088C	PCNA-DAmP	YML023C	NSE5	-0.1353	8.26e-03
YBR088C	PCNA-DAmP	YLR459W	GAB1	-0.1345	7.53e-02
YBR088C	PCNA-DAmP	YDR156W	RPA14	-0.1338	3.34e-02
YBR088C	PCNA-DAmP	YHR122W	YHR122W	-0.1299	5.73e-02
YBR088C	PCNA-DAmP	YLR119W	SRN2	-0.126	5.52e-02
YBR088C	PCNA-DAmP	YGL048C	RPT6	-0.1241	6.07e-02
YBR088C	PCNA-DAmP	YOR157C	PUP1	-0.1227	6.31e-02
YBR088C	PCNA-DAmP	YDL077C	VAM6	-0.1174	1.52e-03
YBR088C	PCNA-DAmP	YKL069W	YKL069W	-0.1172	3.44e-03
YBR088C	PCNA-DAmP	YMR281W	GPI12	-0.1159	3.90e-02
YBR088C	PCNA-DAmP	YOR260W	GCD1	-0.1131	8.78e-06
YBR088C	PCNA-DAmP	YDL105W	NSE4	-0.1118	1.22e-04
YBR088C	PCNA-DAmP	YGL022W	STT3	-0.1079	6.57e-02

Query systematic name	Query standard name	Array systematic name	Array standard name	Epsilon score	p-value
YBR088C	PCNA-DAmP	YKL035W	UGP1	-0.1071	6.00e-02
YBR088C	PCNA-DAmP	YGR264C	MES1	-0.1067	2.14e-04
YBR088C	PCNA-DAmP	YMR240C	CUS1	-0.1051	1.11e-01
YBR088C	PCNA-DAmP	YLR089C	ALT1	-0.1044	1.31e-01
YBR088C	PCNA-DAmP	YDL105W	NSE4	-0.1027	6.12e-04
YBR088C	PCNA-DAmP	YDR478W	SNM1	-0.1012	1.22e-01
YBR088C	PCNA-DAmP	YLR293C	GSP1	-0.1012	6.96e-02
YBR088C	PCNA-DAmP	YDL147W	RPN5	-0.0993	2.73e-04
YBR088C	PCNA-DAmP	YGL130W	CEG1	-0.0987	4.64e-02
YBR088C	PCNA-DAmP	YDR064W	RPS13	-0.0978	3.14e-02
YBR088C	PCNA-DAmP	YHR069C	RRP4	-0.0977	1.72e-02
YBR088C	PCNA-DAmP	YIL150C	MCM10	-0.0956	3.33e-02
YBR088C	PCNA-DAmP	YIR006C	PAN1	-0.0952	1.28e-01
YBR088C	PCNA-DAmP	YNL061W	NOP2	-0.092	7.82e-02
YBR088C	PCNA-DAmP	YGR158C	MTR3	-0.0908	4.75e-02
YBR088C	PCNA-DAmP	YFL038C	YPT1	0.0906	8.57e-02
YBR088C	PCNA-DAmP	YML102W	CAC2	0.0918	2.40e-04
YBR088C	PCNA-DAmP	YJL039C	NUP192	0.092	1.29e-04
YBR088C	PCNA-DAmP	YFL034C-B	MOB2	0.0927	1.22e-01
YBR088C	PCNA-DAmP	YKL045W	PRI2	0.0952	4.24e-02
YBR088C	PCNA-DAmP	YNL118C	DCP2	0.0964	2.06e-09
YBR088C	PCNA-DAmP	YNL041C	COG6	0.098	1.47e-15
YBR088C	PCNA-DAmP	YPL063W	TIM50	0.0982	5.60e-06
YBR088C	PCNA-DAmP	YDL217C	TIM22	0.0987	1.13e-01
YBR088C	PCNA-DAmP	YMR117C	SPC24	0.0992	7.72e-04
YBR088C	PCNA-DAmP	YGL213C	SKI8	0.1009	8.87e-06

Query systematic name	Query standard name	Array systematic name	Array standard name	Epsilon score	p-value
YBR088C	PCNA-DAmP	YDL002C	NHP10	0.1016	2.31e-02
YBR088C	PCNA-DAmP	YPL266W	DIM1	0.1016	8.75e-04
YBR088C	PCNA-DAmP	YGR270W	YTA7	0.1026	9.12e-04
YBR088C	PCNA-DAmP	YJL104W	PAM16	0.1038	1.45e-02
YBR088C	PCNA-DAmP	YLR305C	STT4	0.1053	1.14e-25
YBR088C	PCNA-DAmP	YOL001W	PHO80	0.1056	2.47e-02
YBR088C	PCNA-DAmP	YFL034C-B	MOB2	0.1066	3.78e-06
YBR088C	PCNA-DAmP	YDL030W	PRP9	0.1068	9.85e-06
YBR088C	PCNA-DAmP	YOR020C	HSP10	0.1082	2.39e-03
YBR088C	PCNA-DAmP	YDR182W	CDC1	0.1085	2.08e-14
YBR088C	PCNA-DAmP	YML069W	POB3	0.1098	3.58e-04
YBR088C	PCNA-DAmP	YIR010W	DSN1	0.1119	2.63e-03
YBR088C	PCNA-DAmP	YNL102W	POL1	0.1128	3.29e-01
YBR088C	PCNA-DAmP	YIL144W	TID3	0.113	2.60e-02
YBR088C	PCNA-DAmP	YOL081W	IRA2	0.1132	2.74e-03
YBR088C	PCNA-DAmP	YDR404C	RPB7	0.1137	1.93e-02
YBR088C	PCNA-DAmP	YHR024C	MAS2	0.1152	2.83e-148
YBR088C	PCNA-DAmP	YLR393W	ATP10	0.1157	1.61e-17
YBR088C	PCNA-DAmP	YDR240C	SNU56	0.1184	2.45e-03
YBR088C	PCNA-DAmP	YKR068C	BET3	0.1203	7.42e-03
YBR088C	PCNA-DAmP	YJR076C	CDC11	0.1217	2.42e-02
YBR088C	PCNA-DAmP	YDR182W	CDC1	0.1237	1.13e-01
YBR088C	PCNA-DAmP	YPL174C	NIP100	0.1247	1.35e-09
YBR088C	PCNA-DAmP	YJL081C	ARP4	0.1267	3.12e-04
YBR088C	PCNA-DAmP	YOR057W	SGT1	0.1273	4.66e-03

Query systematic name	Query standard name	Array systematic name	Array standard name	Epsilon score	p-value
YBR088C	PCNA-DAmP	YOL123W	HRP1	0.1349	2.76e-04
YBR088C	PCNA-DAmP	YGR119C	NUP57	0.1356	6.60e-06
YBR088C	PCNA-DAmP	YGR006W	PRP18	0.1378	3.56e-04
YBR088C	PCNA-DAmP	YKL089W	MIF2	0.1415	1.14e-08
YBR088C	PCNA-DAmP	YJR065C	ARP3	0.1473	1.61e-02
YBR088C	PCNA-DAmP	YKL112W	ABF1	0.1513	7.99e-24
YBR088C	PCNA-DAmP	YDR172W	SUP35	0.1561	1.23e-14
YBR088C	PCNA-DAmP	YPL190C	NAB3	0.165	4.47e-11
YBR088C	PCNA-DAmP	YOR236W	DFR1	0.1779	3.01e-03
PCNA-WT					
YBR088C	PCNA-WT	YDL111C	RRP42	-0.3575	3.17e-09
YBR088C	PCNA-WT	YGR195W	SKI6	-0.3298	3.66e-06
YBR088C	PCNA-WT	YDL148C	NOP14	-0.2688	9.93e-05
YBR088C	PCNA-WT	YDR156W	RPA14	-0.2205	6.14e-03
YBR088C	PCNA-WT	YHR101C	BIG1	-0.1945	3.74e-02
YBR088C	PCNA-WT	YML103C	NUP188	-0.1879	4.00e-02
YBR088C	PCNA-WT	YIL115C	NUP159	-0.1813	2.44e-02
YBR088C	PCNA-WT	YHR178W	STB5	-0.181	1.92e-02
YBR088C	PCNA-WT	YGR081C	SLX9	-0.1664	1.55e-02
YBR088C	PCNA-WT	YGR002C	SWC4	-0.1638	1.40e-01
YBR088C	PCNA-WT	YPL057C	SUR1	-0.1545	3.17e-02
YBR088C	PCNA-WT	YLR197W	NOP56	-0.1515	1.45e-01
YBR088C	PCNA-WT	YLR459W	GAB1	-0.1493	3.75e-02
YBR088C	PCNA-WT	YGL044C	RNA15	-0.1451	2.72e-02
YBR088C	PCNA-WT	YDR083W	RRP8	-0.1446	3.86e-02

Query systematic name	Query standard name	Array systematic name	Array standard name	Epsilon score	p-value
YBR088C	PCNA-WT	YIL046W	MET30	-0.1444	3.49e-02
YBR088C	PCNA-WT	YLR218C	COA4	-0.1419	6.93e-02
YBR088C	PCNA-WT	YDR280W	RRP45	-0.1409	6.86e-02
YBR088C	PCNA-WT	YNL064C	YDJ1	-0.1379	2.16e-02
YBR088C	PCNA-WT	YGR140W	CBF2	-0.1301	6.00e-02
YBR088C	PCNA-WT	YDR201W	SPC19	-0.1268	1.05e-01
YBR088C	PCNA-WT	YER161C	SPT2	-0.1266	6.14e-02
YBR088C	PCNA-WT	YOL102C	TPT1	-0.1238	1.12e-01
YBR088C	PCNA-WT	YHR118C	ORC6	-0.1228	1.14e-01
YBR088C	PCNA-WT	YDL084W	SUB2	-0.1226	1.10e-01
YBR088C	PCNA-WT	YJR042W	NUP85	-0.1209	9.54e-02
YBR088C	PCNA-WT	YJR017C	ESS1	-0.1202	6.06e-02
YBR088C	PCNA-WT	YML069W	POB3	-0.1192	7.13e-02
YBR088C	PCNA-WT	YAL011W	SWC3	-0.1184	1.03e-01
YBR088C	PCNA-WT	YJL050W	MTR4	-0.1182	5.40e-02
YBR088C	PCNA-WT	YLR276C	DBP9	-0.1175	1.05e-01
YBR088C	PCNA-WT	YGR172C	YIP1	-0.1168	9.16e-02
YBR088C	PCNA-WT	YDR331W	GPI8	-0.116	9.44e-02
YBR088C	PCNA-WT	YER092W	IES5	-0.1152	5.07e-02
YBR088C	PCNA-WT	YKL089W	MIF2	-0.1152	1.01e-01
YBR088C	PCNA-WT	YGR094W	VAS1	-0.113	1.29e-01
YBR088C	PCNA-WT	YPL169C	MEX67	-0.1104	9.30e-02
YBR088C	PCNA-WT	YDR189W	SLY1	-0.1095	9.31e-02
YBR088C	PCNA-WT	YDR331W	GPI8	-0.1092	5.80e-02
YBR088C	PCNA-WT	YJR141W	YJR141W	-0.1072	9.40e-02
YBR088C	PCNA-WT	YOL021C	DIS3	-0.1051	1.46e-01

Query systematic name	Query standard name	Array systematic name	Array standard name	Epsilon score	p-value
YBR088C	PCNA-WT	YFL008W	SMC1	-0.1048	1.21e-01
YBR088C	PCNA-WT	YHR069C	RRP4	-0.1044	1.22e-01
YBR088C	PCNA-WT	YFR004W	RPN11	-0.1043	1.55e-01
YBR088C	PCNA-WT	YLR452C	SST2	-0.1031	1.94e-01
YBR088C	PCNA-WT	YDR460W	TFB3	-0.1018	1.67e-01
YBR088C	PCNA-WT	YFL009W	CDC4	-0.1012	1.04e-01
YBR088C	PCNA-WT	YMR272C	SCS7	-0.1008	2.49e-01
YBR088C	PCNA-WT	YKL145W	RPT1	-0.0972	9.64e-02
YBR088C	PCNA-WT	YDR170C	SEC7	-0.0954	7.35e-02
YBR088C	PCNA-WT	YFL034C-B	MOB2	-0.0938	2.00e-01
YBR088C	PCNA-WT	YGR113W	DAM1	-0.0924	1.56e-01
YBR088C	PCNA-WT	YPR060C	ARO7	-0.0922	9.69e-02
YBR088C	PCNA-WT	YML069W	POB3	-0.0903	3.18e-02
YBR088C	PCNA-WT	YNL136W	EAF7	-0.0902	1.29e-01
YBR088C	PCNA-WT	YHR036W	BRL1	0.0906	6.40e-02
YBR088C	PCNA-WT	YHR058C	MED6	0.0907	9.47e-02
YBR088C	PCNA-WT	YOL034W	SMC5	0.0911	9.92e-02
YBR088C	PCNA-WT	YDR081C	PDC2	0.0914	1.77e-01
YBR088C	PCNA-WT	YER125W	RSP5	0.0917	8.08e-02
YBR088C	PCNA-WT	YDR361C	BCP1	0.0918	2.16e-02
YBR088C	PCNA-WT	YPR034W	ARP7	0.0924	2.07e-01
YBR088C	PCNA-WT	YOR020C	HSP10	0.0961	1.45e-01
YBR088C	PCNA-WT	YER094C	PUP3	0.0965	2.78e-02
YBR088C	PCNA-WT	YKL208W	CBT1	0.0972	9.18e-02
YBR088C	PCNA-WT	YMR033W	ARP9	0.0974	1.16e-01
YBR088C	PCNA-WT	YML049C	RSE1	0.0988	7.81e-02

Query systematic name	Query standard name	Array systematic name	Array standard name	Epsilon score	p-value
YBR088C	PCNA-WT	YFL039C	ACT1	0.1025	1.47e-01
YBR088C	PCNA-WT	YMR043W	MCM1	0.1042	2.40e-01
YBR088C	PCNA-WT	YPR086W	SUA7	0.1045	1.15e-01
YBR088C	PCNA-WT	YFL039C	ACT1	0.1053	9.75e-02
YBR088C	PCNA-WT	YDL105W	NSE4	0.1057	8.83e-02
YBR088C	PCNA-WT	YNR026C	SEC12	0.1086	3.49e-02
YBR088C	PCNA-WT	YDR145W	TAF12	0.1094	1.36e-01
YBR088C	PCNA-WT	YDR145W	TAF12	0.1105	1.06e-01
YBR088C	PCNA-WT	YNL002C	RLP7	0.115	7.31e-02
YBR088C	PCNA-WT	YOR074C	CDC21	0.1157	1.44e-01
YBR088C	PCNA-WT	YOR181W	LAS17	0.1157	6.32e-02
YBR088C	PCNA-WT	YDL030W	PRP9	0.1159	7.94e-02
YBR088C	PCNA-WT	YOR174W	MED4	0.1192	5.39e-02
YBR088C	PCNA-WT	YDL165W	CDC36	0.12	6.52e-02
YBR088C	PCNA-WT	YDR212W	TCP1	0.1202	1.77e-02
YBR088C	PCNA-WT	YGL247W	BRR6	0.1227	5.76e-02
YBR088C	PCNA-WT	YGL066W	SGF73	0.1339	8.92e-02
YBR088C	PCNA-WT	YDL143W	CCT4	0.138	1.52e-01
YBR088C	PCNA-WT	YOR236W	DFR1	0.1383	5.06e-02
YBR088C	PCNA-WT	YLR078C	BOS1	0.1427	8.27e-02
YBR088C	PCNA-WT	YMR005W	TAF4	0.1489	8.28e-02
YBR088C	PCNA-WT	YFL039C	ACT1	0.1503	5.46e-02
YBR088C	PCNA-WT	YPR103W	PRE2	0.162	3.56e-02
YBR088C	PCNA-WT	YPL043W	NOP4	0.1674	1.78e-01
YBR088C	PCNA-WT	YPR103W	PRE2	0.1875	2.49e-02
YBR088C	PCNA-WT	YNR003C	RPC34	0.1949	2.28e-02

Query systematic name	Query standard name	Array systematic name	Array standard name	Epsilon score	p-value
YBR088C	PCNA-WT	YDR311W	TFB1	0.2307	1.08e-02
YBR088C	PCNA-WT	YDR088C	SLU7	0.2387	1.38e-02
PCNA-K164R Cl.1					
YBR088C	PCNA-K164R Cl.1	YML028W	TSA1	-0.3623	7.30e-15
YBR088C	PCNA-K164R Cl.1	YML032C	RAD52	-0.3205	1.49e-06
YBR088C	PCNA-K164R Cl.1	YGL163C	RAD54	-0.2627	5.20e-05
YBR088C	PCNA-K164R Cl.1	YAR007C	RFA1	-0.2359	3.68e-06
YBR088C	PCNA-K164R Cl.1	YJR093C	FIP1	-0.2258	8.57e-04
YBR088C	PCNA-K164R Cl.1	YMR112C	MED11	-0.1887	2.80e-03
YBR088C	PCNA-K164R Cl.1	YKL145W	RPT1	-0.1781	1.06e-02
YBR088C	PCNA-K164R Cl.1	YFR052W	RPN12	-0.1588	6.03e-04
YBR088C	PCNA-K164R Cl.1	YER157W	COG3	-0.1581	1.24e-02
YBR088C	PCNA-K164R Cl.1	YNR043W	MVD1	-0.1565	1.09e-02
YBR088C	PCNA-K164R Cl.1	YFR028C	CDC14	-0.148	9.46e-02
YBR088C	PCNA-K164R Cl.1	YPL055C	LGE1	-0.1417	2.29e-02
YBR088C	PCNA-K164R Cl.1	YLR197W	NOP56	-0.1411	1.87e-01
YBR088C	PCNA-K164R Cl.1	YDL105W	NSE4	-0.1402	2.20e-02
YBR088C	PCNA-K164R Cl.1	YIR011C	STS1	-0.1358	4.25e-02
YBR088C	PCNA-K164R Cl.1	YDR460W	TFB3	-0.1314	1.09e-01
YBR088C	PCNA-K164R Cl.1	YMR043W	MCM1	-0.1234	2.30e-01
YBR088C	PCNA-K164R Cl.1	YOL094C	RFC4	-0.122	2.04e-05
YBR088C	PCNA-K164R Cl.1	YKL045W	PRI2	-0.1211	7.83e-02
YBR088C	PCNA-K164R Cl.1	YHR058C	MED6	-0.1182	3.25e-02
YBR088C	PCNA-K164R Cl.1	YMR076C	PDS5	-0.1179	3.91e-02
YBR088C	PCNA-K164R Cl.1	YDR288W	NSE3	-0.1172	7.17e-02

Query systematic name	Query standard name	Array systematic name	Array standard name	Epsilon score	p-value
YBR088C	PCNA-K164R Cl.1	YPR135W	CTF4	-0.1168	4.47e-03
YBR088C	PCNA-K164R Cl.1	YGL066W	SGF73	-0.116	5.90e-02
YBR088C	PCNA-K164R Cl.1	YDL105W	NSE4	-0.1156	4.29e-02
YBR088C	PCNA-K164R Cl.1	YNL102W	POL1	-0.1138	7.83e-02
YBR088C	PCNA-K164R Cl.1	YGL112C	TAF6	-0.1123	1.06e-01
YBR088C	PCNA-K164R Cl.1	YJR068W	RFC2	-0.1119	1.12e-02
YBR088C	PCNA-K164R Cl.1	YDL102W	POL3	-0.1104	8.96e-03
YBR088C	PCNA-K164R Cl.1	YLR007W	NSE1	-0.1102	3.40e-02
YBR088C	PCNA-K164R Cl.1	YOR249C	APC5	-0.1087	1.38e-01
YBR088C	PCNA-K164R Cl.1	YLR086W	SMC4	-0.1082	9.78e-02
YBR088C	PCNA-K164R Cl.1	YGR092W	DBF2	-0.1038	8.45e-02
YBR088C	PCNA-K164R Cl.1	YFR004W	RPN11	-0.1025	5.95e-02
YBR088C	PCNA-K164R Cl.1	YOL081W	IRA2	-0.0993	1.27e-01
YBR088C	PCNA-K164R Cl.1	YOR254C	SEC63	-0.0988	7.06e-02
YBR088C	PCNA-K164R Cl.1	YJL074C	SMC3	-0.0957	1.59e-01
YBR088C	PCNA-K164R Cl.1	YFL034C-B	MOB2	-0.0951	1.90e-01
YBR088C	PCNA-K164R Cl.1	YOR259C	RPT4	-0.0949	2.13e-02
YBR088C	PCNA-K164R Cl.1	YMR263W	SAP30	-0.0933	4.16e-02
YBR088C	PCNA-K164R Cl.1	YPR086W	SUA7	-0.0906	4.70e-02
YBR088C	PCNA-K164R Cl.1	YOR204W	DED1	0.09	8.11e-02
YBR088C	PCNA-K164R Cl.1	YGL045W	RIM8	0.0925	3.92e-02
YBR088C	PCNA-K164R Cl.1	YJR057W	CDC8	0.0926	9.06e-02
YBR088C	PCNA-K164R Cl.1	YML069W	POB3	0.1027	4.19e-02
YBR088C	PCNA-K164R Cl.1	YLL050C	COF1	0.1086	1.29e-01
YBR088C	PCNA-K164R Cl.1	YMR117C	SPC24	0.1166	7.05e-02
YBR088C	PCNA-K164R Cl.1	YNR003C	RPC34	0.1427	5.61e-02

Query systematic name	Query standard name	Array systematic name	Array standard name	Epsilon score	p-value
PCNA-K164R Cl. 2					
YBR088C	PCNA-K164R Cl.2	YML028W	TSA1	-0.4585	3.45e-14
YBR088C	PCNA-K164R Cl.2	YML032C	RAD52	-0.2344	6.49e-17
YBR088C	PCNA-K164R Cl.2	YPL055C	LGE1	-0.2238	2.61e-03
YBR088C	PCNA-K164R Cl.2	YAR007C	RFA1	-0.2095	6.48e-04
YBR088C	PCNA-K164R Cl.2	YGL163C	RAD54	-0.1928	1.74e-05
YBR088C	PCNA-K164R Cl.2	YFL034C-B	MOB2	-0.1806	8.62e-02
YBR088C	PCNA-K164R Cl.2	YNR043W	MVD1	-0.1781	7.76e-03
YBR088C	PCNA-K164R Cl.2	YIR011C	STS1	-0.1367	2.72e-02
YBR088C	PCNA-K164R Cl.2	YHR058C	MED6	-0.135	1.08e-02
YBR088C	PCNA-K164R Cl.2	YJR093C	FIP1	-0.1235	2.90e-02
YBR088C	PCNA-K164R Cl.2	YIL040W	APQ12	-0.1217	1.06e-01
YBR088C	PCNA-K164R Cl.2	YER157W	COG3	-0.1202	1.93e-02
YBR088C	PCNA-K164R Cl.2	YNL138W	SRV2	-0.1068	1.88e-01
YBR088C	PCNA-K164R Cl.2	YDL045C	FAD1	-0.1019	1.07e-01
YBR088C	PCNA-K164R Cl.2	YDR512C	EMI1	-0.098	1.45e-01
YBR088C	PCNA-K164R Cl.2	YPR168W	NUT2	0.1042	8.19e-02
YBR088C	PCNA-K164R Cl.2	YML069W	POB3	0.1359	3.14e-02
YBR088C	PCNA-K164R Cl.2	YMR043W	MCM1	0.1525	1.43e-01

Table 3.2

Table 3.2. SGA Screen of PCNA-K164R Cl. 1 and PCNA-K164R Cl. 2 against full genome array. Genetic interactions were scored as described in [Baryshnikova *et al.* 2010]. Only genetic interactions with epsilon scores ε<-0.09 or ε> 0.09 are included.

Query systematic name	Query standard name	Array systematic name	Array standard name	Epsilon score	p-value
PCNA-K164R Cl. 1					
YBR088C	PCNA-K164R Cl.1	YJR011C	YJR011C	-0.3077	6.46e-03
YBR088C	PCNA-K164R Cl.1	YER095W	RAD51	-0.2747	5.39e-46
YBR088C	PCNA-K164R Cl.1	YDR004W	RAD57	-0.2692	1.55e-08
YBR088C	PCNA-K164R Cl.1	YAR029W	YAR029W	-0.2662	3.32e-03
YBR088C	PCNA-K164R Cl.1	YDR076W	RAD55	-0.2634	5.56e-07
YBR088C	PCNA-K164R Cl.1	YML028W	TSA1	-0.2481	7.51e-11
YBR088C	PCNA-K164R Cl.1	YGL163C	RAD54	-0.2476	2.76e-09
YBR088C	PCNA-K164R Cl.1	YER173W	RAD24	-0.2282	8.71e-55
YBR088C	PCNA-K164R Cl.1	YHL033C	RPL8A	-0.2262	2.18e-02
YBR088C	PCNA-K164R Cl.1	YOR368W	RAD17	-0.2147	2.79e-145
YBR088C	PCNA-K164R Cl.1	YOR144C	ELG1	-0.2074	8.23e-18
YBR088C	PCNA-K164R Cl.1	YPL213W	LEA1	-0.1924	9.79e-02
YBR088C	PCNA-K164R Cl.1	YHR046C	INM1	-0.1921	1.25e-01
YBR088C	PCNA-K164R Cl.1	YLR028C	ADE16	-0.1876	9.60e-02
YBR088C	PCNA-K164R Cl.1	YPL194W	DDC1	-0.1871	2.11e-05
YBR088C	PCNA-K164R Cl.1	YDR359C	EAF1	-0.1636	3.48e-04

Query systematic name	Query standard name	Array systematic name	Array standard name	Epsilon score	p-value
YBR088C	PCNA-K164R Cl.1	YER166W	DNF1	-0.1636	1.53e-01
YBR088C	PCNA-K164R Cl.1	YML032C	RAD52	-0.1571	4.95e-07
YBR088C	PCNA-K164R Cl.1	YMR198W	CIK1	-0.1511	0.00e+00
YBR088C	PCNA-K164R Cl.1	YOR311C	DGK1	-0.1507	2.34e-01
YBR088C	PCNA-K164R Cl.1	YPL022W	RAD1	-0.1484	1.83e-01
YBR088C	PCNA-K164R Cl.1	YGL007W	BRP1	-0.1435	1.14e-12
YBR088C	PCNA-K164R Cl.1	YGL212W	VAM7	-0.1391	5.33e-04
YBR088C	PCNA-K164R Cl.1	YIL035C	CKA1	-0.1373	7.94e-02
YBR088C	PCNA-K164R Cl.1	YLR131C	ACE2	-0.1367	2.14e-02
YBR088C	PCNA-K164R Cl.1	YLL023C	POM33	-0.1342	2.56e-01
YBR088C	PCNA-K164R Cl.1	YLR448W	RPL6B	-0.132	7.74e-02
YBR088C	PCNA-K164R Cl.1	YML020W	YML020W	-0.1253	6.69e-03
YBR088C	PCNA-K164R Cl.1	YML007W	YAP1	-0.12	7.58e-03
YBR088C	PCNA-K164R Cl.1	YJL117W	PHO86	-0.1187	1.04e-01
YBR088C	PCNA-K164R Cl.1	YIR002C	MPH1	-0.1174	9.41e-03
YBR088C	PCNA-K164R Cl.1	YOR033C	EXO1	-0.1108	1.94e-02
YBR088C	PCNA-K164R Cl.1	YOL067C	RTG1	-0.1105	9.15e-04
YBR088C	PCNA-K164R Cl.1	YOR334W	MRS2	-0.1095	8.74e-02
YBR088C	PCNA-K164R Cl.1	YDR279W	RNH202	-0.1083	6.31e-02
YBR088C	PCNA-K164R Cl.1	YDL062W	YDL062W	-0.106	2.11e-02
YBR088C	PCNA-K164R Cl.1	YPR045C	THP3	-0.1034	1.60e-02
YBR088C	PCNA-K164R Cl.1	YJR074W	MOG1	-0.103	1.92e-02
YBR088C	PCNA-K164R Cl.1	YPL226W	NEW1	-0.1023	2.03e-01
YBR088C	PCNA-K164R Cl.1	YDL136W	RPL35B	-0.0995	5.14e-02
YBR088C	PCNA-K164R Cl.1	YGR146C	ECL1	-0.0993	9.23e-08
YBR088C	PCNA-K164R Cl.1	YGL066W	SGF73	-0.0972	1.08e-01

Query systematic name	Query standard name	Array systematic name	Array standard name	Epsilon score	p-value
YBR088C	PCNA-K164R Cl.1	YDR217C	RAD9	-0.0957	5.13e-02
YBR088C	PCNA-K164R Cl.1	YLR404W	FLD1	-0.0941	2.12e-01
YBR088C	PCNA-K164R Cl.1	YPR043W	RPL43A	-0.0928	7.97e-02
YBR088C	PCNA-K164R Cl.1	YKL114C	APN1	-0.0926	3.50e-05
YBR088C	PCNA-K164R Cl.1	YGL180W	ATG1	-0.0923	1.71e-01
YBR088C	PCNA-K164R Cl.1	YNL091W	NST1	-0.092	1.98e-02
YBR088C	PCNA-K164R Cl.1	YPL069C	BTS1	-0.0913	8.58e-29
YBR088C	PCNA-K164R Cl.1	YKL087C	CYT2	-0.09	1.18e-01
YBR088C	PCNA-K164R Cl.1	YDR453C	TSA2	0.0909	4.53e-02
YBR088C	PCNA-K164R Cl.1	YDR445C	YDR445C	0.0925	4.03e-02
YBR088C	PCNA-K164R Cl.1	YOR084W	LPX1	0.094	8.84e-02
YBR088C	PCNA-K164R Cl.1	YFR023W	PES4	0.0955	3.21e-07
YBR088C	PCNA-K164R Cl.1	YJL133W	MRS3	0.0957	9.85e-06
YBR088C	PCNA-K164R Cl.1	YDL077C	VAM6	0.0963	5.43e-02
YBR088C	PCNA-K164R Cl.1	YER097W	YER097W	0.0975	9.89e-03
YBR088C	PCNA-K164R Cl.1	YPL140C	MKK2	0.0993	3.04e-02
YBR088C	PCNA-K164R Cl.1	YER087C-A	YER087C-A	0.0997	8.22e-02
YBR088C	PCNA-K164R Cl.1	YFL015C	YFL015C	0.1048	1.42e-36
YBR088C	PCNA-K164R Cl.1	YGR097W	ASK10	0.1075	1.55e-01
YBR088C	PCNA-K164R Cl.1	YER088C	DOT6	0.1088	3.37e-02
YBR088C	PCNA-K164R Cl.1	YGR049W	SCM4	0.1099	4.38e-02
YBR088C	PCNA-K164R Cl.1	YPL174C	NIP100	0.1111	1.84e-03
YBR088C	PCNA-K164R Cl.1	YDR446W	ECM11	0.1123	1.96e-02
YBR088C	PCNA-K164R Cl.1	YJR054W	YJR054W	0.1129	7.21e-08
YBR088C	PCNA-K164R Cl.1	YFR011C	AIM13	0.1154	3.46e-02
YBR088C	PCNA-K164R Cl.1	YFL019C	YFL019C	0.1263	5.20e-08

Query systematic name	Query standard name	Array systematic name	Array standard name	Epsilon score	p-value
YBR088C	PCNA-K164R Cl.1	YER179W	DMC1	0.1382	3.56e-03
YBR088C	PCNA-K164R Cl.1	YLR206W	ENT2	0.1385	1.45e-03
YBR088C	PCNA-K164R Cl.1	YDR046C	BAP3	0.1606	3.47e-06
YBR088C	PCNA-K164R Cl.1	YDR258C	HSP78	0.1618	1.50e-12
PCNA-K164R Cl. 2					
YBR088C	PCNA-K164R Cl.2	YGL163C	RAD54	-0.4341	1.61e-27
YBR088C	PCNA-K164R Cl.2	YER095W	RAD51	-0.3619	3.19e-19
YBR088C	PCNA-K164R Cl.2	YGR050C	YGR050C	-0.284	8.56e-02
YBR088C	PCNA-K164R Cl.2	YPL194W	DDC1	-0.2793	4.41e-11
YBR088C	PCNA-K164R Cl.2	YML032C	RAD52	-0.2685	1.31e-08
YBR088C	PCNA-K164R Cl.2	YOR368W	RAD17	-0.2527	4.97e-08
YBR088C	PCNA-K164R Cl.2	YER173W	RAD24	-0.2377	5.76e-81
YBR088C	PCNA-K164R Cl.2	YDR076W	RAD55	-0.2196	1.36e-46
YBR088C	PCNA-K164R Cl.2	YPL055C	LGE1	-0.2086	1.04e-34
YBR088C	PCNA-K164R Cl.2	YML020W	YML020W	-0.18	6.03e-07
YBR088C	PCNA-K164R Cl.2	YDR004W	RAD57	-0.1691	1.75e-05
YBR088C	PCNA-K164R Cl.2	YIL146C	ATG32	-0.1686	1.77e-03
YBR088C	PCNA-K164R Cl.2	YML028W	TSA1	-0.1668	3.09e-03
YBR088C	PCNA-K164R Cl.2	YIR002C	MPH1	-0.1613	2.44e-05
YBR088C	PCNA-K164R Cl.2	YDR274C	YDR274C	-0.1603	7.36e-49
YBR088C	PCNA-K164R Cl.2	YAL015C	NTG1	-0.1576	9.89e-03
YBR088C	PCNA-K164R Cl.2	YLR278C	YLR278C	-0.1555	1.42e-02
YBR088C	PCNA-K164R Cl.2	YLR089C	ALT1	-0.1507	5.92e-09
YBR088C	PCNA-K164R Cl.2	YHL020C	OPI1	-0.1506	1.26e-02
YBR088C	PCNA-K164R Cl.2	YOR182C	RPS30B	-0.1471	4.92e-02

Query systematic name	Query standard name	Array systematic name	Array standard name	Epsilon score	p-value
YBR088C	PCNA-K164R Cl.2	YDR123C	INO2	-0.1459	3.98e-02
YBR088C	PCNA-K164R Cl.2	YPR151C	SUE1	-0.1454	2.64e-32
YBR088C	PCNA-K164R Cl.2	YMR039C	SUB1	-0.1441	2.83e-03
YBR088C	PCNA-K164R Cl.2	YMR123W	PKR1	-0.1411	7.13e-03
YBR088C	PCNA-K164R Cl.2	YGL244W	RTF1	-0.1374	1.61e-02
YBR088C	PCNA-K164R Cl.2	YPL001W	HAT1	-0.1358	2.53e-07
YBR088C	PCNA-K164R Cl.2	YDR217C	RAD9	-0.132	6.09e-03
YBR088C	PCNA-K164R Cl.2	YJR146W	YJR146W	-0.1307	1.60e-05
YBR088C	PCNA-K164R Cl.2	YPR141C	KAR3	-0.1296	8.35e-02
YBR088C	PCNA-K164R Cl.2	YML095C	RAD10	-0.1295	6.30e-02
YBR088C	PCNA-K164R Cl.2	YDL192W	ARF1	-0.1279	2.60e-02
YBR088C	PCNA-K164R Cl.2	YMR157C	AIM36	-0.1277	1.13e-03
YBR088C	PCNA-K164R Cl.2	YJR119C	JHD2	-0.1234	1.65e-07
YBR088C	PCNA-K164R Cl.2	YDR402C	DIT2	-0.118	5.12e-03
YBR088C	PCNA-K164R Cl.2	YKR099W	BAS1	-0.1152	1.96e-09
YBR088C	PCNA-K164R Cl.2	YMR307W	GAS1	-0.1148	7.44e-21
YBR088C	PCNA-K164R Cl.2	YJR054W	YJR054W	-0.1123	8.71e-02
YBR088C	PCNA-K164R Cl.2	YNL097C	PHO23	-0.1111	1.61e-03
YBR088C	PCNA-K164R Cl.2	YIL035C	CKA1	-0.1102	4.36e-02
YBR088C	PCNA-K164R Cl.2	YLL059C	YLL059C	-0.1089	5.00e-02
YBR088C	PCNA-K164R Cl.2	YDL180W	YDL180W	-0.108	7.49e-07
YBR088C	PCNA-K164R Cl.2	YMR174C	PAI3	-0.1041	3.38e-02
YBR088C	PCNA-K164R Cl.2	YPL178W	CBC2	-0.104	1.74e-01
YBR088C	PCNA-K164R Cl.2	YGL256W	ADH4	-0.102	1.85e-03
YBR088C	PCNA-K164R Cl.2	YJR139C	HOM6	-0.1012	1.17e-01
YBR088C	PCNA-K164R Cl.2	YKL006W	RPL14A	-0.1	6.90e-03

Query systematic name	Query standard name	Array systematic name	Array standard name	Epsilon score	p-value
YBR088C	PCNA-K164R Cl.2	YMR182C	RGM1	-0.0995	1.81e-06
YBR088C	PCNA-K164R Cl.2	YPR135W	CTF4	-0.0995	4.26e-02
YBR088C	PCNA-K164R Cl.2	YPL174C	NIP100	-0.0993	2.32e-03
YBR088C	PCNA-K164R Cl.2	YDL082W	RPL13A	-0.0982	8.26e-07
YBR088C	PCNA-K164R Cl.2	YIR020W-B	YOR198C	-0.0982	5.04e-03
YBR088C	PCNA-K164R Cl.2	YDR149C	YDR149C	-0.0973	2.29e-02
YBR088C	PCNA-K164R Cl.2	YLR434C	YLR434C	-0.0969	6.11e-03
YBR088C	PCNA-K164R Cl.2	YKL114C	APN1	-0.0936	2.55e-02
YBR088C	PCNA-K164R Cl.2	YPR045C	THP3	-0.0924	8.29e-02
YBR088C	PCNA-K164R Cl.2	YJL116C	NCA3	-0.0902	2.24e-02
YBR088C	PCNA-K164R Cl.2	YKR082W	NUP133	0.09	1.26e-04
YBR088C	PCNA-K164R Cl.2	YNL032W	SIW14	0.0921	1.20e-01
YBR088C	PCNA-K164R Cl.2	YGL259W	YPS5	0.0929	5.46e-03
YBR088C	PCNA-K164R Cl.2	YLR395C	COX8	0.0946	6.19e-02
YBR088C	PCNA-K164R Cl.2	YJL098W	SAP185	0.0969	1.24e-03
YBR088C	PCNA-K164R Cl.2	YNL136W	EAF7	0.0981	3.62e-02
YBR088C	PCNA-K164R Cl.2	YDR080W	VPS41	0.099	1.03e-01
YBR088C	PCNA-K164R Cl.2	YDR024W	FYV1	0.1008	1.12e-01
YBR088C	PCNA-K164R Cl.2	YNL082W	PMS1	0.1012	2.10e-01
YBR088C	PCNA-K164R Cl.2	YDR392W	SPT3	0.1016	1.86e-01
YBR088C	PCNA-K164R Cl.2	YGL257C	MNT2	0.103	9.31e-04
YBR088C	PCNA-K164R Cl.2	YJL036W	SNX4	0.1041	1.11e-03
YBR088C	PCNA-K164R Cl.2	YML081C-A	ATP18	0.1045	1.91e-01
YBR088C	PCNA-K164R Cl.2	YGL195W	GCN1	0.1053	9.94e-02
YBR088C	PCNA-K164R Cl.2	YJR077C	MIR1	0.1094	8.47e-02
YBR088C	PCNA-K164R Cl.2	YOR083W	WHI5	0.1103	2.03e-01

Query systematic name	Query standard name	Array systematic name	Array standard name	Epsilon score	p-value
YBR088C	PCNA-K164R Cl.2	YOR078W	BUD21	0.1224	6.82e-02
YBR088C	PCNA-K164R Cl.2	YOR311C	DGK1	0.1314	1.03e-01
YBR088C	PCNA-K164R Cl.2	YDR162C	NBP2	0.1371	3.84e-03
YBR088C	PCNA-K164R Cl.2	YGR270W	YTA7	0.1373	3.54e-07
YBR088C	PCNA-K164R Cl.2	YJR053W	BFA1	0.1435	1.33e-05
YBR088C	PCNA-K164R Cl.2	YHL033C	RPL8A	0.1453	1.71e-01
YBR088C	PCNA-K164R Cl.2	YGR027C	RPS25A	0.1527	5.09e-03
YBR088C	PCNA-K164R Cl.2	YJL188C	BUD19	0.1529	5.24e-02
YBR088C	PCNA-K164R Cl.2	YKR043C	SHB17	0.1555	8.38e-08
YBR088C	PCNA-K164R Cl.2	YNL085W	MKT1	0.1592	1.35e-01
YBR088C	PCNA-K164R Cl.2	YML063W	RPS1B	0.1706	1.76e-02
YBR088C	PCNA-K164R Cl.2	YML010C-B	YDR033W	0.2185	0.00e+00
YBR088C	PCNA-K164R Cl.2	YPR044C	OPI11	0.2298	1.84e-11
YBR088C	PCNA-K164R Cl.2	YMR233W	TRI1	0.2616	1.06e-07

Table 3.3

	PCNA-DAmP	PCNA-WT	PCNA-K164R Cl. 1	PCNA-K164R Cl. 2
elg1Δ	0.551	-0.023	0.356	0.262
pol3-1	0.511	-0.018	0.300	0.267
rfc5-DAmP	0.494	0.041	0.296	0.190
rad27Δ	0.416	-0.077	0.325	0.268
pol31-PH	0.362	-0.058	0.375	0.269
pol1-2	0.300	0.045	0.170	0.147
rad5Δ	0.215	-0.029	0.287	0.288

Table 3.3. Lagging strand replication mutants that correlate strongly with PCNA-DAmP and PCNA-K164R. PCC values for mutant alleles of lagging strand replication genes with TS array signatures that correlated strongly with PCNA-DAmP, PCNA-K164R Cl. 1, and PCNA-K164R Cl.2.

Table 3.4.

Table 3.4. Full results of gene ontology analysis of FG array.

GO Term	Set	Expected	Fold Enrichment	1 Sided Fisher (p-value)
BIOLOGICAL PROCESS				
leading strand elongation	5 of 36 (13.9%)	0.08	61.54	5.52e-09
DNA strand elongation involved in DNA replication	6 of 36 (16.7%)	0.22	27.69	4.19e-08
DNA strand elongation	6 of 36 (16.7%)	0.23	26.59	5.48e-08
DNA replication, removal of RNA primer	4 of 36 (11.1%)	0.06	63.30	1.92e-07
mismatch repair	5 of 36 (13.9%)	0.15	32.58	2.57e-07
DNA replication	9 of 36 (25.0%)	1.04	8.67	4.94e-07
DNA replication, Okazaki fragment processing	4 of 36 (11.1%)	0.08	49.23	6.83e-07
postreplication repair	5 of 36 (13.9%)	0.21	24.08	1.35e-06
lagging strand elongation	4 of 36 (11.1%)	0.12	34.09	3.78e-06
base-excision repair	4 of 36 (11.1%)	0.12	34.09	3.78e-06
DNA repair	10 of 36 (27.8%)	1.78	5.62	5.68e-06
DNA-dependent DNA replication	7 of 36 (19.4%)	0.75	9.34	6.72e-06
RNA-dependent DNA replication	4 of 36 (11.1%)	0.15	26.07	1.23e-05
response to DNA damage stimulus	10 of 36 (27.8%)	2.07	4.84	2.17e-05
cellular response to stress	13 of 36 (36.1%)	3.84	3.39	4.41e-05

GO Term	Set	Expected	Fold Enrichment	1 Sided Fisher (p-value)
DNA metabolic process	11 of 36 (30.6%)	3.10	3.55	0.000136
response to stress	14 of 36 (38.9%)	4.98	2.81	0.000162
DNA biosynthetic process	3 of 36 (8.3%)	0.14	22.16	0.000285
double-strand break repair	5 of 36 (13.9%)	0.66	7.59	0.000434
cellular response to stimulus	14 of 36 (38.9%)	5.89	2.38	0.000951
response to stimulus	16 of 36 (44.4%)	7.49	2.14	0.00115
error-prone translesion synthesis	2 of 36 (5.6%)	0.09	22.16	0.00341
nucleotide-excision repair	3 of 36 (8.3%)	0.34	8.75	0.00459
regulation of biological quality	8 of 36 (22.2%)	2.74	2.92	0.00467
translesion synthesis	2 of 36 (5.6%)	0.11	18.46	0.00494
sister chromatid cohesion	3 of 36 (8.3%)	0.37	8.11	0.00569
RNA catabolic process	4 of 36 (11.1%)	0.74	5.40	0.00593
homeostatic process	6 of 36 (16.7%)	1.72	3.50	0.00636
intracellular accumulation of glycerol	1 of 36 (2.8%)	0.01	110.78	0.00903
cellular magnesium ion homeostasis	1 of 36 (2.8%)	0.01	110.78	0.00903
magnesium ion homeostasis	1 of 36 (2.8%)	0.01	110.78	0.00903
base-excision repair, base-free sugar-phosphate removal	1 of 36 (2.8%)	0.01	110.78	0.00903
peptide pheromone export	1 of 36 (2.8%)	0.01	110.78	0.00903
peptide hormone secretion	1 of 36 (2.8%)	0.01	110.78	0.00903
peptide secretion	1 of 36 (2.8%)	0.01	110.78	0.00903

GO Term	Set	Expected	Fold Enrichment	1 Sided Fisher (p-value)
hormone secretion	1 of 36 (2.8%)	0.01	110.78	0.00903
hormone transport	1 of 36 (2.8%)	0.01	110.78	0.00903
signal release	1 of 36 (2.8%)	0.01	110.78	0.00903
regulation of hormone levels	1 of 36 (2.8%)	0.01	110.78	0.00903
generation of a signal involved in cell-cell signaling	1 of 36 (2.8%)	0.01	110.78	0.00903
cell-cell signaling	1 of 36 (2.8%)	0.01	110.78	0.00903
base-excision repair, gap-filling	1 of 36 (2.8%)	0.01	110.78	0.00903
glycerol-3-phosphate catabolic process	1 of 36 (2.8%)	0.02	55.39	0.018
mitochondrial respiratory chain complex II assembly	1 of 36 (2.8%)	0.02	55.39	0.018
respiratory chain complex II assembly	1 of 36 (2.8%)	0.02	55.39	0.018
mitochondrial respiratory chain complex II biogenesis	1 of 36 (2.8%)	0.02	55.39	0.018
gene conversion at mating-type locus, DNA repair synthesis	1 of 36 (2.8%)	0.02	55.39	0.018
cellular response to water deprivation	1 of 36 (2.8%)	0.02	55.39	0.018
response to water deprivation	1 of 36 (2.8%)	0.02	55.39	0.018
DNA replication proofreading	1 of 36 (2.8%)	0.02	55.39	0.018
nucleotide-excision repair, DNA gap filling	1 of 36 (2.8%)	0.02	55.39	0.018
glycerol-3-phosphate metabolic process	1 of 36 (2.8%)	0.03	36.93	0.0268
response to singlet oxygen	1 of 36 (2.8%)	0.03	36.93	0.0268
free ubiquitin chain polymerization	1 of 36 (2.8%)	0.03	36.93	0.0268
negative regulation of ubiquitin-protein ligase activity involved in mitotic cell cycle	1 of 36 (2.8%)	0.03	36.93	0.0268

GO Term	Set	Expected	Fold Enrichment	1 Sided Fisher (p-value)
cellular macromolecule catabolic process	6 of 36 (16.7%)	2.41	2.49	0.0303
nucleobase-containing compound catabolic process	5 of 36 (13.9%)	1.79	2.80	0.0309
cellular response to abiotic stimulus	2 of 36 (5.6%)	0.30	6.71	0.0351
DNA synthesis involved in DNA repair	1 of 36 (2.8%)	0.04	27.69	0.0356
regulation of ubiquitin homeostasis	1 of 36 (2.8%)	0.04	27.69	0.0356
ubiquitin homeostasis	1 of 36 (2.8%)	0.04	27.69	0.0356
cellular response to water stimulus	1 of 36 (2.8%)	0.04	27.69	0.0356
response to water stimulus	1 of 36 (2.8%)	0.04	27.69	0.0356
negative regulation of ubiquitin-protein ligase activity	1 of 36 (2.8%)	0.04	27.69	0.0356
negative regulation of protein ubiquitination	1 of 36 (2.8%)	0.04	27.69	0.0356
negative regulation of ligase activity	1 of 36 (2.8%)	0.04	27.69	0.0356
exocyst assembly	1 of 36 (2.8%)	0.04	27.69	0.0356
aromatic compound catabolic process	5 of 36 (13.9%)	1.90	2.64	0.0384
macromolecule catabolic process	6 of 36 (16.7%)	2.56	2.34	0.0393
cellular macromolecule biosynthetic process	14 of 36 (38.9%)	8.87	1.58	0.0407
macromolecule biosynthetic process	14 of 36 (38.9%)	8.92	1.57	0.0423
cellular nitrogen compound catabolic process	5 of 36 (13.9%)	1.95	2.56	0.0426
protein ubiquitination	3 of 36 (8.3%)	0.79	3.82	0.0427
double-strand break repair via homologous recombination	2 of 36 (5.6%)	0.33	5.99	0.0433
heterocycle catabolic process	5 of 36 (13.9%)	1.96	2.55	0.0433

GO Term	Set	Expected	Fold Enrichment	1 Sided Fisher (p-value)
phosphorelay signal transduction system	1 of 36 (2.8%)	0.05	22.16	0.0443
regulation of transcription from RNA polymerase II promoter in response to oxidative stress	1 of 36 (2.8%)	0.05	22.16	0.0443
regulation of ubiquitin-protein ligase activity involved in mitotic cell cycle	1 of 36 (2.8%)	0.05	22.16	0.0443
exocyst localization	1 of 36 (2.8%)	0.05	22.16	0.0443
organic cyclic compound catabolic process	5 of 36 (13.9%)	1.99	2.52	0.0455
nucleic acid metabolic process	15 of 36 (41.7%)	9.91	1.51	0.0466
response to oxygen-containing compound	2 of 36 (5.6%)	0.35	5.68	0.0476
catabolic process	10 of 36 (27.8%)	5.71	1.75	0.0485
secretion	2 of 36 (5.6%)	0.36	5.54	0.0499
secretion by cell	2 of 36 (5.6%)	0.36	5.54	0.0499
DEPLETED				
gene expression	4 of 36 (11.1%)	9.82	0.41	0.0168
single-organism metabolic process	3 of 36 (8.3%)	8.02	0.37	0.0261
protein metabolic process	4 of 36 (11.1%)	9.13	0.44	0.0303
RNA processing	0 of 36 (0.0%)	3.20	0.00	0.0347
cellular protein metabolic process	4 of 36 (11.1%)	8.68	0.46	0.0432
MOLECULAR FUNCTION				
exonuclease activity	5 of 36 (13.9%)	0.23	21.30	2.58e-06

GO Term	Set	Expected	Fold Enrichment	1 Sided Fisher (p-value)
single-stranded DNA specific 3'-5' exodeoxyribonuclease activity	3 of 36 (8.3%)	0.04	83.08	2.69e-06
single-stranded DNA specific exodeoxyribonuclease activity	3 of 36 (8.3%)	0.04	83.08	2.69e-06
DNA-directed DNA polymerase activity	4 of 36 (11.1%)	0.14	29.54	7.12e-06
DNA polymerase activity	4 of 36 (11.1%)	0.14	29.54	7.12e-06
3'-5'-exodeoxyribonuclease activity	3 of 36 (8.3%)	0.05	55.39	1.33e-05
exodeoxyribonuclease activity, producing 5'-phosphomonoesters	3 of 36 (8.3%)	0.06	47.48	2.31e-05
exodeoxyribonuclease activity	3 of 36 (8.3%)	0.07	41.54	3.67e-05
nucleotidyltransferase activity	5 of 36 (13.9%)	0.45	11.08	7.11e-05
deoxyribonuclease activity	4 of 36 (11.1%)	0.23	17.04	7.26e-05
DNA binding	11 of 36 (30.6%)	3.42	3.22	0.000332
nuclease activity	5 of 36 (13.9%)	0.62	8.03	0.000333
3'-5' exonuclease activity	3 of 36 (8.3%)	0.14	20.77	0.000349
exonuclease activity, active with either ribo- or deoxyribonucleic acids and producing 5'-phosphomonoesters	3 of 36 (8.3%)	0.14	20.77	0.000349
DNA clamp loader activity	2 of 36 (5.6%)	0.04	55.39	0.00047
protein-DNA loading ATPase activity	2 of 36 (5.6%)	0.04	55.39	0.00047
5'-3' exonuclease activity	2 of 36 (5.6%)	0.05	44.31	0.000779
DNA-dependent ATPase activity	3 of 36 (8.3%)	0.42	7.22	0.00786
deoxycytidyl transferase activity	1 of 36 (2.8%)	0.01	110.78	0.00903
ubiquitin-protein ligase inhibitor activity	1 of 36 (2.8%)	0.01	110.78	0.00903

GO Term	Set	Expected	Fold Enrichment	1 Sided Fisher (p-value)
ligase inhibitor activity	1 of 36 (2.8%)	0.01	110.78	0.00903
endopeptidase activator activity	1 of 36 (2.8%)	0.01	110.78	0.00903
hydrolase activity, acting on ester bonds	6 of 36 (16.7%)	1.87	3.21	0.00958
nucleic acid binding	12 of 36 (33.3%)	6.26	1.92	0.0151
damaged DNA binding	2 of 36 (5.6%)	0.20	10.07	0.0163
glycerol-3-phosphate dehydrogenase [NAD+] activity	1 of 36 (2.8%)	0.02	55.39	0.018
lysophospholipase activity	1 of 36 (2.8%)	0.02	55.39	0.018
peptidase activator activity	1 of 36 (2.8%)	0.02	55.39	0.018
GTP-Rho binding	1 of 36 (2.8%)	0.02	55.39	0.018
hydrolase activity	11 of 36 (30.6%)	5.89	1.87	0.0247
magnesium ion transmembrane transporter activity	1 of 36 (2.8%)	0.03	36.93	0.0268
peptide-transporting ATPase activity	1 of 36 (2.8%)	0.03	36.93	0.0268
four-way junction helicase activity	1 of 36 (2.8%)	0.03	36.93	0.0268
Y-form DNA binding	1 of 36 (2.8%)	0.03	36.93	0.0268
ATPase activity, coupled	4 of 36 (11.1%)	1.16	3.43	0.0276
phosphorelay response regulator activity	1 of 36 (2.8%)	0.04	27.69	0.0356
ubiquitin-protein ligase regulator activity	1 of 36 (2.8%)	0.04	27.69	0.0356
ligase regulator activity	1 of 36 (2.8%)	0.04	27.69	0.0356
endopeptidase regulator activity	1 of 36 (2.8%)	0.04	27.69	0.0356
Rho GTPase binding	1 of 36 (2.8%)	0.04	27.69	0.0356
5'-flap endonuclease activity	1 of 36 (2.8%)	0.05	22.16	0.0443

GO Term	Set	Expected	Fold Enrichment	1 Sided Fisher (p-value)
flap endonuclease activity	1 of 36 (2.8%)	0.05	22.16	0.0443
sterol binding	1 of 36 (2.8%)	0.05	22.16	0.0443
steroid binding	1 of 36 (2.8%)	0.05	22.16	0.0443
four-way junction DNA binding	1 of 36 (2.8%)	0.05	22.16	0.0443
phospholipase activity	1 of 36 (2.8%)	0.05	22.16	0.0443
peptidase regulator activity	1 of 36 (2.8%)	0.05	22.16	0.0443
CELLULAR COMPONENT				
delta DNA polymerase complex	3 of 36 (8.3%)	0.03	110.78	6.76e-07
replication fork	6 of 36 (16.7%)	0.37	16.21	1.25e-06
Elg1 RFC-like complex	3 of 36 (8.3%)	0.04	83.08	2.69e-06
DNA polymerase complex	3 of 36 (8.3%)	0.07	41.54	3.67e-05
chromosomal part	10 of 36 (27.8%)	2.34	4.28	6.31e-05
chromosome	10 of 36 (27.8%)	2.56	3.90	0.000138
nuclear replisome	3 of 36 (8.3%)	0.13	23.74	0.00023
replisome	3 of 36 (8.3%)	0.13	23.74	0.00023
DNA replication factor C complex	2 of 36 (5.6%)	0.03	73.85	0.000236
Rad17 RFC-like complex	2 of 36 (5.6%)	0.04	55.39	0.00047
protein-DNA complex	4 of 36 (11.1%)	0.40	10.07	0.000587
Ctf18 RFC-like complex	2 of 36 (5.6%)	0.05	36.93	0.00116
nuclear replication fork	3 of 36 (8.3%)	0.32	9.50	0.00363
nuclear chromosome part	6 of 36 (16.7%)	1.80	3.34	0.00795
nuclear chromosome	6 of 36 (16.7%)	1.98	3.04	0.0125

GO Term	Set	Expected	Fold Enrichment	1 Sided Fisher (p-value)
extracellular region	3 of 36 (8.3%)	0.55	5.45	0.017
fungal-type cell wall	3 of 36 (8.3%)	0.57	5.28	0.0185
cell wall	3 of 36 (8.3%)	0.60	5.04	0.0209
external encapsulating structure	3 of 36 (8.3%)	0.60	5.04	0.0209
glycerol-3-phosphate dehydrogenase complex	1 of 36 (2.8%)	0.03	36.93	0.0268
mating projection tip	3 of 36 (8.3%)	0.70	4.32	0.0313
cell projection part	3 of 36 (8.3%)	0.72	4.15	0.0345
chromosome, telomeric region	2 of 36 (5.6%)	0.30	6.71	0.0351
proteasome core complex, beta-subunit complex	1 of 36 (2.8%)	0.04	27.69	0.0356
mating projection	3 of 36 (8.3%)	0.79	3.82	0.0427
cell projection	3 of 36 (8.3%)	0.79	3.82	0.0427
nucleus	19 of 36 (52.8%)	13.53	1.40	0.0447

Table 3.5

Table 3.5. Full results of gene ontology analysis of SGA screen against TS array.

GO Term	Set	Expected	Fold Enrichment	1 Sided Fisher (p-value)
BIOLOGICAL				
DNA repair	23 of 29 (79.3%)	2.04	11.27	1.89e-22
response to DNA damage stimulus	23 of 29 (79.3%)	2.29	10.05	3.09e-21
DNA metabolic process	24 of 29 (82.8%)	3.45	6.96	1.57e-18
cellular response to stress	23 of 29 (79.3%)	3.54	6.49	9.76e-17
DNA recombination	16 of 29 (55.2%)	1.17	13.66	5.31e-16
double-strand break repair	14 of 29 (48.3%)	0.84	16.65	3.47e-15
response to stress	23 of 29 (79.3%)	4.13	5.56	3.48e-15
DNA-dependent DNA replication	15 of 29 (51.7%)	1.13	13.27	9.88e-15
cellular response to stimulus	23 of 29 (79.3%)	4.85	4.74	1.33e-13
cell cycle phase	20 of 29 (69.0%)	3.31	6.05	2.6e-13
DNA replication	15 of 29 (51.7%)	1.41	10.67	3.04e-13
recombinational repair	11 of 29 (37.9%)	0.52	21.00	3.85e-13
cell cycle process	21 of 29 (72.4%)	4.12	5.10	1.25e-12
double-strand break repair via homologous recombination	10 of 29 (34.5%)	0.45	21.99	3.34e-12
response to stimulus	23 of 29 (79.3%)	5.71	4.03	5.04e-12
cell cycle	21 of 29 (72.4%)	4.81	4.37	2.88e-11
base-excision repair	7 of 29 (24.1%)	0.17	42.32	3.29e-11
M phase	16 of 29 (55.2%)	2.76	5.80	5.59e-10
non-recombinational repair	7 of 29 (24.1%)	0.26	26.73	1.96e-09

DNA strand elongation involved in DNA replication	8 of 29 (27.6%)	0.43	18.72	2.93e-09
DNA strand elongation	8 of 29 (27.6%)	0.43	18.72	2.93e-09
cellular process involved in reproduction	13 of 29 (44.8%)	2.14	6.08	2.79e-08
single organism reproductive process	13 of 29 (44.8%)	2.14	6.08	2.79e-08
reproductive process	13 of 29 (44.8%)	2.14	6.08	2.79e-08
lagging strand elongation	6 of 29 (20.7%)	0.22	27.21	2.89e-08
chromosome segregation	11 of 29 (37.9%)	1.39	7.90	3.05e-08
meiosis I	8 of 29 (27.6%)	0.58	13.82	3.97e-08
sister chromatid cohesion	8 of 29 (27.6%)	0.59	13.50	4.83e-08
meiosis	10 of 29 (34.5%)	1.25	7.97	1.42e-07
M phase of meiotic cell cycle	10 of 29 (34.5%)	1.25	7.97	1.42e-07
meiotic cell cycle	10 of 29 (34.5%)	1.27	7.89	1.58e-07
double-strand break repair via break-induced replication	6 of 29 (20.7%)	0.29	20.73	1.87e-07
reproduction	13 of 29 (44.8%)	2.51	5.18	1.98e-07
mitotic sister chromatid cohesion	7 of 29 (24.1%)	0.48	14.51	2.26e-07
double-strand break repair via nonhomologous end joining	5 of 29 (17.2%)	0.18	27.90	4.14e-07
sister chromatid segregation	8 of 29 (27.6%)	0.80	10.01	5.58e-07
nucleic acid metabolic process	24 of 29 (82.8%)	10.97	2.19	7.82e-07
mitotic cell cycle	13 of 29 (44.8%)	2.88	4.51	1.03e-06
cellular macromolecule metabolic process	27 of 29 (93.1%)	15.38	1.76	3.14e-06
telomere maintenance	6 of 29 (20.7%)	0.45	13.19	3.41e-06
anatomical structure homeostasis	6 of 29 (20.7%)	0.45	13.19	3.41e-06
maintenance of fidelity involved in DNA-dependent DNA replication	4 of 29 (13.8%)	0.12	32.25	3.5e-06
chromosome organization	13 of 29 (44.8%)	3.23	4.03	3.83e-06

telomere organization	6 of 29 (20.7%)	0.47	12.80	4.1e-06
macromolecule metabolic process	27 of 29 (93.1%)	15.70	1.72	5.25e-06
mitotic sister chromatid segregation	7 of 29 (24.1%)	0.76	9.23	5.66e-06
DNA replication initiation	6 of 29 (20.7%)	0.52	11.46	8.1e-06
mismatch repair	4 of 29 (13.8%)	0.15	26.38	9e-06
nucleobase-containing compound metabolic process	24 of 29 (82.8%)	12.34	1.95	9.39e-06
leading strand elongation	4 of 29 (13.8%)	0.17	24.18	1.34e-05
cellular aromatic compound metabolic process	24 of 29 (82.8%)	12.57	1.91	1.39e-05
heterocycle metabolic process	24 of 29 (82.8%)	12.63	1.90	1.52e-05
interphase of mitotic cell cycle	7 of 29 (24.1%)	0.91	7.69	1.96e-05
interphase	7 of 29 (24.1%)	0.92	7.58	2.17e-05
cellular nitrogen compound metabolic process	24 of 29 (82.8%)	12.90	1.86	2.38e-05
organic cyclic compound metabolic process	24 of 29 (82.8%)	12.91	1.86	2.43e-05
postreplication repair	4 of 29 (13.8%)	0.19	20.73	2.65e-05
mitosis	9 of 29 (31.0%)	1.76	5.10	3.06e-05
regulation of DNA metabolic process	6 of 29 (20.7%)	0.66	9.07	3.27e-05
nuclear division	9 of 29 (31.0%)	1.79	5.02	3.47e-05
homeostatic process	7 of 29 (24.1%)	0.99	7.05	3.5e-05
regulation of cell cycle	8 of 29 (27.6%)	1.39	5.75	3.97e-05
organelle fission	9 of 29 (31.0%)	1.83	4.91	4.17e-05
DNA replication checkpoint	3 of 29 (10.3%)	0.08	36.28	4.58e-05
negative regulation of G2/M transition of mitotic cell cycle	3 of 29 (10.3%)	0.08	36.28	4.58e-05
nitrogen compound metabolic process	24 of 29 (82.8%)	13.48	1.78	5.84e-05
single-organism cellular process	28 of 29 (96.6%)	18.87	1.48	5.88e-05
regulation of cell cycle process	7 of 29 (24.1%)	1.08	6.51	5.94e-05

M phase of mitotic cell cycle	9 of 29 (31.0%)	1.92	4.70	5.95e-05
negative regulation of DNA metabolic process	4 of 29 (13.8%)	0.23	17.07	6.13e-05
G2/M transition of mitotic cell cycle	5 of 29 (17.2%)	0.45	10.99	6.3e-05
organic substance metabolic process	28 of 29 (96.6%)	18.97	1.48	6.74e-05
mitotic recombination	4 of 29 (13.8%)	0.25	16.12	7.81e-05
negative regulation of mitotic cell cycle	3 of 29 (10.3%)	0.10	31.09	7.95e-05
DNA replication, removal of RNA primer	3 of 29 (10.3%)	0.10	31.09	7.95e-05
DNA catabolic process	3 of 29 (10.3%)	0.10	31.09	7.95e-05
single-organism process	28 of 29 (96.6%)	19.10	1.47	8.16e-05
meiotic chromosome segregation	4 of 29 (13.8%)	0.26	15.27	9.79e-05
cellular metabolic process	28 of 29 (96.6%)	19.32	1.45	0.000111
maintenance of DNA repeat elements	3 of 29 (10.3%)	0.11	27.21	0.000126
meiotic DNA double-strand break formation	3 of 29 (10.3%)	0.11	27.21	0.000126
DNA biosynthetic process	3 of 29 (10.3%)	0.11	27.21	0.000126
regulation of mitotic cell cycle	6 of 29 (20.7%)	0.84	7.14	0.000131
replication fork protection	2 of 29 (6.9%)	0.03	72.55	0.000184
regulation of endodeoxyribonuclease activity	2 of 29 (6.9%)	0.03	72.55	0.000184
regulation of deoxyribonuclease activity	2 of 29 (6.9%)	0.03	72.55	0.000184
regulation of nuclease activity	2 of 29 (6.9%)	0.03	72.55	0.000184
gene conversion at mating-type locus, DNA repair synthesis	2 of 29 (6.9%)	0.03	72.55	0.000184
cell cycle checkpoint	5 of 29 (17.2%)	0.57	8.85	0.000184
regulation of cell cycle arrest	5 of 29 (17.2%)	0.57	8.85	0.000184
DNA replication, Okazaki fragment processing	3 of 29 (10.3%)	0.12	24.18	0.000187
cell cycle arrest	5 of 29 (17.2%)	0.58	8.64	0.000207
negative regulation of cell cycle	5 of 29 (17.2%)	0.59	8.44	0.000232
metabolic process	28 of 29 (96.6%)	19.97	1.40	0.000264

DNA geometric change	3 of 29 (10.3%)	0.14	21.77	0.000265
primary metabolic process	27 of 29 (93.1%)	18.50	1.46	0.000299
nucleic acid phosphodiester bond hydrolysis	7 of 29 (24.1%)	1.42	4.93	0.000352
regulation of G2/M transition of mitotic cell cycle	3 of 29 (10.3%)	0.15	19.79	0.000361
DNA conformation change	5 of 29 (17.2%)	0.68	7.40	0.000434
mating type switching	3 of 29 (10.3%)	0.17	18.14	0.000477
biological regulation	18 of 29 (62.1%)	9.01	2.00	0.000517
S phase of mitotic cell cycle	3 of 29 (10.3%)	0.18	16.74	0.000614
mating type determination	3 of 29 (10.3%)	0.18	16.74	0.000614
sex determination	3 of 29 (10.3%)	0.18	16.74	0.000614
cell fate commitment	3 of 29 (10.3%)	0.18	16.74	0.000614
cellular macromolecule biosynthetic process	17 of 29 (58.6%)	8.35	2.04	0.000705
macromolecule biosynthetic process	17 of 29 (58.6%)	8.38	2.03	0.000736
regulation of DNA recombination	3 of 29 (10.3%)	0.19	15.55	0.000774
RNA-dependent DNA replication	3 of 29 (10.3%)	0.21	14.51	0.000959
DNA topological change	2 of 29 (6.9%)	0.06	36.28	0.00108
resolution of meiotic recombination intermediates	2 of 29 (6.9%)	0.06	36.28	0.00108
meiotic chromosome separation	2 of 29 (6.9%)	0.06	36.28	0.00108
negative regulation of DNA-dependent DNA replication	2 of 29 (6.9%)	0.06	36.28	0.00108
double-strand break repair via synthesis-dependent strand annealing	2 of 29 (6.9%)	0.06	36.28	0.00108
DNA synthesis involved in DNA repair	2 of 29 (6.9%)	0.06	36.28	0.00108
gene conversion at mating-type locus	2 of 29 (6.9%)	0.06	36.28	0.00108
S phase	3 of 29 (10.3%)	0.22	13.60	0.00117
regulation of interphase of mitotic cell cycle	3 of 29 (10.3%)	0.22	13.60	0.00117
negative regulation of cellular process	9 of 29 (31.0%)	2.87	3.14	0.0013

negative regulation of biological process	9 of 29 (31.0%)	2.88	3.12	0.00135
regulation of cellular process	16 of 29 (55.2%)	8.06	1.98	0.00162
cell differentiation	5 of 29 (17.2%)	0.91	5.50	0.00173
heteroduplex formation	2 of 29 (6.9%)	0.07	29.02	0.00179
meiotic DNA double-strand break processing	2 of 29 (6.9%)	0.07	29.02	0.00179
DNA double-strand break processing	2 of 29 (6.9%)	0.07	29.02	0.00179
DNA catabolic process, exonucleolytic	2 of 29 (6.9%)	0.07	29.02	0.00179
DNA integrity checkpoint	3 of 29 (10.3%)	0.26	11.46	0.00197
regulation of biological quality	7 of 29 (24.1%)	1.89	3.71	0.00198
regulation of biological process	16 of 29 (55.2%)	8.31	1.93	0.0023
cellular component organization	19 of 29 (65.5%)	11.07	1.72	0.00245
chromosome separation	2 of 29 (6.9%)	0.08	24.18	0.00266
double-strand break repair via single-strand annealing	2 of 29 (6.9%)	0.08	24.18	0.00266
gene conversion	2 of 29 (6.9%)	0.08	24.18	0.00266
negative regulation of DNA recombination	2 of 29 (6.9%)	0.08	24.18	0.00266
developmental process	6 of 29 (20.7%)	1.49	4.03	0.00287
cellular biosynthetic process	18 of 29 (62.1%)	10.46	1.72	0.00369
positive regulation of cell cycle process	2 of 29 (6.9%)	0.10	20.73	0.00369
telomere maintenance via recombination	2 of 29 (6.9%)	0.10	20.73	0.00369
reproductive process in single-celled organism	4 of 29 (13.8%)	0.68	5.92	0.00402
cellular developmental process	5 of 29 (17.2%)	1.10	4.53	0.00406
organic substance biosynthetic process	18 of 29 (62.1%)	10.61	1.70	0.00442
regulation of macromolecule metabolic process	12 of 29 (41.4%)	5.57	2.16	0.00465
regulation of DNA replication	3 of 29 (10.3%)	0.36	8.37	0.00495
biosynthetic process	18 of 29 (62.1%)	10.72	1.68	0.00502
regulation of catalytic activity	4 of 29 (13.8%)	0.73	5.48	0.00535

nucleotide-excision repair	3 of 29 (10.3%)	0.37	8.06	0.00552
negative regulation of cell cycle process	3 of 29 (10.3%)	0.37	8.06	0.00552
DNA duplex unwinding	2 of 29 (6.9%)	0.12	16.12	0.00622
negative regulation of DNA replication	2 of 29 (6.9%)	0.12	16.12	0.00622
developmental process involved in reproduction	4 of 29 (13.8%)	0.79	5.09	0.00694
regulation of cellular metabolic process	12 of 29 (41.4%)	5.84	2.05	0.00701
regulation of primary metabolic process	12 of 29 (41.4%)	5.87	2.04	0.00729
chromatin silencing at silent mating-type cassette	3 of 29 (10.3%)	0.41	7.26	0.00745
negative regulation of nucleobase-containing compound metabolic process	6 of 29 (20.7%)	1.83	3.27	0.00809
organelle organization	15 of 29 (51.7%)	8.45	1.78	0.00834
negative regulation of nitrogen compound metabolic process	6 of 29 (20.7%)	1.85	3.25	0.00838
regulation of molecular function	4 of 29 (13.8%)	0.84	4.76	0.00883
regulation of metabolic process	12 of 29 (41.4%)	6.05	1.98	0.00935
negative regulation of macromolecule metabolic process	6 of 29 (20.7%)	1.97	3.04	0.0114
activation of mitotic anaphase-promoting complex activity	1 of 29 (3.4%)	0.01	72.55	0.0138
positive regulation of ubiquitin-protein ligase activity involved in mitotic cell cycle	1 of 29 (3.4%)	0.01	72.55	0.0138
activation of anaphase-promoting complex activity	1 of 29 (3.4%)	0.01	72.55	0.0138
positive regulation of ubiquitin-protein ligase activity	1 of 29 (3.4%)	0.01	72.55	0.0138
positive regulation of protein ubiquitination	1 of 29 (3.4%)	0.01	72.55	0.0138
positive regulation of ligase activity	1 of 29 (3.4%)	0.01	72.55	0.0138

activation of anaphase-promoting complex activity involved in meiotic cell cycle	1 of 29 (3.4%)	0.01	72.55	0.0138
positive regulation of ubiquitin-protein ligase activity involved in meiotic cell cycle	1 of 29 (3.4%)	0.01	72.55	0.0138
regulation of ubiquitin-protein ligase activity involved in meiotic cell cycle	1 of 29 (3.4%)	0.01	72.55	0.0138
meiotic anaphase I	1 of 29 (3.4%)	0.01	72.55	0.0138
positive regulation of endodeoxyribonuclease activity	1 of 29 (3.4%)	0.01	72.55	0.0138
positive regulation of deoxyribonuclease activity	1 of 29 (3.4%)	0.01	72.55	0.0138
positive regulation of nuclease activity	1 of 29 (3.4%)	0.01	72.55	0.0138
cell shape checkpoint	1 of 29 (3.4%)	0.01	72.55	0.0138
base-excision repair, base-free sugar-phosphate removal	1 of 29 (3.4%)	0.01	72.55	0.0138
replication fork arrest	1 of 29 (3.4%)	0.01	72.55	0.0138
negative regulation of endodeoxyribonuclease activity	1 of 29 (3.4%)	0.01	72.55	0.0138
negative regulation of deoxyribonuclease activity	1 of 29 (3.4%)	0.01	72.55	0.0138
negative regulation of nuclease activity	1 of 29 (3.4%)	0.01	72.55	0.0138
negative regulation of metabolic process	6 of 29 (20.7%)	2.11	2.85	0.0157
negative regulation of cellular metabolic process	6 of 29 (20.7%)	2.11	2.85	0.0157
nucleobase-containing compound catabolic process	5 of 29 (17.2%)	1.56	3.21	0.0172
cellular macromolecule catabolic process	6 of 29 (20.7%)	2.16	2.77	0.0177
aromatic compound catabolic process	5 of 29 (17.2%)	1.57	3.18	0.0179
regulation of nucleobase-containing compound metabolic process	10 of 29 (34.5%)	4.98	2.01	0.018

regulation of nitrogen compound metabolic process	10 of 29 (34.5%)	4.99	2.00	0.0183
cellular nitrogen compound catabolic process	5 of 29 (17.2%)	1.59	3.15	0.0185
cellular process	29 of 29 (100.0%)	25.32	1.15	0.019
heterocycle catabolic process	5 of 29 (17.2%)	1.60	3.13	0.0191
organic cyclic compound catabolic process	5 of 29 (17.2%)	1.60	3.13	0.0191
reproduction of a single-celled organism	4 of 29 (13.8%)	1.06	3.77	0.0197
macromolecule catabolic process	6 of 29 (20.7%)	2.23	2.69	0.0204
regulation of DNA-dependent DNA replication	2 of 29 (6.9%)	0.23	8.54	0.022
replicative cell aging	2 of 29 (6.9%)	0.26	7.64	0.0271
meiotic mismatch repair	1 of 29 (3.4%)	0.03	36.28	0.0274
DNA replication proofreading	1 of 29 (3.4%)	0.03	36.28	0.0274
base-excision repair, gap-filling	1 of 29 (3.4%)	0.03	36.28	0.0274
nucleotide-excision repair, DNA gap filling	1 of 29 (3.4%)	0.03	36.28	0.0274
positive regulation of proteasomal ubiquitin-dependent protein catabolic process	1 of 29 (3.4%)	0.03	36.28	0.0274
positive regulation of mitotic metaphase/anaphase transition	1 of 29 (3.4%)	0.03	36.28	0.0274
regulation of proteasomal ubiquitin-dependent protein catabolic process	1 of 29 (3.4%)	0.03	36.28	0.0274
positive regulation of proteasomal protein catabolic process	1 of 29 (3.4%)	0.03	36.28	0.0274
regulation of proteasomal protein catabolic process	1 of 29 (3.4%)	0.03	36.28	0.0274
positive regulation of proteolysis	1 of 29 (3.4%)	0.03	36.28	0.0274
positive regulation of mitosis	1 of 29 (3.4%)	0.03	36.28	0.0274
positive regulation of nuclear division	1 of 29 (3.4%)	0.03	36.28	0.0274

regulation of ubiquitin-protein ligase activity involved in mitotic cell cycle	1 of 29 (3.4%)	0.03	36.28	0.0274
regulation of ubiquitin-protein ligase activity	1 of 29 (3.4%)	0.03	36.28	0.0274
regulation of ligase activity	1 of 29 (3.4%)	0.03	36.28	0.0274
cyclin catabolic process	1 of 29 (3.4%)	0.03	36.28	0.0274
septin checkpoint	1 of 29 (3.4%)	0.03	36.28	0.0274
cytokinesis checkpoint	1 of 29 (3.4%)	0.03	36.28	0.0274
regulation of cell cycle cytokinesis	1 of 29 (3.4%)	0.03	36.28	0.0274
free ubiquitin chain polymerization	1 of 29 (3.4%)	0.03	36.28	0.0274
regulation of ubiquitin homeostasis	1 of 29 (3.4%)	0.03	36.28	0.0274
ubiquitin homeostasis	1 of 29 (3.4%)	0.03	36.28	0.0274
donor selection	1 of 29 (3.4%)	0.03	36.28	0.0274
cellular component organization or biogenesis	19 of 29 (65.5%)	13.44	1.41	0.0287
chromatin silencing at telomere	3 of 29 (10.3%)	0.69	4.35	0.0299
RNA catabolic process	3 of 29 (10.3%)	0.72	4.19	0.0331
reciprocal meiotic recombination	2 of 29 (6.9%)	0.30	6.60	0.0357
reciprocal DNA recombination	2 of 29 (6.9%)	0.30	6.60	0.0357
single-organism developmental process	4 of 29 (13.8%)	1.30	3.09	0.0377
DNA recombinase assembly	1 of 29 (3.4%)	0.04	24.18	0.0408
meiotic DNA recombinase assembly	1 of 29 (3.4%)	0.04	24.18	0.0408
positive regulation of cellular catabolic process	1 of 29 (3.4%)	0.04	24.18	0.0408
anaphase	1 of 29 (3.4%)	0.04	24.18	0.0408
regulation of transcription during meiosis	1 of 29 (3.4%)	0.04	24.18	0.0408
premeiotic DNA replication	1 of 29 (3.4%)	0.04	24.18	0.0408
DNA replication, synthesis of RNA primer	1 of 29 (3.4%)	0.04	24.18	0.0408
negative regulation of hydrolase activity	1 of 29 (3.4%)	0.04	24.18	0.0408

Table 3.6

Table 3.6. Leading and lagging strand replication gene lists.

Leading Strand	Lagging Strand
POL2	*POL1*
DPB3	*POL12*
MCM2	*PRI1*
MCM3	*PRI2*
MCM4	*MCM10*
MCM5	*CTF4*
MCM6	*POL3*
MCM7	*POL31*
	POL32
	RAD27
	DNA2
	CDC9
	ELG1
	POL30
	RFC1
	RFC2
	RFC3
	RFC4
	RFC5

Table 3.7

Table 3.7. Yeast strains used in Chapter 3

Strain Name	Relevant Genotype	Source
EFS20	*MATα, ade5-1, lys2-A12, trp1-289, his7-2, leu2-3,112, ura3-52, bar1*	[Tran *et al.* 1997]
AByb1724	*rad27::kanMX*	This study
AByb1733	*pol30::POL30 (LEU2)*	This study
AByb1735	*pol30::pol30-K164R (LEU2)*	This study
AByb1809	*rad27::kanMX, pol30::POL30 (LEU2)*	This study
AByb1810	*rad27::kanMX, pol30::pol30-K164R (LEU2)*	This study
AByb2049	*rad5::TRP1*	This study
AByb2051	*rad27::kanMX, rad5::TRP1*	This study
AByb2053	*rad18::TRP1*	This study
AByb2055	*rad27::kanMX, rad18::TRP1*	This study
AByb2062	*leu2::His-POL30 (LEU2), pol30::TRP1*	This study
AByb2083	*rev3::LEU2*	This study

Strain Name	Relevant Genotype	Source
AByb2085	*rad27::kanMX, rev3::LEU2*	This study
AByb2086	*rev3::LEU2, rad5::TRP1*	This study
AByb2087	*rad27::kanMX, rev3::LEU2, rad5::TRP1*	This study
AByb2169	*leu2::His-POL30 (LEU2), pol30::TRP1, rad27::URA3*	This study
AByb2171	*leu2::His-pol30-K164R (LEU2), pol30::TRP1, rad27::URA3*	This study
AByb2192	*elg1::TRP1, pol30::pol30-K164R (LEU2)*	This study
AByb2193	*siz1::TRP1*	This study
AByb2200	*elg1::TRP1*	This study
AByb2213	*leu2::His-pol30-K164R (LEU2), pol30::TRP1, elg1::URA3*	This study
AByb2233	*leu2::His-POL30 (LEU2), pol30::TRP1, elg1::URA3*	This study
AByb2242	*rad27::kanMX, leu2::His-POL30 (LEU2), pol30::URA3, pRS424gal-EV (TRP1)*	This study
AByb2243	*rad27::kanMX, leu2::His-POL30 (LEU2), pol30::URA3, pBL336 (TRP1)*	This study
AByb2244	*rad27::kanMX, leu2::His-POL30 (LEU2), pol30::URA3, pBL336-01 (TRP1)*	This study
AByb2252	*leu2::His-POL30 (LEU2), pol30::URA3, pRS424gal-EV (TRP1)*	This study

Strain Name	Relevant Genotype	Source
AByb2253	*leu2::His-POL30 (LEU2), pol30::URA3, pBL336 (TRP1)*	This study
AByb2254	*leu2::His-POL30 (LEU2), pol30::URA3, pBL336-01 (TRP1)*	This study
AByb2277	*leu2::His-POL30 (LEU2), pol30::TRP1, pJS227 (URA3)*	This study
AByb2278	*leu2::His-POL30 (LEU2), pol30::TRP1, gal-DNA2 (URA3)*	This study
AByb2281	*rad27::kanMX, leu2::His-POL30 (LEU2), pol30::TRP1, pJS227 (URA3)*	This study
AByb2282	*rad27::kanMX, leu2::His-POL30 (LEU2), pol30::TRP1, gal-DNA2 (URA3)*	This study
AByb2299	*leu2::His-POL30 (LEU2), pol30::TRP1, pRS316 (URA3)*	This study
AByb2300	*leu2::His-POL30 (LEU2), pol30::TRP1, gal-EXO1 (URA3)*	This study
AByb2301	*leu2::His-pol30-K164R (LEU2), pol30::TRP1, pRS316 (URA3)*	This study
AByb2303	*rad27::kanMX, leu2::His-POL30 (LEU2), pol30::TRP1, pRS316 (URA3)*	This study
AByb2304	*rad27::kanMX, leu2::His-POL30 (LEU2), pol30::TRP1, gal-EXO1 (URA3)*	This study
AByb2410	*rad27::kanMX, siz1::TRP1*	This study
AByb2412	*leu2::His-POL30 (LEU2), pol30::TRP1, gal-exo1-D173A (URA3)*	This study
AByb2414	*rad27::kanMX, leu2::His-POL30 (LEU2), pol30::TRP1, gal-exo1-D173A (URA3)*	This study

Strain Name	Relevant Genotype	Source
SSL204	*MATα, ade2, his3Δ200, trp1, leu2, ura3-52*	Becker *et al*. 2014
ABy2430	*leu2::His-POL30 (LEU2), pol30::TRP1, pRS316 (URA3)*	This Study
ABy2432	*leu2::His-POL30 (LEU2), pol30::TRP1, gal-EXO1 (URA3)*	This Study
ABy2434	*pol1-1, leu2::His-POL30 (LEU2), pol30::TRP1, pRS316 (URA3)*	This Study
ABy2436	*pol1-1, leu2::His-POL30 (LEU2), pol30::TRP1, gal-EXO1 (URA3)*	This Study
ABy2438	*pol1-1, leu2::His-pol30-K164R (LEU2), pol30::TRP1, pRS316 (URA3)*	This Study
ABy2440	*pol1-1, leu2::His-pol30-K164R (LEU2), pol30::TRP1, gal-EXO1 (URA3)*	This Study

CHAPTER 4

Flap endonuclease overexpression is a potent driver of genome instability and mutation

(The work in this chapter is in preparation for publication as Becker, J.R., Gallo, D., Nguyen, H.D., Thu, Y.M., Croissant, T., Leung, W., Brown, G.W., and Bielinsky, A.K. (2016))

Author contributions:

Experiments were designed and conceived by J.R.B., D.G., H.D.N. and A.K.B. and performed by J.R.B., D.G., T.C., Y.M.T., and W.L. All results were interpreted and prepared for publication by J.R.B. and A.K.B.

INTRODUCTION

Complete replication of the genome before cell division is a fundamental requirement for the multigenerational viability of all organisms. As a result of the necessity to complete this process repeatedly and successfully, evolution has provided a highly conserved set of replication factors, which carry out a magnificently coordinated array of activities. In the event of difficulty or error, a network of repair and checkpoint pathways has arisen to facilitate the completion of replication with a minimum of inherited mutations. The high level of conservation in these replication-, repair- and checkpoint pathways has allowed us to utilize relatively simpler model organisms such as *S. cerevisiae* to better understand how these processes are carried out in more complex metazoan systems. As such, in this study we started with an observation that has been made repeatedly in human cancer samples of increased expression of the replication factor flap endonuclease 1 (FEN1) and attempted to understand, beginning in *S. cerevisiae*, the effect that this has on DNA replication and genome stability.

FEN1 and its yeast homolog radiation sensitive 27 (*RAD27*) have a conserved function in DNA replication to process 5' flaps which are generated at the junction of Okazaki fragments on the lagging strand [Ayyagari *et al.* 2003, Jin *et al.* 2003]. Synthesis of the lagging strand is carried out primarily by polymerase (pol-) δ in conjunction with the homotrimeric replication clamp and processivity factor proliferating cell nuclear antigen (PCNA). Synthesis continues until the polymerase collides with the 5' end of the previous Okazaki fragment and

displaces it into a 5' flap [Burgers 2009]. PCNA then coordinates the processing of this flap in a manner that is dependent on a conserved interaction between the PCNA interacting peptide (PIP) box of Rad27/FEN1 and the interdomain connector loop of PCNA [Gary *et al.* 1999, Chapados *et al.* 2004, Tsutakawa *et al.* 2011]. Flap cleavage results in a ligatable nick, which is sealed by DNA ligase I, completing Okazaki fragment maturation [Burgers 2009]. In addition to its well described function in DNA replication, Rad27/FEN1 has also been implicated in 5'-deoxyribophosphate removal at abasic sites during base excision repair (BER) [Memisoglu and Samson 2000].

Deletion mutants of *RAD27* in yeast are viable but exhibit temperature sensitive growth, increased mutation rate, hyper-recombination, repeat tract instability and DNA damage sensitivity [Reagan *et al.* 1995, Tishkoff *et al.* 1997, Freudenreich *et al.* 1998, Becker *et al.* 2015]. FEN1 is essential in mammalian cells and has furthermore been found to be haploinsufficient in a mouse model where deletion of one copy leads to rapid cancer formation [Kucherlapati *et al.* 2002]. Mutant forms of FEN1 with reduced nuclease activity have been mapped in a variety of human cancer samples and at least one such allele leads to cancer formation in mice [Zheng *et al.* 2007, Larsen *et al.* 2008]. In addition to these loss of function mutations, FEN1 overexpression has been observed in a wide variety of cancer types including gastric, prostate, testis, brain, lung, breast, ovarian, and prostate and is a marker for poor prognosis in breast cancer [Kim *et al.* 2005, Lam *et al.* 2006, Singh *et al.* 2008, Nikolova *et al.* 2009, Abdel-Fatah *et al.* 2014, Zhang

et al. 2014]. Despite the prevalence of overexpression in cancer, remarkably little is understood as to the effect of FEN1 overabundance on DNA replication, cell cycle progression or genome stability. We hypothesized that overexpression of an enzyme capable of cleaving DNA strands that also interacts with PCNA and plays a crucial function in DNA replication could lead to negative effects on genome stability through the deregulation of any of these functions.

In addition to its coordinating role in unperturbed replication, PCNA is also subject to a number of post-translational modifications which endow it with the ability to coordinate cellular responses to replication stress [Ulrich 2009]. Ubiquitination of PCNA at the residue of lysine (K)164 by Rad6-Rad18 is an evolutionarily conserved response to replication stress triggered by persistent regions of replication protein A (RPA) coated single stranded (ss) DNA [Hoege *et al.* 2002, Davies *et al.* 2008]. This modification can activate two potential postreplicative repair (PRR) pathways dependent on the length of the ubiquitin chain [Hoege *et al.* 2002]. Mono-ubiquitin facilitates a switch from the processive replicative polymerases to specialized translesion polymerases that are able to tolerate replication over damaged DNA, albeit with an increased rate of nucleotide misincorporation [Prakash *et al.* 2005]. Alternatively, poly-ubiquitination facilitates an error-free template switching pathway of PRR capable of bypassing damage sites and filling in ssDNA gaps [Branzei 2011]. The mechanistic details of this pathway are not yet well understood. K164 is also a conserved target for attachment of a small ubiquitin-like modifier (SUMO). Unlike ubiquitination, this

modification occurs during unperturbed S phase and serves to inhibit illegitimate recombination between nascent sister chromatids by recruiting the helicase/anti-recombinase suppressor of rad six 2 (Srs2) [Papouli *et al.* 2005, Pfander *et al.* 2005]. Srs2 is thought to inhibit recombination at replication forks by disrupting the formation of Rad51 nucleoprotein filaments [Krejci *et al.* 2003, Veaute *et al.* 2003]. Conversely, recent studies have pointed to a pro-recombination role for Srs2 that is independent of its interaction with PCNA [Miura *et al.* 2013, Kolesar *et al.* 2016].

In the present study we have used an inducible overexpression system to modulate *RAD27* expression levels. Our findings indicate that overexpression causes marked impairment of DNA replication leading to delayed S phase progression and accumulation of DNA damage in a manner that is dependent on its interaction with PCNA. Unexpectedly, overexpression also dramatically increases DNA damage sensitivity that is linked to an inability to transfer ubiquitin onto PCNA. Instead, PCNA is heavily sumoylated and SUMO dependent pathways – including those targeting PCNA – promote viability under these conditions. Finally, we demonstrate that transient overexpression of FEN1 in human cell culture leads to an elevation of markers for genome instability. We conclude that overexpression of flap endonuclease is a potent driver of genome instability and mutation, both enabling characteristics of cancer, and that this widespread phenomenon has the potential to be an active contributor to cancer formation and evolution.

RESULTS

RAD27 overexpression promotes genome instability

Overexpression of the Rad27 homolog FEN1 has been observed in a variety of different cancers originating from varying tissue types. We therefore hypothesized that it may impact a fundamental enabling characteristic of cancer, such as genome instability [Kim *et al.* 2005, Lam *et al.* 2006, Singh *et al.* 2008, Nikolova *et al.* 2009, Abdel-Fatah *et al.* 2014, Zhang *et al.* 2014]. While overexpression may reflect an increased demand for FEN1 as a replication factor in rapidly dividing cells, overabundance of a PCNA-binding enzyme with DNA processing activity could also promote genome instability by disrupting normal replication kinetics.

To investigate this possibility, we utilized a galactose inducible overexpression system in *S. cerevisiae*, which allowed us to rapidly and effectively overexpress *RAD27* and track the effect on cell cycle progression and genome maintenance. Asynchronous cultures with a plasmid-borne, galactose-inducible copy of *RAD27* (gal-*RAD27*) or an empty control vector (gal-EV) were grown to log phase before addition of galactose. Upon galactose addition, we observed increased accumulation of cells in G1 in all cultures (Figures 4.1A and B). Importantly, only upon *RAD27* overexpression did we observe a significant accumulation of cells in S phase, indicating difficulty in the completion of replication (Figures 4.1A and B). Overexpression of *RAD27* was rapidly observable and

coincided with increased phosphorylation of histone H2A at serine (S)129, a mitosis entry checkpoint 1 (Mec1) target and marker for DNA damage (Figure 4.1C) [Downs *et al.* 2000]. We also observed increased phosphorylation of the checkpoint kinase Rad53, further indicating replication stress or DNA damage (Figure 4.1C) [Osborn and Elledge 2003]. Whereas a baseline level of hyperphosphorylated Rad53 was present in both gal-EV and gal-*RAD27* containing cultures, we noted that only *RAD27* overexpressing cultures exhibited a progressive shift of the fast migrating unphosphorylated form to a slower migrating phosphorylated form (Figure 4.1C). The persistent hyperphosphorylated form (marked by an asterisk in Figure 4.1C) may result from growth in medium containing the sub-optimal carbon sources galactose and raffinose leading to metabolic stress and increased to difficulty making the G1 to S phase transition [Barford and Hall 1976]. Taken together, these observations suggested that replication stress and DNA damage resulting from *RAD27* overexpression was interfering with the normal replication program.

In agreement with the presence of increased DNA damage, we also observed reduced viability upon deletion of the homologous recombination (HR) gene *RAD52* (Figure 4.1D). In contrast, there was no such requirement for the non-homologous end joining (NHEJ) factor *DNL4*. If anything, growth was moderately more robust in *dnl4Δ* mutants (Figure 4.1D). We concluded that *RAD27* overexpression leads to replication stress and eventually double-strand breaks (DSB) that require HR but not NHEJ for efficient repair. Interestingly, a recent study

found that coincident overexpression of FEN1 and the HR factor RAD54B in lung adenocarcinomas was predictive of poor patient survival, suggesting that the dynamic between flap endonuclease overexpression and HR may be evolutionarily conserved [Hwang *et al.* 2015].

PCNA ubiquitination is impaired in *RAD27* overexpressing cultures

The accumulation of *RAD27* overexpressing cells in S phase, increased phosphorylation of H2A-S129, and activation of Rad53 led us to further investigate the relationship between flap endonuclease overexpression and replication stress. To this end, we examined ubiquitination of PCNA as a marker of replication stress that indicates the presence of ssDNA gaps [Davies *et al.* 2008]. We purified His_6-tagged PCNA (His_6-PCNA) from *RAD27* overexpressing cells and probed its ubiquitination and sumoylation status by western blot (Figure 4.2A). Treatment with UV light, which is known to induce PCNA ubiquitination was included as a positive control. Unexpectedly, *RAD27* overexpression did not trigger PCNA ubiquitination, and it drastically reduced the level of ubiquitination in response to UV light (Figure 4.2A). In contrast, PCNA sumoylation was vastly enhanced when *RAD27* was overexpressed (Figure 4.2A). This was likely due to an increase of cells in S phase during which PCNA is sumoylated to recruit Srs2 and inhibit illegitimate recombination between sister chromatids [Papouli *et al.* 2005, Pfander *et al.* 2005]. We also measured a higher rate of mutation at the *CAN1* locus in *RAD27* overexpressing cells compared to wild-type (Figure 4.2B). As expected, this was

independent of PCNA-K164, consistent with the observation that PCNA was not ubiquitinated (Figure 4.2A). Thus, mutagenesis was operating outside of ubiquitination-dependent translesion synthesis (TLS) (Figure 4.2B).

We considered the possibility that overexpression of *RAD27* may decrease ubiquitination by occluding PCNA binding surfaces and sterically hindering access for the Rad6-Rad18 ubiquitination complex. However, overexpression of a dominant negative nuclease dead allele identified as *rad27-n* (D179A) led to robust ubiquitination in the absence of UV, arguing against this model (Figure 4.2C) [Gary *et al.* 1999]. Interestingly, in *rad27-n* overexpressing cells we observed ubiquitination of PCNA at K164 as well as at an alternate site, which we mapped to K242 (Figure 4.2C). Whereas a K164R mutation moderately reduced cell viability, K242 was dispensable for growth (Figure 4.3). In contrast to cells overexpressing wild-type *RAD27*, the mutation rate in *rad27-n* expressing cells was significantly increased in a manner that was dependent on both K164 and K242 (Figure 4.2D). These findings support that TLS was primarily responsible for the increase in the mutation rate and that K242 is sufficient, but not necessary, to facilitate TLS under these conditions.

We next considered the possibility that ubiquitination of PCNA may have simply been delayed in *RAD27* overexpressing cells due to reduced replication fork progression. However, ubiquitination rapidly reached its maximum level 15 min after UV treatment in the presence or absence of *RAD27* overexpression, albeit this level was much lower in the former cell poplulation (Figure 4.2E). From

these observations we concluded that high abundance of flap endonuclease interferes with the ubiquitination of PCNA, but that this phenomenon is not due to steric hindrance.

Sumoylation promotes viability in *RAD27* overexpressing cells

Although overexpression of *RAD27* did not lead to PCNA ubiquitination and in fact suppressed ubiquitination in response to UV treatment, we tested for a genetic interaction with a PCNA-K164R mutation, which resulted in a very mild but reproducible growth defect (Figure 4.4A). In contrast, the deletion of PRR pathway components *REV3* and *RAD5* had no effect on viability (Figure 4.4A). To investigate whether the observed genetic interaction between the *pol30-K164R* allele and *RAD27* overexpression was due to the loss of sumoylation at this residue, we induced flap endonuclease in *siz1Δ* mutants deficient for the E3 SUMO ligase, which targets PCNA at K164 [Pfander *et al.* 2005]. Interestingly, the loss of *SIZ1* had a more severe effect on viability than the *pol30-K164R* mutation alone, suggesting that additional targets of Siz1 are necessary to fully counteract the genotoxic effects of *RAD27* overexpression (Figure 4.4B). We also observed a significant reduction in viability in strains carrying a catalytically inactive allele of the E3 SUMO ligase *MMS21* (*mms21-CH*) (Figure 4.4B). Deletion of *siz2Δ* had no impact on viability. Together, these findings indicate that sumoylation by Siz1 and Mms21 is enhancing growth under conditions of *RAD27* overexpression.

Sumoylation of PCNA at K164 is thought to primarily act to recruit the helicase/anti-recombinase Srs2 which suppresses illegitimate HR between nascent sister chromatids at the replication fork [Papouli *et al.* 2005, Pfander *et al.* 2005]. Deletion of *SRS2* resulted in a very mild growth defect, similar to that observed in K164R mutants (Figure 4.4C). Combination of the two alleles revealed an additive effect in reducing viability, indicating that PCNA-K164 and Srs2 have independent functions under these conditions (Figure 4.4C). This, in turn, is consistent with Srs2 having a pro-recombination role that is independent of its interaction with PCNA and promotes cell viability [Miura *et al.* 2013, Kolesar *et al.* 2016]. It may be that Srs2 is required at replication forks in *RAD27* overexpressing cells to inhibit illegitimate recombination, but facilitates HR at DSB sites. *pol30-K164R siz1Δ* mutants on the other hand behaved similarly to *siz1Δ* mutants, further supporting the notion that Siz1 dependent sumoylation, including that of PCNA at K164, is promoting the viability of *RAD27* overexpressing cells (Figure 4.4C).

We next sought to determine whether the *pol30*-K164R, *siz1Δ*, *mms21-CH*, or *rad52Δ* alleles, which decreased the viability of *RAD27* overexpressing cells, also led to increased DNA damage sensitivity. Consistent with previous reports, *pol30-K164R*, *mms21-CH*, and *rad52Δ* mutants all exhibited enhanced sensitivity to DNA damage even in the absence of *RAD27* overexpression (Figure 4.5A and B) [Stelter and Ulrich 2003, Sacher *et al.* 2006, Cremona *et al.* 2012]. Remarkably however, when combined with *RAD27* overexpression, the sensitivity to the UV

mimic 4-nitroquinoline 1-oxide (4-NQO), alkylating drug methyl methanesulfonate (MMS), or replication inhibitor hydroxyurea (HU) was dramatically enhanced (Figure 4.5A-4.5C). *RAD27* overexpression alone was sufficient to acutely sensitize cells to 4-NQO, MMS and HU at concentrations that had a minimal effect on the control (gal-EV) strain. This sensitivity was not further enhanced by *SIZ1* mutation (Figure 4.5A-4.5C). These results suggested that elevated levels of Rad27 simulate DNA repair or DNA damage tolerance pathway deficiencies. This is compounded by our finding that *RAD27* overexpression impeded normal ubiquitination of PCNA and this may provide a mechanistic explanation for the observed sensitivity to DNA damaging agents.

PCNA is the primary target for sumoylation

Our finding that *siz1Δ* mutants overexpressing *RAD27* had a reduction in viability greater than that resulting from the loss of K164 sumoylation alone led us to conclude that additional Siz1 targets might be contributing to the growth of these cells. Western blot analysis of whole cell extracts of cells overexpressing *RAD27* showed an increase in SUMO-conjugates relative to controls (Figure 4.6A). A side-by-side comparison of the same blot developed with a PCNA specific antibody revealed a banding pattern highly similar to the pattern of sumoylated proteins, suggesting that PCNA is the primary target for increased sumoylation under these conditions (Figure 4.6A). In addition, we isolated His_8-tagged SUMO-conjugates by cobalt affinity purification to identify sumoylated species by liquid

chromatography coupled tandem mass spectrometry (MS) (Figure 4.6B). PCNA was the most abundant sumoylated protein in our purification (Figure 4.6C). We also identified increased sumoylation of the glyceraldehyde-3-phosphate dehydrogenase (GAPDH) isozyme triose-phosphate dehydrogenase 1 (Tdh1). Tdh1 protein levels have been reported to increase under conditions of replication stress although both the biological significance of this increase and the function of Tdh1 sumoylation remain unclear [Tkach *et al.* 2012]. However, considering the role of Tdh1 in sugar metabolism and the change of sugar conditions in the growth medium necessary to induce *RAD27* overexpression, it would be difficult to conclude that these changes are exclusively a result of genome instability. Furthermore, both Tdh1 and Rad27 were abundant in a control with untagged SUMO, arguing that they may have contaminated the His_8-SUMO preparation due to high overall abundance (Figure 4.6C). Taken together, these data indicate that the primary target for sumoylation as measured by abundance under conditions of *RAD27* overexpression is PCNA.

Genome instability in RAD27 overexpressing cells is dependent on its interaction with PCNA

We demonstrated that overexpression of *RAD27* is a source of replication stress, genome instability, and mutation. To better understand the underlying mechanism, we considered two potential models: 1) *RAD27* overexpression leads to spurious or unregulated processing of replication intermediates causing DNA

breakage, or 2) genome instability is simply a side-effect of having an over-abundance of a PCNA interacting protein interfering with the kinetics of replication as it pertains to PCNA binding.

To test these hypotheses, we generated a variant of the overexpression construct carrying a *rad27-FFAA* allele in which two crucial phenylalanine residues (F346, F347) located in the PIP box of Rad27 were mutated to alanine, ablating its interaction with PCNA [Gary *et al.* 1999]. Remarkably, we found that overexpression of this PCNA binding mutant did not result in any observable increase in phosphorylation of H2A-S129 or Rad53 over that observed in an empty vector control (Figure 4.7A). Additionally, the severe S-phase delay observed in *RAD27* overexpressing cells was absent when overexpressing *rad27-FFAA* (Figure 4.7B and C). Expression of this mutant in combination with *pol30-K164R*, *siz1Δ*, *mms21-CH*, or *rad52Δ*, which all displayed negative genetic interactions with *RAD27* overexpression, did not result in growth inhibition (Figure 4.7D and E). In fact, the *rad27-FFAA* mutation rescued the proliferation defect and the other observed genome instability phenotypes inherent to *RAD27* overexpression (Figure 4.7D and E). These results suggested that *RAD27* overexpression interfered with normal progression of active replication forks, likely by blocking binding sites on PCNA. However, this experiment did not allow us to distinguish whether Rad27 simply acted as a spatial block or caused DNA damage by spurious or unregulated DNA processing.

To address whether the over-abundance of a PCNA interacting protein alone is sufficient to explain the phenotype of *RAD27* overexpressing cells, we generated a fusion protein composed of the full sequence of GFP with the C-terminal 48 amino acids of Rad27 fused to its C-terminus (GFP-PIP) (Figure 4.8A). This fragment of Rad27 contains the PIP motif and nuclear localization sequence (NLS) but none of the catalytic domains. While overexpression of GFP-PIP led to a mild accumulation of cells in S phase, this phenotype was not ameliorated when the PIP motif contained the inactivating FFAA mutation (Figure 4.8B and C). Furthermore, GFP-PIP expressing cells were not sensitive to 4-NQO at the concentrations examined and only mildly sensitive to MMS or HU treatment (Figure 4.9 A-C). This partial phenotype supports the contention that the impact of *RAD27* overexpression on genome stability is at least partially unique to Rad27 and not entirely generalizable to all PCNA interacting peptides.

Overexpression of FEN1 in 293T cells causes genome instability

Overexpression of flap endonuclease in yeast impaired DNA replication and promoted genome instability. To investigate whether the same held true for overexpression of the human Rad27 homolog FEN1, we transiently transfected 293T cells with a vector encoding FLAG-tagged FEN1 under control of a CMV promoter. Transient overexpression of FLAG-FEN1 led to a temporary increase in the phosphorylation of RPA32-S4/S8, an ATM target and marker for DSB processing, which subsided at the 48 h timepoint (Figure 4.10A) [Sartori *et al.*

2007, Liu *et al.* 2012]. It is possible that reduced RPA phosphorylation at 48 h was reflective of Rad51 displacing RPA for repair by HR. Levels of γH2AX, a marker for DSB formation were also increased at 24 and 48 h timepoints [Rogakou *et al.* 1998]. These findings are indicative of DNA damage induction upon FLAG-FEN1 expression. However, in contrast to our findings in yeast, we did not observe any significant reorganization of the cell cycle distribution of these cultures as measured by DNA content (Figure 4.10B).

A hypomorphic E160D mutation in the catalytic domain of FEN1 primarily causes lung tumors in mice [Zheng *et al.* 2007]. We wondered whether overexpression of FEN1 would similarly affect lung tissue. Relative expression levels of FEN1 mRNA in matched normal and tumor tissues from lung adenocarcinoma patients as measured by RNAseq were obtained from The Cancer Genome Atlas (TCGA). In accordance with what has been previously reported, we found overexpression of FEN1 to be prevalent in the vast majority of tumor samples (Figure 4.10C) [Sato *et al.* 2003, Nikolova *et al.* 2009, Yang *et al.* 2009]. The median level of overexpression was ~5-fold with individual samples and ranged as high as 10-fold over normal tissue. It is possible that disrupting the balance of flap processing by mutation or overexpression of FEN1 manifests with particular penetrance in lung tissue. The mechanism underlying any lung-specific effect remains unclear.

Altogether, it appears that increased expression of flap endonuclease has a conserved effect between yeast and human cell systems marked by a significant

increase in genome instability. When taken into consideration with the high prevalence of FEN1 overexpression in a wide variety of cancers we believe that this phenomenon is likely not a passenger effect, but may be a direct contributor to, and driver of genome instability and mutation (Figure 4.10C).

DISCUSSION

Here, we have demonstrated that overexpression of the FEN1 homolog Rad27 in yeast impairs DNA replication in a manner that is dependent on its interaction with PCNA and leads to the accumulation of DNA damage and mutations. Overexpression of FEN1 has been observed in cancers derived from a variety of tissue types at levels approaching 50-fold greater than matched normal tissues in some cases [Nikolova *et al.* 2009]. With this in mind, we modeled FEN1 overexpression using the strong *GAL1/10* promoter to enforce overexpression of *RAD27* at a high level. This promoter has the dual advantages of inducible control and expression at sufficiently high levels to model what has been observed in human cancers.

Sumoylation suppresses the effects of *RAD27* overexpression

Work over the past two decades has vastly increased our understanding of the complex networks of posttranslational modifications that are mobilized in response to replication stress and DNA damage [Cremona *et al.* 2012, Jackson and Durocher 2013]. Among these, the ubiquitination of PCNA at the conserved

residue K164 plays a crucial role in coordinating PRR pathways [Hoege *et al.* 2002]. Because the appearance of this modification is a sensitive marker for replication stress, we were surprised that *RAD27* overexpression not only failed to elicit this response, but suppressed it following UV treatment. This was particularly puzzling given the preponderance of other replication stress markers.

The observation that sumoylation, but not ubiquitination, of PCNA at K164 enhanced the viability of *RAD27* overexpressing cells prompted us to investigate the role of the three yeast SUMO ligases under these conditions. Genetic interaction studies with mutant alleles of *SIZ1*, *SIZ2* and *MMS21* revealed a significant decrease in viability in combination with *siz1Δ* and *mms21-CH*, but not *siz2Δ*, suggestive of broader applications for sumoylation beyond the attachment to PCNA. Although our analysis of the SUMO proteome in *RAD27* overexpressing cells identified PCNA as the most abundant target, it is possible that additional Siz1 and Mms21 targets of importance remain unidentified due to lower relative abundance. More sensitive and quantitative techniques will be necessary to identify these targets. It is also possible that multiple targets of low individual importance have an additive effect on viability. Additional studies will be necessary to fully understand the role of SUMO in mediating Rad27-induced replication stress.

Interaction with PCNA mediates *RAD27* overexpression effects

Our finding that mutation of the *RAD27* PIP box in *rad27-FFAA* mutants abrogates the negative impacts of *RAD27* overexpression suggests two possible mechanisms by which expression of the wild-type enzyme imperils genome stability. First, it could be interpreted that overabundance of Rad27 as a PCNA interacting protein disrupts the kinetics of replication by impeding the ability of other PCNA binding replication factors to be appropriately localized. Such a model has been proposed to explain the detrimental effects of DNA ligase I overexpression on genome stability and is also thought to be one of the mechanisms by which p21 regulates DNA replication [Waga *et al.* 1994, Subramanian *et al.* 2005]. If this model were to withstand examination, it would stand to reason that overexpression of any PCNA binding protein would have a similar effect on replication and that there is nothing intrinsic to *RAD27* that causes the observed phenotypes. However, overexpression of a GFP-Rad27 fusion protein (GFP-PIP) which retains the PIP box and NLS of *RAD27* but none of the nucleolytic domains failed to fully reproduce the results of expressing full-length *RAD27*, arguing that this model does not completely explain our observations.

Instead, we favor a second model in which the effect of *RAD27* overexpression is at least partially due to its catalytic activity. Unfortunately, we were not able to directly test this model as a catalytically dead mutant of *RAD27* (*rad27-n*) displays a dominant negative phenotype [Gary *et al.* 1999]. This is thought to be the result of substrate binding by the catalytically dead enzyme which

is then unable to complete its catalytic cycle [Gary *et al.* 1999]. The enzyme substrate complex then acts as an impediment to processing by alternative enzymes, severely disrupting Okazaki fragment processing and inhibiting the completion of DNA replication. It is, however, telling that a mutation in the PIP box of Rad27-n alleviates the dominant negative phenotype of the mutant [Gary *et al.* 1999]. This demonstrates that the PIP box mutation not only abrogates the Rad27:PCNA physical interaction, but it also must impair substrate binding and processing *in vivo* [Li *et al.* 1995]. Furthermore, the observation that overexpression of catalytically inert GFP-PIP fusion protein does not completely reproduce overexpression of full length Rad27, let us conclude that the phenotypes we observed are not entirely a generalizable effect of any PIP box containing protein, but are at least partially unique to *RAD27*.

The fact that all observed growth and genome instability phenotypes upon *RAD27* overexpression are completely dependent on the interaction between Rad27 and PCNA and result in a severe S phase delay argues that the effect is linked to replication. We can speculate that due to the well described role of Rad27 in Okazaki fragment processing, disruption of this process is a likely side-effect of overexpression. It is possible that too much flap endonuclease present during Okazaki fragment processing interferes with RNA primer removal, fill-in DNA synthesis and eventual ligation, leading to unligated nicks [Ayyagari *et al.* 2003, Jin *et al.* 2003, Garg *et al.* 2004]. If left unrepaired, these nicks would form DSB

during the next round of replication, explaining the observed dependence on HR of *RAD27* overexpressing cells.

RAD27 overexpression causes DNA damage sensitivity

One of the more striking phenotypes that we observed upon Rad27 overexpression was an acute sensitivity to DNA damage. High abundance of flap endonuclease rendered multiple strains uniformly sensitive to both 4-NQO and MMS treatment at concentrations that failed to impact the growth of control cells that harbored an empty vector. Considering that Rad27 is involved in BER, which is the primary pathway for removal of MMS-induced lesions, it is somewhat counterintuitive that overexpression would sensitize cells to this type of damage [Memisoglu and Samson 2000, Ma *et al.* 2008]. Nevertheless, we propose two reasons for why this is the case. First, we have thoroughly demonstrated that *RAD27* overexpression leads to genome instability and impaired replication. It may be that given the amount of replication stress already present in these cells, they are unable to tolerate additional damage and easily succumb to drug treatment. Second, we observed that ubiquitination of PCNA in response to DNA damage was severely impaired (Figure 4.2). It has been well established that both 4-NQO and MMS treatment lead to an increased dependence on PRR for viability [Hoege *et al.* 2002, Stelter and Ulrich 2003]. It is therefore possible that the inability to ubiquitinate PCNA and activate PRR renders these cells highly sensitive to DNA damage. If this relationship between flap endonuclease overexpression and DNA

damage sensitivity is conserved in human cancer cells, it may offer an effective therapeutic target for cancers with high levels of FEN1. Because the mode of action for many clinical chemotherapeutics relies on causing damage to DNA or otherwise inducing replication stress, this would be a highly implementable strategy with a readily identifiable marker in FEN1.

FEN1 overexpression and cancer

Overexpression of FEN1 in cancers from a wide variety of tissue types may suggest simply that dividing cancer cells require elevated levels of this replication factor to enable proliferation. However, our finding that overexpression of flap endonuclease in both yeast and human systems is a potent source of genome instability raises the possibility that overabundance of FEN1 presents an active mechanism to drive cancer evolution irrespective of tissue type. Based solely on the results presented in this study, it is impossible to determine whether FEN1 overexpression is a driving factor in carcinogenesis, a promoter of cancer progression, or a combination of the two. Nonetheless, inhibition of FEN1 has already been investigated as a potential chemotherapeutic strategy with promising results, although none of these studies have analyzed the effect of FEN1 inhibitors specifically in cancers with elevated expression levels [McManus *et al.* 2009, McWhirter *et al.* 2013, van Pel *et al.* 2013]. Such studies will be necessary to determine whether some cancers become “addicted” to overexpression and whether this is exploitable as a therapeutic strategy.

In summary, we report that overexpression of flap endonuclease impairs DNA replication leading to S phase delay, DNA damage and mutation in a manner that is dependent on its interaction with PCNA. Furthermore, overabundance of Rad27 impairs ubiquitination of PCNA in response to DNA damaging agents and renders these cells acutely sensitive to DNA damage. Our findings provide evidence that this common occurrence in cancer cells may not be simply a passenger effect but must be considered as a driver of genome instability.

MATERIALS AND METHODS

Yeast Strains and culture conditions

All yeast strains with the exception of those used for MS analysis were derived from E133 wild-type cells (Table 4.1) [Tran *et al.* 1997]. Strains used for MS were derived from W303-1a [Thomas and Rothstein 1989]. Cultures carrying plasmid-borne galactose inducible constructs were grown in synthetic medium lacking uracil and containing 2% raffinose as a sugar source. Induction of gene expression was accomplished by adding galactose to a final concentration of 2% once cultures had reached an OD_{600} of ~0.600. All genetic knockouts were generated by PCR mediated gene disruption [Lorenz *et al.* 1995]. The *mms21-CH* allele was introduced via a two-fragment PCR method that has been described previously [Nguyen *et al.* 2013]. Briefly, one fragment containing *mms21-CH* was generated from genomic DNA using a 5' primer upstream of the *mms21-CH* locus

and a downstream 3' primer with a region complementary to the 5' end of a second PCR fragment containing a *LEU2* marker. Equal molar ratios of the two fragments were mixed, denatured at 95°C for 5 min and allowed to anneal at room temperature for 30 min before being transformed into competent yeast cells.

Plasmids

Overexpression of *RAD27*, *rad27-n*, and *rad27-FFAA* was under control of an inducible *GAL1-10* promoter in a YEp195SPGAL plasmid backbone[Clark *et al.* 1999]. These constructs were obtained from D. Gordenin and have been described [Gary *et al.* 1999]. His_6-PCNA strains were constructed using Yip128-P30-POL30 (a gift from H.D. Ulrich, IMB Mainz). This construct was linearized with AflII and integrated at the genomic *LEU2* locus. Expression was analyzed by western blot to ensure similar protein levels to endogenous untagged PCNA. Endogenous *POL30* was then knocked out *via* PCR mediated gene disruption.

The GFP-PIP construct was generated by PCR amplification of GFP using 5'_GFP_SalI (5'-TATATGTCGACATGAGTAAAGGAGAAGAACTTTTCAC-3') and 3'_GFP_PIP_1 (5'-CTTGGAAGAACCCATCTAACCTACCCTGAATGCCAGATTTTTTGTATAGTTCATCCATGC-3'), followed by sequential overlapping PCR extensions at the 3' end using 3'_GFP_PIP_2 (5'-TTCGCCGCAGCAGCCAGCTGTTCCTTTGTCTTAGGCACCACTTGGAAGAACCCATCTAAC-3'), 3'_GFP_PIP_3 (5'-

ATTCTTATTTTTGTTCAATTTTTTATTTTCTTGTGCTCTTTTCGCCGCAGCAGC CAGCT-3'), 3'_GFP_PIP_4 (5'-TCATCTTCTTCCCTTTGTGACTTTATTCTTATTTTTGTTCAATTTTTTATTTTC-3'), and 3'_GFP_PIP_NotI (5'-TATATGCGGCCGCTCATCTTCTTCCCTTTGTGACTTTAT-3'). The resulting fragment was composed of GFP in its entirety with the terminal 144 nucleotides of *RAD27* fused to the 3' end. This fragment was then digested with SalI and NotI restriction enzymes before ligation into a YEp195SPGAL backbone. Expression was confirmed by the visualization of GFP fluorescence after the addition of galactose to cultures carrying the GFP-PIP construct. The GFP-PIP-FFAA variant was generated by site directed mutagenesis with a previously published primer set [Gary *et al.* 1999].

Strains with a PCNA-K164R mutation were generated by transformation of a single PCR fragment amplified from pCH1654 (a gift from L. Prakash, UTMB) or derivatives with additional lysine mutations introduced using the QuikChange Lightning Site-Directed Mutagenesis kit (Agilent). The resulting fragment was composed of the PCNA coding sequence and a *LEU2* marker flanked by homology arms targeting it for integration at the endogenous PCNA locus. Integration and incorporation of the mutant allele were confirmed by PCR and sequencing.

3xFLAG-FEN1 was transiently overexpressed in 293T cells from a pShuttle-3xFLAG-FEN1 vector under the control of a CMV promoter (S. Stewart, Washington U).

His_6-PCNA and His_8-SUMO purification

Purification of His_6-PCNA was performed as previously described [Becker *et al.* 2014, Becker *et al.* 2015]. Briefly, cultures were grown to OD_{600} ~0.600 in medium containing 2% raffinose. Galactose was then added to a final concentration of 2% to induce *RAD27* overexpression. In experiments with UV treatment, induction was carried out for 2 h before treatment with 100 J/m^2 of 254 nm light using a UV crosslinker (CL-1000, UVP). After collection, cell pellets were stored at -80°C overnight before processing. The pellets were then subjected to lysis under denaturing conditions and protein extracts were prepared in 8 M urea buffer. His_6-PCNA was bound to Ni-NTA conjugated agarose overnight at room temperature before washing with buffers of decreasing pH to successively increase stringency. Bound His_6-PCNA was eluted with EDTA-containing buffer and the eluates were fractionated by SDS-PAGE for western blot analysis with antibodies raised against PCNA, ubiquitin and SUMO. His_8-SUMO was also purified under denaturing conditions from cultures that were grown to OD_{600} ~0.600 in medium containing 2% raffinose. Galactose was added to a final concentration of 2% to induce *RAD27* overexpression in cells with tagged or untagged SUMO. Cultures were harvested after 3 h for His_8-SUMO pulldown with TALON metal affinity beads (Clonetech). Purification was carried out as described in Thu, *et al*. and submitted for MS [Thu *et al.* 2016].

Protein extraction and western blotting

Protein extracts were isolated by lysing cells under denaturing conditions, precipitating protein with trichloracetic acid, and resuspending the precipitated protein pellet in SDS loading buffer [Ricke and Bielinsky 2006]. Extracts were fractionated by SDS-PAGE, transferred to a PVDF membrane and analyzed by western blot with the following antibodies as indicated in each figure; anti-FEN1 (ab2619, Abcam) at a 1:1000 dilution in 5% blocking solution overnight, anti-Rad53 (a gift from JFX Diffley, LRI) at a 1:1000 dilution in 5% blocking solution for 1 h, anti-phospho-S129 H2A (ab15083, Abcam) at a 1:500 dilution in blocking solution overnight, anti-tubulin (MMS-407R, Covance) at a 1:5000 dilution in 5% blocking solution overnight, anti-PCNA (a gift from B. Stillman, CSHL) at a 1:4000 dilution in TBST for 2 h, anti-ubiquitin (P4D1, Covance) at a 1:1000 dilution in 5% blocking solution overnight, anti-SUMO (a gift from X. Zhao, MSKCC) at a 1:3000 dilution in TBST for 1 h, anti-phospho-S4/8 RPA32 (A300-245A, Bethyl Laboratories) at a 1:2000 dilution in 5% blocking solution overnight, and anti-γH2AX (A300-081A, Bethyl Laboratories) at a 1:2000 dilution in 5% blocking solution overnight. The anti-FEN1 antibody was raised against human FEN1 and only cross-reacted with yeast Rad27 sufficiently to visualize by western blot when Rad27 was overexpressed.

Mutation rate estimation

Mutation rates were estimated using the forward rate of mutations at the *CAN1* locus that conferred resistance to canavanine. Individual colonies were inoculated in medium lacking uracil and containing 2% raffinose as well as 2% galactose. Under these conditions the cultures required 8 days of growth at 25°C to reach saturation. Saturated cultures were washed and appropriate dilutions were plated on medium lacking arginine and containing canavanine (60 mg/L) or on rich medium to obtain a viable cell count. Mutation rates were calculated using Drake's formula and significance was determined using the Mann-Whitney U test [Mann and Whitney 1947, Drake 1991, Foster 2006]. Determinations were made from at least 16 independent cultures for each strain.

Cell cycle analysis

DNA content in yeast cells was measured by flow cytometry using a BD Accuri C6 flow cytometer and Sytox Green (Invitrogen) DNA dye. Measurement of DNA content in 293T cells was carried out using the same machine with propidium iodide (Sigma-Aldrich) as the DNA stain.

Viability analysis

The relative viability of yeast strains was examined in a "spotting" assay. We began by inoculating 10 ml cultures in medium lacking uracil and containing 2% glucose as a sugar source. These cultures were grown to saturation for 4 days

at 25°C, harvested, washed with 10 ml water, and resuspended in 5 ml water. The cells in the resulting suspension were quantified and 10-fold serial dilutions were then prepared in a 96 well plate from a starting cell count of $2x10^7$. The spots were then plated using a multi-pronged plating instrument on medium lacking uracil and containing either 2% glucose or 2% galactose. Images were taken after 4 days growth at 25°C. Strains containing the *mms21-CH* allele had an inherent growth defect made direct comparison with other strains difficult to visualize. To account for this, 5-fold more cells (10^8) were used as the starting cell count for all *mms21-CH* strains.

Human cell culture

293T cells were cultured in Dulbecco's modified eagle medium (DMEM). Transient transfection was carried out with Lipofectamine LTX (Thermo Fisher). In these experiments 10 µg of circular plasmid DNA was transfected into 293T cells at ~60% confluency on a 10 cm plate. Cells were harvested at 24 and 48 h for protein extraction and DNA content analysis by flow cytometry. For protein extraction cells were lysed in NETN (20 mM Tris-HCl at pH 8.0, 100 mM NaCl, 1 mM EDTA, 0.5% Nonidet P-40 and protease inhibitors) for 10 min and then centrifuged at 16,000*g* for 10 min. Cleared lysates were collected, mixed with SDS loading buffer, and boiled before fractionation by SDS-PAGE and analysis by western blot.

Figure 4.1

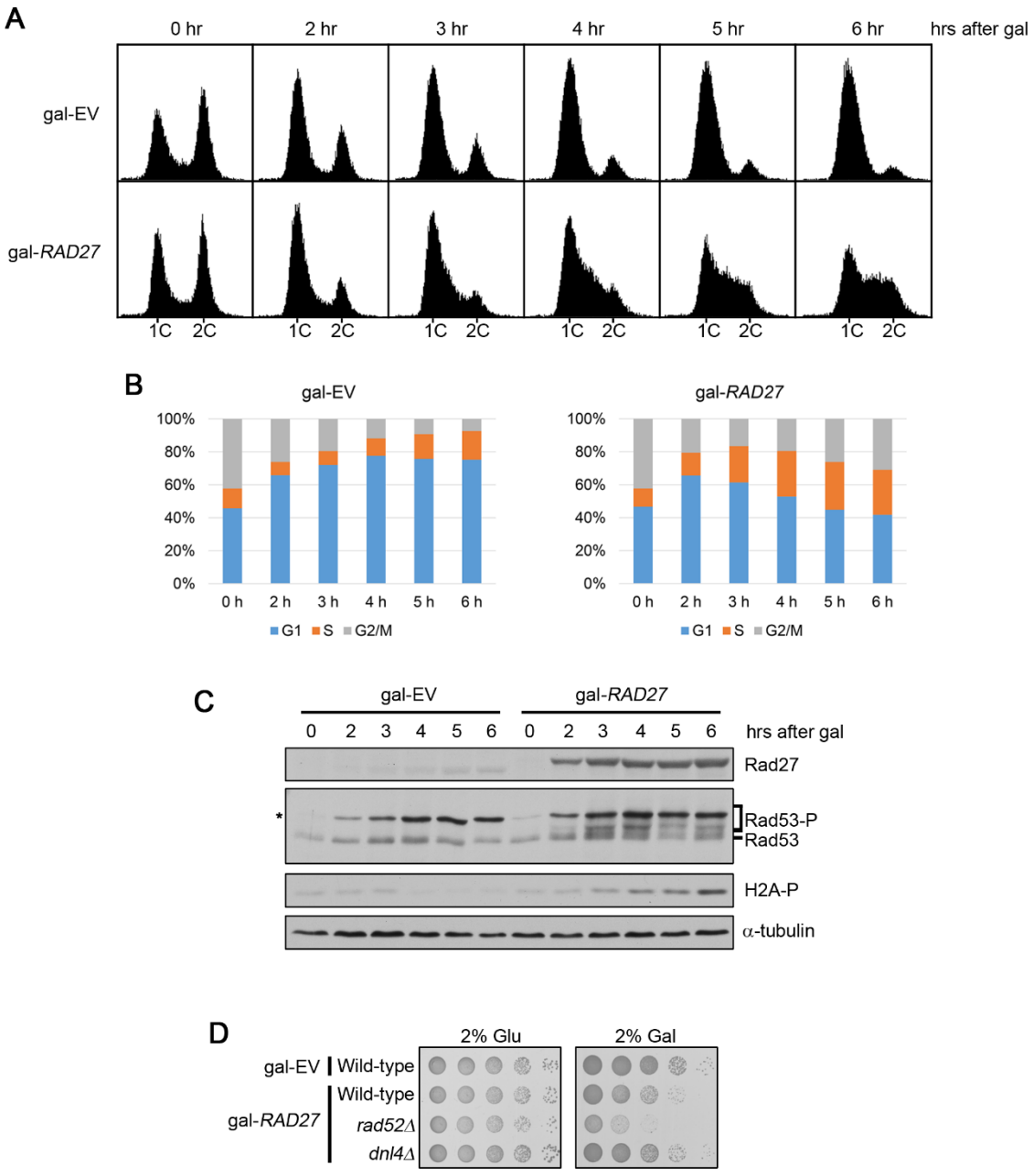
A
0 hr
2 hr
3 hr
4 hr
5 hr
6 hr
hrs after gal
gal-EV
gal-RAD27
1C 2C
B
gal-EV
gal-RAD27
100%
80%
60%
40%
20%
0%
0 h 2 h 3 h 4 h 5 h 6 h
G1 S G2/M
C
gal-EV
gal-RAD27
0 2 3 4 5 6 0 2 3 4 5 6
hrs after gal
Rad27
*
Rad53-P
Rad53
H2A-P
α-tubulin
D
2% Glu
2% Gal
gal-EV
Wild-type
gal-RAD27
Wild-type
rad52Δ
dnl4Δ

Figure 4.1. *RAD27* overexpression causes genome instability and impairs S phase progression. (A) Strains containing either gal-EV or gal-*RAD27* expression vectors were grown to OD_{600} ~0.600 in synthetic medium lacking uracil and containing 2% raffinose as a sugar source. Galactose was then added to a final concentration of 2% and samples were collected at the indicated time points for analysis by western blot and flow cytometry. DNA content was measured by flow cytometry on a BD Accuri C6 flow cytometer. (B) Quantification of the cell cycle distribution of the profiles in panel B. Quantification was carried out using the BD Accuri C6 software. This result is representative of 3 independent experiments. (C) Samples from the same cultures described above were harvested at the indicated timepoints and protein extracts were prepared by TCA precipitation. Extracts were fractionated by SDS-PAGE for western blot analysis with anti-Rad27, anti-Rad53, anti-phospho-S129 H2A, and anti-tubulin antibodies. The asterisk on the Rad53 blot marks the galactose-dependent effect. (D) 10-fold serial dilutions of the indicated strains were plated on medium lacking uracil and containing either 2% glucose to suppress gal-*RAD27* or 2% galactose to induce *RAD27* overexpression. Plates were incubated at 25°C for 4 days before imaging.

Figure 4.2

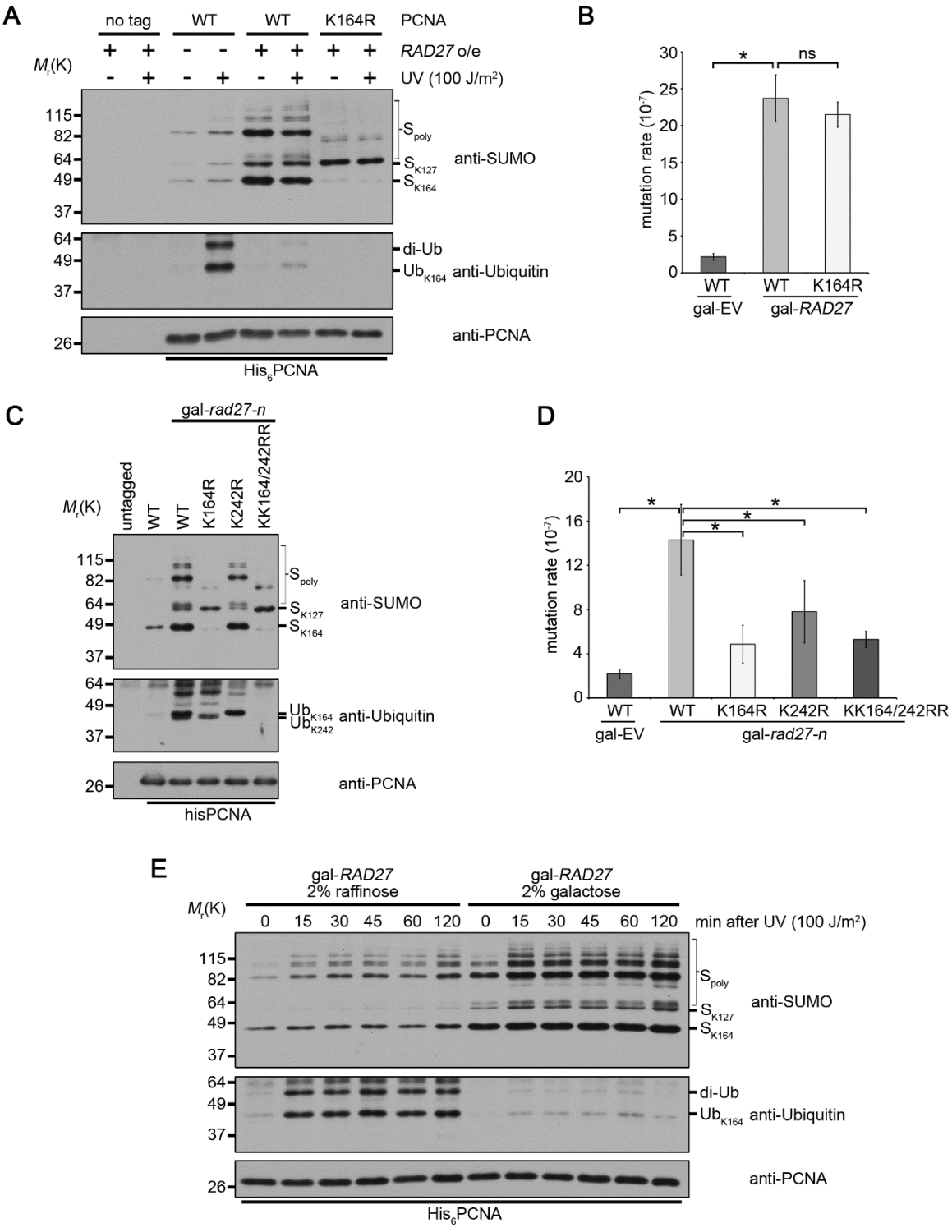
A
no tag
WT
WT
K164R
PCNA
RAD27 o/e
UV (100 J/m2)
Mr(K)
115
82
64
49
37
Spoly
SK127
SK164
anti-SUMO
di-Ub
UbK164
anti-Ubiquitin
anti-PCNA
His6PCNA
B
mutation rate (10-7)
*
ns
WT
WT
K164R
gal-EV
gal-RAD27
C
gal-rad27-n
untagged
WT
K164R
K242R
KK164/242RR
anti-SUMO
UbK164
UbK242
anti-Ubiquitin
anti-PCNA
hisPCNA
D
mutation rate (10-7)
WT
WT
K164R
K242R
KK164/242RR
gal-EV
gal-rad27-n
E
gal-RAD27
2% raffinose
gal-RAD27
2% galactose
0
15
30
45
60
120
min after UV (100 J/m2)
anti-SUMO
di-Ub
anti-Ubiquitin
anti-PCNA
His6PCNA

Figure 4.2. *RAD27* overexpression inhibits PCNA ubiquitination. (A) Strains with either untagged PCNA, His_6-PCNA, or His_6-PCNA-K164R and all carrying gal-*RAD27* were grown to OD_{600}~0.600 in medium lacking uracil. Overexpression of *RAD27* was then induced where indicated by the addition of galactose to a final concentration of 2%. UV treatment was applied 2 h after addition of galactose and the cultures were harvested 1 h later. His_6-PCNA was purified under denaturing conditions and analyzed by western blot with antibodies against PCNA, ubiquitin, and SUMO. (B) The mutation rate at the *CAN1* locus was measured in the indicated strains after growth to saturation in galactose containing medium. Each bar represents the median of at least 16 independent determinations. Error bars indicate standard error. Significance was determined by the Mann-Whitney U-test. (C) The indicated strains were grown to OD_{600}~0.600 in complete medium with 2% raffinose before addition of galactose to a final concentration of 2%. Cells were harvested after 3 h and His_6-PCNA was purified under denaturing conditions before analysis by western blot with antibodies against PCNA, ubiquitin, and SUMO. (D) The mutation rate at the *CAN1* locus was measured as in (B). (E) A strain with His_6-PCNA and carrying gal-*RAD27* was grown to OD_{600}~0.600 in medium lacking uracil and containing 2% raffinose. The culture was then split in half with one half receiving an additional 2% raffinose and the other having galactose added to a final concentration of 2%. Both cultures were treated with

Figure 4.3

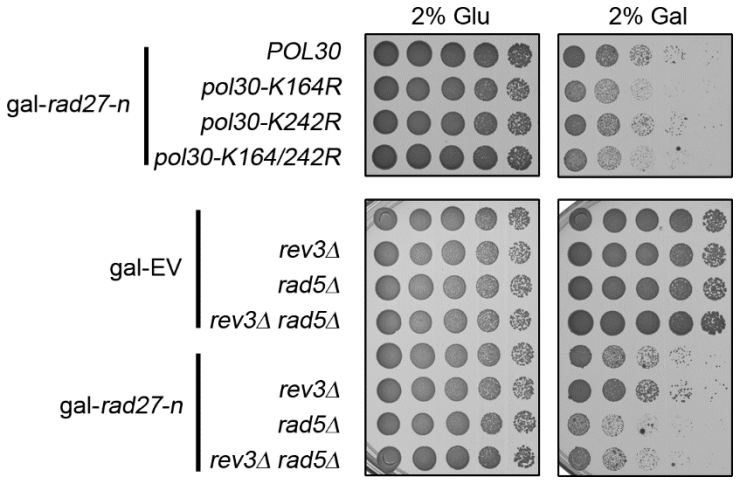

Figure 4.3. *rad27-n* overexpressing cells rely on error-free PRR for viability. 5-fold serial dilutions of the indicated strains were plated on medium lacking uracil and containing either 2% glucose to suppress overexpression or 2% galactose to induce *rad27-n* overexpression. Plates were incubated at 25°C for 4 days before imaging.

Figure 4.4

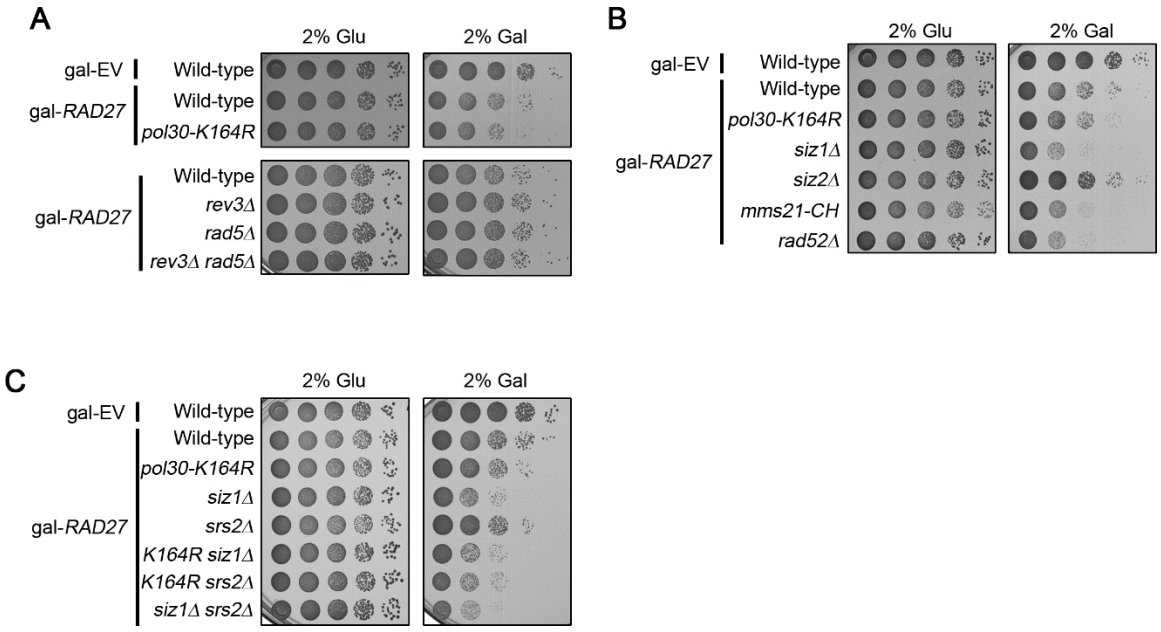

Figure 4.4. Sumoylation promotes the viability of *RAD27* overexpressing cells. (A-C) 10-fold serial dilutions of the indicated strains were plated on medium lacking uracil and containing either 2% glucose to suppress gal-*RAD27* or 2% galactose to induce *RAD27* overexpression. Plates were incubated at 25°C for 4 days before imaging.

Figure 4.5

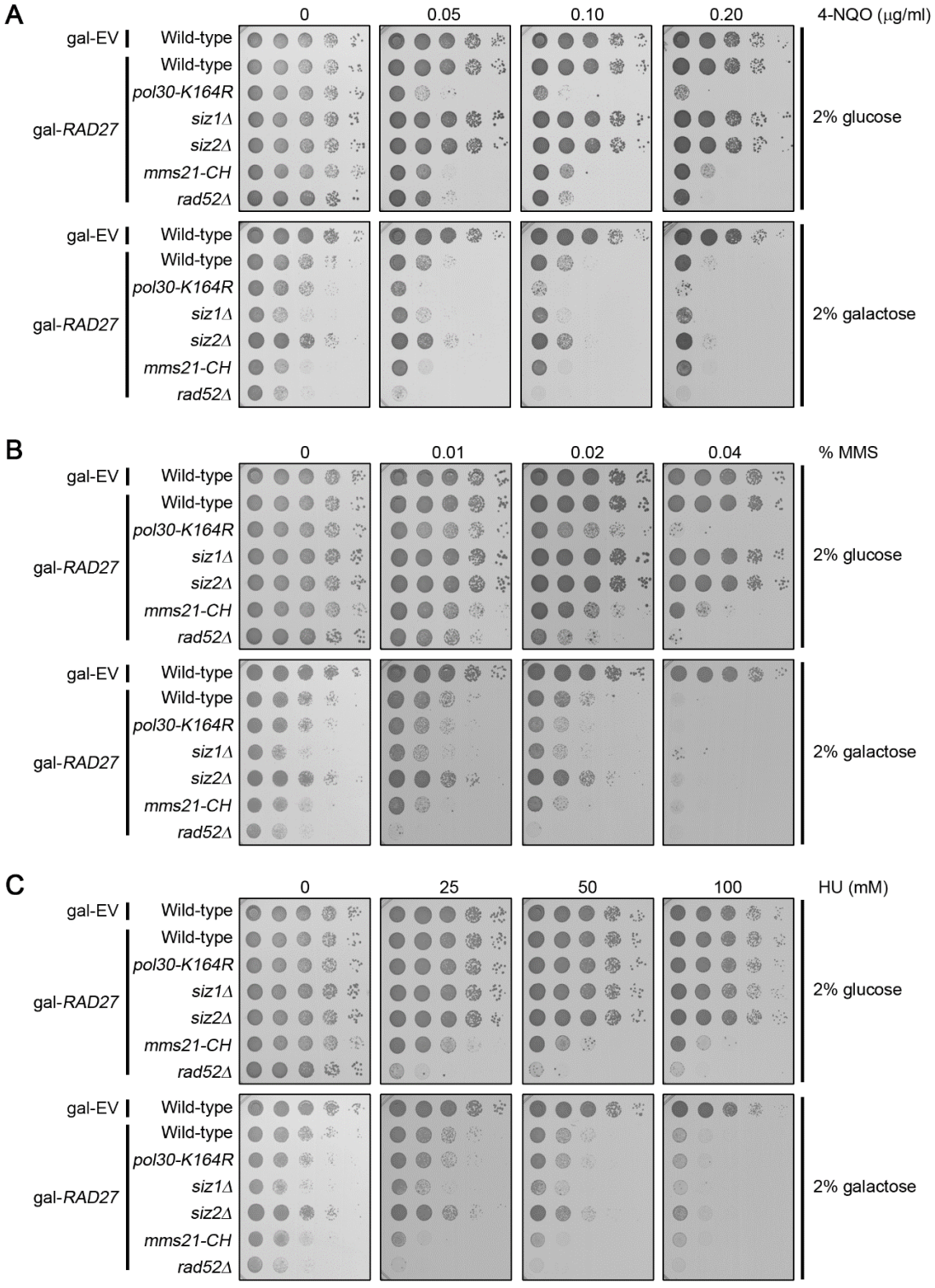
A
0
0.05
0.10
0.20
4-NQO (μg/ml)
gal-EV
Wild-type
gal-RAD27
Wild-type
pol30-K164R
siz1Δ
siz2Δ
mms21-CH
rad52Δ
2% glucose
2% galactose
B
0
0.01
0.02
0.04
% MMS
C
0
25
50
100
HU (mM)

Figure 4.5. Sumoylation promotes the viability of *RAD27* overexpressing cells. (A-C) 10-fold serial dilutions of the indicated strains were plated on medium lacking uracil and containing either 2% glucose to suppress gal-*RAD27* or 2% galactose to induce *RAD27* overexpression. Plates were incubated at 25°C for 4 days before imaging.

Figure 4.6

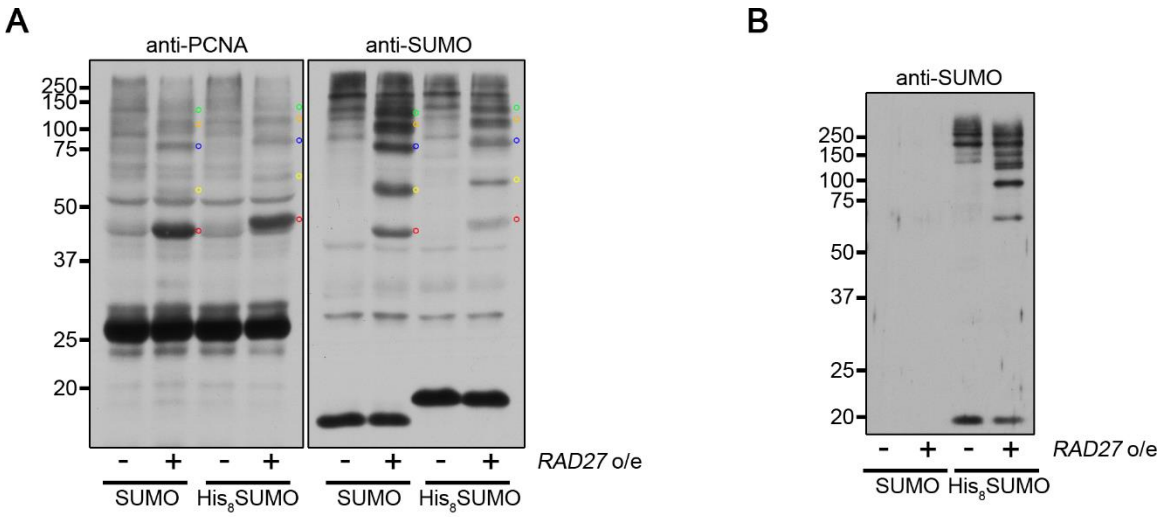

C

Exclusively present with *RAD27* overexpression	Spectral counts	Spectral counts in untagged SUMO
Pol30	9	0
Tdh1	7	8
Rad27	6	10
Zap1	3	2
Por1p	3	0
Sam2	2	0
Ape3	2	1
Vma2	2	3
HSC82	2	3
Pbp1	2	0
RPL4B	2	0
RPL4A	2	0
Suc2	2	0
Pir1	2	0
Ald3	2	0
Dbp7	2	2

Figure 4.5. PCNA is the most abundant sumoylation target. (A) Strains with either untagged SUMO or His_8-SUMO and carrying gal-*RAD27* were grown to OD_{600}~0.600 in medium lacking uracil and containing 2% raffinose. The cultures were then each split in half with one half receiving an additional 2% raffinose and the other having galactose added to a final concentration of 2%. Samples were harvested after 3 h and whole cell protein extracts were made by TCA precipitation. Extracts were fractionated by SDS-PAGE and analyzed by western blot with antibodies against PCNA and SUMO. The blots in this image were run side-by-side on the same gel. Corresponding bands between the SUMO and PCNA blots are marked with circles of the same color. (B) His_8-SUMO was purified under denaturing conditions from the cultures described in (A), fractionated by SDS-PAGE and analyzed by western blot with and anti-SUMO antibody. This purification was subsequently subjected to mass spectrometry analysis. (C) The most abundant proteins identified by mass spectrometry analysis under conditions of *RAD27* overexpression.

Figure 4.7

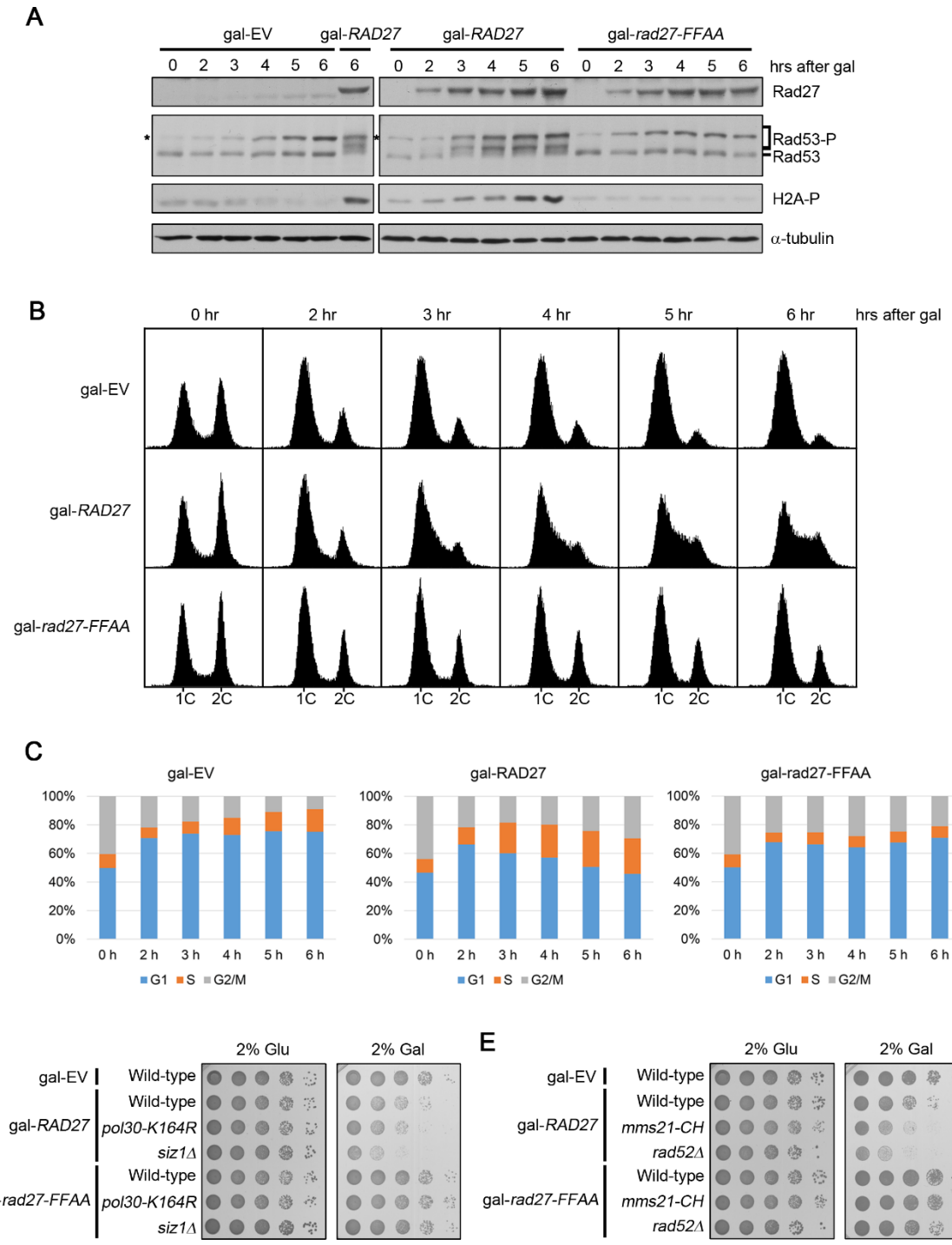
A
gal-EV
gal-RAD27
gal-RAD27
gal-rad27-FFAA
0 2 3 4 5 6 6 0 2 3 4 5 6 0 2 3 4 5 6
hrs after gal
Rad27
Rad53-P
Rad53
H2A-P
α-tubulin
B
0 hr
2 hr
3 hr
4 hr
5 hr
6 hr
hrs after gal
gal-EV
gal-RAD27
gal-rad27-FFAA
1C 2C
C
gal-EV
gal-RAD27
gal-rad27-FFAA
100%
80%
60%
40%
20%
0%
0 h 2 h 3 h 4 h 5 h 6 h
G1 S G2/M
D
2% Glu
2% Gal
gal-EV
gal-RAD27
gal-rad27-FFAA
Wild-type
Wild-type
pol30-K164R
siz1Δ
Wild-type
pol30-K164R
siz1Δ
E
2% Glu
2% Gal
gal-EV
gal-RAD27
gal-rad27-FFAA
Wild-type
Wild-type
mms21-CH
rad52Δ
Wild-type
mms21-CH
rad52Δ

Figure 4.6. Rad27-PCNA interaction mediates the effects of *RAD27* overexpression. (A) Strains containing either gal-EV, gal-*RAD27*, or gal-*rad27-FFAA* expression vectors were grown to OD_{600} ~0.600 in synthetic medium lacking uracil and containing 2% raffinose as a sugar source. Galactose was then added to a final concentration of 2% and samples were collected at the indicated time points for analysis by western blot and flow cytometry. Protein extracts were prepared by TCA precipitation and fractionated by SDS-PAGE for western blot analysis with anti-Rad27, anti-Rad53, anti-phospho-S129 H2A, and anti-tubulin antibodies. The asterisk on both Rad53 blots marks the galactose-dependent effect. (B) Samples from the same cultures described above were harvested at the indicated time points and DNA content was measured by flow cytometry on a BD Accuri C6 flow cytometer. (C) Quantification of the cell cycle distribution of the profiles in panel B. Quantification was carried out using the BD Accuri C6 software. (D and E) 10-fold serial dilutions of the indicated strains were plated on medium lacking uracil and containing either 2% glucose to suppress overexpression or 2% galactose to induce *RAD27* or *rad27-FFAA* overexpression. Plates were incubated at 25°C for 4 days before imaging.

Figure 4.8

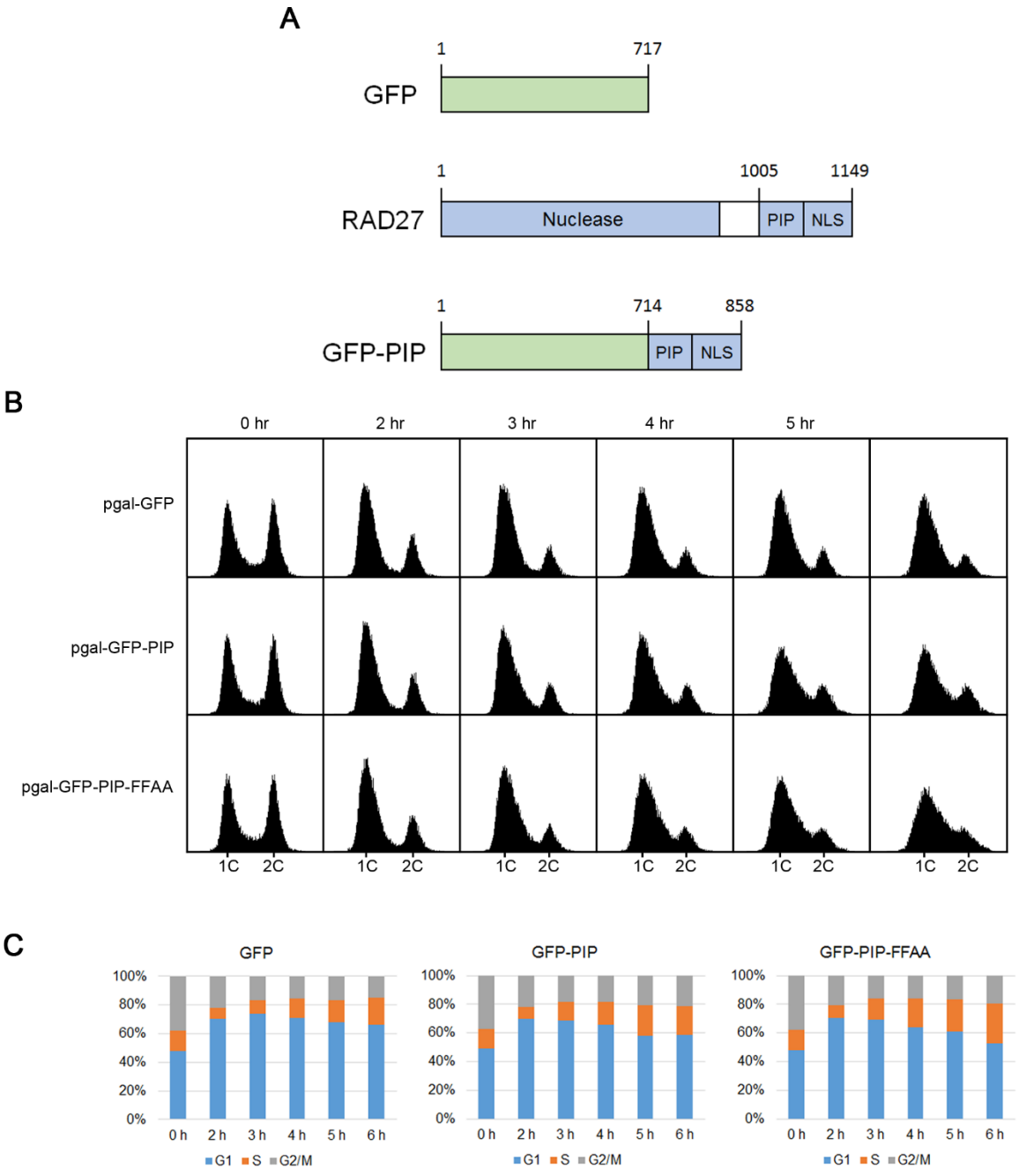
A
1
717
GFP
1
1005
1149
RAD27
Nuclease
PIP
NLS
1
714
858
GFP-PIP
PIP
NLS
B
0 hr
2 hr
3 hr
4 hr
5 hr
pgal-GFP
pgal-GFP-PIP
pgal-GFP-PIP-FFAA
1C
2C
C
GFP
GFP-PIP
GFP-PIP-FFAA
100%
80%
60%
40%
20%
0%
0 h
2 h
3 h
4 h
5 h
6 h
G1
S
G2/M

Figure 4.7. Overexpression of GFP-PIP does not fully replicate *RAD27* overexpression. (A) GFP-PIP was constructed by fusing the PIP motif and NLS of *RAD27* to the C terminus of full length GFP. The variant in which the PIP box contains the inactivating FFAA mutation was generated by site directed mutagenesis. (B) Cells overexpressing either GFP, GFP-PIP, or GFP-PIP-FFAA were harvested at the indicated time points after galactose addition and DNA content was measured by flow cytometry on a BD Accuri C6 flow cytometer. (C) Quantification of the cell cycle distribution of the profiles in panel B. Quantification was carried out using the BD Accuri C6 software.

Figure 4.9

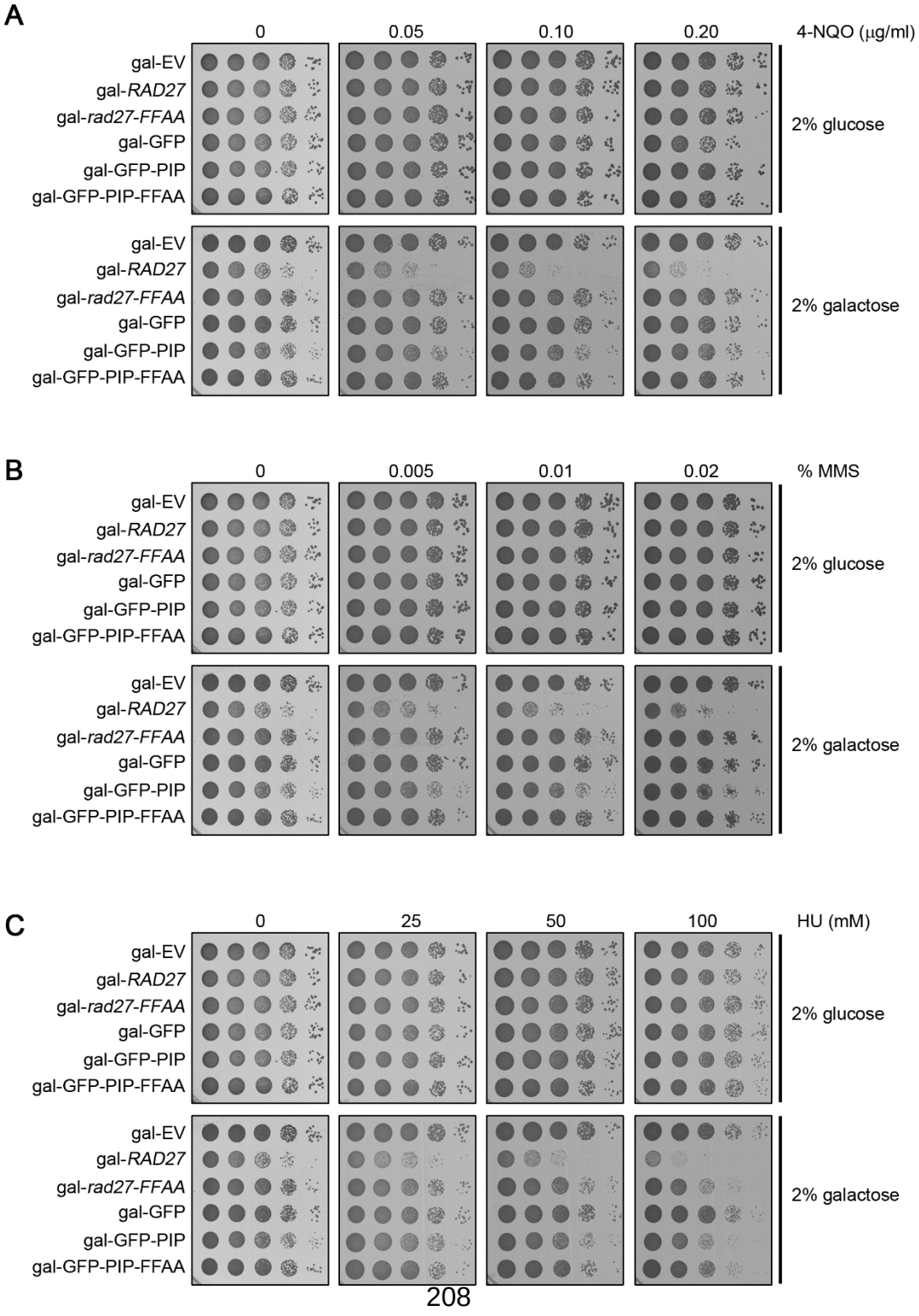
A
0
0.05
0.10
0.20
4-NQO (μg/ml)
gal-EV
gal-RAD27
gal-rad27-FFAA
gal-GFP
gal-GFP-PIP
gal-GFP-PIP-FFAA
2% glucose
2% galactose
B
0
0.005
0.01
0.02
% MMS
C
0
25
50
100
HU (mM)

Figure 4.8. GFP-PIP overexpression confers mild DNA damage sensitivity. (A) 10-fold serial dilutions of the indicated strains were plated on medium lacking uracil and containing either 2% glucose to suppress gal-*RAD27* or 2% galactose to induce *RAD27* overexpression. The medium contained either 0.05, 0.10 or 0.20 µg/ml 4-NQO as indicated. Plates were incubated at 25°C for 4 days before imaging. (B) 10-fold serial dilutions of the indicated strains were plated on medium lacking uracil and containing either 2% glucose to suppress gene expression or 2% galactose to induce overexpression. The medium contained either 0.005%, 0.01% or 0.02% MMS as indicated. Plates were incubated at 25°C for 4 days before imaging.

Figure 4.10

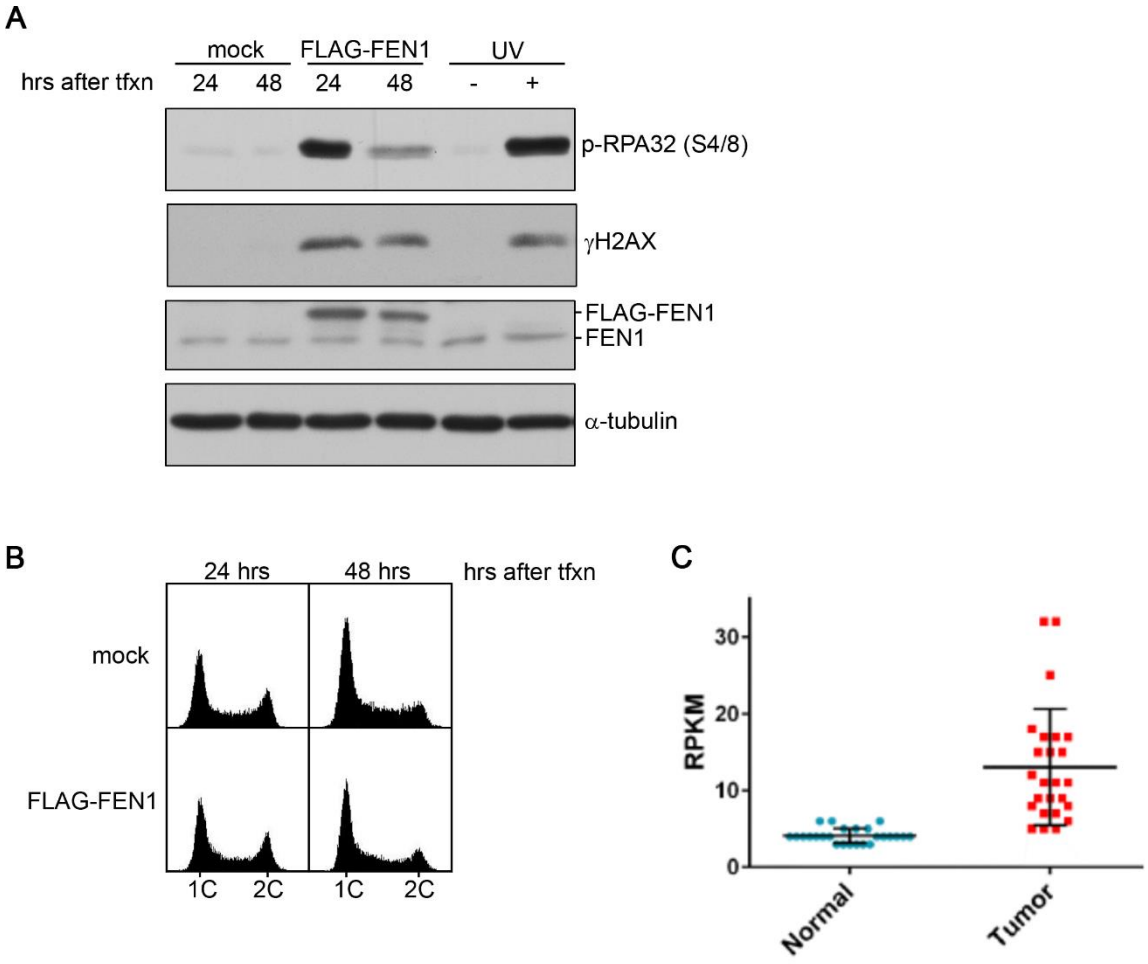
A
mock
FLAG-FEN1
UV
hrs after tfxn
24
48
24
48
-
+
p-RPA32 (S4/8)
γH2AX
FLAG-FEN1
FEN1
α-tubulin
B
24 hrs
48 hrs
hrs after tfxn
mock
FLAG-FEN1
1C
2C
1C
2C
C
RPKM
30
20
10
0
Normal
Tumor

Figure 4.9. FEN1 overexpression promotes genome instability. (A) 293T cells were either mock transfected or transiently transfected with FLAG-FEN1 under control of a CMV promoter and collected 24 or 48 h after transfection. Treatment with 10 J/m^2 UV was included as a positive control for DNA damage. UV treated cultures were harvested 24 h after irradiation. Whole cell extracts were isolated and fractionated by SDS-PAGE for western blot analysis with anti-phospho-S4/8 RPA32, anti-γH2AX, anti-FEN1, and anti-α-tubulin. (B) A portion of the cells collected from the experiment described in (A) were fixed in ethanol and DNA content was measured by flow cytometry on a BD Accuri C6 flow cytometer. (C) FEN1 reads per kilobase of transcript per million mapped reads (RPKM) from lung adecarcinoma and matched normal tissue were compared. Of the 162 RNASeq datasets available, these 50 were paired tumor/normal samples from 25 patients. Lines indicate mean values and bars represent standard deviations. Source: The Cancer Genome Atlas (TCGA): http://cancergenome.nih.gov/.

Table 4.1

Table 4.1. Yeast Strains used in Chapter 4

Strain Name	Relevant Genotype	Source
	E133 derived strains	
EFS20	*MATα, ade5-1, lys2-A12, trp1-289, his7-2, leu2-3,112, ura3-52, bar1*	[Tran *et al.* 1997]
AByb1541	pYEP195spgal-EV (*URA3*)	This study
AByb1542	pRG105A (*URA3*)	This study
AByb1543	pRG106A (*URA3*)	This study
AByb1800	pRG106A (*URA3*), *pol30::pol30-K164R (LEU2)*	This study
AByb2205	pRG106A (*URA3*), *rad52*::*TRP1*	This study
AByb2216	pRG106A (*URA3*), *dnl4*::*TRP1*	This study
AByb2108	pRG106A (URA3), leu2*::His-POL30 (LEU2), pol30::TRP1*	This study
AByb2110	pRG106A (URA3), *leu2::His-pol30-K164R (LEU2), pol30::TRP1*	This study
EFS3101	*rad27::gal-rad27-D179A*	This study

Strain Name	Relevant Genotype	Source
AByb1549	*rad27::gal-RAD27*, leu2*::His-POL30 (LEU2), pol30::URA3*	This study
AByb1550	*rad27::gal-rad27-D179A*, leu2*::His-POL30 (LEU2), pol30::URA3*	This study
AByb1554	*rad27::gal-rad27-D179A*, *leu2::His-pol30-K164R (LEU2), pol30::URA3*	This study
AByb1805	*rad27::gal-rad27-D179A*, *leu2::His-pol30-K242R (LEU2), pol30::URA3*	This study
AByb1806	*rad27::gal-rad27-D179A*, *leu2::His-pol30-KK164/242RR (LEU2), pol30::URA3*	This study
AByb1795	pRG105A (*URA3*), *pol30::POL30 (LEU2)*	This study
AByb1797	pRG105A (*URA3*), *pol30::pol30-K164R (LEU2)*	This study
AByb1798	pRG106A (*URA3*), *pol30::POL30 (LEU2)*	This study
AByb1834	pRG105A (*URA3*), *pol30::pol30-K242R (LEU2)*	This study
AByb1836	pRG105A (*URA3*), *pol30::pol30-KK164/242RR (LEU2)*	This study
AByb1835	pRG106A (*URA3*), *pol30::pol30-K242R (LEU2)*	This study
AByb1837	pRG106A (*URA3*), *pol30::pol30-KK164/242RR (LEU2)*	This study
AByb2094	YEP195spgal-EV (URA3), rev3::*LEU2*	This study
AByb2096	YEP195spgal-EV (*URA3*), *rad5*::*TRP1*	This study

Strain Name	Relevant Genotype	Source
AByb2098	YEP195spgal-EV (*URA3*), *rad5*::*TRP1*, *rev3*::*LEU2*	This study
AByb2100	pRG106A (URA3), rev3::*LEU2*	This study
AByb2102	pRG106A (*URA3*), *rad5*::*TRP1*	This study
AByb2104	pRG106A (*URA3*), *rad5*::*TRP1*, *rev3*::*LEU2*	This study
AByb2469	pRG106A-FFAA (*URA3*)	This study
AByb2165	pRG106A (*URA3*), *siz1*::*TRP1*	This study
AByb2289	pRG106A (*URA3*), *mms21::mms21-CH* (*LEU2*)	This study
AByb2471	pRG106A-FFAA (*URA3*), *pol30::pol30-K164R (LEU2)*	This study
AByb2477	pRG106A-FFAA (*URA3*), *siz1::TRP1*	This study
AByb2483	pRG106A-FFAA (*URA3*), *mms21::mms21-CH* (*LEU2*)	This study
AByb2473	pRG106A-FFAA (*URA3*), *rad52*::*TRP1*	This study
AByb2124	pRG105A (URA3), rev3::*LEU2*	This study
AByb2057	pRG105A (*URA3*), *rad5*::*TRP1*	This study
AByb2126	pRG105A (*URA3*), *rad5*::*TRP1*, *rev3*::*LEU2*	This study

Strain Name	Relevant Genotype	Source
AByb2525	gal-GFP (URA3)	This study
AByb2518	gal-GFP-PIP (URA3)	This study
AByb2520	gal-GFP-PIP-FFAA (URA3)	This study
	W303-1a derived strains	
AByb2382	pRG106A (URA3), smt3::*SMT3* (*TRP1)*	
AByb2384	pRG106A (URA3), *smt3::His-SMT3* (*TRP*)	

CHAPTER 5

Discussion and Future Directions

The work described in this dissertation is aimed at understanding the role of PCNA ubiquitination and PRR in the absence of DNA damage. A wealth of evidence gathered over the past 50 years has described the function of these pathways in the tolerance of chemical damage, which impairs the progress of DNA polymerases and prevents complete replication. Only more recently have we come to appreciate that PRR pathways are also operational in the absence of DNA damage. This was first identified in yeast strains carrying hypomorphic alleles of genes encoding the replication polymerases Pol-α, Pol-δ, and Pol-ε [Northam *et al.* 2006, Suzuki *et al.* 2009, Becker *et al.* 2014]. It is likely that the replication defect in these cells is very similar to DNA damage insofar as the activity of the polymerases is incapable of maintaining pace with DNA unwinding, causing ssDNA regions to be formed [Byun *et al.* 2005, Lopes *et al.* 2006, Suzuki *et al.* 2009]. In chapter 3, I describe a role for PRR in mutants of genes unrelated to DNA synthesis, further widening the scope of conditions under which these pathways operate. The picture that is emerging is that PCNA ubiquitination and PRR act as general suppressors of replication stress under a variety of compromising conditions.

The findings summarized in chapter 2 provide greater detail for the activity of PRR in mutants impaired for nascent DNA priming. This study identifies a requirement for PRR in Mcm10 mutants and establishes that the basis for this dependence is separable between Mcm10's activity in priming/DNA synthesis and its role in origin activation [Becker *et al.* 2014]. These findings support the notion

that Mcm10 has functions beyond origin activation, which had hitherto been controversial in the field. To extend the analysis beyond obvious defects in the replication machinery that affect DNA synthesis, in chapter 3, I have taken a systematic approach to characterizing PRR in the absence of DNA damage through the use of a genome-wide genetic screen. Two particularly exciting conclusions were derived from this study. First, mutations that disrupt lagging strand replication exhibited a much greater requirement for PRR than those affecting leading strand synthesis. Second, I demonstrated that PRR acts to rescue DNA processing defects at the junction of Okazaki fragments in *rad27Δ* mutants [Becker *et al.* 2015]. This is to my knowledge the first example of PRR acting in response to disruption of a non-DNA synthesis related process of replication. Finally, in chapter 4 I have studied the effect of *RAD27* overexpression on genome stability. Whereas overexpression markedly impairs replication and leads to the accumulation of DNA damage and mutations, I observed no dependence on PRR. In fact, PRR was largely suppressed under these conditions as measured by the level of PCNA ubiquitination. Instead, SUMO-dependent pathways, including those that target PCNA, were highly upregulated and played a critical role in supporting cell viability.

Altogether this work has illuminated conditions that lead to a requirement for PRR, particularly on the lagging strand, and show that *RAD27* overexpression is a potent driver of genome instability. These studies leave some old questions unanswered as well as raising several new ones. For the remainder of this chapter,

I will address outstanding questions resulting from this work that would provide interesting avenues for further research.

1) How does SUMO improve the viability of RAD27 overexpressing cells? In chapter 4, I identified a genetic requirement for the SUMO E3 ligases Siz1 and Mms21 in cells that overexpress *RAD27*. Furthermore, I determined that PCNA-K164 is not the only SUMO target of importance for Siz1 under these conditions (Figure 4.4). No specific targets of Mms21 were identified despite the fact that it has been previously reported to be activated in response to replication stress [Branzei *et al.* 2006]. Identification of Siz1 and Mms21 targets would provide valuable mechanistic insight into how these proteins counteract replication stress, particularly when *RAD27* is overexpressed.

In the experiment described in Figure 4.6, His_8-tagged SUMO was purified under denaturing conditions in the presence or absence of *RAD27* overexpression. Analysis by SDS-PAGE fractionation and anti-SUMO western blot revealed a noticeable change in the pattern of sumoylated proteins in cells overexpressing *RAD27* (Figure 4.6A). A single pilot experiment was performed to identify these SUMO targets by mass spectrometry using spectral counts as a measure of abundance. PCNA was the only clear candidate identified in this analysis. However, as discussed in chapter 4, the minimal effect on viability of ablating PCNA-K164 sumoylation in comparison to deleting the SUMO ligases *SIZ1* or *MMS21* indicates that there are additional targets of importance (Figure 4.4).

Recent work in our laboratory has exploited the same purification strategy to isolate SUMO conjugates and quantified changes in their abundance between wild-type and mutant conditions [Thu *et al.* 2016]. Quantification was carried out using a novel label-free method known as DRIPPER [Thu *et al.* 2016, Van Riper *et al.* 2016]. Optimization of the His_8-SUMO purification strategy with *RAD27* overexpression and utilization of this sensitive quantification method could potentially identify additional targets that were missed in the first analysis.

It may also be that the relatively high amount of PCNA identified masks our ability to detect other target proteins. Performing the same experiment in a ***siz1Δ*** or PCNA-K164R mutant background that lacks sumoylated PCNA would be a strategy to increase our detection of non-PCNA targets. The ***siz1Δ*** background in particular would allow us to identify targets that are specific to Mms21 and assist in dissecting the divergent functions of these E3 SUMO ligases. The simplicity of the yeast system and the abundance of genetic tools at our disposal make it ideally suited for solving mechanistic questions such as this. Principles established in yeast can then be used in guiding similar investigations in the more complex human system.

We already know that many cancers have elevated levels of genome instability and chronic replication stress [Gaillard *et al.* 2015]. How they are able to manage this stress over many rounds of replication is not entirely clear. A cursory review of MMS21 status in a variety of cancers available in the TCGA database reveals that its expression is frequently amplified in many cancer cell types (Figure

5.1). It is possible that this is reflective of an increased requirement for MMS21-dependent sumoylation pathways. Unfortunately, this line of inquiry is woefully understudied at the moment. A better understanding for the targets of MMS21 during stressed replication holds the potential to reveal mechanisms at work in cancer cells that are relied upon to manage rapid proliferation in the face of chronic replication stress. Such pathways would be attractive therapeutic targets for anti-cancer treatment. Yeast research offers the opportunity to understand mechanistically how MMS21 amplification acts as a compensatory mechanism that enables the tolerance of chronic replication stress.

2) What are the functions of non-K164 sites of PCNA ubiquitination? Since the original discovery of PCNA-K164 as a site of ubiquitin attachment at least two additional sites in yeast, K107 and K242, have been identified [Das-Bradoo *et al.* 2010, Nguyen *et al.* 2013]. Alternate sites of ubiquitination have also been mapped in proteomic screens of human cells after UV irradiation or treatment with the spindle formation inhibitor colchicine [Xu *et al.* 2010, Povlsen *et al.* 2012, Elia *et al.* 2015]. The conventional dogma in the field has long stated that K164 is the sole site for ubiquitination. However, in light of these recent findings, it is becoming increasingly apparent that modification of PCNA by ubiquitin is not as exclusive to K164 as initially thought.

Chapter 4 includes the first description of K242 as a site for ubiquitin attachment in yeast. This was observed in cells overexpressing the nuclease dead

allele of *RAD27* known as *rad27-n* (Figure 4.2C). Interestingly, whereas K242 is not evolutionarily conserved, a nearby lysine residue (K240) is conserved in higher eukaryotes (Figure 5.2). These residues map to very similar positions on the PCNA trimer and could conceivably be functionally redundant (Figure 5.2). However, K240 has not yet been reported as a site of ubiquitination on human PCNA. Because substitution of K242 with arginine reduced the mutation rate of *rad27-n* expressing cells, we inferred that K242, like K164, is capable of facilitating mutagenic TLS. Given that ubiquitination at this site has never been previously observed and that no *in vivo* evidence has linked TLS to ubiquitination of a non-K164 site, investigation of K242 modification and its regulation may be of importance in understanding the factors that govern PRR usage.

Determining the ubiquitin conjugating enzymes that target K242 will be crucial in understanding its relationship to PRR. Because I have already established detection tools for ubiquitination at this site *via* His_6-PCNA purification and western blot analysis with anti-PCNA and anti-ubiquitin antibodies (Figure 4.2C), I would begin by knocking out candidate ubiquitin conjugating enzymes and ubiquitin ligases. First, I would delete Rad6-Rad18 to immediately determine whether the same pathway that attaches ubiquitin to K164 regulates K242. If deletion of these enzymes were not to have any impact on K242 ubiquitination, the relative simplicity of yeast would make a systematic approach manageable. *S. cerevisiae* has twelve described E2 ubiquitin conjugating enzymes [Ye and Rape 2009]. Three have no known nuclear functions and can be initially discounted. Of

the nine remaining E2 enzymes, eight could be deleted individually in *rad27-n* overexpressing mutants. One is known to be essential but its activity can be modulated through the use of a temperature sensitive allele [Goebl *et al.* 1988]. Candidate E2 enzyme(s) can be used to narrow the number of potential E3 ubiquitin ligases based on their known E2 preferences [Ye and Rape 2009]. This information may give insight into how K242 ubiquitination is regulated based on what is already known about the enzymes that target it and may reveal co-regulated pathways. Furthermore, identification of E2 and E3 enzymes would provide genetic tools to alter ubiquitination status that are independent of PCNA mutation.

In addition to K242, our laboratory has described K107 as an alternative site of PCNA ubiquitination in yeast [Das-Bradoo *et al.* 2010, Nguyen *et al.* 2013]. Similar to K242, targeting of this residue has only been observed under a specific genetic condition, namely, DNA ligase I deficiency. With the exception of K107, very little is known about the enzymatic pathways that underlie targeting of alternative residues or the downstream effectors impacted by such modifications. However, the fact that K242 and K107 are both targeted in response to very specific mutations may indicate that different sites are involved in the cellular response to specific replication defects [Das-Bradoo *et al.* 2010]. If K242 were targeted for ubiquitination in a Rad6-Rad18 independent manner it would further support the notion that different sites of PCNA ubiquitination are linked to different sources of replication stress. This suggests a model in which different sites of

ubiquitination act as a sort of “DNA damage code” that enables cells to distinguish between different replication stress intermediates and respond appropriately.

3) Do RPA coated 5’ flaps directly recruit Rad6-Rad18? In Chapter 3, I provided genetic evidence that flap endonuclease (*rad27Δ*) deficient yeast cells accumulate long RPA-coated flaps, which act as a substrate for Rad6-Rad18 recruitment and subsequent PCNA ubiquitination (Figure 3.8D). This conclusion is predicated on the assumption that the *rad27Δ* mutants do not form ssDNA gaps, which are also a stimulus for PCNA ubiquitination. The foundation of our argument in this study was that overexpression of *DNA2*, which cleaves 5’ flaps *after* they have grown long enough to bind RPA, had no impact on the level of PCNA ubiquitination in *rad27Δ* mutants. In contrast, overexpression of *EXO1*, which cleaves short DNA flaps *before* they become long enough to bind RPA *did* alleviate PCNA ubiquitination. Together, these two pieces of evidence support a model in which long RPA-bound flaps present in *rad27Δ* are sufficient to recruit Rad6-Rad18 and ubiquitinate PCNA. However, we lack direct biochemical evidence that RPA-bound 5’ flaps are a direct substrate for Rad6-Rad18 recruitment. We therefore cannot exclude the possibility that overexpression of *EXO1*, a close evolutionary relative of *RAD27*, more effectively rescues the *rad27Δ* mutant phenotype than *DNA2* and compensates for any deficiency that leads to ssDNA gap formation [Orans *et al.* 2011, Tsutakawa *et al.* 2011, Miętus *et al.* 2014]. Evidence of a more direct nature

will be necessary to confirm the model that long RPA-coated flaps stimulate PCNA ubiquitination.

Previous *in vitro* work has shown that long flaps are capable of binding RPA and indeed a robust body of evidence suggests that this is necessary for flap processing by *DNA2* [Bae and Seo 2000, Bae *et al.* 2001, Ayyagari *et al.* 2003]. Furthermore, genetic evidence has suggested that RPA-bound 5' flaps are sufficient to propagate Mec1-Ddc2 binding and checkpoint activation [Budd *et al.* 2011, Nguyen *et al.* 2013]. Although the theory that long RPA coated flaps participate in DNA damage response signaling has existed for at least 5 years, it has never been directly demonstrated. Confirmation that such flaps are key participants in checkpoint/PRR signaling would force us to reconsider the dynamic relationship between Okazaki fragment processing and the DNA damage response. This finding would also have implications for other processes such as BER which involve 5' flap intermediates [Krokan and Bjørås 2013].

To prove that RPA-bound 5' flaps are sufficient to recruit Rad6-Rad18 to ubiquitinate PCNA, I would carry out a set of *in vitro* experiments using a biotin labelled 5' flapped DNA substrate with purified PCNA, RPA, ubiquitin, and Rad6-Rad18. Purification of the biotin-labelled DNA substrate from this mixture over streptavidin conjugated resin, fractionation by SDS-PAGE, and analysis by western blot with antibodies directed against components of the RPA complex will be necessary to demonstrate that RPA is binding the 5' flap under defined reaction conditions. Western blot analysis for Rad6 and Rad18 that might co-purify with the

biotin-DNA substrate in the presence or absence of RPA would determine whether RPA-bound flaps recruit this complex. A DNA substrate with a single-stranded gap would serve as a positive control, whereas a dsDNA fragment of equal length would act as a negative control. If the addition of RPA in the presence of a 5' flapped DNA substrate significantly enhanced PCNA ubiquitination, I would conclude that Rad6-Rad18 ubiquitinated PCNA by directly binding RPA-coated 5' flaps.

Such an experimental system could also be adapted to assay the involvement of RPA-bound flaps in other DNA damage response transactions, including binding and activation of the kinase Mec1. Between BER and Okazaki fragment processing, the frequency with which 5' flaps appear throughout the cell cycle suggests that their involvement in intracellular signaling could be a powerful regulatory element for DNA replication and cell cycle progression.

Figure 5.1

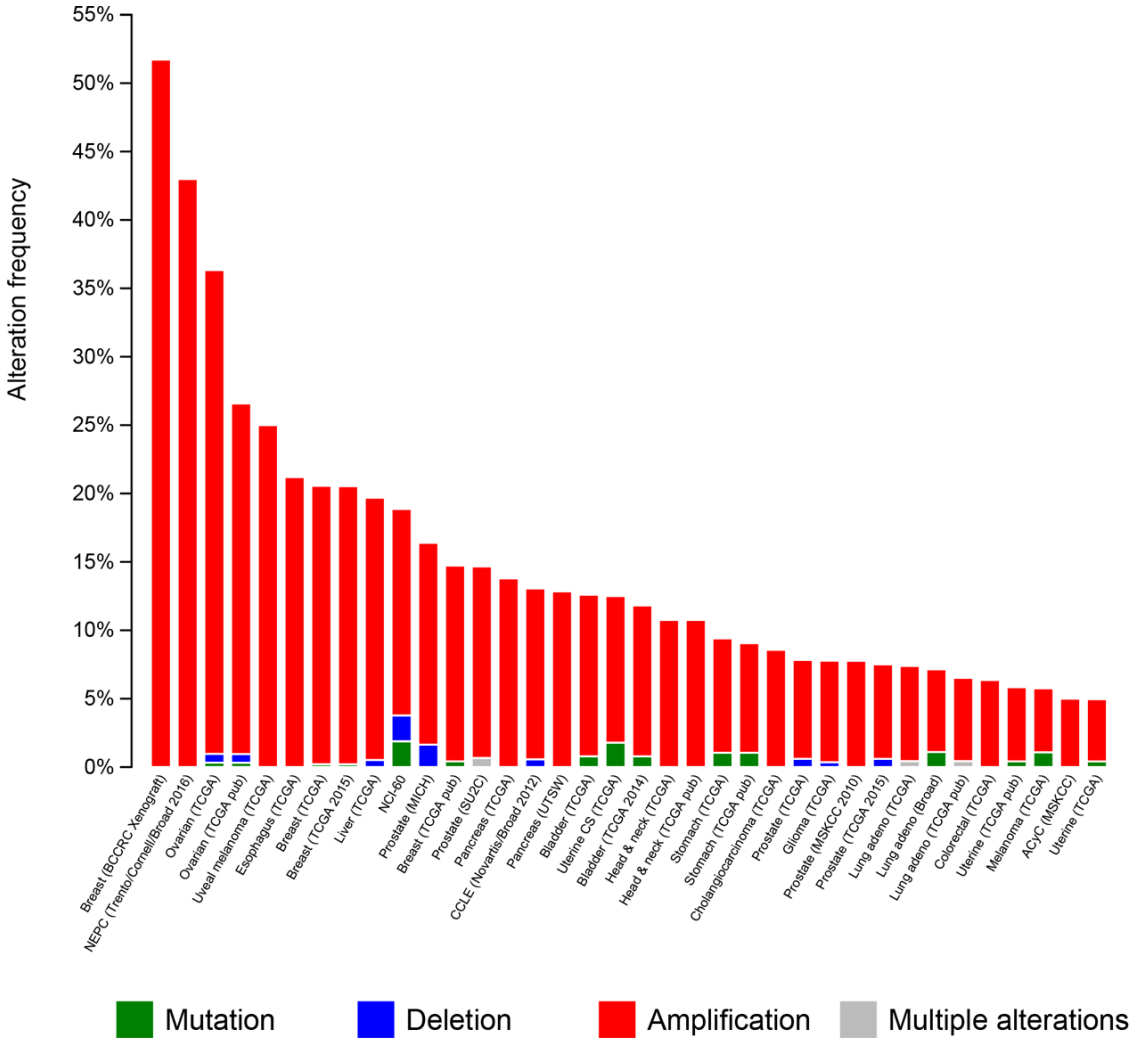

Figure 5.1. MMS21 expression is frequently amplified in cancer. Illustrated are the genetic alterations of MMS21 associated with a variety of cancers. This data is freely available from TCGA and was accessed via cBioportal for Cancer Genomics (http://www.cbioportal.org/). This figure was adapted from an image downloaded from cBioportal [Cerami *et al.* 2012, Gao *et al.* 2013].

Figure 5.2

```
mouse        ALRYLNFFTKATPLSPTVTLSMSADVPLVVEYKIADMGHLKYYLAPKIEDE-EAS 261
human        ALRYLNFFTKATPLSSTVTLSMSADVPLVVEYKIADMGHLKYYLAPKIEDE-EGS 261
chicken      ALRYLNFFTKATPLSPTVTLSMSADVPLVVEYKIADMGHLKYYLAPKIEDQQEGS 262
Xenopus      ALRYLNFFTKATPLSPTVILSMSADIPLVVEYKIADMEHVKYYLAPKIEDE-EAS 261
Drosophila   ACRYLNAFTKATPLSTQVQLSMCADVPLVVEYAIKDLGHIRYYLAPKIEDN-ET- 260
pombe        SLKYLAQFTKATPLATRVTLSMSNDVPLLVEYKMES-GFLRFYLAPKIGEEDE-- 259
Cerevisiae   GAKYLLDIIKGSSLSDRVGIRLSSEAPALFQFDLKS-GFLQFFLAPKFNDE-E-- 258
                                            240 242
```

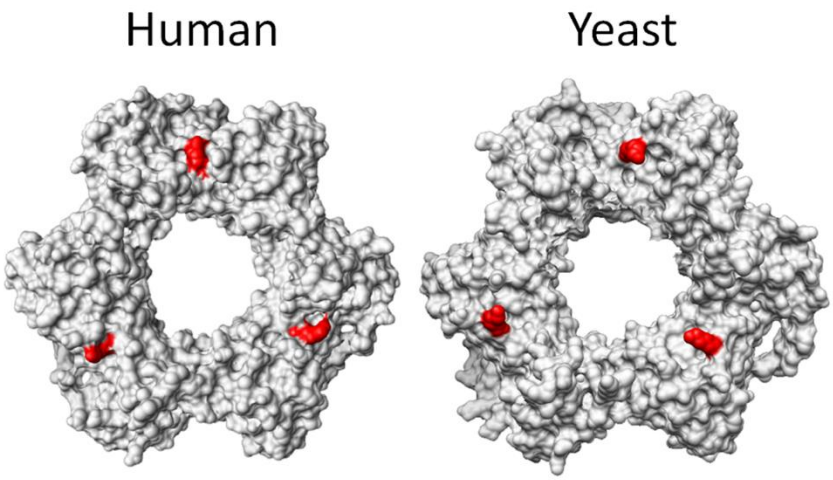

Figure 5.2. Yeast PCNA-K242 is positionally conserved in higher eukaryotes. An alignment between yeast PCNA and that of other eukaryotic organisms was generated using Clustal Omega (http://www.ebi.ac.uk/Tools/msa/clustalo/) (top). Residues 240 and 242 are highlighted with red boxes. The space filling models of human and yeast PCNA (bottom) were obtained from the RCSB Protein Database (PDB) (http://www.rcsb.org/pdb/home/home.do) and modeled using the Chimera program (https://www.cgl.ucsf.edu/chimera/). In the human PCNA structure K240 is highlighted in red and in the yeast structure K242 is highlighted [Krishna *et al.* 1994, Gulbis *et al.* 1996].

REFERENCES

Abdel-Fatah, T. M., R. Russell, N. Albarakati, D. J. Maloney, D. Dorjsuren, O. M. Rueda, P. Moseley, V. Mohan, H. Sun and R. Abbotts (2014). "Genomic and protein expression analysis reveals flap endonuclease 1 (FEN1) as a key biomarker in breast and ovarian cancer." Molecular oncology **8**(7): 1326-1338.

Acharya, N., R. E. Johnson, S. Prakash and L. Prakash (2006). "Complex formation with Rev1 enhances the proficiency of Saccharomyces cerevisiae DNA polymerase ζ for mismatch extension and for extension opposite from DNA lesions." Molecular and cellular biology **26**(24): 9555-9563.

Albertella, M. R., A. Lau and M. J. O'Connor (2005). "The overexpression of specialized DNA polymerases in cancer." DNA repair **4**(5): 583-593.

Alcasabas, A. A., A. J. Osborn, J. Bachant, F. Hu, P. J. Werler, K. Bousset, K. Furuya, J. F. Diffley, A. M. Carr and S. J. Elledge (2001). "Mrc1 transduces signals of DNA replication stress to activate Rad53." Nature Cell Biology **3**(11): 958-965.

Arezi, B. and R. D. Kuchta (2000). "Eukaryotic DNA primase." Trends in biochemical sciences **25**(11): 572-576.

Ayyagari, R., X. V. Gomes, D. A. Gordenin and P. M. Burgers (2003). "Okazaki fragment maturation in yeast I. Distribution of functions between FEN1 and DNA2." Journal of Biological Chemistry **278**(3): 1618-1625.

Bae, S.-H., K.-H. Bae, J.-A. Kim and Y.-S. Seo (2001). "RPA governs endonuclease switching during processing of Okazaki fragments in eukaryotes." Nature **412**(6845): 456-461.

Bae, S.-H. and Y.-S. Seo (2000). "Characterization of the enzymatic properties of the yeast dna2 Helicase/endonuclease suggests a new model for Okazaki fragment processing." Journal of Biological Chemistry **275**(48): 38022-38031.

Balakrishnan, L., J. Stewart, P. Polaczek, J. L. Campbell and R. A. Bambara (2010). "Acetylation of Dna2 endonuclease/helicase and flap endonuclease 1 by p300 promotes DNA stability by creating long flap intermediates." Journal of Biological Chemistry **285**(7): 4398-4404.

Baranovskiy, A. G., A. G. Lada, H. M. Siebler, Y. Zhang, Y. I. Pavlov and T. H. Tahirov (2012). "DNA polymerase δ and ζ switch by sharing accessory subunits of DNA polymerase δ." Journal of Biological Chemistry **287**(21): 17281-17287.

Barford, J. and R. Hall (1976). "Estimation of the length of cell cycle phases from asynchronous cultures of Saccharomyces cerevisiae." Experimental cell research **102**(2): 276-284.

Bartkova, J., Z. Hořejší, K. Koed, A. Krämer, F. Tort, K. Zieger, P. Guldberg, M. Sehested, J. M. Nesland and C. Lukas (2005). "DNA damage response as a candidate anti-cancer barrier in early human tumorigenesis." Nature **434**(7035): 864-870.

Baryshnikova, A., M. Costanzo, S. Dixon, F. J. Vizeacoumar, C. L. Myers, B. Andrews and C. Boone (2010). "Synthetic genetic array (SGA) analysis in Saccharomyces cerevisiae and Schizosaccharomyces pombe." Methods in enzymology **470**: 145-179.

Baryshnikova, A., M. Costanzo, Y. Kim, H. Ding, J. Koh, K. Toufighi, J.-Y. Youn, J. Ou, B.-J. San Luis and S. Bandyopadhyay (2010). "Quantitative analysis of fitness and genetic interactions in yeast on a genome scale." Nature methods **7**(12): 1017-1024.

Baxley, R. M., Y. M. Thu and A.-K. Bielinsky (2016). The Role of Mcm10 in Replication Initiation. The Initiation of DNA Replication in Eukaryotes, Springer**:** 319-341.

Becker, J. R., H. D. Nguyen, X. Wang and A.-K. Bielinsky (2014). "Mcm10 deficiency causes defective-replisome-induced mutagenesis and a dependency on error-free postreplicative repair." Cell Cycle **13**(11): 1737-1748.

Becker, J. R., C. Pons, H. D. Nguyen, M. Costanzo, C. Boone, C. L. Myers and A.-K. Bielinsky (2015). "Genetic Interactions Implicating Postreplicative Repair in Okazaki Fragment Processing." PLoS Genet **11**(11): e1005659.

Bell, S. P. and A. Dutta (2002). "DNA replication in eukaryotic cells." Annual review of biochemistry **71**(1): 333-374.

Bellaoui, M., M. Chang, J. Ou, H. Xu, C. Boone and G. W. Brown (2003). "Elg1 forms an alternative RFC complex important for DNA replication and genome integrity." The EMBO journal **22**(16): 4304-4313.

Beltrao, P., G. Cagney and N. J. Krogan (2010). "Quantitative genetic interactions reveal biological modularity." Cell **141**(5): 739-745.

Ben-Aroya, S., A. Koren, B. Liefshitz, R. Steinlauf and M. Kupiec (2003). "ELG1, a yeast gene required for genome stability, forms a complex related to replication factor C." Proceedings of the National Academy of Sciences **100**(17): 9906-9911.

Branzei, D. (2011). "Ubiquitin family modifications and template switching." FEBS letters **585**(18): 2810-2817.

Branzei, D. and M. Foiani (2010). "Maintaining genome stability at the replication fork." Nature reviews Molecular cell biology **11**(3): 208-219.

Branzei, D., M. Seki and T. Enomoto (2004). "Rad18/Rad5/Mms2-mediated polyubiquitination of PCNA is implicated in replication completion during replication stress." Genes to cells **9**(11): 1031-1042.

Branzei, D., J. Sollier, G. Liberi, X. Zhao, D. Maeda, M. Seki, T. Enomoto, K. Ohta and M. Foiani (2006). "Ubc9-and mms21-mediated sumoylation

counteracts recombinogenic events at damaged replication forks." Cell **127**(3): 509-522.
Budd, M. E., I. A. Antoshechkin, C. Reis, B. J. Wold and J. L. Campbell (2011). "Inviability of a DNA2 deletion mutant is due to the DNA damage checkpoint." Cell Cycle **10**(10): 1690-1698.
Budd, M. E., C. C. Reis, S. Smith, K. Myung and J. L. Campbell (2006). "Evidence suggesting that Pif1 helicase functions in DNA replication with the Dna2 helicase/nuclease and DNA polymerase δ." Molecular and Cellular Biology **26**(7): 2490-2500.
Budd, M. E., A. H. Y. Tong, P. Polaczek, X. Peng, C. Boone and J. L. Campbell (2005). "A network of multi-tasking proteins at the DNA replication fork preserves genome stability." PLoS genetics **1**(6): e61.
Burgers, P. M. (2009). "Polymerase dynamics at the eukaryotic DNA replication fork." Journal of Biological Chemistry **284**(7): 4041-4045.
Byun, T. S., M. Pacek, M.-c. Yee, J. C. Walter and K. A. Cimprich (2005). "Functional uncoupling of MCM helicase and DNA polymerase activities activates the ATR-dependent checkpoint." Genes & development **19**(9): 1040-1052.
Callahan, J. L., K. J. Andrews, V. A. Zakian and C. H. Freudenreich (2003). "Mutations in yeast replication proteins that increase CAG/CTG expansions also increase repeat fragility." Molecular and cellular biology **23**(21): 7849-7860.
Cerami, E., J. Gao, U. Dogrusoz, B. E. Gross, S. O. Sumer, B. A. Aksoy, A. Jacobsen, C. J. Byrne, M. L. Heuer and E. Larsson (2012). "The cBio cancer genomics portal: an open platform for exploring multidimensional cancer genomics data." Cancer discovery **2**(5): 401-404.
Chabes, A., B. Georgieva, V. Domkin, X. Zhao, R. Rothstein and L. Thelander (2003). "Survival of DNA damage in yeast directly depends on increased dNTP levels allowed by relaxed feedback inhibition of ribonucleotide reductase." Cell **112**(3): 391-401.
Chapados, B. R., D. J. Hosfield, S. Han, J. Qiu, B. Yelent, B. Shen and J. A. Tainer (2004). "Structural basis for FEN-1 substrate specificity and PCNA-mediated activation in DNA replication and repair." Cell **116**(1): 39-50.
Chattopadhyay, S. and A.-K. Bielinsky (2007). "Human Mcm10 regulates the catalytic subunit of DNA polymerase-α and prevents DNA damage during replication." Molecular biology of the cell **18**(10): 4085-4095.
Chen, J., W. Bozza and Z. Zhuang (2011). "Ubiquitination of PCNA and its essential role in eukaryotic translesion synthesis." Cell biochemistry and biophysics **60**(1-2): 47-60.
Chen, X. L., H. R. Silver, L. Xiong, I. Belichenko, C. Adegite and E. S. Johnson (2007). "Topoisomerase I-dependent viability loss in Saccharomyces cerevisiae mutants defective in both SUMO conjugation and DNA repair." Genetics **177**(1): 17-30.

Ciosk, R., W. Zachariae, C. Michaelis, A. Shevchenko, M. Mann and K. Nasmyth (1998). "An ESP1/PDS1 complex regulates loss of sister chromatid cohesion at the metaphase to anaphase transition in yeast." Cell **93**(6): 1067-1076.

Clark, A. B., M. E. Cook, H. T. Tran, D. A. Gordenin, M. A. Resnick and T. A. Kunkel (1999). "Functional analysis of human MutSα and MutSβ complexes in yeast." Nucleic acids research **27**(3): 736-742.

Cleaver, J. E. (2005). "Cancer in xeroderma pigmentosum and related disorders of DNA repair." Nature Reviews Cancer **5**(7): 564-573.

Cohen-Fix, O., J.-M. Peters, M. W. Kirschner and D. Koshland (1996). "Anaphase initiation in Saccharomyces cerevisiae is controlled by the APC-dependent degradation of the anaphase inhibitor Pds1p." Genes & development **10**(24): 3081-3093.

Coleman, T. R., P. B. Carpenter and W. G. Dunphy (1996). "The Xenopus Cdc6 protein is essential for the initiation of a single round of DNA replication in cell-free extracts." Cell **87**(1): 53-63.

Collins, N. S., S. Bhattacharyya and R. S. Lahue (2007). "Rev1 enhances CAG· CTG repeat stability in Saccharomyces cerevisiae." DNA repair **6**(1): 38-44.

Costa, A., I. Ilves, N. Tamberg, T. Petojevic, E. Nogales, M. R. Botchan and J. M. Berger (2011). "The structural basis for MCM2–7 helicase activation by GINS and Cdc45." Nature structural & molecular biology **18**(4): 471-477.

Costanzo, M., J. L. Nishikawa, X. Tang, J. S. Millman, O. Schub, K. Breitkreuz, D. Dewar, I. Rupes, B. Andrews and M. Tyers (2004). "CDK activity antagonizes Whi5, an inhibitor of G1/S transcription in yeast." Cell **117**(7): 899-913.

Cremona, C. A., P. Sarangi, Y. Yang, L. E. Hang, S. Rahman and X. Zhao (2012). "Extensive DNA damage-induced sumoylation contributes to replication and repair and acts in addition to the mec1 checkpoint." Molecular cell **45**(3): 422-432.

Daee, D. L., T. Mertz and R. S. Lahue (2007). "Postreplication repair inhibits CAG· CTG repeat expansions in Saccharomyces cerevisiae." Molecular and cellular biology **27**(1): 102-110.

Daigaku, Y., A. A. Davies and H. D. Ulrich (2010). "Ubiquitin-dependent DNA damage bypass is separable from genome replication." Nature **465**(7300): 951-955.

Das-Bradoo, S., H. D. Nguyen and A.-K. Bielinsky (2010). "Damage-specific modification of PCNA." Cell Cycle **9**(18): 3674-3679.

Das-Bradoo, S., H. D. Nguyen, J. L. Wood, R. M. Ricke, J. C. Haworth and A.-K. Bielinsky (2010). "Defects in DNA ligase I trigger PCNA ubiquitylation at Lys 107." Nature cell biology **12**(1): 74-79.

Das-Bradoo, S., R. M. Ricke and A.-K. Bielinsky (2006). "Interaction between PCNA and diubiquitinated Mcm10 is essential for cell growth in budding yeast." Molecular and cellular biology **26**(13): 4806-4817.
Davidson, M. B., Y. Katou, A. Keszthelyi, T. L. Sing, T. Xia, J. Ou, J. A. Vaisica, N. Thevakumaran, L. Marjavaara and C. L. Myers (2012). "Endogenous DNA replication stress results in expansion of dNTP pools and a mutator phenotype." The EMBO journal **31**(4): 895-907.
Davies, A. A., D. Huttner, Y. Daigaku, S. Chen and H. D. Ulrich (2008). "Activation of ubiquitin-dependent DNA damage bypass is mediated by replication protein a." Molecular cell **29**(5): 625-636.
Dirick, L., T. Böhm and K. Nasmyth (1995). "Roles and regulation of Cln-Cdc28 kinases at the start of the cell cycle of Saccharomyces cerevisiae." The EMBO journal **14**(19): 4803.
Dornfeld, K. J. and D. M. Livingston (1991). "Effects of controlled RAD52 expression on repair and recombination in Saccharomyces cerevisiae." Molecular and cellular biology **11**(4): 2013-2017.
Downs, J. A., N. F. Lowndes and S. P. Jackson (2000). "A role for Saccharomyces cerevisiae histone H2A in DNA repair." Nature **408**(6815): 1001-1004.
Drake, J. W. (1991). "A constant rate of spontaneous mutation in DNA-based microbes." Proceedings of the National Academy of Sciences **88**(16): 7160-7164.
Elia, A. E., A. P. Boardman, D. C. Wang, E. L. Huttlin, R. A. Everley, N. Dephoure, C. Zhou, I. Koren, S. P. Gygi and S. J. Elledge (2015). "Quantitative Proteomic Atlas of Ubiquitination and Acetylation in the DNA Damage Response." Molecular cell.
Evrin, C., P. Clarke, J. Zech, R. Lurz, J. Sun, S. Uhle, H. Li, B. Stillman and C. Speck (2009). "A double-hexameric MCM2-7 complex is loaded onto origin DNA during licensing of eukaryotic DNA replication." Proceedings of the National Academy of Sciences **106**(48): 20240-20245.
Feldman, R. R., C. C. Correll, K. B. Kaplan and R. J. Deshaies (1997). "A complex of Cdc4p, Skp1p, and Cdc53p/cullin catalyzes ubiquitination of the phosphorylated CDK inhibitor Sic1p." Cell **91**(2): 221-230.
Fien, K., Y.-S. Cho, J.-K. Lee, S. Raychaudhuri, I. Tappin and J. Hurwitz (2004). "Primer utilization by DNA polymerase α-primase is influenced by its interaction with Mcm10p." Journal of Biological Chemistry **279**(16): 16144-16153.
Fitch, I., C. Dahmann, U. Surana, A. Amon, K. Nasmyth, L. Goetsch, B. Byers and B. Futcher (1992). "Characterization of four B-type cyclin genes of the budding yeast Saccharomyces cerevisiae." Molecular biology of the cell **3**(7): 805-818.
Flynn, R. L. and L. Zou (2011). "ATR: a master conductor of cellular responses to DNA replication stress." Trends in biochemical sciences **36**(3): 133-140.

Foster, P. L. (2006). "Methods for determining spontaneous mutation rates." Methods in enzymology **409**: 195-213.
Freudenreich, C. H., S. M. Kantrow and V. A. Zakian (1998). "Expansion and length-dependent fragility of CTG repeats in yeast." Science **279**(5352): 853-856.
Freudenthal, B. D., L. Gakhar, S. Ramaswamy and M. T. Washington (2010). "Structure of monoubiquitinated PCNA and implications for translesion synthesis and DNA polymerase exchange." Nature structural & molecular biology **17**(4): 479-484.
Fu, Y. V., H. Yardimci, D. T. Long, A. Guainazzi, V. P. Bermudez, J. Hurwitz, A. van Oijen, O. D. Schärer and J. C. Walter (2011). "Selective bypass of a lagging strand roadblock by the eukaryotic replicative DNA helicase." Cell **146**(6): 931-941.
Fu, Y. V., H. Yardimci, D. T. Long, T. V. Ho, A. Guainazzi, V. P. Bermudez, J. Hurwitz, A. van Oijen, O. D. Schärer and J. C. Walter (2011). "Selective bypass of a lagging strand roadblock by the eukaryotic replicative DNA helicase." Cell **146**(6): 931-941.
Fumasoni, M., K. Zwicky, F. Vanoli, M. Lopes and D. Branzei (2015). "Error-Free DNA Damage Tolerance and Sister Chromatid Proximity during DNA Replication Rely on the Polα/Primase/Ctf4 Complex." Molecular cell **57**(5): 812-823.
Gai, D., Y. P. Chang and X. S. Chen (2010). "Origin DNA melting and unwinding in DNA replication." Current opinion in structural biology **20**(6): 756-762.
Gaillard, H., T. García-Muse and A. Aguilera (2015). "Replication stress and cancer." Nature Reviews Cancer **15**(5): 276-289.
Gambus, A., F. Van Deursen, D. Polychronopoulos, M. Foltman, R. C. Jones, R. D. Edmondson, A. Calzada and K. Labib (2009). "A key role for Ctf4 in coupling the MCM2-7 helicase to DNA polymerase α within the eukaryotic replisome." The EMBO journal **28**(19): 2992-3004.
Ganesan, A. K. (1974). "Persistence of pyrimidine dimers during post-replication repair in ultraviolet light-irradiated Escherichia coli K12." Journal of molecular biology **87**(1): 103-119.
Gao, J., B. A. Aksoy, U. Dogrusoz, G. Dresdner, B. Gross, S. O. Sumer, Y. Sun, A. Jacobsen, R. Sinha and E. Larsson (2013). "Integrative analysis of complex cancer genomics and clinical profiles using the cBioPortal." Science signaling **6**(269): pl1.
Garg, P. and P. M. Burgers (2005). "Ubiquitinated proliferating cell nuclear antigen activates translesion DNA polymerases η and REV1." Proceedings of the National Academy of Sciences of the United States of America **102**(51): 18361-18366.
Garg, P., C. M. Stith, N. Sabouri, E. Johansson and P. M. Burgers (2004). "Idling by DNA polymerase δ maintains a ligatable nick during lagging-strand DNA replication." Genes & development **18**(22): 2764-2773.

Gary, R., M. S. Park, J. P. Nolan, H. L. Cornelius, O. G. Kozyreva, H. T. Tran, K. S. Lobachev, M. A. Resnick and D. A. Gordenin (1999). "A novel role in DNA metabolism for the binding of Fen1/Rad27 to PCNA and implications for genetic risk." Molecular and cellular biology **19**(8): 5373-5382.

Goebl, M. G., J. Yochem, S. Jentsch, J. P. McGrath, A. Varshavsky and B. Byers (1988). "The yeast cell cycle gene CDC34 encodes a ubiquitin-conjugating enzyme." Science **241**(4871): 1331-1335.

Gulbis, J. M., Z. Kelman, J. Hurwitz, M. O'Donnell and J. Kuriyan (1996). "Structure of the C-terminal region of p21 WAF1/CIP1 complexed with human PCNA." Cell **87**(2): 297-306.

Gutiérrez, P. J. and T. S.-F. Wang (2003). "Genomic instability induced by mutations in Saccharomyces cerevisiae POL1." Genetics **165**(1): 65-81.

Haase, S. B., M. Winey and S. I. Reed (2001). "Multi-step control of spindle pole body duplication by cyclin-dependent kinase." Nature cell biology **3**(1): 38-42.

Hanahan, D. and R. A. Weinberg (2011). "Hallmarks of cancer: the next generation." Cell **144**(5): 646-674.

Haracska, L., C. A. Torres-Ramos, R. E. Johnson, S. Prakash and L. Prakash (2004). "Opposing effects of ubiquitin conjugation and SUMO modification of PCNA on replicational bypass of DNA lesions in Saccharomyces cerevisiae." Molecular and Cellular Biology **24**(10): 4267-4274.

Haracska, L., I. Unk, R. E. Johnson, E. Johansson, P. M. Burgers, S. Prakash and L. Prakash (2001). "Roles of yeast DNA polymerases δ and ζ and of Rev1 in the bypass of abasic sites." Genes & Development **15**(8): 945-954.

Harkins, V., C. Gabrielse, L. Haste and M. Weinreich (2009). "Budding yeast Dbf4 sequences required for Cdc7 kinase activation and identification of a functional relationship between the Dbf4 and Rev1 BRCT domains." Genetics **183**(4): 1269-1282.

Hartwell, L. H., J. Culotti, J. R. Pringle and B. J. Reid (1974). "Genetic control of the cell division cycle in yeast." Science **183**(4120): 46-51.

Haworth, J., R. C. Alver, M. Anderson and A.-K. Bielinsky (2010). "Ubc4 and Not4 regulate steady-state levels of DNA polymerase-α to promote efficient and accurate DNA replication." Molecular biology of the cell **21**(18): 3205-3219.

Heller, R. C., S. Kang, W. M. Lam, S. Chen, C. S. Chan and S. P. Bell (2011). "Eukaryotic origin-dependent DNA replication in vitro reveals sequential action of DDK and S-CDK kinases." Cell **146**(1): 80-91.

Hereford, L. M. and L. H. Hartwell (1974). "Sequential gene function in the initiation of Saccharomyces cerevisiae DNA synthesis." Journal of molecular biology **84**(3): 445-461.

Hishida, T., Y. Kubota, A. M. Carr and H. Iwasaki (2009). "RAD6–RAD18–RAD5-pathway-dependent tolerance to chronic low-dose ultraviolet light." Nature **457**(7229): 612-615.
Hoege, C., B. Pfander, G.-L. Moldovan, G. Pyrowolakis and S. Jentsch (2002). "RAD6-dependent DNA repair is linked to modification of PCNA by ubiquitin and SUMO." Nature **419**(6903): 135-141.
Homesley, L., M. Lei, Y. Kawasaki, S. Sawyer, T. Christensen and B. K. Tye (2000). "Mcm10 and the MCM2–7 complex interact to initiate DNA synthesis and to release replication factors from origins." Genes & development **14**(8): 913-926.
Huang, D., B. D. Piening and A. G. Paulovich (2013). "The preference for error-free or error-prone postreplication repair in Saccharomyces cerevisiae exposed to low-dose methyl methanesulfonate is cell cycle dependent." Molecular and cellular biology **33**(8): 1515-1527.
Huang, M.-E. and R. D. Kolodner (2005). "A biological network in Saccharomyces cerevisiae prevents the deleterious effects of endogenous oxidative DNA damage." Molecular cell **17**(5): 709-720.
Hubscher, U. and Y.-S. Seo (2001). "Replication of the lagging strand: a concert of at least 23 polypeptides." Molecules and cells **12**(2): 149-157.
Hwang, J.-C., W.-W. Sung, H.-P. Tu, K.-C. Hsieh, C.-M. Yeh, C.-J. Chen, H.-C. Tai, C.-T. Hsu, G. S. Shieh and J.-G. Chang (2015). "The Overexpression of FEN1 and RAD54B May Act as Independent Prognostic Factors of Lung Adenocarcinoma." PloS one **10**(10): e0139435.
Jackson, S. P. and J. Bartek (2009). "The DNA-damage response in human biology and disease." Nature **461**(7267): 1071-1078.
Jackson, S. P. and D. Durocher (2013). "Regulation of DNA damage responses by ubiquitin and SUMO." Molecular cell **49**(5): 795-807.
Jentsch, S., J. P. McGrath and A. Varshavsky (1986). "The yeast DNA repair gene RAD6 encodes a ubiquitin-conjugating enzyme." Nature **329**(6135): 131-134.
Jin, Y. H., R. Ayyagari, M. A. Resnick, D. A. Gordenin and P. M. Burgers (2003). "Okazaki Fragment Maturation in Yeast II. COOPERATION BETWEEN THE POLYMERASE AND 3′–5′-EXONUCLEASE ACTIVITIES OF POL δ IN THE CREATION OF A LIGATABLE NICK." Journal of Biological Chemistry **278**(3): 1626-1633.
Jin, Y. H., R. Obert, P. M. Burgers, T. A. Kunkel, M. A. Resnick and D. A. Gordenin (2001). "The 3′→ 5′ exonuclease of DNA polymerase δ can substitute for the 5′ flap endonuclease Rad27/Fen1 in processing Okazaki fragments and preventing genome instability." Proceedings of the National Academy of Sciences **98**(9): 5122-5127.
Jiyang, O., K. Kawamura, Y. Tada, H. Ohmori, H. Kimura, S. Sakiyama and M. Tagawa (2001). "DNA polymerase κ, implicated in spontaneous and DNA

damage-induced mutagenesis, is overexpressed in lung cancer." Cancer research **61**(14): 5366-5369.
Johnson, R. E., S. T. Henderson, T. D. Petes, S. Prakash, M. Bankmann and L. Prakash (1992). "Saccharomyces cerevisiae RAD5-encoded DNA repair protein contains DNA helicase and zinc-binding sequence motifs and affects the stability of simple repetitive sequences in the genome." Molecular and Cellular Biology **12**(9): 3807-3818.
Kanellis, P., R. Agyei and D. Durocher (2003). "Elg1 forms an alternative PCNA-interacting RFC complex required to maintain genome stability." Current biology **13**(18): 1583-1595.
Kanke, M., Y. Kodama, T. S. Takahashi, T. Nakagawa and H. Masukata (2012). "Mcm10 plays an essential role in origin DNA unwinding after loading of the CMG components." The EMBO journal **31**(9): 2182-2194.
Kao, H.-I., J. Veeraraghavan, P. Polaczek, J. L. Campbell and R. A. Bambara (2004). "On the roles of Saccharomyces cerevisiae Dna2p and Flap endonuclease 1 in Okazaki fragment processing." Journal of Biological Chemistry **279**(15): 15014-15024.
Karras, G. I., M. Fumasoni, G. Sienski, F. Vanoli, D. Branzei and S. Jentsch (2013). "Noncanonical role of the 9-1-1 clamp in the error-free DNA damage tolerance pathway." Molecular cell **49**(3): 536-546.
Karras, G. I. and S. Jentsch (2010). "The< i> RAD6</i> DNA Damage Tolerance Pathway Operates Uncoupled from the Replication Fork and Is Functional Beyond S Phase." Cell **141**(2): 255-267.
Karras, G. I. and S. Jentsch (2010). "The RAD6 DNA damage tolerance pathway operates uncoupled from the replication fork and is functional beyond S phase." Cell **141**(2): 255-267.
Kenyon, C. J. and G. C. Walker (1980). "DNA-damaging agents stimulate gene expression at specific loci in Escherichia coli." Proceedings of the National Academy of Sciences **77**(5): 2819-2823.
Kim, J.-M., H.-Y. Sohn, S. Y. Yoon, J.-H. Oh, J. O. Yang, J. H. Kim, K. S. Song, S.-M. Rho, H. S. Yoo and Y. S. Kim (2005). "Identification of gastric cancer–related genes using a cDNA microarray containing novel expressed sequence tags expressed in gastric cancer cells." Clinical Cancer Research **11**(2): 473-482.
Kochenova, O. V., D. L. Daee, T. M. Mertz, P. V. Shcherbakova and S. Jinks-Robertson (2015). "DNA Polymerase ζ-Dependent Lesion Bypass in Saccharomyces cerevisiae Is Accompanied by Error-Prone Copying of Long Stretches of Adjacent DNA." PLoS genetics **11**(3).
Kolesar, P., V. Altmannova, S. Silva, M. Lisby and L. Krejci (2016). "Pro-recombination role of Srs2 requires SUMO but is independent of PCNA interaction." Journal of Biological Chemistry: jbc. M115. 685891.
Kolodner, R. D., C. D. Putnam and K. Myung (2002). "Maintenance of genome stability in Saccharomyces cerevisiae." Science **297**(5581): 552-557.

Krejci, L., S. Van Komen, Y. Li, J. Villemain, M. S. Reddy, H. Klein, T. Ellenberger and P. Sung (2003). "DNA helicase Srs2 disrupts the Rad51 presynaptic filament." Nature **423**(6937): 305-309.

Krishna, T. S., X.-P. Kong, S. Gary, P. M. Burgers and J. Kuriyan (1994). "Crystal structure of the eukaryotic DNA polymerase processivity factor PCNA." Cell **79**(7): 1233-1243.

Krokan, H. E. and M. Bjørås (2013). "Base excision repair." Cold Spring Harbor perspectives in biology **5**(4): a012583.

Kubota, T., Y. Katou, R. Nakato, K. Shirahige and A. D. Donaldson (2015). "Replication-Coupled PCNA Unloading by the Elg1 Complex Occurs Genome-wide and Requires Okazaki Fragment Ligation." Cell Reports.

Kubota, T., K. Nishimura, M. T. Kanemaki and A. D. Donaldson (2013). "The Elg1 replication factor C-like complex functions in PCNA unloading during DNA replication." Molecular cell **50**(2): 273-280.

Kucherlapati, M., K. Yang, M. Kuraguchi, J. Zhao, M. Lia, J. Heyer, M. F. Kane, K. Fan, R. Russell and A. M. Brown (2002). "Haploinsufficiency of Flap endonuclease (Fen1) leads to rapid tumor progression." Proceedings of the National Academy of Sciences **99**(15): 9924-9929.

Lam, J. S., D. B. Seligson, H. Yu, A. Li, M. Eeva, A. J. Pantuck, G. Zeng, S. Horvath and A. S. Belldegrun (2006). "Flap endonuclease 1 is overexpressed in prostate cancer and is associated with a high Gleason score." BJU international **98**(2): 445-451.

Larsen, E., L. Kleppa, T. J. Meza, L. A. Meza-Zepeda, C. Rada, C. G. Castellanos, G. F. Lien, G. J. Nesse, M. S. Neuberger and J. K. Laerdahl (2008). "Early-onset lymphoma and extensive embryonic apoptosis in two domain-specific Fen1 mice mutants." Cancer research **68**(12): 4571-4579.

Lawrence, C. W. and R. Christensen (1976). "UV mutagenesis in radiation-sensitive strains of yeast." Genetics **82**(2): 207-232.

Lazzaro, F., D. Novarina, F. Amara, D. L. Watt, J. E. Stone, V. Costanzo, P. M. Burgers, T. A. Kunkel, P. Plevani and M. Muzi-Falconi (2012). "RNase H and postreplication repair protect cells from ribonucleotides incorporated in DNA." Molecular cell **45**(1): 99-110.

Lee, C., I. Liachko, R. Bouten, Z. Kelman and B. K. Tye (2010). "Alternative mechanisms for coordinating polymerase α and MCM helicase." Molecular and cellular biology **30**(2): 423-435.

Lee, G.-H., H. Nishimori, Y. Sasaki, H. Matsushita, T. Kitagawa and T. Tokino (2003). "Analysis of lung tumorigenesis in chimeric mice indicates the Pulmonary adenoma resistance 2 (Par2) locus to operate in the tumor-initiation stage in a cell-autonomous manner: detection of polymorphisms in the Polı gene as a candidate for Par2." Oncogene **22**(15): 2374-2382.

Lee, G. H. and H. Matsushita (2005). "Genetic linkage between Polı deficiency and increased susceptibility to lung tumors in mice." Cancer science **96**(5): 256-259.
Lee, M., C.-H. Lee, A. A. Demin, P. R. Munashingha, T. Amangyeld, B. Kwon, T. Formosa and Y.-S. Seo (2014). "Rad52/Rad59-dependent recombination as a means to rectify faulty Okazaki fragment processing." Journal of Biological Chemistry **289**(21): 15064-15079.
Lei, M., Y. Kawasaki, M. R. Young, M. Kihara, A. Sugino and B. K. Tye (1997). "Mcm2 is a target of regulation by Cdc7–Dbf4 during the initiation of DNA synthesis." Genes & development **11**(24): 3365-3374.
Lemée, F., V. Bergoglio, A. Fernandez-Vidal, A. Machado-Silva, M.-J. Pillaire, A. Bieth, C. Gentil, L. Baker, A.-L. Martin and C. Leduc (2010). "DNA polymerase θ up-regulation is associated with poor survival in breast cancer, perturbs DNA replication, and promotes genetic instability." Proceedings of the National Academy of Sciences **107**(30): 13390-13395.
Lemontt, J. F. (1971). "Mutants of yeast defective in mutation induced by ultraviolet light." Genetics **68**(1): 21.
Levikova, M. and P. Cejka (2015). "The Saccharomyces cerevisiae Dna2 can function as a sole nuclease in the processing of Okazaki fragments in DNA replication." Nucleic acids research: gkv710.
Lew, D. J. and S. I. Reed (1993). "Morphogenesis in the yeast cell cycle: regulation by Cdc28 and cyclins." The Journal of cell biology **120**(6): 1305-1320.
Lew, D. J. and S. I. Reed (1995). "A cell cycle checkpoint monitors cell morphogenesis in budding yeast." The Journal of Cell Biology **129**(3): 739-749.
Lewis, L. K., G. Karthikeyan, J. W. Westmoreland and M. A. Resnick (2002). "Differential suppression of DNA repair deficiencies of Yeast rad50, mre11 and xrs2 mutants by EXO1 and TLC1 (the RNA component of telomerase)." Genetics **160**(1): 49-62.
Li, X., J. Li, J. Harrington, M. R. Lieber and P. M. Burgers (1995). "Lagging strand DNA synthesis at the eukaryotic replication fork involves binding and stimulation of FEN-1 by proliferating cell nuclear antigen." Journal of Biological Chemistry **270**(38): 22109-22112.
Li, Z., F. J. Vizeacoumar, S. Bahr, J. Li, J. Warringer, F. S. Vizeacoumar, R. Min, B. VanderSluis, J. Bellay and M. DeVit (2011). "Systematic exploration of essential yeast gene function with temperature-sensitive mutants." Nature biotechnology **29**(4): 361-367.
Liang, C., M. Weinreich and B. Stillman (1995). "ORC and Cdc6p interact and determine the frequency of initiation of DNA replication in the genome." Cell **81**(5): 667-676.
Liu, S., S. O. Opiyo, K. Manthey, J. G. Glanzer, A. K. Ashley, C. Amerin, K. Troksa, M. Shrivastav, J. A. Nickoloff and G. G. Oakley (2012). "Distinct

roles for DNA-PK, ATM and ATR in RPA phosphorylation and checkpoint activation in response to replication stress." Nucleic acids research **40**(21): 10780-10794.
Lopes, M., M. Foiani and J. M. Sogo (2006). "Multiple mechanisms control chromosome integrity after replication fork uncoupling and restart at irreparable UV lesions." Molecular cell **21**(1): 15-27.
Lopez-Mosqueda, J., N. L. Maas, Z. O. Jonsson, L. G. DeFazio-Eli, J. Wohlschlegel and D. P. Toczyski (2010). "Damage-induced phosphorylation of Sld3 is important to block late origin firing." Nature **467**(7314): 479-483.
Lorenz, M. C., R. S. Muir, E. Lim, J. McElver, S. C. Weber and J. Heitman (1995). "Gene disruption with PCR products in Saccharomyces cerevisiae." Gene **158**(1): 113-117.
Lorenz, M. C., R. S. Muir, E. Lim, J. McElver, S. C. Weber and J. Heitman (1995). "Gene disruption with PCR products in< i> Saccharomyces cerevisiae</i>." Gene **158**(1): 113-117.
Lucchini, G., M. M. Falconi, A. Pizzagalli, A. Aguilera, H. L. Klein and P. Plevani (1990). "Nucleotide sequence and characterization of temperature-sensitive< i> pol1</i> mutants of< i> Saccharomyces cerevisiae</i>." Gene **90**(1): 99-104.
Lucchini, G., C. Mazza, E. Scacheri and P. Plevani (1988). "Genetic mapping of the Saccharomyces cerevisiae DNA polymerase I gene and characterization of a pol1 temperaturesensitive mutant altered in DNA primase-polymerase complex stability." Molecular and General Genetics MGG **212**(3): 459-465.
Ma, W., M. A. Resnick and D. A. Gordenin (2008). "Apn1 and Apn2 endonucleases prevent accumulation of repair-associated DNA breaks in budding yeast as revealed by direct chromosomal analysis." Nucleic acids research **36**(6): 1836-1846.
Maiorano, D., J. Moreau and M. Méchali (2000). "XCDT1 is required for the assembly of pre-replicative complexes in Xenopus laevis." Nature **404**(6778): 622-625.
Majka, J. and P. M. Burgers (2004). "The PCNA–RFC families of DNA clamps and clamp loaders." Progress in nucleic acid research and molecular biology **78**: 227-260.
Makarova, A. V., J. L. Stodola and P. M. Burgers (2012). "A four-subunit DNA polymerase ζ complex containing Pol δ accessory subunits is essential for PCNA-mediated mutagenesis." Nucleic acids research **40**(22): 11618-11626.
Mann, H. B. and D. R. Whitney (1947). "On a test of whether one of two random variables is stochastically larger than the other." The annals of mathematical statistics: 50-60.

Mann, H. B. and D. R. Whitney (1947). "On a test of whether one of two random variables is stochastically larger than the other." The annals of mathematical statistics **18**(1): 50-60.

Masutani, C., R. Kusumoto, A. Yamada, N. Dohmae, M. Yokoi, M. Yuasa, M. Araki, S. Iwai, K. Takio and F. Hanaoka (1999). "The XPV (xeroderma pigmentosum variant) gene encodes human DNA polymerase η." Nature **399**(6737): 700-704.

McDonald, J. P., A. S. Levine and R. Woodgate (1997). "The Saccharomyces cerevisiae RAD30 gene, a homologue of Escherichia coli dinB and umuC, is DNA damage inducible and functions in a novel error-free postreplication repair mechanism." Genetics **147**(4): 1557-1568.

McDonald, J. P., V. Rapić-Otrin, J. A. Epstein, B. C. Broughton, X. Wang, A. R. Lehmann, D. J. Wolgemuth and R. Woodgate (1999). "Novel human and mouse homologs of Saccharomyces cerevisiae DNA polymerase η." Genomics **60**(1): 20-30.

McElhinny, S. A. N., C. M. Stith, P. M. Burgers and T. A. Kunkel (2007). "Inefficient proofreading and biased error rates during inaccurate DNA synthesis by a mutant derivative of Saccharomyces cerevisiae DNA polymerase δ." Journal of Biological Chemistry **282**(4): 2324-2332.

McManus, K. J., I. J. Barrett, Y. Nouhi and P. Hieter (2009). "Specific synthetic lethal killing of RAD54B-deficient human colorectal cancer cells by FEN1 silencing." Proceedings of the National Academy of Sciences **106**(9): 3276-3281.

McWhirter, C., M. Tonge, H. Plant, I. Hardern, W. Nissink and S. T. Durant (2013). "Development of a high-throughput fluorescence polarization DNA cleavage assay for the identification of FEN1 inhibitors." Journal of biomolecular screening **18**(5): 567-575.

Memisoglu, A. and L. Samson (2000). "Base excision repair in yeast and mammals." Mutation Research/Fundamental and Molecular Mechanisms of Mutagenesis **451**(1): 39-51.

Mendenhall, M. D. and A. E. Hodge (1998). "Regulation of Cdc28 cyclin-dependent protein kinase activity during the cell cycle of the yeast Saccharomyces cerevisiae." Microbiology and Molecular Biology Reviews **62**(4): 1191-1243.

Merchant, A. M., Y. Kawasaki, Y. Chen, M. Lei and B. K. Tye (1997). "A lesion in the DNA replication initiation factor Mcm10 induces pausing of elongation forks through chromosomal replication origins in Saccharomyces cerevisiae." Molecular and cellular biology **17**(6): 3261-3271.

Miętus, M., E. Nowak, M. Jaciuk, P. Kustosz, J. Studnicka and M. Nowotny (2014). "Crystal structure of the catalytic core of Rad2: insights into the mechanism of substrate binding." Nucleic acids research **42**(16): 10762-10775.

Miura, T., T. Shibata and K. Kusano (2013). "Putative antirecombinase Srs2 DNA helicase promotes noncrossover homologous recombination avoiding loss of heterozygosity." Proceedings of the National Academy of Sciences **110**(40): 16067-16072.
Moldovan, G.-L., B. Pfander and S. Jentsch (2007). "PCNA, the maestro of the replication fork." Cell **129**(4): 665-679.
Moreau, S., E. A. Morgan and L. S. Symington (2001). "Overlapping functions of the Saccharomyces cerevisiae Mre11, Exo1 and Rad27 nucleases in DNA metabolism." Genetics **159**(4): 1423-1433.
Morgan, D. O. (1999). "Regulation of the APC and the exit from mitosis." Nature Cell Biology **1**(2): E47-E53.
Motegi, A., K. Kuntz, A. Majeed, S. Smith and K. Myung (2006). "Regulation of gross chromosomal rearrangements by ubiquitin and SUMO ligases in Saccharomyces cerevisiae." Molecular and cellular biology **26**(4): 1424-1433.
Moyer, S. E., P. W. Lewis and M. R. Botchan (2006). "Isolation of the Cdc45/Mcm2–7/GINS (CMG) complex, a candidate for the eukaryotic DNA replication fork helicase." Proceedings of the National Academy of Sciences **103**(27): 10236-10241.
Muramatsu, S., K. Hirai, Y.-S. Tak, Y. Kamimura and H. Araki (2010). "CDK-dependent complex formation between replication proteins Dpb11, Sld2, Pol ε, and GINS in budding yeast." Genes & development **24**(6): 602-612.
Myung, K., C. Chen and R. D. Kolodner (2001). "Multiple pathways cooperate in the suppression of genome instability in Saccharomyces cerevisiae." Nature **411**(6841): 1073-1076.
Nagai, S., K. Dubrana, M. Tsai-Pflugfelder, M. B. Davidson, T. M. Roberts, G. W. Brown, E. Varela, F. Hediger, S. M. Gasser and N. J. Krogan (2008). "Functional targeting of DNA damage to a nuclear pore-associated SUMO-dependent ubiquitin ligase." Science **322**(5901): 597-602.
Nelson, J. R., C. W. Lawrence and D. C. Hinkle (1996). "Thymine-thymine dimer bypass by yeast DNA polymerase ζ." Science **272**(5268): 1646-1649.
Nguyen, H. D., J. Becker, Y. M. Thu, M. Costanzo, E. N. Koch, S. Smith, K. Myung, C. L. Myers, C. Boone and A.-K. Bielinsky (2013). "Unligated Okazaki fragments induce PCNA ubiquitination and a requirement for Rad59-dependent replication fork progression." PloS one **8**(6): e66379.
Nikolova, T., M. Christmann and B. Kaina (2009). "FEN1 is overexpressed in testis, lung and brain tumors." Anticancer research **29**(7): 2453-2459.
Nishitani, H., Z. Lygerou, T. Nishimoto and P. Nurse (2000). "The Cdt1 protein is required to license DNA for replication in fission yeast." Nature **404**(6778): 625-628.
Northam, M. R., P. Garg, D. M. Baitin, P. M. Burgers and P. V. Shcherbakova (2006). "A novel function of DNA polymerase ζ regulated by PCNA." The EMBO journal **25**(18): 4316-4325.

Northam, M. R., H. A. Robinson, O. V. Kochenova and P. V. Shcherbakova (2010). "Participation of DNA Polymerase ζ in Replication of Undamaged DNA in Saccharomyces cerevisiae." Genetics **184**(1): 27-42.

Orans, J., E. A. McSweeney, R. R. Iyer, M. A. Hast, H. W. Hellinga, P. Modrich and L. S. Beese (2011). "Structures of human exonuclease 1 DNA complexes suggest a unified mechanism for nuclease family." Cell **145**(2): 212-223.

Osborn, A. J. and S. J. Elledge (2003). "Mrc1 is a replication fork component whose phosphorylation in response to DNA replication stress activates Rad53." Genes & Development **17**(14): 1755-1767.

Pacek, M., A. V. Tutter, Y. Kubota, H. Takisawa and J. C. Walter (2006). "Localization of MCM2-7, Cdc45, and GINS to the site of DNA unwinding during eukaryotic DNA replication." Molecular cell **21**(4): 581-587.

Papouli, E., S. Chen, A. A. Davies, D. Huttner, L. Krejci, P. Sung and H. D. Ulrich (2005). "Crosstalk between SUMO and ubiquitin on PCNA is mediated by recruitment of the helicase Srs2p." Molecular cell **19**(1): 123-133.

Parenteau, J. and R. J. Wellinger (1999). "Accumulation of single-stranded DNA and destabilization of telomeric repeats in yeast mutant strains carrying a deletion of RAD27." Molecular and Cellular Biology **19**(6): 4143-4152.

Parnas, O., A. Zipin-Roitman, B. Pfander, B. Liefshitz, Y. Mazor, S. Ben-Aroya, S. Jentsch and M. Kupiec (2010). "Elg1, an alternative subunit of the RFC clamp loader, preferentially interacts with SUMOylated PCNA." The EMBO Journal **29**(15): 2611-2622.

Pascal, J. M., P. J. O'Brien, A. E. Tomkinson and T. Ellenberger (2004). "Human DNA ligase I completely encircles and partially unwinds nicked DNA." Nature **432**(7016): 473-478.

Pessoa-Brandão, L. and R. A. Sclafani (2004). "CDC7/DBF4 functions in the translesion synthesis branch of the RAD6 epistasis group in Saccharomyces cerevisiae." Genetics **167**(4): 1597-1610.

Pfander, B., G.-L. Moldovan, M. Sacher, C. Hoege and S. Jentsch (2005). "SUMO-modified PCNA recruits Srs2 to prevent recombination during S phase." nature **436**(7049): 428-433.

Pizzagalli, A., P. Valsasnini, P. Plevani and G. Lucchini (1988). "DNA polymerase I gene of Saccharomyces cerevisiae: nucleotide sequence, mapping of a temperature-sensitive mutation, and protein homology with other DNA polymerases." Proceedings of the National Academy of Sciences **85**(11): 3772-3776.

Povlsen, L. K., P. Beli, S. A. Wagner, S. L. Poulsen, K. B. Sylvestersen, J. W. Poulsen, M. L. Nielsen, S. Bekker-Jensen, N. Mailand and C. Choudhary (2012). "Systems-wide analysis of ubiquitylation dynamics reveals a key role for PAF15 ubiquitylation in DNA-damage bypass." Nature cell biology **14**(10): 1089-1098.

Prakash, S., R. E. Johnson and L. Prakash (2005). "Eukaryotic translesion synthesis DNA polymerases: specificity of structure and function." Annu. Rev. Biochem. **74**: 317-353.
Pursell, Z. F., I. Isoz, E.-B. Lundström, E. Johansson and T. A. Kunkel (2007). "Yeast DNA polymerase ε participates in leading-strand DNA replication." Science **317**(5834): 127-130.
Quah, S.-K., R. Von Borstel and P. Hastings (1980). "The origin of spontaneous mutation in Saccharomyces cerevisiae." Genetics **96**(4): 819-839.
Quammen, D. (2008). "CONTAGIOUS CANCER The evolution of a killer." HARPERS **1895**: 33.
Ran, F. A., P. D. Hsu, J. Wright, V. Agarwala, D. A. Scott and F. Zhang (2013). "Genome engineering using the CRISPR-Cas9 system." Nature protocols **8**(11): 2281-2308.
Randell, J. C., J. L. Bowers, H. K. Rodríguez and S. P. Bell (2006). "Sequential ATP hydrolysis by Cdc6 and ORC directs loading of the Mcm2-7 helicase." Molecular cell **21**(1): 29-39.
Raveendranathan, M., S. Chattopadhyay, Y.-T. Bolon, J. Haworth, D. J. Clarke and A.-K. Bielinsky (2006). "Genome-wide replication profiles of S-phase checkpoint mutants reveal fragile sites in yeast." The EMBO journal **25**(15): 3627-3639.
Reagan, M. S., C. Pittenger, W. Siede and E. C. Friedberg (1995). "Characterization of a mutant strain of Saccharomyces cerevisiae with a deletion of the RAD27 gene, a structural homolog of the RAD2 nucleotide excision repair gene." Journal of bacteriology **177**(2): 364-371.
Reed, S. I., J. A. Hadwiger and A. T. Lörincz (1985). "Protein kinase activity associated with the product of the yeast cell division cycle gene CDC28." Proceedings of the National Academy of Sciences **82**(12): 4055-4059.
Remus, D., F. Beuron, G. Tolun, J. D. Griffith, E. P. Morris and J. F. Diffley (2009). "Concerted loading of Mcm2–7 double hexamers around DNA during DNA replication origin licensing." Cell **139**(4): 719-730.
Richardson, H. E., C. Wittenberg, F. Cross and S. I. Reed (1989). "An essential G1 function for cyclin-like proteins in yeast." Cell **59**(6): 1127-1133.
Ricke, R. M. and A.-K. Bielinsky (2004). "Mcm10 regulates the stability and chromatin association of DNA polymerase-α." Molecular cell **16**(2): 173-185.
Ricke, R. M. and A.-K. Bielinsky (2006). "A conserved Hsp10-like domain in Mcm10 is required to stabilize the catalytic subunit of DNA polymerase-α in budding yeast." Journal of Biological Chemistry **281**(27): 18414-18425.
Robertson, P. D., B. Chagot, W. J. Chazin and B. F. Eichman (2010). "Solution NMR structure of the C-terminal DNA binding domain of Mcm10 reveals a conserved MCM motif." Journal of Biological Chemistry **285**(30): 22942-22949.

Rogakou, E. P., D. R. Pilch, A. H. Orr, V. S. Ivanova and W. M. Bonner (1998). "DNA double-stranded breaks induce histone H2AX phosphorylation on serine 139." Journal of biological chemistry **273**(10): 5858-5868.

Rossi, M. L. and R. A. Bambara (2006). "Reconstituted Okazaki fragment processing indicates two pathways of primer removal." Journal of Biological Chemistry **281**(36): 26051-26061.

Rossi, M. L., J. E. Pike, W. Wang, P. M. Burgers, J. L. Campbell and R. A. Bambara (2008). "Pif1 helicase directs eukaryotic Okazaki fragments toward the two-nuclease cleavage pathway for primer removal." Journal of Biological Chemistry **283**(41): 27483-27493.

Rouse, J. and S. P. Jackson (2000). "LCD1: an essential gene involved in checkpoint control and regulation of the MEC1 signalling pathway in Saccharomyces cerevisiae." The EMBO journal **19**(21): 5801-5812.

Rupp, W. D. and P. Howard-Flanders (1968). "Discontinuities in the DNA synthesized in an excision-defective strain of Escherichia coli following ultraviolet irradiation." Journal of molecular biology **31**(2): 291-304.

Sacher, M., B. Pfander, C. Hoege and S. Jentsch (2006). "Control of Rad52 recombination activity by double-strand break-induced SUMO modification." Nature cell biology **8**(11): 1284-1290.

Sakabe, K. and R. Okazaki (1966). "A unique property of the replicating region of chromosomal DNA." Biochimica et Biophysica Acta (BBA)-Nucleic Acids and Protein Synthesis **129**(3): 651-654.

Sakiyama, T., T. Kohno, S. Mimaki, T. Ohta, N. Yanagitani, T. Sobue, H. Kunitoh, R. Saito, K. Shimizu and C. Hirama (2005). "Association of amino acid substitution polymorphisms in DNA repair genes TP53, POLI, REV1 and LIG4 with lung cancer risk." International journal of cancer **114**(5): 730-737.

Sanchez, Y., B. A. Desany, W. J. Jones, Q. Liu, B. Wang and S. J. Elledge (1996). "Regulation of RAD53 by the ATM-like kinases MEC1 and TEL1 in yeast cell cycle checkpoint pathways." Science **271**(5247): 357-360.

Santocanale, C. and J. F. Diffley (1998). "A Mec1-and Rad53-dependent checkpoint controls late-firing origins of DNA replication." Nature **395**(6702): 615-618.

Sartori, A. A., C. Lukas, J. Coates, M. Mistrik, S. Fu, J. Bartek, R. Baer, J. Lukas and S. P. Jackson (2007). "Human CtIP promotes DNA end resection." Nature **450**(7169): 509-514.

Sato, M., L. Girard, I. Sekine, N. Sunaga, R. D. Ramirez, C. Kamibayashi and J. D. Minna (2003). "Increased expression and no mutation of the Flap endonuclease (FEN1) gene in human lung cancer." Oncogene **22**(46): 7243-7246.

Sawyer, S. L., I. H. Cheng, W. Chai and B. K. Tye (2004). "Mcm10 and Cdc45 Cooperate in Origin Activation in< i> Saccharomyces cerevisiae</i>." Journal of molecular biology **340**(2): 195-202.

Schneider, B., Q.-H. Yang and A. Futcher (1996). "Linkage of replication to start by the Cdk inhibitor Sic1." Science **272**(5261): 560-562.
Schuldiner, M., S. R. Collins, N. J. Thompson, V. Denic, A. Bhamidipati, T. Punna, J. Ihmels, B. Andrews, C. Boone and J. F. Greenblatt (2005). "Exploration of the function and organization of the yeast early secretory pathway through an epistatic miniarray profile." Cell **123**(3): 507-519.
Schweitzer, J. K. and D. M. Livingston (1998). "Expansions of CAG repeat tracts are frequent in a yeast mutant defective in Okazaki fragment maturation." Human molecular genetics **7**(1): 69-74.
Schweitzer, J. K. and D. M. Livingston (1999). "The effect of DNA replication mutations on CAG tract stability in yeast." Genetics **152**(3): 953-963.
Schwob, E. and K. Nasmyth (1993). "CLB5 and CLB6, a new pair of B cyclins involved in DNA replication in Saccharomyces cerevisiae." Genes & Development **7**(7a): 1160-1175.
Serero, A., C. Jubin, S. Loeillet, P. Legoix-Né and A. G. Nicolas (2014). "Mutational landscape of yeast mutator strains." Proceedings of the National Academy of Sciences **111**(5): 1897-1902.
Seufert, W., B. Futcher and S. Jentsch (1995). "Role of a ubiquitin-conjugating enzyme in degradation of S-and M-phase cyclins."
Sheu, Y.-J. and B. Stillman (2006). "Cdc7-Dbf4 phosphorylates MCM proteins via a docking site-mediated mechanism to promote S phase progression." Molecular cell **24**(1): 101-113.
Sheu, Y.-J. and B. Stillman (2010). "The Dbf4–Cdc7 kinase promotes S phase by alleviating an inhibitory activity in Mcm4." Nature **463**(7277): 113-117.
Simon, I., J. Barnett, N. Hannett, C. T. Harbison, N. J. Rinaldi, T. L. Volkert, J. J. Wyrick, J. Zeitlinger, D. K. Gifford and T. S. Jaakkola (2001). "Serial regulation of transcriptional regulators in the yeast cell cycle." Cell **106**(6): 697-708.
Singh, P., M. Yang, H. Dai, D. Yu, Q. Huang, W. Tan, K. H. Kernstine, D. Lin and B. Shen (2008). "Overexpression and hypomethylation of flap endonuclease 1 gene in breast and other cancers." Molecular Cancer Research **6**(11): 1710-1717.
Smith, S., J.-Y. Hwang, S. Banerjee, A. Majeed, A. Gupta and K. Myung (2004). "Mutator genes for suppression of gross chromosomal rearrangements identified by a genome-wide screening in Saccharomyces cerevisiae." Proceedings of the National Academy of Sciences of the United States of America **101**(24): 9039-9044.
Stelter, P. and H. D. Ulrich (2003). "Control of spontaneous and damage-induced mutagenesis by SUMO and ubiquitin conjugation." Nature **425**(6954): 188-191.
Stewart, J. A., A. S. Miller, J. L. Campbell and R. A. Bambara (2008). "Dynamic removal of replication protein A by Dna2 facilitates primer cleavage during

Okazaki fragment processing in Saccharomyces cerevisiae." Journal of Biological Chemistry **283**(46): 31356-31365.
Stinchcomb, D., K. Struhl and R. Davis (1979). "yeast chromosomal replicator." Nature **282**: 1.
Subramanian, J., S. Vijayakumar, A. E. Tomkinson and N. Arnheim (2005). "Genetic instability induced by overexpression of DNA ligase I in budding yeast." Genetics **171**(2): 427-441.
Sun, X., D. Thrower, J. Qiu, P. Wu, L. Zheng, M. Zhou, J. Bachant, D. M. Wilson and B. Shen (2003). "Complementary functions of the Saccharomyces cerevisiae Rad2 family nucleases in Okazaki fragment maturation, mutation avoidance, and chromosome stability." DNA repair **2**(8): 925-940.
Sun, Z., D. S. Fay, F. Marini, M. Foiani and D. Stern (1996). "Spk1/Rad53 is regulated by Mec1-dependent protein phosphorylation in DNA replication and damage checkpoint pathways." Genes & Development **10**(4): 395-406.
Sung, P., S. Prakash and L. Prakash (1988). "The RAD6 protein of Saccharomyces cerevisiae polyubiquitinates histones, and its acidic domain mediates this activity." Genes & development **2**(11): 1476-1485.
Suzuki, M., A. Niimi, S. Limsirichaikul, S. Tomida, Q. M. Huang, S. Izuta, J. Usukura, Y. Itoh, T. Hishida and T. Akashi (2009). "PCNA mono-ubiquitination and activation of translesion DNA polymerases by DNA polymerase α." Journal of biochemistry **146**(1): 13-21.
Symington, L. S. (1998). "Homologous recombination is required for the viability of rad27 mutants." Nucleic acids research **26**(24): 5589-5595.
Tanaka, S., T. Umemori, K. Hirai, S. Muramatsu, Y. Kamimura and H. Araki (2007). "CDK-dependent phosphorylation of Sld2 and Sld3 initiates DNA replication in budding yeast." Nature **445**(7125): 328-332.
Taylor, M., K. Moore, J. Murray, S. J. Aves and C. Price (2011). "Mcm10 interacts with Rad4/Cut5< sup> TopBP1</sup> and its association with origins of DNA replication is dependent on Rad4/Cut5< sup> TopBP1</sup>." DNA repair **10**(11): 1154-1163.
Tercero, J. A. and J. F. Diffley (2001). "Regulation of DNA replication fork progression through damaged DNA by the Mec1/Rad53 checkpoint." Nature **412**(6846): 553-557.
Thomas, B. J. and R. Rothstein (1989). "Elevated recombination rates in transcriptionally active DNA." Cell **56**(4): 619-630.
Thu, Y. M. and A.-K. Bielinsky (2013). "Enigmatic roles of Mcm10 in DNA replication." Trends in biochemical sciences.
Thu, Y. M. and A.-K. Bielinsky (2014). MCM10: One tool for all—Integrity, maintenance and damage control. Seminars in cell & developmental biology, Elsevier.
Thu, Y. M., S. Van Riper, L. Higgins, T. Zhang, J. R. Becker, T. W. Markowski, H. D. Nguyen, T. J. Griffin and A.-K. Bielinsky (2016). "Slx5/Slx8 promotes

replication stress tolerance by facilitating mitotic progression." Cell Reports ***In press***.

Tishkoff, D. X., A. L. Boerger, P. Bertrand, N. Filosi, G. M. Gaida, M. F. Kane and R. D. Kolodner (1997). "Identification and characterization of Saccharomyces cerevisiae EXO1, a gene encoding an exonuclease that interacts with MSH2." Proceedings of the National Academy of Sciences **94**(14): 7487-7492.

Tishkoff, D. X., N. Filosi, G. M. Gaida and R. D. Kolodner (1997). "A novel mutation avoidance mechanism dependent on S. cerevisiae RAD27 is distinct from DNA mismatch repair." Cell **88**(2): 253-263.

Tkach, J. M., A. Yimit, A. Y. Lee, M. Riffle, M. Costanzo, D. Jaschob, J. A. Hendry, J. Ou, J. Moffat and C. Boone (2012). "Dissecting DNA damage response pathways by analysing protein localization and abundance changes during DNA replication stress." Nature cell biology **14**(9): 966-976.

Tomkinson, A. E., S. Vijayakumar, J. M. Pascal and T. Ellenberger (2006). "DNA ligases: structure, reaction mechanism, and function." Chemical reviews **106**(2): 687-699.

Tong, A. H. Y., M. Evangelista, A. B. Parsons, H. Xu, G. D. Bader, N. Pagé, M. Robinson, S. Raghibizadeh, C. W. Hogue and H. Bussey (2001). "Systematic genetic analysis with ordered arrays of yeast deletion mutants." Science **294**(5550): 2364-2368.

Tran, H. T., J. D. Keen, M. Kricker, M. A. Resnick and D. A. Gordenin (1997). "Hypermutability of homonucleotide runs in mismatch repair and DNA polymerase proofreading yeast mutants." Molecular and Cellular Biology **17**(5): 2859-2865.

Tran, P. T., N. Erdeniz, S. Dudley and R. M. Liskay (2002). "Characterization of nuclease-dependent functions of Exo1p in Saccharomyces cerevisiae." DNA repair **1**(11): 895-912.

Tsutakawa, S. E., S. Classen, B. R. Chapados, A. S. Arvai, L. D. Finger, G. Guenther, C. G. Tomlinson, P. Thompson, A. H. Sarker and B. Shen (2011). "Human flap endonuclease structures, DNA double-base flipping, and a unified understanding of the FEN1 superfamily." Cell **145**(2): 198-211.

Tyers, M. (1996). "The cyclin-dependent kinase inhibitor p40SIC1 imposes the requirement for Cln G1 cyclin function at Start." Proceedings of the National Academy of Sciences **93**(15): 7772-7776.

Uhlmann, F., F. Lottspeich and K. Nasmyth (1999). "Sister-chromatid separation at anaphase onset is promoted by cleavage of the cohesin subunit Scc1." Nature **400**(6739): 37-42.

Ulrich, H. D. (2009). "Regulating post-translational modifications of the eukaryotic replication clamp PCNA." DNA repair **8**(4): 461-469.

Ulrich, H. D. (2009). SUMO protocols, Humana Press New York, NY.

van Deursen, F., S. Sengupta, G. De Piccoli, A. Sanchez-Diaz and K. Labib (2012). "Mcm10 associates with the loaded DNA helicase at replication origins and defines a novel step in its activation." The EMBO journal **31**(9): 2195-2206.

van Pel, D. M., I. J. Barrett, Y. Shimizu, B. V. Sajesh, B. J. Guppy, T. Pfeifer, K. J. McManus and P. Hieter (2013). "An evolutionarily conserved synthetic lethal interaction network identifies FEN1 as a broad-spectrum target for anticancer therapeutic development." PLoS Genet **9**(1): e1003254.

Van Riper, S. K., L. Higgins, J. V. Carlis and T. J. Griffin (2016). "RIPPER: A Framework for MS1 Only Metabolomics and Proteomics Label-Free Relative Quantification." Bioinformatics: btw091.

Vanoli, F., M. Fumasoni, B. Szakal, L. Maloisel and D. Branzei (2010). "Replication and recombination factors contributing to recombination-dependent bypass of DNA lesions by template switch." PLoS genetics **6**(11): e1001205.

Varrin, A. E., A. A. Prasad, R.-P. Scholz, M. D. Ramer and B. P. Duncker (2005). "A mutation in Dbf4 motif M impairs interactions with DNA replication factors and confers increased resistance to genotoxic agents." Molecular and cellular biology **25**(17): 7494-7504.

Veaute, X., J. Jeusset, C. Soustelle, S. C. Kowalczykowski, E. Le Cam and F. Fabre (2003). "The Srs2 helicase prevents recombination by disrupting Rad51 nucleoprotein filaments." Nature **423**(6937): 309-312.

Vialard, J. E., C. S. Gilbert, C. M. Green and N. F. Lowndes (1998). "The budding yeast Rad9 checkpoint protein is subjected to Mec1/Tel1-dependent hyperphosphorylation and interacts with Rad53 after DNA damage." The EMBO journal **17**(19): 5679-5688.

Waga, S., G. J. Hannon, D. Beach and B. Stillman (1994). "The p21 inhibitor of cyclin-dependent kinases controls DNA replication by interaction with PCNA." Nature **369**(6481): 574-578.

Warren, E. M., H. Huang, E. Fanning, W. J. Chazin and B. F. Eichman (2009). "Physical interactions between MCM10, DNA, AND DNA polymerase α." Journal of Biological Chemistry **284**(36): 24662-24672.

Warren, E. M., S. Vaithiyalingam, J. Haworth, B. Greer, A.-K. Bielinsky, W. J. Chazin and B. F. Eichman (2008). "Structural basis for DNA binding by replication initiator Mcm10." Structure **16**(12): 1892-1901.

Watanabe, K., S. Tateishi, M. Kawasuji, T. Tsurimoto, H. Inoue and M. Yamaizumi (2004). "Rad18 guides polη to replication stalling sites through physical interaction and PCNA monoubiquitination." The EMBO journal **23**(19): 3886-3896.

Watase, G., H. Takisawa and M. T. Kanemaki (2012). "Mcm10 plays a role in functioning of the eukaryotic replicative DNA helicase, Cdc45-Mcm-GINS." Current Biology **22**(4): 343-349.

Waters, L. S., B. K. Minesinger, M. E. Wiltrout, S. D'Souza, R. V. Woodruff and G. C. Walker (2009). "Eukaryotic translesion polymerases and their roles and regulation in DNA damage tolerance." Microbiology and Molecular Biology Reviews **73**(1): 134-154.

Waters, L. S. and G. C. Walker (2006). "The critical mutagenic translesion DNA polymerase Rev1 is highly expressed during G2/M phase rather than S phase." Proceedings of the National Academy of Sciences **103**(24): 8971-8976.

Whelan, W. L., E. Gocke and T. R. Manney (1979). "The CAN1 locus of Saccharomyces cerevisiae: fine-structure analysis and forward mutation rates." Genetics **91**(1): 35-51.

Whittaker, A. J., I. Royzman and T. L. Orr-Weaver (2000). "Drosophila double parked: a conserved, essential replication protein that colocalizes with the origin recognition complex and links DNA replication with mitosis and the down-regulation of S phase transcripts." Genes & Development **14**(14): 1765-1776.

Windecker, H. and H. D. Ulrich (2008). "Architecture and assembly of poly-SUMO chains on PCNA in Saccharomyces cerevisiae." Journal of molecular biology **376**(1): 221-231.

Wohlschlegel, J. A., S. K. Dhar, T. A. Prokhorova, A. Dutta and J. C. Walter (2002). "< i> Xenopus</i> Mcm10 Binds to Origins of DNA Replication after Mcm2-7 and Stimulates Origin Binding of Cdc45." Molecular cell **9**(2): 233-240.

Xu, G., J. S. Paige and S. R. Jaffrey (2010). "Global analysis of lysine ubiquitination by ubiquitin remnant immunoaffinity profiling." Nature biotechnology **28**(8): 868-873.

Yang, J., Z. Chen, Y. Liu, R. J. Hickey and L. H. Malkas (2004). "Altered DNA polymerase ı expression in breast cancer cells leads to a reduction in DNA replication fidelity and a higher rate of mutagenesis." Cancer research **64**(16): 5597-5607.

Yang, M., H. Guo, C. Wu, Y. He, D. Yu, L. Zhou, F. Wang, J. Xu, W. Tan and G. Wang (2009). "Functional FEN1 polymorphisms are associated with DNA damage levels and lung cancer risk." Human mutation **30**(9): 1320-1328.

Yang, X., J. Gregan, K. Lindner, H. Young and S. Kearsey (2005). "Nuclear distribution and chromatin association of DNA polymerase α-primase is affected by TEV protease cleavage of Cdc23 (Mcm10) in fission yeast." BMC molecular biology **6**(1): 13.

Ye, Y. and M. Rape (2009). "Building ubiquitin chains: E2 enzymes at work." Nature reviews Molecular cell biology **10**(11): 755-764.

Yeeles, J. T., T. D. Deegan, A. Janska, A. Early and J. F. Diffley (2015). "Regulated eukaryotic DNA replication origin firing with purified proteins." Nature.

Yu, C., H. Gan, J. Han, Z.-X. Zhou, S. Jia, A. Chabes, G. Farrugia, T. Ordog and Z. Zhang (2014). "Strand-Specific Analysis Shows Protein Binding at Replication Forks and PCNA Unloading from Lagging Strands when Forks Stall." Molecular cell **56**(4): 551-563.

Zegerman, P. and J. F. Diffley (2007). "Phosphorylation of Sld2 and Sld3 by cyclin-dependent kinases promotes DNA replication in budding yeast." Nature **445**(7125): 281-285.

Zegerman, P. and J. F. Diffley (2010). "Checkpoint-dependent inhibition of DNA replication initiation by Sld3 and Dbf4 phosphorylation." Nature **467**(7314): 474-478.

Zeman, M. K. and K. A. Cimprich (2014). "Causes and consequences of replication stress." Nature cell biology **16**(1): 2-9.

Zhang, B., W.-H. Jia, K. Matsuda, S.-S. Kweon, K. Matsuo, Y.-B. Xiang, A. Shin, S. H. Jee, D.-H. Kim and Q. Cai (2014). "Large-scale genetic study in East Asians identifies six new loci associated with colorectal cancer risk." Nature genetics **46**(6): 533-542.

Zheng, L., H. Dai, M. Zhou, M. Li, P. Singh, J. Qiu, W. Tsark, Q. Huang, K. Kernstine and X. Zhang (2007). "Fen1 mutations result in autoimmunity, chronic inflammation and cancers." Nature medicine **13**(7): 812-819.

Zhong, Y., T. Nellimoottil, J. M. Peace, S. R. Knott, S. K. Villwock, J. M. Yee, J. M. Jancuska, S. Rege, M. Tecklenburg and R. A. Sclafani (2013). "The level of origin firing inversely affects the rate of replication fork progression." The Journal of cell biology **201**(3): 373-383.

Zhu, W., C. Ukomadu, S. Jha, T. Senga, S. K. Dhar, J. A. Wohlschlegel, L. K. Nutt, S. Kornbluth and A. Dutta (2007). "Mcm10 and And-1/CTF4 recruit DNA polymerase α to chromatin for initiation of DNA replication." Genes & development **21**(18): 2288-2299.

Zou, L. and S. J. Elledge (2003). "Sensing DNA damage through ATRIP recognition of RPA-ssDNA complexes." Science **300**(5625): 1542-1548.

Zou, L. and B. Stillman (2000). "Assembly of a complex containing Cdc45p, replication protein A, and Mcm2p at replication origins controlled by S-phase cyclin-dependent kinases and Cdc7p-Dbf4p kinase." Molecular and Cellular Biology **20**(9): 3086-3096.